SLIP AND FALL RISKS:

PRE-SLIP GAIT CONTRIBUTIONS AND POST-SLIP RESPONSE EFFECTS

by

Brian E. Moyer

B. S. in Mechanical Engineering, Carnegie Mellon University, 1993

M. S. in Mechanical Engineering, University of Pittsburgh, 1997

Submitted to the Graduate Faculty of

School of Engineering in partial fulfillment

of the requirements for the degree of

Doctor of Philosophy in Bioengineering

University of Pittsburgh

2006

UNIVERSITY OF PITTSBURGH

SCHOOL OF ENGINEERING

This dissertation was presented

by

Brian E. Moyer

It was defended on

July 20, 2006

and approved by

Richard E. Debski, Associate Professor, Department of Bioengineering

Jessica K. Hodgins, Professor, Robotics Institute, Carnegie Mellon University

Chris G. Atkeson, Professor, Robotics Institute, Carnegie Mellon University

Rakié Cham, Assistant Professor, Department of Bioengineering

Dissertation Director: Mark S. Redfern, Professor, Department of Bioengineering

SLIP AND FALL RISKS: PRE-SLIP GAIT CONTRIBUTIONS

AND POST-SLIP RESPONSE EFFECTS

Brian E. Moyer, PhD

University of Pittsburgh, 2006

This thesis describes analysis methods and results from slip-perturbed gait experiments. The risk for falls was related both to the conditions present at heel strike and to the nature of the response. Gait analysis was performed using the Human Movement and Balance Laboratory (HMBL) model, a fifteen segment, fourteen joint model of the human body that was developed as part of this thesis effort.   Resulting kinematics and kinetics included three-dimensional angles describing relative segment rotations, segmental and whole-body centers-of-mass, and joint actuation torques for the entire body.

The relationship between pre-slip gait characteristics and the magnitude of slips was explored for both younger and older adults. Slip severity, either hazardous or non-hazardous, was determined using a 1.0 m/s peak slip velocity threshold. Hazardous slips were associated with greater step lengths normalized by leg length, larger and more rapidly changing foot-floor angles at heel strike, and increased cadence across the two subject groups. These results suggest that gait characteristics play an important role in the severity of slips. Older adults were found to walk with shorter step lengths and with smaller and more slowly changing foot-floor angles at heel strike compared to younger subjects, suggesting that age effects also impact slip severity.

The effects of slipping and trailing leg response on slip outcome (falls or recoveries) were explored. Slip severity was found to be the most significant parameter related to outcome. Response strategies were classified, based on trailing leg dynamics, as either minimal, foot-flat, mid-flight, or toe-down. Slipping and trailing leg hip and knee torques were determined using the HMBL model and timing and magnitude parameters from these torques were then identified. Relationships between these parameters, age group (younger/older), response strategy, and outcome were then explored. Age was not found to be significantly related to response strategy or outcome, nor was response strategy found to be related to outcome. Slipping leg knee torque timing and magnitude parameters were related to slip severity and to outcome for hazardous

slips. These results suggest that slip responses, coupled with slip severity, determine fall or recovery outcomes.

TABLE OF CONTENTS

LIST OF TABLES

LIST OF FIGURES

PREFACE

"The most important motive for work in school and in life is pleasure in work, pleasure in its result, and the knowledge of the value of the result to the community."

    Albert Einstein (1879 - 1955), *On Education*

Patience has a name and she is called Heather – thank you, my love, for your support, your advice, and your formatting expertise. I could not have finished this without you. Bridget and Grayson, I have tried to give you as much attention as I could through this process but it was less than you deserved (daddy doesn't have to work tonight), thanks for behaving while I had to focus elsewhere. Mom and dad and Christy and Bill: I thank you for being there when I needed you. Mark, my brother-from-a-different-mother, having had you to talk at was worth more than gold. I can think of no one else who I would rather have shared this experience. Rakié, it was your effort that made this project possible. I only hope that my work helps you as your work surely did help me. Although there are too many of you to address individually, I thank all of the lab assistants who helped with collection and analysis software development, subject recruitment, data collection, and post-processing. Finally, although it likely goes without saying that one's advisor deserves appreciation, I am especially grateful to the kindness, generosity, and wisdom that Mark shared with me – I have learned much beyond how to read a journal article from you and will continue to emulate you in my dealings with others for the rest of my life.

NOMENCLATURE

AJC	Ankle Joint Center
ASIS	Midpoint of the anterior superior iliac spine
C7	7th Cervical Vertebra
CAD	Cadence
COM	Center of mass
DAT	Analog data file collected via LabVIEW
EJC	Elbow Joint Center
FF	Foot-Flat Response Strategy
FFA	Angle between the foot and the floor at heel strike
FFAS	Rate of change of FFA at heel strike
GCS	Global Coordinate System
GS	Gait speed
H or HAZ	Hazardous slip as defined by PSV > 1.0 m/s
H_VEL	Horizontal velocity of the left heel at heel strike
HJC	Hip Joint Center, left and right
HMBL	Human Movement and Balance Laboratory
HS	Heel strike - the beginning of stance.
I, Ix, Iy, Iz	Moment of inertia, moments of inertia about the axes of the local coordinate system
KJC	Knee Joint Center
LCS	Local Coordinate System
MASTER	Computer responsible for data acquisition and synchronization with the Vicon system
MID	Mid-Swing Response Strategy
MIDH	Midpoint between left and right HJC
MIN	Response Strategy Minimally Different from Baseline
MP	Metatarsal-Phalangeal - an imaginary axis through the feet roughly differentiating the hind-foot and toe segments
NH or NHAZ	Non Hazardous
PSIS	posterior superior iliac spine
PSV	Peak slip velocity
R, Rx, Ry, Rz (or, K, Kx, Ky, Kz)	Radii of gyration about the axes of the local coordinate system
SD	Slip distance
SJC	Shoulder Joint Center

SLR	Step length normalized to leg length
T10	10th Thoracic Vertebra
TD	Toe-Down Response Strategy
TO	Toe-off - the end of double support.
V_VEL	Vertical velocity of the left heel at heel strike
VAD	Vicon Analog Data File
VICON	The motion capture computer
WJC	Wrist Joint Center

1.0   INTRODUCTION

Slips and falls are a significant health issue resulting in serious injuries and deaths. There are many factors that contribute to slip and fall risks. Some of these factors, such as the presence of surface contamination, are related to the environment while myriad others are related to human factors, such as a person's ability to sense slip risks in a timely manner. Generally, the human factors of slip and fall risk can be differentiated into pre-slip gait contributions and post-slip response effects with biomechanics being important for both of these categories. This thesis reports analysis techniques and results from experimental investigations of pre and post-slip biomechanics. Because both the frequency and cost of slip and fall accidents increase with age, biomechanical differences between younger and older adults were explored as part of this effort. The primary goal of this research was to better understand the effects of pre-slip gait and post-slip response biomechanics on the risk for falls. The insights resulting from this thesis may make it possible to identify individuals at risk for slip induced falls and may suggest methods to reduce fall risks.

Chapter 2.0 of this thesis describes the development of a laboratory data collection system enabling experiments to study human movement. This customized hardware and software system includes an eight camera, reflective marker based motion capture component, two ground-embedded force plates, and an integrated safety support structure to prevent ground contact injuries. A new segmental model of the human body was developed. This model uses continuously measured locations from nearly 80 points on the body to produce a dynamic postural record of human movement. Variables such as the three dimensional rotations at the ankles, knees, and hips result from the application of this model. When these postural variables are further coupled with measurements of ground reaction forces and subject-specific segmental mass estimates, forces and torques acting between segments (at joints) can be derived. Of particular interest for this thesis were the hip and knee joint torques characterizing slip responses.

1

Experimental data were analyzed in two parts. The first analysis, detailed in Chapter 3.0, examined pre-slip gait characteristics such as step length and the angle between the foot and the floor at heel strike, looking for relationships between such parameters and the risk for hazardous slips (i.e., those with an increased risk for falls) for younger and older adults. The second analysis, detailed in Chapter 4.0, examined lower extremity responses to slips, attempting to identify differences in joint torques for responses leading to falls compared to responses leading to recoveries and exploring relationships among age, slip severity, response biomechanics, and outcomes. The results of Chapter 3.0 and Chapter 4.0 suggest that, for unexpected slips, pre-slip biomechanics are the most critical human factors.

1.1   SCOPE OF THE PROBLEM

Falls are among the leading causes of both work-related and non work-related injuries. Slips are recognized as a major contributor to falls. Injuries resulting from slips include traumatic injuries due to contact with the ground or other objects and overexertion injuries (sprains and strains) resulting from recovery efforts. These injuries can cause serious reductions in quality of life, lead to huge costs, and can even result in death. Slips were identified as the second leading accidental cause of death in the United States [51]. In 2002, over 1.6 million people in the United States suffered a non-fatal, falling-related injury [83]. In 2000, falls caused the highest number (854,600) of hospitalized injuries for the general US population [52]. These injuries equated to 309 hospitalizations per 100,000 persons – three times higher than the next leading injury mechanism [52]. In addition, falls led to an estimated 10.7 million less-severe, non-hospitalization injuries and caused 14,052 deaths – when taken together, injuries due to falls accounted for 23% of all injuries (Figure 1) [52].
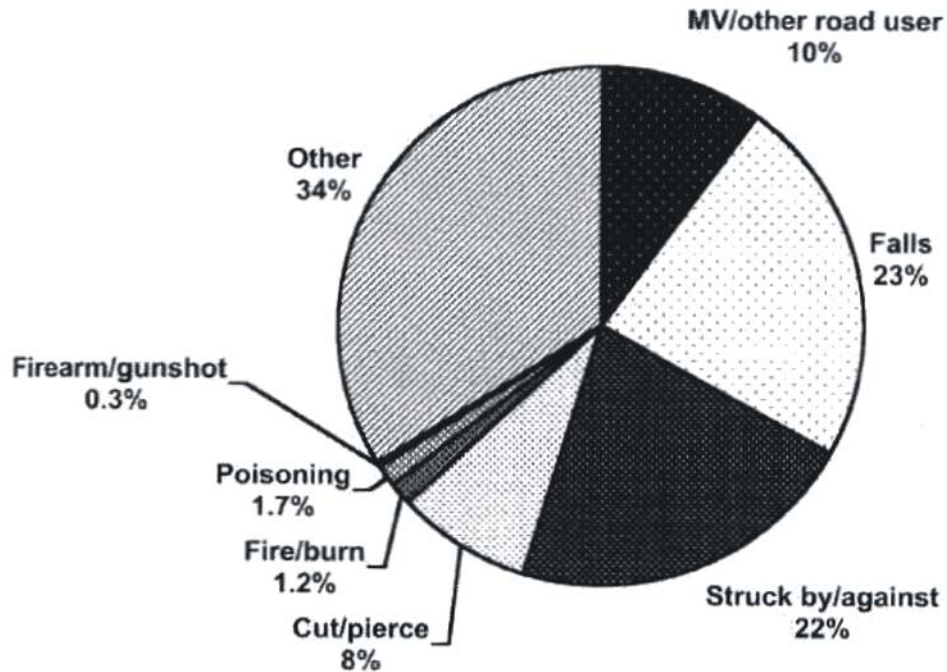
Figure 1: Injury incidence rates by mechanism for 2000 [taken from 52]

1.1.1 The Link Between Slips and Falls

Slips are a leading cause for falls. Slips were the most frequent event leading to fall and overexertion related injuries in the Swedish labor force [44] and were the most common fall initiating event for employees in the UK [55]. Britain ranked slips, trips and falls as the most frequent mechanism, accounting for 29.8% of all reported injuries occurring on the same floor level [63]. The US National Health Interview Survey questionnaire administered by the National Center for Health Statistics in 1997 revealed a clear majority (64%) of work-related falls were attributable to slipping, tripping, or stumbling and indicated that 43% of occupational same-level fatal falls were most commonly triggered by a slip [44].

1.1.2 The Relationship Between Age and Slip Risk, Outcome, and Costs

Both the risk for slips and the associated costs increase with age. Lloyd and Stevenson [85] indicated that while slips and trips caused 32% of falls for young people, 67% of falls for the

3

elderly were initiated by slips. Injuries to the elderly resulting from falls cause significant mortality, disability, and loss of independence [125]. More than one third of older adults fall each year [62, 69] and these falls are the leading cause of unintentional injury and death among older adults. As Figure 2 illustrates, the highest rates for fall related deaths were for persons over 75 years old – 5 times greater than any other age group [52].
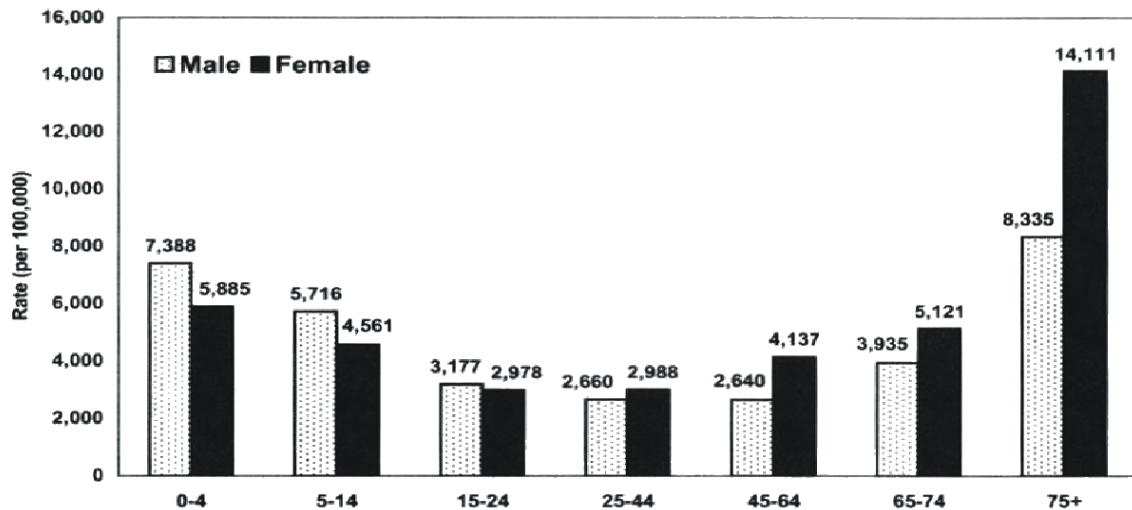
Figure 2: Incidence rate (per 100,000) of fall injuries by age group and gender [taken from 52]

The relationship between age and slip and fall risk is influenced by many age related physiological and psychological changes. Muscle weakness and loss of lower body strength, often caused by inactivity, are well know risk factors for falling [124]. Aging has been shown to diminish sensory and musculoskeletal acuity [71, 131, 138] as well as cognitive function [140] perhaps leading to late or erroneous perception of slips or inadequate responses. As an example of age related psychophysical gait changes, fear of falling has been shown to impact balance and movement patterns for the elderly [12, 19, 35, 77, 93].

Not only does the risk for slips and falls increase with age, but related injuries to the elderly are often more serious. Osteoporosis increases in prevalence as a person ages, greatly increasing the chance that a person who falls will suffer a hip fracture [56, 99]. Because the elderly are more likely to experience falls, weighting the impact of this population segment, and because injury treatment for the elderly is more expensive, the lifetime costs for falls are

disproportionately high compared to other injury mechanisms (Figure 3) – $26.9 billion or 34% of all medical costs in 2000 [52].
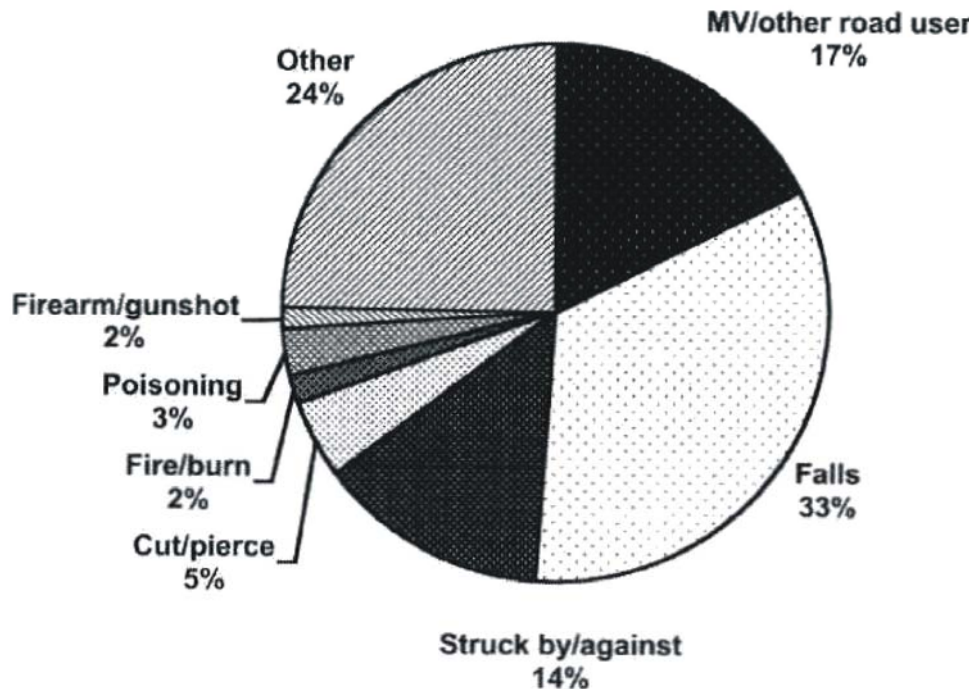
Figure 3: Distribution of total lifetime medical costs by mechanism for 2000 [taken from 52]

1.2   EXPERIMENTAL INVESTIGATIONS

This experimental portion of this research effort utilized laboratory-based, slip-perturbed gait testing to explore two potential biomechanical contributors to the results of unexpected slips. Specifically, a study of pre-slip gait characteristics and an examination of the timing and magnitude of lower extremity responses to slip perturbations were performed.

1.2.1 Pre-Slip Gait Characteristics

Previous experimental efforts demonstrated that slip outcomes can include falls and recoveries, as expected, for larger slips. However, additional outcomes were also observed. These additional outcomes included non-slips (slip distance < 1.0 cm), mini-slips (slip distance < 3 cm), and larger slips with indeterminate outcomes where participants either slipped beyond the contaminated area but did not fall or relied on the safety support harness to an unknown degree to prevent falls. Therefore, a new classification for fall risk was devised based on the motion of the slipping foot. Longer and faster slips were classified as hazardous, implying an increased risk for falls, while shorter and slower slips were classified as non-hazardous. Severity classification using a 1.0 m/s peak slip velocity threshold for hazardous slips allowed all observed outcomes to be included in analyses relating pre-slip gait parameters to slip severity (hazardous or non-hazardous).

The first specific aim of the thesis, with results reported in Chapter 3.0, was to investigate the impact of AGE GROUP and INITIAL CONDITIONS on the SLIP SEVERITY (hazardous or non-hazardous) for induced slips during gait in the laboratory. It was hoped that the results of this study would identify characteristics of gait that determine why individuals experience hazardous slips. If such gait style parameters were found to impact slip risk, these results could be used to a) determine a person's risk for slip-induced falls a priori or to b) reduce a person's risk through training such that they could walk in a safer manner.

Individual differences in gait, due either to personal walking style differences [18, 100] or due to expectations of slips [97, 33] have been reported to impact the magnitude of resulting slips. The pre-slip gait variables analyzed for this study were chosen because of their importance in existing gait and slip literature and because they were believed to be variables that could be changed through appropriate interventions if they were found to be related to slip and fall risks for this study. Sixteen younger adults, aged 20 to 35 years old, and eleven older adults, aged 55 to 70 years old, participated in this study and each participant experienced a single unexpected slip.

The results of the analyses in Chapter 3.0 indicated that slip severity was related to cadence, step length, and the angle that the slipping foot makes with the floor at heel strike. Two logistic regression models are presented in Chapter 3.0 that link these variables to slip severity.

Interestingly, older participants' gait was characterized generally by safer pre-slip gait (shorter step lengths, and shallower foot-floor contact angles) yet they did not appear to benefit from this safer gait: older participants experienced hazardous slips in the lab at about the same rate as younger subjects. This apparent paradox suggests that some other age-related variable, either pre or post-slip, may influence slip severity.

1.2.2 Responses to Slips

In addition to environmental and pre-slip gait effects, slip severity and outcome (falls or recoveries) may also depend on how individuals respond to slips. Thus examining slip responses may further the goal of understanding human factor contributions to slip and fall risks. Additionally, early responses to slips (prior to peak slip velocity) may contribute to slip severity and could explain the why older participants appeared to walk more conservatively *pre-slip* and yet experienced hazardous slips at approximately the same rate as younger participants.

In addition to the effect that slips have on the sliding foot, slips also cause changes to the dynamic posture of the entire body. Thus, responses to slips combine, in a coordinated fashion, passive (i.e., driven by the momentum of body segments), reflexive, and active components of response across many body segments. Although a primary goal of this response must be to arrest the slip [32], stabilizing the body to prevent falls or to resume gait could also be objectives. It has been reported that small slips occur with every step [32, 81]. Clearly, these smaller slips are often not perceived nor do they appear to require active response: passive or reflexive responses correctly compensate for these slips and gait continues naturally. However, responses to larger slips combine these passive and reflexive components with coordinated, multi-segment active components of response. Whether these active responses are purely open-loop, pre-programmed automatic postural responses generated when some slip-severity threshold has been exceeded [66], are more carefully modulated responses using sensory feedback to adjust response magnitude [95], or some combination of these two [3] remains open for debate. Active responses may also involve subject choice related to experience as indicated by differences in response seen after repeated exposures [33, 97] to slips.

Chapter 4.0 focuses on slipping and trailing leg responses to slips. Response biomechanics were characterized through examinations of the timing and magnitudes of knee

and hip joint torques. Based on observations of trailing leg postural responses to laboratory-induced slips, responses were categorized into four strategies, thought to result from either subject choice or from natural postural dynamics. The same older and younger participants for the study described in Chapter 3.0 were analyzed for this study with two additional older and two additional younger subjects. Outcomes of hazardous slips for this study were divided into falls and recoveries based on a hip height criteria. Finally, in addition to using a 1.0 m/s peak slip velocity threshold to identify hazardous slips, peak slip velocity and the time at which the 1.0 m/s threshold was exceeded (related to heel acceleration) for hazardous slips were used as continuous measures of slip severity for hazardous slips.

The specific aim for the second study of this thesis was to investigate the relationships among AGE GROUP, SLIP SEVERITY (both hazardous and non-hazardous AND continuous measures of severity), trailing leg response STRATEGY, lower extremity RESPONSE BIOMECHANICS (timing and magnitude), and OUTCOMES (falls or recoveries) for slip perturbed gait. Understanding how hazardous slip outcomes are related to response biomechanics, response strategy, age, and slip severity could explain the epidemiological finding that older people fall more than younger people and may suggest methods to reduce falls risks, even when hazardous slips do occur.

Although the limited number of unexpected slip trials weakens the strength of any conclusions for this study, continuous severity measures appear to be primarily driven by initial conditions prior to any active response. In addition, the magnitude of hazardous slips (peak slip velocity or heel acceleration) appears to be the most important contributor to fall outcomes. Perhaps because the older study participants were not significantly old and were healthy enough to volunteer for a slip and fall study, age group was not found to be significantly related to response characteristics, strategy, or outcome. Although limited due to the small number of observations, response strategy was not found to be related to outcome, age, or severity for hazardous slips. Slipping leg knee torque was identified as the primary response for ending slips. Slipping leg hip and trailing leg knee and hip responses were not found to be related to ending slips; rather, these torques appear to be related to postural stability, i.e., for positioning the base of support appropriately to arrest COM acceleration or to allow the resumption of normal gait as quickly as possible.

2.0 A WHOLE BODY MODEL USED IN THREE-DIMENSIONAL INVERSE DYNAMICS SIMULATIONS OF HUMAN GAIT

The research conducted at the Human Movement and Balance Laboratory (HMBL) at the University of Pittsburgh requires consistent mathematical characterization of the states of the assumed-to-be-rigid segments that make up the human body (arm, head, pelvis, etc) as well as the body as a whole. This chapter describes the equipment, data collection procedures, and analysis tools used to provide this characterization. The primary equipment used to characterize human movement at HMBL includes two gait-path embedded force plates and a motion capture system. Data from this hardware is collected using a unique software coupling of vendor provided software and a customized LabVIEW based graphical user interface. The marker-based model used to determine subject kinematics, kinetics, and center of mass motion is the most critical component of post-collection motion characterization and will be completely described.

2.1 EQUIPMENT

Individual hardware components of the data acquisition system, schematically illustrated in Figure 4, will be described in the following section. Although illustrated, details concerning the EMG system are described elsewhere.
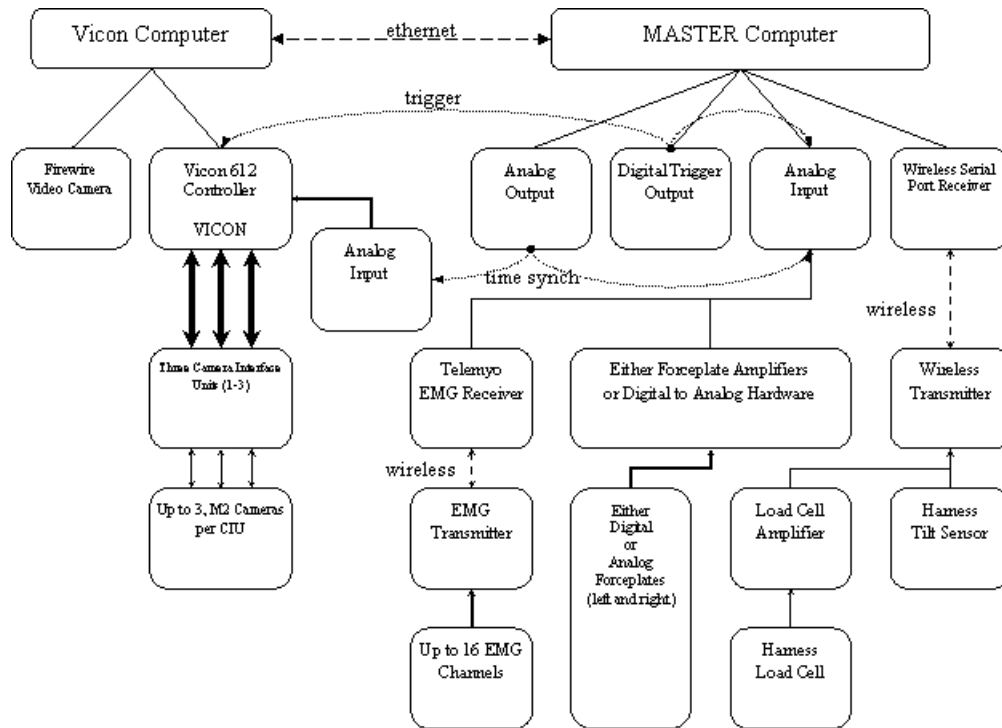
Figure 4: Schematic illustration of HMBL data acquisition hardware

2.1.1 Motion Capture

Motion data was collected using a Vicon 612 (Oxford Metrics, Vicon Peak–UK) motion analysis system. Specifically, eight Vicon M2 cameras were placed around the laboratory (Figure 5) and calibrated to track motion in a volume approximately 4 m (length) x 2.5 m (width) x 2.5 m (height), centered along the gait path. Motion data was sampled at 120 Hz.
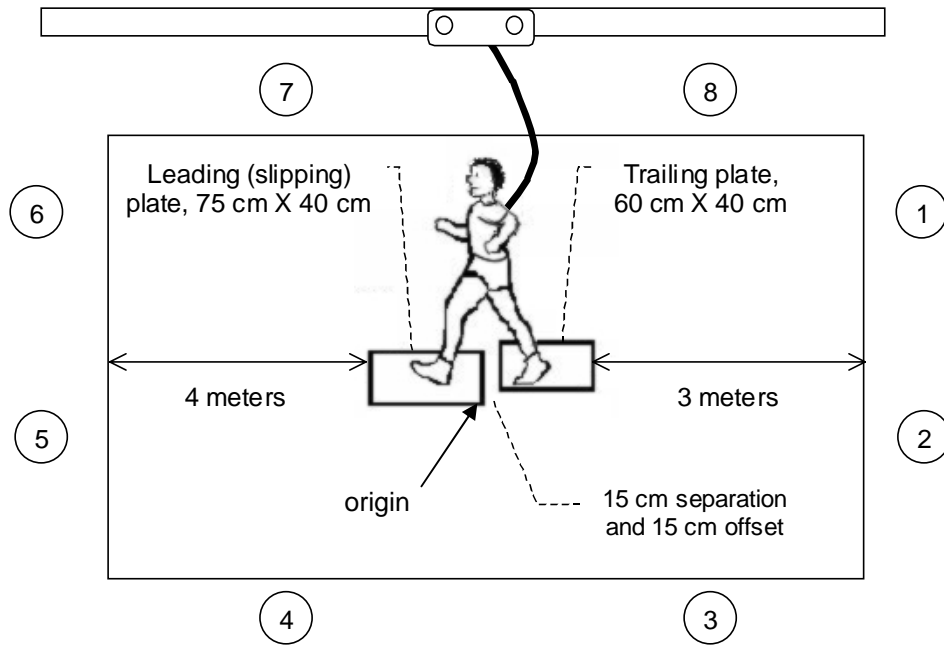
Figure 5: Gait path illustration

All cameras were configured to a medium gain control setting of 5 and were outfitted with 20 mm aspherical lenses set to a 2.8 aperture and a focal length of ∞. Vicon Workstation software was used to further set both the camera sensitivities (between 0.5 and 0.8) and the overall system strobe intensity (between 5 and 8) such that, using Vicon's static clinical L and 240 mm dynamic wand, calibrations resulted in camera residuals of less than 1 (unitless), wand visibility of greater than 75%, and static reproducibility of less than 2%. The origin of the volume was configured to lie at the first, left corner of the leading foot force plate (Figure 5).

2.1.2   Force Plates

As illustrated in Figure 5, the gait path included two embedded force plates (Type 4060) by Bertec (Bertec Corporation) offset such that each plate would receive contact from only one foot per normal gait trial – always the right foot on the first plate and the left foot on the second plate. Two different hardware configurations were used requiring significantly different hardware. The first of these two configurations utilized analog force plates with external amplification and software calibration. These plates were connected to the data acquisition system through Bertec

AM-6 series amplifiers with channel gains set to 20, 20, 10, 20, 20, and 10 (Fx, Fy, Fz, Mx, My, Mz respectively) and with an internal low-pass filter (1000 Hz cutoff frequency). Any DC offsets were removed via the amplifiers' autozero function prior to actual data collection. The second force plate configuration replaced the external analog circuitry with internal calibration and digitization (digital force plates). For compatibility with data acquisition hardware, the digital force plate data was converted back to analog using Bertec's AM-6501 modules. For both configurations, force plate data was acquired at 1080 Hz only after ample warm-up time (at least twenty minutes).

2.1.3   Process Control

A master computer (MASTER) was used to control the data acquisition process using a custom, LabVIEW (National Instruments Corporation) based, graphical user interface and a National Instruments multifunction card (NI PCI-6071E) with 64, 12-bit analog inputs, programmable analog output, and several lines of digital I/O. MASTER was responsible for analog and serial data acquisition and for triggering and synchronizing motion capture with the Vicon 612 controller (VICON) and its related computer running Vicon's Workstation software. Both MASTER and VICON were triggered to begin new acquisitions with the same digital output from MASTER. This signal was wired to VICON's J1 connector and to MASTER's analog input start trigger. Workstation was configured to wait for both start and stop triggers to initiate and terminate trials.
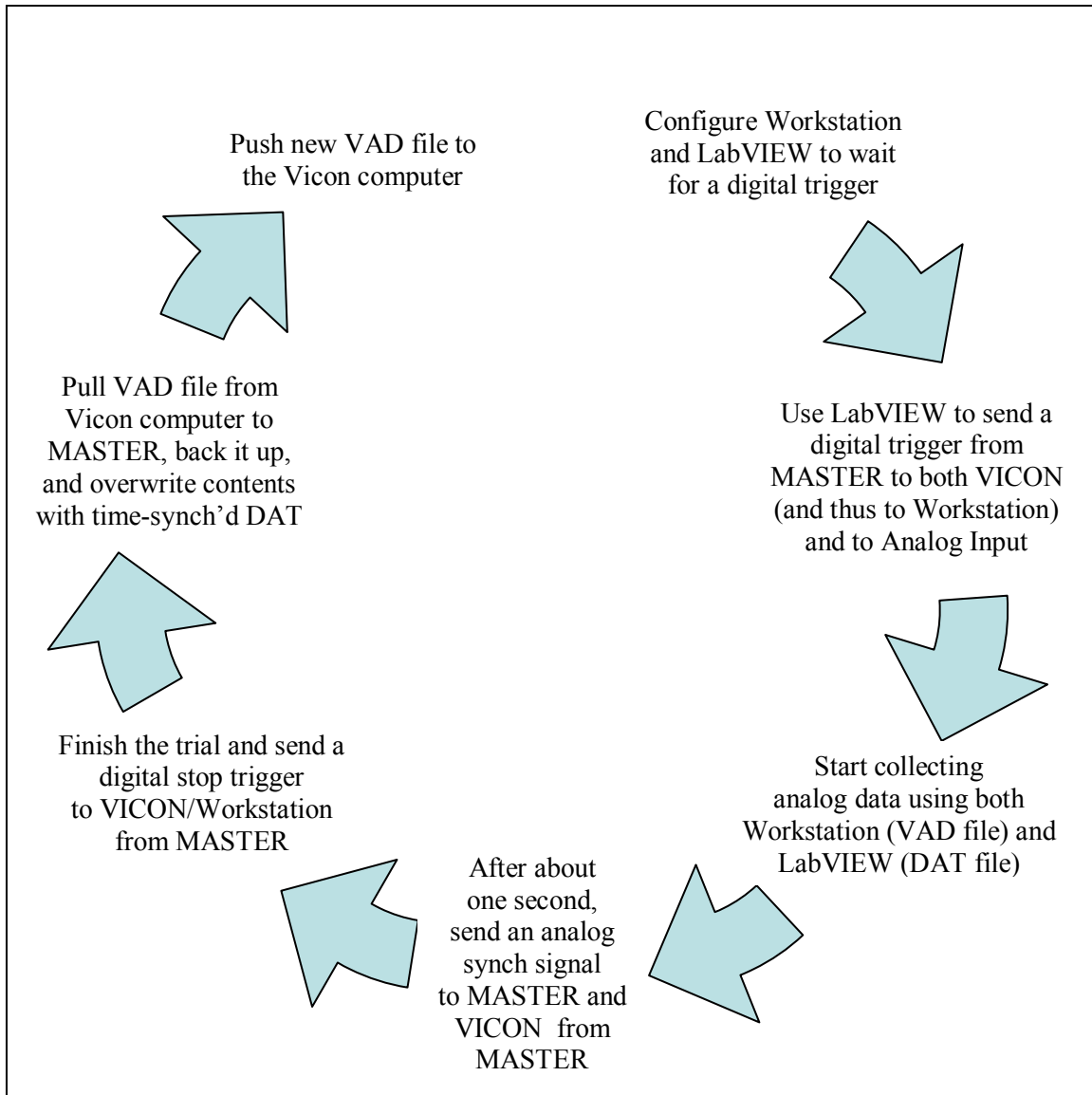
Figure 6: Data acquisition process diagram

As illustrated in Figure 4, both MASTER and VICON collected a single channel of analog data for time synchronization from an analog output from MASTER. This channel was programmed to deliver a step change from zero to five volts, about one second after each new acquisition was triggered, and was later used to align the timestamps from data in the Workstation created analog data file (VAD) and the LabVIEW created analog data file (DAT). MASTER saved both analog and interpolated serial port data (actual serial port rate varied due to wireless hardware limitations but was always equally spaced in time at a slower rate) at 1080 Hz.

VICON's analog input card (64 channel, 16 bit) was configured to sample all channels at 1080 Hz but was only physically wired to the synchronization channel.

Vicon's Workstation software is designed to maintain time synchronicity between its analog data in the VAD file and marker trajectory data stored separately. Therefore, a synchronization channel was simultaneously collected by VICON and MASTER allowing the DAT file to be correctly aligned to the marker trajectories post-collection using the process illustrated in Figure 6. MASTER retrieved the VAD file containing only time synchronization information using an ethernet connection from VICON. The synchronization channel from this file was then aligned with the synchronization channel data in the DAT file from MASTER and the remaining analog channels in the DAT file were then appropriately padded or chopped, potentially both at the beginning and at the end of the data set, to be the same length as, and temporally aligned with, the VAD file whose blank data was then overwritten. This time-synced VAD/DAT hybrid data file was then pushed back to the Vicon computer to replace the original VAD file for future analysis.

2.2   METHODS

2.2.1   Experimental Procedures

Subjects wore tight fitting clothing and PVC soled shoes and were equipped with a safety harness to prevent ground contact injuries resulting from losses of balance. The total body mass, shoe size, and height of each subject were recorded prior to testing. Subjects were instructed to walk at a self-selected, purposeful pace while focusing on a target at eye-height on the far wall.

2.2.2   Marker Set

Seventy-nine reflective markers were placed on each subject at locations corresponding to various palpable anatomical locations (see Table 5 and Table 18). Of this total, twenty-two, 9.5 mm diameter markers were placed on the feet and sixty-one, 14mm diameter markers were

placed on the rest of the body. Nineteen of the reflective markers, referred to as "static markers", were present only during static posture "calibration" trials, which were collected at the beginning of each testing session (Table 18). The calibration trial relative location of static markers to other, same-segment markers were later used to approximate static marker locations for dynamic trials. Rigid plates with multiple affixed markers were attached to the subjects' arm segments (upper and lower) and thigh segments. Both the upper arm plates and the thigh plates utilized four markers per plate while the forearm plates had three markers each. The markers on these plates were often used to relocate static markers from the same segment for dynamic trials.
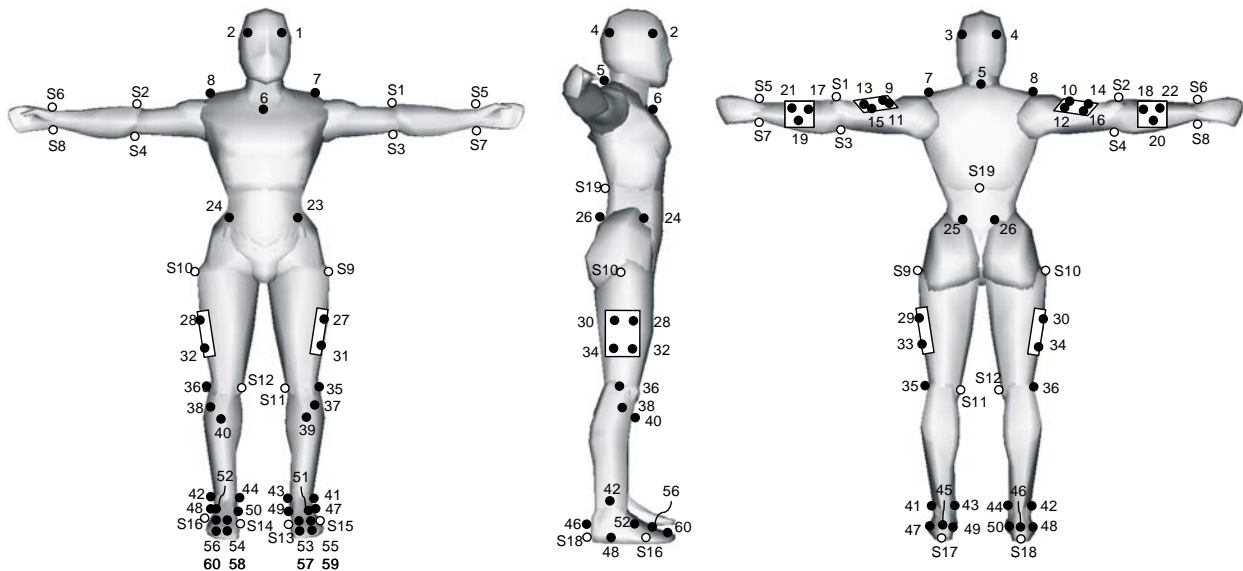
Figure 7: Dynamic and static reflective markers – static posture illustrated

In Figure 7, solid circles represent markers present for both static and dynamic trials while hollow circles illustrate markers present only for static trials. Table 5 and Table 18 label and describe these numbered markers.

Marker positions were tracked via a Vicon 512 motion tracking system and were reconstructed from individual camera data to full three dimensional trajectories automatically by Vicon's Workstation software using reconstruction parameters typified by those illustrated in Figure 8. The typical parameters illustrated in Figure 8 were not used for every trial; rather, these parameters were customized to achieve useful trajectories for each trial. Even with

15

reconstruction parameter customization, complete marker trajectories for every marker were not always available due to marker occlusions. When sections of marker data were missing, the missing sections were either:

- replaced using Workstation's "Copy Pattern" function. Trajectory information from another marker on the same rigid body was used to fill in the gap in a meaningful way.

- replaced using Workstation's "Fill Gaps" function which used cubic splines to complete missing sections based on the shape of the trajectory before and after the gap. When this option was chosen, the maximum gap size that was filled was seven frames and the trajectory information before and after the gap was inspected to remove spurious endpoints.

- replaced using a post-processing macro, REPLACE4 (see Appendix D) which used the average marker location relative to three other markers on the same rigid body to replace the marker when missing.

- or, when a marker was accidentally absent for an entire dynamic trial, by treating it in the same manner as a static marker, i.e., by using its relative location to other markers on the same rigid body from a static trial to form its dynamic trial trajectory.
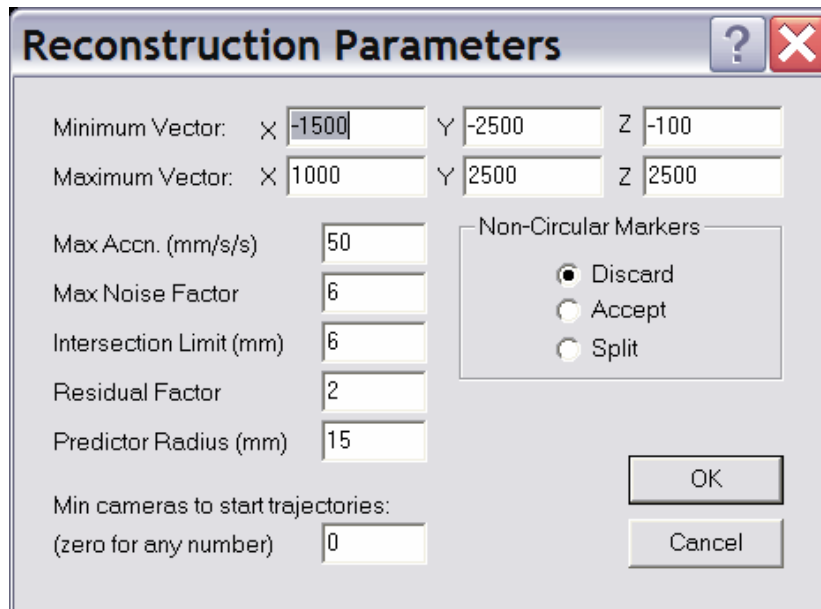
Figure 8: Workstation reconstruction parameters used to combine camera data to three dimensional marker trajectories

16

2.2.3 Modeling

A whole body model comprised of 15 segments was developed for analysis using Vicon's BodyBuilder software. This model included toe, heel, shank, thigh, upper arm, and forearm segments for the right and left sides of the body, as well as pelvis, torso and head segments. No assumptions concerning the rotational degrees of freedom for the joints between the rigid bodies were made; i.e., all joints were capable of three rotational degrees of freedom.

"Static" markers (Table 18) were removed from locations that were susceptible to errors due to skin/clothing movement or due to obstructions from the safety harness or body movements. The three-dimensional relationships between markers belonging to rigid segments were obtained from static calibration trials and then used in subsequent dynamic gait trials to mathematically recreate the static marker trajectories (and any other marker that may have been obstructed during walking). Although the forearm segments had only three markers each for dynamic trials, all other segments were tracked using at least four markers during the dynamic trials allowing any one marker to be mathematically determined based on its relative location to at least three other, same segment markers. This redundancy was extremely valuable for markers on the lower extremities which were often difficult to track for an entire trial due to occlusions.

Figure 7 and Figure 9 to Figure 17 illustrate marker placements (both static and dynamic markers), mathematically determined virtual trajectories for segment origins and centers-of-mass, and local coordinate system definitions for each segment. Solid circles (black for foreground, gray for background markers) represent markers present for both static and dynamic trials (Table 5). Hollow circles illustrate the placement of static markers (Table 18). Hollow diamonds represent calculated trajectories (Table 19). The center of mass of each segment is illustrated as a hollow circle with an X while whole body center of mass is illustrated by a solid circle with an X). Local coordinate systems (origins and axes) for each segment were defined using markers on that segment and were based on segment definitions as reported by de Leva [47] whenever possible. Reasonable effort was also extended to align local coordinate systems with ISB recommendations for the pelvis, thigh, shank, and feet segments [142]. However, modifications to these segment definitions were made as required and are described in the following segment specific sections.

2.2.3.1 Pelvis Segment
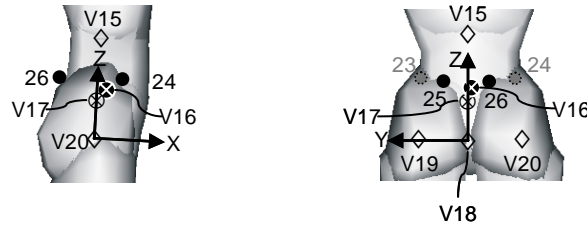
Figure 9: Pelvis segment – right side and rear views

A temporary pelvis segment was used to locate the hip joint centers (HJCs) based on a coordinate system from Leardini et al. [82]. This temporary segment was defined with its origin at the midpoint of the anterior superior iliac spine (ASIS) markers. The first axis (Y) defined for this segment pointed from the right ASIS to the left ASIS marker. A temporary vector (*temp*) defined the plane containing the ASIS markers and the midpoint between the two posterior superior iliac spine (PSIS) markers. The vector orthogonal to the first axis and to *temp* was used as the second axis (X) with positive roughly anterior in static posture. The third axis (Z) was then orthogonal to the other two with positive roughly superior in static posture.

This segment definition was used to locate the HJCs using regression equations with the Z, Y, and X axes corresponding to the -X, -Z, and Y axes from Leardini's original regression equations [82]. The modified form of these regression equations were used to determine HJC locations relative to the midpoint of the two ASIS markers.

```
Right HJCx = -0.096 * L          Left HJCx = -0.096 * L
Right HJCy = 0.09 * PW - 111     Left HJCy = -0.09 * PW + 111
Right HJCz = -0.31 * PD          Left HJCz = -0.31 * PD
```

Pelvic width (PW), pelvic depth (PD), and the distance from the same-side ASIS to maleoli (L) used in the regression equations were determined using static trial average marker locations for the ASIS, PSIS, and medial maleoli markers: the distance between the right and left ASIS markers for PW, the distance from the mid point between the ASIS markers to the mid point between the PSIS markers for PD, and the distance between the ASIS and same side medial maleolus for L.

Once the hip centers had been located, the origin for the pelvis segment was shifted to the mid-point of the HJCs (mid-HJC) (the axes definitions remained the same) to define the segment used for kinematic and kinetic analysis.

The attachment point between the torso segment and the pelvic segment (torso-attach), which for de Leva [47] was placed at the same height as the navel for static posture, was assumed be at the same height (global Z location) as the static posture 10th thoracic vertebra (T10) marker for this model because navel height was unavailable from existing markers. Assuming that the attachment point between the two segments was on the pelvis Z axis determined the X and Y coordinates of the attachment point (torso-attach). The location of this attachment point relative to the pelvis LCS was then used to place it for dynamic trials. Pelvis segment length was measured from mid-HJC to torso-attach. The pelvis segment's center of mass (COM) location, mass, and radii of gyration were determined from de Leva [47] using total body mass and segment length (see Table 3).

2.2.3.2 Torso Segment
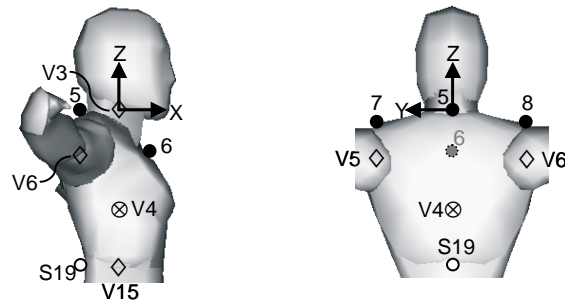
Figure 10: Torso segment – right side and rear views

The origin of the torso for static posture was positioned using the average global X and Y coordinates of the mid-point between the 7th cervical vertebra (C7) and Sternum markers while the Z coordinate was set to static posture C7 height (global Z coordinate). The relative location of this origin to other markers on the torso of static posture was then used to determine its position for dynamic trials. Torso length was defined as the difference between the origin and torso-attach (see Pelvis definition for a description of this point) – this line also defined the Z axis of the torso with positive pointing in the direction of torso-attach to origin. A temporary

vector, *temp*, defined the plane containing the torso-attach point and the two acromium markers. A vector orthogonal to the first axis and to *temp* was used as the second (Y) axis (roughly pointing to the subject's left in static posture). The third axis (X) was orthogonal to the other two axes roughly pointing anteriorly in static posture.

The torso segment's center of mass (COM) location, total mass, and radii of gyration were determined by combining parameters from two torso segments (UPT using alternative endpoints and MPT) as defined in de Leva [47] using each subject's total body mass and the torso length as previously described (see Table 3). The COM estimate (for the combined segment) along the long axis of the torso was found by combining the two segments' mass locations (from de Leva [47]) relative to a common origin using a weighted average technique.

$$\textbf{COM}_{\textbf{new}} = (\textbf{COM}_{\textbf{1}} * m_1 + \textbf{COM}_{\textbf{2}} * m_2) / (m_1 + m_2)$$

Where $\textbf{COM}_{\textbf{1,2}}$ were vectors to the individual segment centers of mass (UPT and MPT respectively) as measured from the origin and $m_{\textbf{1,2}}$ were the two segment masses from de Leva [47]. Because the two COM points and the origin were all located along the same Z axis, the **COM** vectors were reduced to scalars for that axis and the other two elements were set to zero.

The torso's radii of gyration were determined using the parallel axis theory to combine the contributions of the two sub-segments (from de Leva [47]) to the moments of inertia about the new center of mass location.

$$\textbf{R}_{new} = \sqrt{\frac{\left(\textbf{R}_1^2 + \textbf{d}_1^2\right) * m_1 + \left(\textbf{R}_2^2 + \textbf{d}_2^2\right) * m_2}{m_1 + m_2}}$$

where $\textbf{R}_{\textbf{new}}$ and $\textbf{R}_{\textbf{1,2}}$ contain three quantities representing the principal radii of gyration for the combined segment and the UPT and the MPT segments respectively and $\textbf{d}_{\textbf{1,2}}$ are the vectors from the COMs of de Leva's two torso segments to the new combined COM. For the mid and upper torso, it was assumed that the long axes of the two segments were co-linear and the other two axes were parallel from segment–to-segment. Thus each **d** had two non-zero components, the distance from the sub-segment COM to the combined COM for the Y and Z axes. The new moments if inertia, $\textbf{I}_{\textbf{new}}$, were then found using:

$$\mathbf{I}_{new} = \mathbf{R}_{new}^{2} * \left(m_1 + m_2\right) = \left(\mathbf{R_1}^{2} + \mathbf{d}_1^{2}\right) * m_1 + \left(\mathbf{R_2}^{2} + \mathbf{d}_2^{2}\right) * m_2$$

To correctly report angle signs for shoulder rotations (issues resulting from axes definition differences between the torso and the upper arms), the local coordinate system for the torso was modified for shoulder rotations determination such that the modified LCS used the original LCS but rotated 180 degrees about the original Z axis, resulting in the Y axis directed to the subject's right and the X axis directed posteriorly.

2.2.3.3 Head
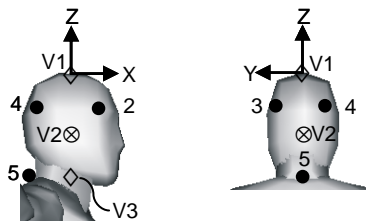
Figure 11: Head segment – right side and rear views

The origin of the head segment was initially placed at the average of the head's anterior and posterior, medial and lateral markers (4 total). The height to the top of the head was then located relative to the height of this origin using static trial data and measured subject heights. Head length was determined using measured subject heights and the average height (global Z location) of the C7 marker for static trials. A roughly vertical vector was established as orthogonal to both (1) a vector defining the plane of the C7 marker and the two posterior head markers (roughly pointing anteriorly for static posture) and (2) the vector pointing from the right side of the head to the left side of the head using the two anterior markers. This vertical vector was then used to locate the top of the head relative to the initial head origin for dynamic trials. The head segment was then redefined with the top of the head as its origin. The local coordinate system for the head included Y from right to left, Z (as previously discussed) roughly vertical with positive pointing superiorly for static postures, and X orthogonal to the other two, roughly pointing anteriorly for static posture. Head mass, COM location, and radii of gyration were determined using total body mass and head length (distance from origin to the top of the head) in conjunction with relationships reported by de Leva [47] (see Table 3).

2.2.3.4 Upper Arms
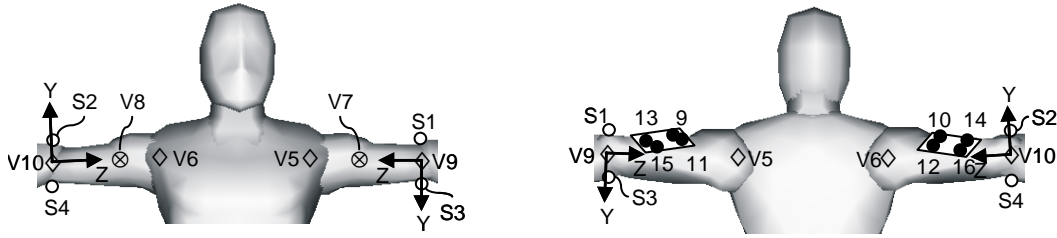
Figure 12: Upper arm segments – front and rear views

The segment definitions for the upper arms follow those proposed by Roux et al. [118] with subtle modification to better fit BodyBuilder segment definition requirements and the rest of the model's axes choices. De Leva [47] cites several anthropometric references for shoulder joint center (SJC) location and suggests locating the SJC at 33.7 mm (female) and 34.5 mm (male) down from the acromia following the torso's long axis (NB, the height from the acromia to the middle of our reflective markers was also included to account for marker height). The origins for the upper arm segments were placed at the elbow joint centers (EJC), which were estimated to lie midway between the medial and lateral static elbow trajectories. Upper arm lengths were then found using the distance from the EJC to the SJC from static posture.

The first axis (Z) defined for the upper arm local coordinate system was the vector from the EJC to the SJC. A reference vector was defined using the elbow markers: for the right arm from the medial to the lateral elbow marker and for the left arm from the lateral to the medial elbow marker. The second axis (X) was then the vector orthogonal to the first axis and the reference vector with positive generally inferior and posterior for static posture. The last axis (Y) was orthogonal to the other two axes to approximate the flexion axis for the elbow joint (positive for flexion rotations). The mass, COM locations, and radii of gyration for the upper arm segments were found using the de Leva [47] estimates based on segment length and total subject mass (see Table 3).

2.2.3.5 Lower Arms and Hands
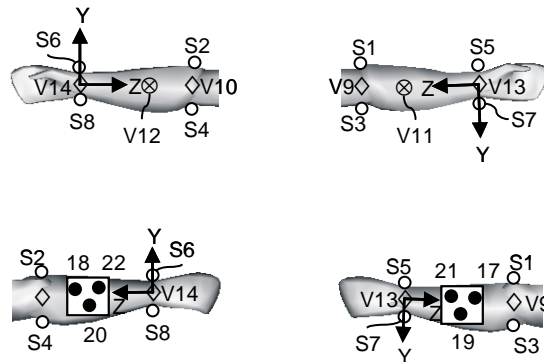
Figure 13: Lower arm segments – front and rear views

The origin for a combined forearm and hand segment was located at the wrist joint center (WJC) which was assumed to lie midway between the medial and lateral wrist markers. The long axis (Z) of the segment pointed from the WJC to the EJC. The second axis (X) was defined to be orthogonal to the first axis and to a line containing the markers on the medial and lateral sides of the wrist with positive pointing away from the palm side of the hand. The third axis (Y) was orthogonal to the other two axes with positive roughly from pinky side to thumb side for the right arm and opposite for the left arm. The mass and COM locations of the lower arm segments were found using the de Leva [47] estimates but an estimate for the mass of the hand was added to the lower arm segment definition as well. The COM location for this combined segment (hand and forearm) required estimates of the length of the hand and of the distance to the COM of the hand but this was complicated by a lack of markers on the hand. De Leva's [47] measurements of hand length relative to total body height were used to estimate both hand length and hand COM location for our subjects assuming a fused wrist joint oriented such that the hand's long axis extended in the same direction as the long axis of the lower arm. Combined hand and lower arm masses, COM locations, and radii of gyration were then found following the same procedure as previously described for the combined upper and lower torso segments (see Table 3).

2.2.3.6 Thighs
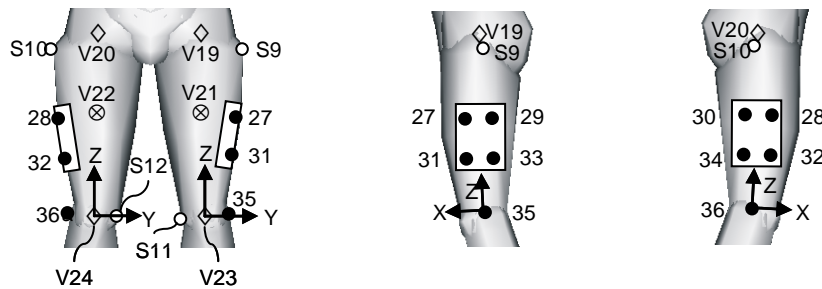
Figure 14: Thigh segments – front, left side and right side views

Thigh segment definitions were fairly straight-forward with the origin for the segment located at the knee joint center (KJC) which was assumed to lie at the midpoint between the lateral and medial femoral epicondyles trajectories. The first axis (X) was defined as the vector describing the plane containing the femoral epicondyles and the HJC with positive roughly anterior for static posture. A second axis (Y) was orthogonal to the first axis and to a vector pointing from the KJC to the HJC with positive generally pointed to a subject's left side. The third axis (Z) was orthogonal to the other two and was roughly the long axis of the segment pointing from the KJC to the HJC. Thigh length was also defined as the distance from the KJC to the HJC and was used with subject mass to determine segment COM locations, masses, and radii of gyration based again on de Leva [47] (see Table 3).

2.2.3.7 Shanks
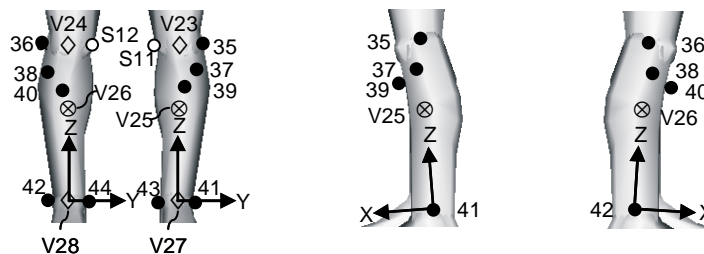
Figure 15: Shank segments – front, left side and right side views

24

Like the thighs, segment definitions for the shank segments were fairly straight-forward. The origins for the shank segments were placed at the ankle joint centers (AJC) which were assumed to lie at the midpoint between the lateral and medial maleoli trajectories. The first shank axis (X) was defined as the vector describing the plane containing the maleoli and the KJC with positive roughly anterior for static posture. The second axis (Y) was orthogonal to the first axis and to the vector pointing from the AJC to the KJC with positive roughly to a subject's left side for static posture. The third axis (Z) was orthogonal to the other two and was roughly the long axis of the shank pointing from AJC to KJC. Shank length was also defined as the distance from the AJC to the KJC and was used with subject mass to determine segment COM locations, masses, and radii of gyration based on relationships from de Leva [47].

Rotations at the ankle were determined using a modified shank segment such that dorsi-flexion at the ankle was positive and so that the flexion rotation for static posture was approximately zero. This modified LCS was based on the previously described LCS but with the X and Z axes switched and the Y axis changed to point to the subject's right rather than left. In other words, the temporary shank LCS was well aligned with the foot LCS which is defined in the next section.

2.2.3.8 Feet A massless toe segment was attached to a lumped mass heel and shoe segment to define the feet. Thus the mass, center of mass location, and radii of gyration for the feet were obtained by combining the contributions from the entire foot and the shoe and applying them to the heel segment only (appropriate assumption for swing phase and foot flat). A massless toe segment, split from the heel segment at approximately the metatarsal-phalangeal (MP) joint, was included for improved lower limb kinematics and kinetics near toe-off. This toe segment definition renders meaningless any loads at the MP joint which could be estimated via inverse dynamics. Limitations related to the connection of multiple segments with mass (heel and toe) to ground reaction forces for inverse dynamics calculations required that the toe segment have no mass. Because postural changes at the MP joint are minimal during heel-strike, foot-flat and flight phases of gait and because the moment of inertia and mass for the toe segment are small, lumping this mass into the heel segment introduced acceptably small errors to the inverse dynamics calculations.

Heel Segments
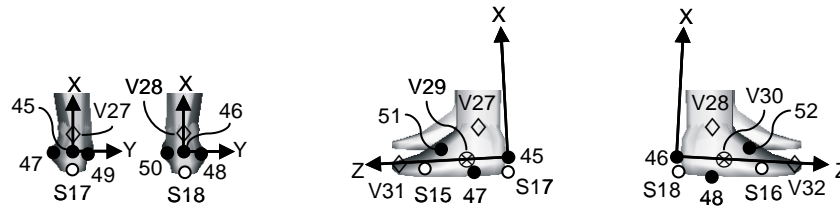
Figure 16: Heel segments – rear, left side and right side views

In Figure 16, markers V31 and V32 were located based on the static posture location of a point midway between the two toe markers. Although V31 and V32 were related to markers on the toe segment from static trials, for dynamic trials, these markers were mathematically relocated based on dynamic markers from the heel segments.

The heel segment was defined using a marker placed near the calcaneous as the origin. The first axis (X) was orthogonal to the plane containing the origin and markers placed near the fifth and first metatarsal heads with positive roughly up for static posture. The second axis (Y) was orthogonal to the first axis and to the vector from the origin to the midpoint between the most distal medial and lateral markers on the shoe's toe section (mid-toe) *from static trials* with positive to the subject's right. The third axis (Z) was orthogonal to the other two axes with positive roughly from the origin to mid-toe and was assumed to lie in the same direction as a vector pointing from the origin to the second metatarsal head to agree with Zatsiorsky [144] which referenced Cappozzo et al. [27]. For the heel segment, the center of mass location, segment mass as a percentage of total body mass, and the radii of gyration were calculated, *for the whole foot*, using relationships reported in de Leva [47] with the length of the foot measured from the marker placed on calcaneous (accounting for marker diameter) to mid-toe which, for dynamic trials, was located *relative to other heel segment markers* using its static trial location.

The rotations of the foot with respect to global were determined by defining a temporary foot LCS which was better aligned with the global LCS. This temporary foot LCS was based on the previously described foot LCS but with the Z and X axes swapped and the Y axis to the subject's left. Thus, for static posture Z was directed vertically up and X was directed anteriorly for this temporary foot LCS.

The mass of the foot was adjusted to include the mass of the shoe which was found from shoe size using:

```
ShoeMass = (ShoeSize * 0.0425 + 0.5375) / 2
```

where ShoeSize was the U.S. shoe size (from 7 to 13) and ShoeMass was in Kg. This equation was derived by massing out two shoes plus twenty-two markers for four different size shoes and finding the line of best fit ($r^2 = 0.9797$). The contribution of the shoes to the center of mass and moments of inertia was approximated by modeling the shoe as an elliptical plate attached to the bottom of the foot, in essence, assuming that the thin material of the upper part of the shoes did not contribute to the mass or moments of inertia.

The sole was modeled as an elliptical plate of the same length as the foot (Ln) with a maximum width of 90 mm and a constant thickness of 20 mm. The moment of inertia of this sole plate about its center of mass was thus:

$$Ix = 1/2 * Ms * (Ln^2 / 4 + 45^2)$$
$$Iy = 1/6 * Ms * (3 * Ln^2 / 4 + 4 * 20^2)$$
$$Iz = 1/6 * Ms * (3 * 45^2 + 4 * 20^2)$$

These moments of inertia were then combined with the moments of inertia of the foot to find the combined moments of inertia at the combined COM using the same approach as previously described for combining the upper and mid torso segments into a single torso segment.

Toe Segments
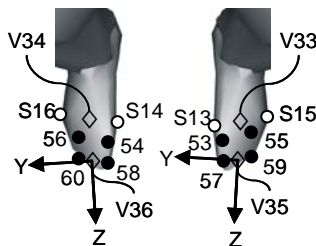
Figure 17: Toe segments – top down view

In Figure 17, markers V35 and V36 were located between the two most distal toe markers for both static and dynamic trials. The massless toe segment was connected to the heel segment at the MP joint, which was located midway between markers on the medial side of the first metatarsal and the lateral side of the fifth metatarsal. This additional toe segment remained in contact with the floor during toe-off which aided BodyBuilder's automatic connection of force plate data to the feet for inverse dynamic calculations and resulted in better foot-to-floor and ankle angles.

The origin of the toe segment was located at the MP joint center. The first axis (X) was the vector defining the plane of a new mid-toe marker, which was located at the mid-point between the two most distal toe trajectories for both static and dynamic trials, and the two metatarsal markers with positive generally up from horizontal for static posture. The second axis (Y) was orthogonal to the first axis and to the line from the origin to the new mid-toe trajectory with positive to the subject's right such that dorsi-flexion about that axis would be positive. The third axis (Z) was orthogonal to the other two axes with positive roughly along the long axis of the toe segment from the origin to the new mid-toe trajectory.

2.2.3.9 Segment Definition Summary
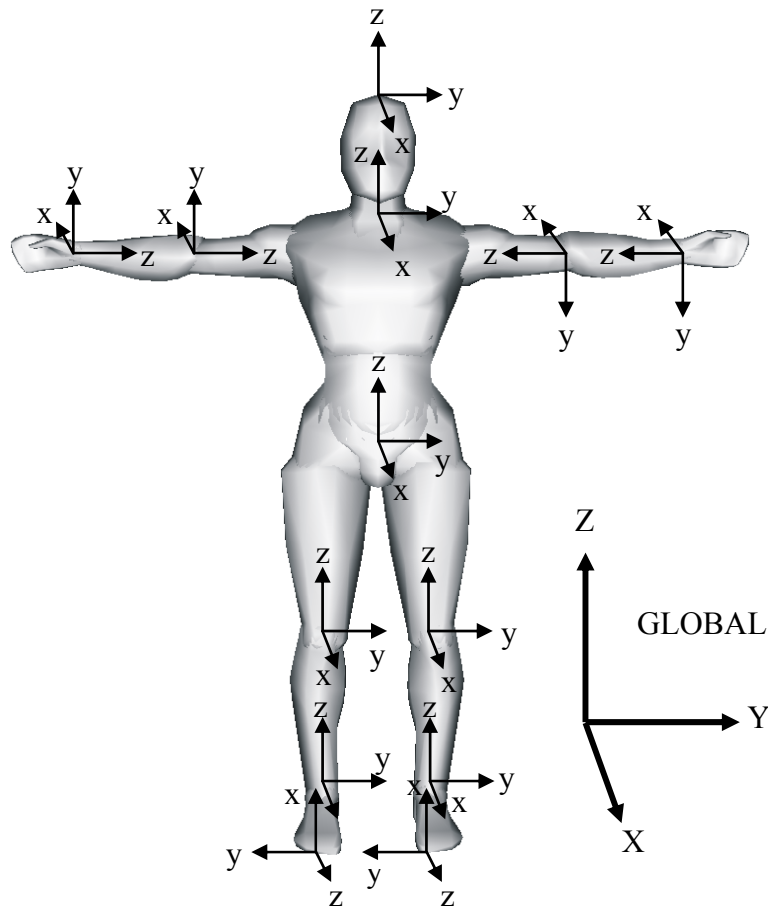
Figure 18: Whole body model summary with local coordinate systems illustrated at segment origins

Table 1 reiterates segment definitions, described in the preceding text sections and illustrated in Figure 18. In Figure 18, heel segments are not illustrated; however, their local coordinate systems, with origins at the calcanei, are similar to the toe segment LCSs. The vectors and points listed in Table 1 correspond to those used to follow the Vicon BodyBuilder convention for segment definitions. Specifically, the second axis is determined by crossing the reference line onto the first axis and the third axis determined by crossing the first axis onto the second axis with a token determining axis labels. (T)rajectory labels include prepended (V) for Virtual (calculated) trajectories, (S) for markers reproduced from static trials, and (L or R) for Left or Right. See Appendix B and Table 5, Table 18, and Table 19 for additional information about specific trajectory labels. A modified torso segment definition was used for shoulder JCS

rotations, modified shank segments were used for ankle JCS rotations, and modified heel segments were used for Euler rotations of the feet relative to the global coordinate system. Note, the token illustrated in Table 1 is not related to Euler angle rotation tokens described later.

Table 1: Segment Definition Summary

Segment	Origin	First Axis	Reference Line	Plane Explanation	Token
Head	TV_Head_Origin	TR_ANT_Head to TL_ANT_Head	Plane 4 to {0:0:0}	(T_C7 to TR_POS_Head) CROSS (T_C7 to TL_POS_Head)	yzx
Torso	TV_Torso_Origin	TV_Torso_Attach to TV_Torso_Origin	Plane 3 to {0:0:0}	(TL_Acr to TR_Acr) CROSS (TL_Acr to TV_Torso_Attach)	zyx
Modified Torso	TV_Torso_Origin	TV_Torso_Attach to TV_Torso_Origin	{0:0:0} to Plane 3	(TL_Acr to TR_Acr) CROSS (TL_Acr to TV_Torso_Attach)	zyx
Right Upper Arm	TVR_EJC	TVR_EJC to TVR_SJC	TSR_LAT_Elb to TSR_MED_Elb	NA	zxy
Right Forearm & Hand	TVR_WJC	TVR_WJC to TVR_EJC	TSR_LATDIS_Radius to TSR_MEDDIS_Radius	NA	zxy
Left Upper Arm	TVL_EJC	TVL_EJC to TVL_SJC	TSL_MED_Elb to TSL_LAT_Elb	NA	zxy
Left Forearm & Hand	TVL_WJC	TVL_WJC to TVL_EJC	TSL_LATDIS_Radius to TSL_MEDDIS_Radius	NA	zxy
Pelvis	TV_MIDH	TR_ASIS to TL_ASIS	{0:0:0} to Plane 1	(TR_ASIS to TL_ASIS) CROSS (TR_ASIS to MID_PSIS)	yxz
Right Thigh	TVR_KJC	{0:0:0} to Plane 5	TVR_KJC to TVR_HJC	(TVR_HJC to TR_LAT_EpiC) CROSS (TVR_HJC to TR_MED_EpiC)	xyz
Right Shank	TVR_AJC	{0:0:0} to Plane 7	TVR_AJC to TVR_KJC	(TVR_KJC to TR_LAT_Mal) CROSS (TVR_KJC to TR_MED_Mal)	xyz
Modified Right Shank	TVR_AJC	{0:0:0} to Plane 7	TVR_KJC to TVR_AJC	(TVR_KJC to TR_LAT_Mal) CROSS (TVR_KJC to TR_MED_Mal)	zyx
Right Heel	TR_SUPPOS_Heel	{0:0:0} to Plane 9	TR_SUPPOS_Heel to TVR_FF_Origin	(Origin to TSR_LATPRX_Met5) CROSS (Origin to TSR_MEDPRX_Met1)	xyz
Modified Right Heel	TR_SUPPOS_Heel	{0:0:0} to Plane 9	TVR_FF_Origin to TR_SUPPOS_Heel	(Origin to TSR_LATPRX_Met5) CROSS (Origin to TSR_MEDPRX_Met1)	zyx
Right Toe	TVR_Toe	{0:0:0} to Plane 11	TVR_MPJC to TVR_Toe	(TVR_Toe to TSR_MEDPRX_Met1) CROSS (TVR_Toe to TSR_LATPRX_Met5)	xyz
Left Thigh	TVL_KJC	{0:0:0} to Plane 6	TVL_KJC to TVL_HJC	(TVL_HJC to TSL_MED_EpiC) CROSS (TVL_HJC to TSL_LAT_EpiC)	xyz
Left Shank	TVL_AJC	{0:0:0} to Plane 8	TVL_AJC to TVL_KJC	(TVL_KJC to TL_MED_Mal) CROSS (TVL_KJC to TL_LAT_Mal)	xyz
Modified Left Shank	TVL_AJC	{0:0:0} to Plane 8	TVL_KJC to TVL_AJC	(TVL_KJC to TL_MED_Mal) CROSS (TVL_KJC to TL_LAT_Mal)	zyx
Left Heel	TL_SUPPOS_Heel	{0:0:0} to Plane 10	TL_SUPPOS_Heel to TVL_FF_Origin	(Origin to TSL_MEDPRX_Met1) CROSS (Origin to TSL_LATPRX_Met5)	xyz
Modified Left Heel	TL_SUPPOS_Heel	{0:0:0} to Plane 10	TVL_FF_Origin to TL_SUPPOS_Heel	(Origin to TSL_MEDPRX_Met1) CROSS (Origin to TSL_LATPRX_Met5)	zyx
Left Toe	TVL_Toe	{0:0:0} to Plane 12	TVL_MPJC to TVL_Toe	(TVL_Toe to TSL_LATPRX_Met5) CROSS (TVL_Toe to TSL_MEDPRX_Met1)	xyz

30

2.2.4 Processing

The kinematic, kinetic, center of mass, and temporal event identification processing details are presented in the following sections. These analysis components were automated through a Vicon BodyBuilder model and additional MATLAB (The Mathworks, Inc) code.

2.2.4.1 Kinematics The standard Vicon BodyBuilder convention for fixed (rotations about the fixed axes of the parent) Euler angle determination is:

```
E_Angles = <Child Segment, Parent Segment, token>
```

This convention was used for rotations of the feet (modified LCS), pelvis, torso, and head with respect to global using a token of ZXY (see Figure 18 for global LCS illustration).

```
E_Angles = <Child Segment, Global, zxy>
```

This equation resulted in angles about the Z, X, and Y axes respectively.

For segment-to-segment rotations at major joints, a floating convention was chosen based on the algorithm of Cole et al. [41, 59] resulting in Cardan/Joint Coordinate System (JCS) angles. For these rotations, the parent's flexion axis was used for the first rotation and the child's long axis was chosen for the last rotation with the second rotation about an axis orthogonal to the other two. Vicon BodyBuilder implements this convention by simply inverting the sign of rotations of the parent with respect to the child using an opposite token.

```
J_Angles = -<Parent Segment, Child Segment, zxy>
```

Rotation magnitudes were determined based on the orientation of the LCSs between the parent and child segments; therefore, zero rotations do not necessarily occur during static posture where near-constant rotations may be observed about the axes of certain joints (e.g., the

abduction axis of the elbow). Typical rotations from a static posture trial are listed in Table 4 for comparison to the dynamic rotations observed from the same subject as illustrated in Appendix A.

2.2.4.2 Kinetics Gender specific segmental mass (as a percentage of total body mass), center of mass locations, and radii of gyration were adapted from de Leva [47] using link lengths as determined from markers placed at anatomical landmarks as previously described and summarized in Table 3.

Table 2: Segment hierarchy and connectivity for kinetic analyses and link length determination

Segment	Parent Segment	Origin	Attachment Point
Head	Torso	TV_Head_Top	TV_Torso_Origin
Torso	Pelvis	TV_Torso_Origin	TV_Torso_Attach
Right Upper Arm	Torso	TVR_EJC	TVR_SJC
Right Fore Arm	Torso	TVR_WJC	TVR_EJC
Left Upper Arm	Right Upper Arm	TVL_EJC	TVL_SJC
Left Fore Arm	Left Upper Arm	TVL_WJC	TVL_EJC
Pelvis	This is the root segment	TVL_MIDH	–
Right Thigh	Pelvis	TVR_KJC	TVR_HJC
Right Shank	Right Thigh	TVR_AJC	TVR_KJC
Right Heel	Right Shank	TR_SUPPOS_Heel	TVR_AJC
Right Toe	Right Heel	TVR_Toe	TVR_MPJC
Left Thigh	Pelvis	TVL_KJC	TVL_HJC
Left Shank	Left Thigh	TVL_AJC	TVL_KJC
Left Heel	Left Shank	TL_SUPPOS_Heel	TVL_AJC
Left Toe	Left Heel	TVL_Toe	TVL_MPJC

Using the postural chain illustrated in Table 2, the BodyBuilder inverse dynamics algorithm [134] was utilized to determine torques and forces at the lower extremity joints by working up from the ground reaction forces as measured by the two Bertec force plates. Upper body kinetic variables were also determined by working distally to proximally toward the pelvis root segment. Specifically, Bodybuilder's REACTION function was used to calculate the forces and moments on a segment's proximal end by accounting for inertial loading, loads from segments lower in the chain, and external forces including gravity. Joint moments have been

reported in the coordinate system of the more proximal segment and have been normalized to body mass.

The attachment of ground reaction forces to the model is a critical factor influencing Bodybuilder's inverse dynamic algorithm. Automatic connection between a force plate and a segment is assumed using distance (perpendicular distance from surface to origin or attachment must be less than the threshold), force (normal force must exceed the force threshold), and velocity thresholds (the model used to produce the included plots used:

```
ForceThreshold = 2 (Newtons),
DistanceThreshold = 80 (mm), and
VelocityThreshold = 4000 (mm /s)
```

However, because there were two segments per foot (Heel and Toe) in this model, either of which could have been within the force, distance, and velocity threshold limits during foot-flat, it remained unclear to which segment the ground reaction forces would be applied. Therefore, since the algorithm could mistakenly attach the ground reaction forces to the wrong foot segment, moments at the MP joint resulting from inverse dynamics analyses were not considered meaningful and are thus not reported.

2.2.4.3 Whole Body Center Of Mass A common method for COM positional estimation is to assume that COM motion follows roughly the same trajectory of an external marker on the pelvis [68]. For pseudo-static postures, the center of pressure (COP), as estimated from ground reaction force measurements [119, 137], has been compared to the horizontal plane projection of the COM. COM trajectory during gait with perturbations is likely to be highly variable; therefore, these simpler methods of COM estimation were deemed inadequate. Rather, a weighted average of segmental COM locations was used to calculate a more accurate COM estimation [30].

2.2.4.4 Further Data Processing When ground reaction force data was available, heel strike (HS) and toe off (TO) for both feet were identified as the points where vertical ground reaction forces changed from no load levels. HS was identified as the first data point, occurring after an unloaded period, where the normal force was larger than the mean plus two standard deviations

of the unloaded data with the additional requirement that from this point forward in time, the force did not return to lower than the mean plus two standard deviation without first passing 20 Newtons (Appendix F, 'Get_HS_and_TO.m). HS determination was verified both by visual inspection of the normal force trace and through inspection of the heel marker vertical velocity (see Appendix F, 'Verify_HS_and_TO.m'). Toe off was determined using the same method but with the data reversed in time and was verified by inspection of virtual toe marker vertical displacement. When force data was unavailable due to technical difficulties, HS and TO were determined and verified using heel vertical velocity and toe marker vertical displacement only (Appendix F, 'Get_HS_and_TO2.m and 'Verify_HS_and_TO2.m').

For comparative analyses (trial to trial, subject to subject, etc), all time dependent data were normalized using MATLAB's (The MathWorks, Inc.) `interp1` function with 2000 points interpolated from the original data (collected at 120 Hz) from -50% to +150% (0% = HS, 100% = TO) using shape-preserving piecewise cubic interpolation ('pchip' or cubic Hermite) (Appendix F, 'main.m').

Trajectory velocities, including center of mass velocity, were calculated using a centered finite difference formula with fourth order error terms [40] using a macro in the model script (Appendix D).

$$\dot{x}(k) = \frac{x(k-2) - 8 * x(k-1) + 8 * x(k+1) - x(k+2)}{12 * \Delta t}$$

Where Δt was typically 0.0083 seconds (1 / 120 Hz).

Table 3: Segment masses, longitudinal COM locations, and radii of gyration

Segment	Mass (%)		COM position (%)		Rx (Ab/Ad duction) (%)		Ry (Flex/Ext) (%)		Rz (Int/Ext Rot) (%)	
	F	M	F	M	F	M	F	M	F	M
Head	6.68	6.94	48.41	50.02	27.1	30.3	29.5	31.5	26.1	26.1
Torso (UPT & MPT)	30.10	32.29	*49.65	*50.73	*32.8	*34.3	*29.0	*29.4	*21.8	*23.3
Upper Arm	2.55	2.71	42.46	42.28	27.8	28.5	26.0	26.9	14.8	15.8
Fore Arm & Hand	1.94	2.23	*32.34	*32.49	*91.0	*102.8	*88.1	*97.7	*9.5	*12.3
Pelvis	12.47	11.17	50.80	38.85	49.2	61.5	40.2	55.1	44.4	58.7
Thigh	14.78	14.16	63.88	59.05	36.9	32.9	36.4	36.4	16.2	14.9
Shank	4.81	4.33	56.48	56.05	26.7	25.1	26.3	24.6	9.2	10.2
Foot **	1.29	1.37	40.14	44.15	29.9	25.7	27.9	24.5	13.9	12.4
Toe	0.00	0.00	NA	NA	NA	NA	NA	NA	NA	NA

In Table 3, segment masses given as percentages of total body mass. COM position given as percentages of link lengths from the segment origin toward the attachment point (see Table 2). Radii of gyration are given as percentages of link lengths. Typical values resulting from the combination of multiple segment components are identified with *. The foot segment used in the model combined masses and radii of gyration from the shoe sole with the foot for inverse dynamics calculations; however, the contributions of the shoe sole have not been included in this table. This table is based in large part on de Leva [47].

2.3   RESULTS

Appendix A illustrates typical (i.e., a single trial) kinematic and kinetic results for the same young (age 22) male subject with a total body mass of 83.6 Kg and a height of 1.78 meters. This subject was instructed to walk at a "purposeful" pace while focusing on a distant target placed at eye-level; however, no attempt was made to control gait speed. The subject wore sized 10 PVC soled dress shoes (with the heels slightly abraded to simulate light wear) and practiced walking along the laboratory gait path to ensure that the right and left feet cleanly struck the two force plates during normal gait.

The analyses presented in Appendix A were from a unperturbed gait trial which followed several other typical gait trials and a single static posture trial. Motion capture data was labeled and processed as previously described to remove gaps and unlabeled trajectories. The data was

then modeled, heel strike and toe off for both feet were identified, and all trajectories were then time-normalized to left foot heel strike (0%) and toe off (100%). This subject was observed to walk with very little right arm swing but with a gait that appeared to be otherwise typical of younger subjects observed in The Human Movement and Balance Laboratory.

Table 4: Sign conventions and typical static posture rotations for comparison with dynamic trial results as illustrated in Appendix A

Rotation	Sign Conventions and Clinical Terminology						Typical Static Posture Rotations (deg)		
	First		Second		Third		First	Second	Third
E_Head_Global	+	Forward Tilt	+	Right Lean	+	Left Twist	10.4	3.5	3.5
J_Neck	+	Flexion	+	Right Lean	+	Left Twist	6.5	5.0	2.3
JL_Shld	+	Flexion	+	Adduction	+	External Rotation	2.5	-80.4	49.9
JR_Shld	+	Flexion	+	Abduction	+	Internal Rotation	-23.3	72.4	-71.6
JL_Elbow	+	Flexion	+	Adduction	+	External Rotation	12.2	-18.4	-69.6
JR_Elbow	+	Flexion	+	Abduction	+	Internal Rotation	22.1	16.0	77.9
E_Torso_Global	+	Forward Tilt	+	Right Lean	+	Left Twist	3.8	-1.3	1.3
J_Waist	+	Flexion	+	Right Lean	+	Left Twist	1.7	-4.2	1.1
E_Pelvis_Global	+	Forward Tilt	+	Right Lean	+	Left Twist	2.2	2.9	0.1
JL_Hip	+	Extension	+	Adduction	+	External Rotation	0.8	-1.2	14.9
JR_Hip	+	Extension	+	Abduction	+	Internal Rotation	1.9	-4.6	-8.0
JL_Knee	+	Flexion	+	Adduction	+	External Rotation	-0.2	2.8	-1.8
JR_Knee	+	Flexion	+	Abduction	+	Internal Rotation	-1.0	-1.9	-2.4
JL_Ankle	+	Dorsiflexion	+	External Rotation (toe out)	+	Abduction, Pronation, Inversion	-2.7	-8.6	-4.7
JR_Ankle	+	Dorsiflexion	+	Internal Rotation (toe in)	+	Adduction, Supination, Eversion	-2.9	6.4	3.9
EL_FFA	+	Forward Tilt	+	Right Lean	+	Left Twist	5.7	-0.8	4.9
ER_FFA	+	Forward Tilt	+	Right Lean	+	Left Twist	5.9	0.6	-3.9
JL_MP	+	Dorsiflexion	+	External Rotation (toe out)	+	Abduction, Pronation, Inversion	9.5	-2.1	-0.6
JR_MP	+	Dorsiflexion	+	Internal Rotation (toe in)	+	Adduction, Supination, Eversion	11.7	6.6	0.3

In Table 4, J(R/L)_Joint indicate JCS, 'floating' rotations and E(R/L)_Joint indicate 'fixed' Euler angles.

2.3.1 Kinematic Results

The following sections compare results generated by the model described in this chapter to results from existing literature where appropriate. Due to differences in segment local coordinate systems and mathematical approaches, it is expected that no two studies will report exactly the

same magnitude for either joint angles or joint torques. However, it is expected that the shapes and ranges of the joint angles and joint torques will be similar.

2.3.1.1 HEAD   Reports of head orientation during gait are not common. Hirasaki et al. [64] referred to other work [15, 16, 111] to support the idea that the head pitches up and down to compensate for vertical translation at higher walking velocities. Thus, the head and the trunk work together to maintain a stable head pitch in global space. For gait speeds around 1.4 m/s, Hirasaki [64] reported head pitch ranging between 8 and 12 degrees with maximum forward tilt occurring around double support and minimum forward tilt occurring just prior to TO. This range and timing agrees well with the data illustrated in Figure 37 for sagittal plane head orientation. Data for comparison to the typical head orientation in planes other than sagittal during gait was not available.

2.3.1.2 NECK   Because neck rotation can be thought of as the difference between head rotation and torso rotation when only sagittal plane rotations are considered, relatively little work has been reported focusing on any other details for neck rotations during gait. Hirasaki et al. [64] reported neck rotation (pitch only) as the difference between torso and head tilts and indicated a range of almost 5 degrees (from 5 to 10 degrees of forward pitch) with maxima occurring just after TO and minima occurring just prior to HS. These results appear to agree with those illustrated in Figure 38. Data reporting neck rotations during gait for the other two rotations (other than sagittal plane rotations) were not identified.

2.3.1.3 SHOULDERS AND ELBOWS   Murray et al. [100] reported typical sagittal plane shoulder rotations during gait with peaks of about +5 degrees of flexion (contralateral shoulder) and -20 degrees of extension (same side shoulder) occurring at HS during free speed walking. The timing of these peaks agrees well with the timing of the peaks illustrated in the flexion and extension JCS shoulder rotations in Figure 39; however, the magnitude of these peaks appears to depend, in large measure, on each individual's arm swing during gait. The subject whose data is illustrated in Appendix A did not appear to use much right arm swing during gait.

Similarly, Murray et al. [100] reported elbow flexion rotations of about the same shape as shoulder rotations (peaks occurred at about the same time) with a range of between 20 degrees of

flexion at contralateral HS to about 40 degrees of flexion at contralateral TO. This trend agrees well with the data depicted in Figure 40, at least for the left arm. Shoulder and elbow rotations other than flexion/extension during gait for comparison to the data in Figure 39 and Figure 40 was not available.

2.3.1.4 Torso Studies separating the orientation of the torso from the rest of the upper body during gait are not common. However, Winter [136] did illustrate sagittal plane pitch of the trunk during gait as varying by about +/- 1 degree over a stride. Hirasaki [64] reported a slightly larger trunk pitch range of between +3 degrees (forward tilt) to -2 degrees (backward tilt) with minima occurring just after toe off and maxima occurring just before heel strike for gait at around 1.4 m/s. Thorstensson et al. [130] reported both pitch and side to side roll trunk motion during gait with ranges of about 4 and 5 degrees respectively for gait at around 1.0 m/s. According to Thorstensson's data, peak forward tilt occurred prior to HS and minimum tilt occurring after TO. Lateral trunk rotation was typified by maxima and minima occurring near mid-swing.

In comparison, the sagittal plane orientation of the torso illustrated in Figure 37 includes a peak forward tilt just prior to HS and a minimum forward tilt around TO of the right foot. The range of torso pitch illustrated in Figure 37 also seems to be consistent with previous research. The frontal plane rotations reported in Figure 37 includes angles ranging from about -4 to +2 degrees, which seems consistent with the results from other researchers.

2.3.1.5 Waist Waist angle during gait has not often been reported. Most researchers lump the pelvis and the torso (and often head as well) together, assuming a rigid waist and then report HAT (head, arms, torso) orientation which is probably closer to our torso orientation. Reports of both pelvic and HAT orientation may exist in the literature and would allow one to determine waist rotation as the relative difference between the two rigid body rotations. Because we have assumed rigid torso and pelvis segments, waist rotations are a simplified way of reporting spinal deformations and do not indicate in any meaningful manner the rotations about any one joint in the body. Waist rotations during gait, as presented in Figure 40, have not been compared to data existing in the literature.

2.3.1.6 Pelvis   Pelvic orientation in space has commonly been included in the set of lower extremity kinematics making comparisons of the results of our model to existing literature possible. Pelvic orientation, as illustrated in Figure 37, was compared to results from three specific papers, Kadaba et al. [72], Apkarian et al. [8], and Frigo et al. [53]. Kadaba reported pelvic tilt (sagittal plane) rotations ranging from about 4 degrees to about 10 degrees on average with near constant value shape (no obvious peaks or valleys) other than a barely discernable peak prior to mid-stance with minima near TO. Apkarian reported pelvic tilt for three subjects, with all three typified with peaks near mid-stance and minima near TO. Apkarian's subjects had diverse average values of pelvic tilt ranging from around -10 degrees to about +10 degrees with peak-to-peak ranges of between 15 and 25 degrees. Frigo's data was very different from these other two studies in that the pelvis appeared to tilt forward at a near constant 20 degrees from HS to TO with about a 5 degree peak-to-peak range but with the opposite shape; in-other-words, the pelvis was tilted forward less at mid-stance than at HS and TO. The typical data illustrated in Figure 37 indicates pelvic tilt ranging between 1 and 4 degrees with a peak forward tilt occurring just after mid-stance and minima around TO. Summarizing, our typical subject's pelvic tilt was comparable to the data from other studies in both range and shape.

Pelvic obliquity (rotation in the frontal plane) from Kadaba's and Frigo's studies seems to have a shape that is similar to that of our typical male subject with peak's at around 20 percent and 70 percent of stance duration (just after and just before contralateral TO and HS). The magnitude of this rotation ranges from about 0 to about 5 degrees for both the two previous studies and our results. Apkarian, on the other hand, did not indicate an consistent pattern across three subjects.

Comparisons of the magnitude and shape of transverse plane rotation to existing literature were very difficult. Frigo indicated that these rotations were about 180 degrees out of phase with pelvic obliquity, Kadaba suggested a sinusoidal pattern of about +/- 5 degrees with maxima and minima around TO, and Apkarian's data does not suggest a discernable pattern. Our typical subject's transverse plane pelvic rotation seemed to remain constant at around 0 degrees until just before TO and then grew to about 6 degrees. Whether this data indicates a sinusoidal oscillation with peaks around TO is inconclusive. However, the magnitude of this rotation does seem to agree with the previously published data.

2.3.1.7 Hips In addition to the three studies used for pelvic orientation relative to the global coordinate system, a fourth study, Besier et al. [11] was examined to validate the rotations at the hips from the model described herein.

The plots in Appendix A indicate typical hip rotations with peak extension of around 10 degrees occurring in the contralateral hip at HS and near constant flexion minima of around -30 degrees occurring at +/- 20 percent of same-side HS. The shape, the magnitude, and the rotational range of this hip flexion rotation agrees well with all four previous studies. Likewise, hip ab/adduction angles appear to be consistent with the data reported by Frigo et al. [53] and Kadaba et al. [72] with a near constant abducted plateau of around 5 degrees during foot flat. However, Apkarian et al. [8] and Besier et al. [11] report hip ab/adduction of similar magnitudes and ranges but with different shapes; Besier's data indicates a rather sharp peak rather than a plateau and Apkarian's data does not indicate any discernable shape. Data in Figure 41 indicates that int/external rotation at the hip for our typical subject is periodic with a peak-to-peak range of about 12 degrees with minima around HS and long plateau maxima beginning around 20% of stance duration and ending around TO. This shape seems to match Besier, Apkarian, and Frigo well while Kadaba's is less similar.

2.3.1.8 Knees Many studies have reported knee rotations during gait, both as a primary objective of the research and in support of new analysis methods. Although many of these would have been appropriate choices for comparisons to the knee rotation results from the typical young male subject as illustrated in Figure 42, only three were chosen in addition to the four studies used for hip rotation comparisons. These three additional papers, which reported knee rotations for gait exclusively, were Chao et al. [39], Growney et al. [60], and Lafortune et al. [79].

Knee flexion results for all studies, including the current model, indicate a similar pattern with maximum extension occurring just prior to heel strike, a smaller flexion peak near 25% of stance duration, a local minimum flexion occurring at around mid-stance, and a larger flexion peak occurring just after TO for the same side knee joint. Figure 42 illustrates the magnitude of the typical extension peak at around 3 degrees, of the two flexion peaks at about 25 degrees and 70 degrees respectively, and the mid-stance minimum at around 16 degrees. These values agree

very well with the results from the literature as evinced in Table 5. All ranges are based on mean and standard deviations where available or estimated from plots.

Table 5: Knee flexion points of interest from existing literature compared to typical results from the current model

Paper	Max Extension near HS (degrees)	Initial Flexion Peak (degrees)	Mid-Stance Flexion (degrees)	Post-TO Flexion Peak (degrees)
Kadaba et al. (1989)	5 to 10	15 to 20	2 to 10	53 to 58
Apkarian et al. (1989)	0 to 5	10 to 20	0 to 15	60 to 75
Chao et al. (1983)	3 to 11	7 to 19	26 to 38	60 to 76
La Fortune et al. (1992)	0 to 7	14 to 21	-2 to 7	56 to 64
Growney et al. (1997)	0	20 to 25	5 to10	~65
Figro et al. (1998)	0 to 10	10 to 20	-2 to 10	58 to 72
Besier et al (2003)	-2 to 0	15 to 20	5 to 10	~70
Current model	3	25	16	70

Abduction and adduction (Varus-Valgus) angles for the knee were not as easily comparable. Generally, a shape mirroring joint flexion but at much smaller magnitudes was observed with small adduction peaks around 25% of step (left foot), a larger peak occurring near TO, and a local minimum occurring at about 125% of stance duration. The magnitude and shape of this trend were comparable for many of the previously identified studies and appeared in the typical subject's data illustrated in Figure 42. Similarly, higher frequency oscillations in int/external rotation for the knee from previous studies made comparisons to the current model difficult. However, the magnitude of the rotations from most studies were comparable to those illustrated in Figure 42; small rotations of between 20 degrees internal and 10 degrees external rotation for the left knee were not uncommon. The left knee rotation was internally rotated for the majority of left foot stance based on the current model and this agrees well with most of the existing literature.

2.3.1.9 Ankles Current model typical rotations at the hip were compared to the results of four previous studies [8, 11, 53, 72] and thus these same studies were used for ankle rotation comparisons. As illustrated in Figure 43, typical ankle rotation for a young male subject walking

naturally followed a pattern with a plantar flexion peak occurring after HS transitioning smoothly to dorsiflexion around mid stance, peaking at around 80% of stance duration and then rapidly moving to a plantar flexion peak around TO. This pattern was observed in all four of the referenced studies with good agreement in angular magnitudes although Frigo et al. used a slightly different local coordinate system resulting in a constant shift from zero of about 70 degrees.

Int/external rotation at the ankle joint likewise was similar to results from the literature. For the current model, this rotation was observed to change from its maximum value of internal rotation at HS to a slightly less internally rotated value at about 80% of stance duration and then return to its original value for TO. This shape was repeated in Kadaba's results and in Apkarian's results although with an external rotation bias.

The structure of the ankle joint is very complicated and the degrees of freedom there are not independent. However, most biomechanical models describe ankle movement using a flexion axis, an abduction axis (the long axis of the foot), and an axis which is roughly normal to the floor during foot flat. Inversion (facing the soles of the feet toward each other) is sometimes termed supination, vargus, or adduction while eversion (facing the soles of the feet away from each other) is termed pronation, valgus, or abduction. Interestingly, neither Frigo nor Besier reported int/external rotation as such but rather reported one rotation as ab/adduction and another as inversion/eversion [11] or pronation/supination. This misnomer is fairly confusing as one of the two plots must clearly be int/external rotation while the other must be ad/abduction. Adding to the difficulty is that Kadaba did not report ab/adduction at all. Thus, it must be assumed that the current model is performing similarly to existing research as far as ankle ab/adduction and int/external rotations are concerned: results agree when comparisons can be made and do not seem unreasonable otherwise.

2.3.1.10   Foot Rotations Relative to Global   Although the angle that the foot makes with the horizontal plane has been reported often, this has primarily been reported as the sagittal plane projection of the orientation of the foot with respect to the floor [18]. The current model produces three rotations, one in the global sagittal plane, one in the global frontal plane, and one in the transverse plane. This sagittal plane rotation has also been loosely referred to as the foot-to-floor angle (FFA) while it is really an Euler rotation relating the LCS of the foot to the global

coordinate system. We assume that this approach to FFA determination will result in angles that will be comparable to the projection angles previously reported as the angle that the foot makes with the floor.

The current model results in a typical pattern of sagittal plane rotations of the foot with respect to the floor where the foot is at its maximum toe-up orientation at or just before HS and is at its maximum toe-down orientation near TO. As expected, this FFA is nearly constant during foot-flat; however, the reported angle is greater than zero, indicating that the LCS for the foot is not perfectly horizontal but rather is oriented with the toe slightly lower than the heel.

2.3.1.11   MP Joint Rotations Most gait modeling and characterization literature treat the foot as a single rigid link or use so much detail as to make the resulting kinematics difficult to interpret. Figure 45 illustrates the effect of including a simple joint at the metatarsal-phalangeal line. As expected, the primary motion at this joint is one of dorsiflexion near TO. However, because the break of the shoe does not exactly coincide with the identified axis, there is some minor crosstalk that presents itself as a small amount of int/external rotation, also near TO. The dorsiflexion rotation illustrated in Figure 45 agrees with Bojsen-Moller et al. [17], especially near TO although the expected dorsiflexion prior to HS is missing from this subject's MP joint rotation.

2.3.1.12   Kinematic Summary Generally, the rigid body rotations and joint angles resulting from the current model and illustrated in Appendix A agree well with kinematic results from existing literature. Where discrepancies do exist, these may be due to local coordinate system definition differences or mathematical/motion tracking issues but this seems much less likely than simple subjective gait style differences for our typical subject (i.e., right shoulder and elbow rotations were obviously different for this subject). The majority of the angles reported in this section agreed with the literature leading to a high confidence in the resulting kinematic analyses from the current model.

2.3.2 Ground Reaction Forces and Moments

Figure 46 presents typical ground reaction forces for the same young male subject whose kinematics have previously been compared to the literature. The normal and shear forces and the moments in the sagittal, frontal, and transverse planes are both qualitatively and quantitatively similar to results from numerous works [136].

2.3.3 Lower Extremity Kinetics

Although the results of kinetic analyses for every joint in the 15 segment model have been presented in Appendix A, only the results for the lower extremities (ankle, knee, and hip moments) will be compared to existing literature in this section as these are commonly used for gait characterization. Because the kinematics resulting from the current model agreed well with the existing literature, we expect the kinetics of the lower extremities will likewise agree with the literature. However, it is also likely that subtle differences in joint center locations, link lengths, and mass distributions could affect the kinetic results significantly. As indicated in the segment definition sections of this document, the centers of mass and radii of gyration for the lower extremity segments were based in large part on the work of de Leva [47]. Table 3 summarizes parameters relevant for kinetic analyses.

2.3.3.1 Ankles The typical subject's ankle flexion moment (Figure 43) followed the pattern as reported by Apkarian et al. [8], Kadaba et al. [72], Eng and Winter [49], Doriot and Cheze [48], and Besier et al. [11] with ankle flexion moments starting near zero at HS, hitting a small peak dorsiflexion moment at around 10% of stance duration, transitioning to plantar-flexion by about 20% of stance duration with a peak at around 80%, and then returning to near zero at TO. Although studies have normalized moments differently making magnitude comparisons difficult, the shape, magnitudes, and timing of the flexion ankle moments generated using the model discussed herein matched much of the existing literature.

The ankle ab/adduction moments from the same sources have not demonstrated nearly as consistent a pattern, possibly due to differences in subject gait styles. It does appear that subjects generally maintained inversion (i.e., adduction or vargus) moments during the stance phase of

gait for most studies – although Eng and Winter [49] reported moments transitioning from eversion to inversion and back to eversion. Besier et al. [11] was difficult to interpret due to scale labeling confusion for ankle moments other than flexion. The model discussed herein generated results for a typical subject indicating consistent inversion moments from HS to TO, the small magnitude of which seems reasonable giving the variability in the literature.

The int/external ankle joints reported in Figure 43 followed a pattern, repeated in Kadaba et al. [72], Eng and Winter [49], and Doriot and Cheze [48] that was somewhat similar to ankle flexion: from 0 near HS, to a small internal rotation moment peak at around 10% of stance duration, and then transitioning to primarily external rotation with a peak at around 75% of stance before returning to near zero at TO. The int/external ankle moments in Apkarian et al. [8] were difficult to interpret due to plot scaling and were likewise difficult in Besier et al. [11] due to plot labeling issues as previously discussed.

2.3.3.2 Knees Knee flexion moments during gait have been widely reported [8, 48, 49, 72] and typically follow a pattern of slight flexion at HS, peak extensor moment at about 20% of stance duration, a minimum moment at around 75% of stance duration and another, lesser flexion moment peak near TO. Figure 42 illustrates that the typical young male subject, as analyzed using the model discussed herein, exhibited knee flexion moments that closely followed the same pattern as previously reported, both in terms of shape and magnitudes. Unlike the flexion moments typically reported, Besier et al. [11] reported knee flexions that seemed very different in shape and magnitudes from others and comparisons to this data were not favorable.

Knee ab/adduction moments during gait, as illustrated in Figure 42 for our young male subject, followed a typically M-shaped pattern with peak adduction moments occurring at around 25 and 75% of stance duration. This shape with similar magnitudes has also been reported previously [11, 48, 49, 72]. The knee abduction moments presented by Apkarian et al. [8] were atypical in that the first peak in the M shape was significantly greater than the second for all three of their subjects.

Knee internal and external rotation moments were very difficult to compare across studies with no typical pattern presenting itself, other than an external moment peak occurring late during stance in some of the literature [11, 48, 49, 72] which matches the moments resulting from the current model as illustrated in Figure 42.

2.3.3.3 Hips Hip moments resulting from the inverse dynamics analysis are illustrated in Figure 41. As in the existing literature, the typical flexion moment resulting from the current model exhibited a sinusoidal trend with peak extensor moments occurring near HS and peak flexor moments occurring near TO [8, 11, 48, 49, 72].

The peak ab/adduction moments at the hips were typically of about the same magnitude of the peak flexion moments, with M-shape of adduction peaks at around 25 and 75% of stance of almost 1 Nm/kg. The same shape with similar ratios of peak flexion versus adduction moments was demonstrated in the results from Kadaba et al. [72], Apkarian et al. [8], Eng and Winter [49], Besier et al. [11] and Doriot and Cheze [48].

Finally, the observed int/external rotational moments at the hips, which for the typical male's data in Figure 41 seemed to move from an internal moment peak at around 25% of stance to an external moment peak at around 75% of stance, also agreed well, both in shape and in magnitudes, with previously reported results [8, 11, 48, 72] with one exception: Eng and Winter [49] reported moments that were inverted from the typical with an external moment transitioning to an internal moment - likely due to a sign error.

2.3.3.4 Kinetic Summary The shape and magnitudes of the results of kinetic analyses from Appendix A seemed to agreed well with data from the literature. There are many sources of error that could explain any slight discrepancies including joint center location errors, mass distribution estimation differences (anthropometry references for many of the existing studies were different from the reference chosen for the current model), and subjective gait style differences are obvious candidates. However, the consistently high degree of agreement between the results from the current model and other studies suggests that a high level of confidence in the appropriateness of the current model would be well founded.

2.3.4   Center of Mass

The global position of the three-dimensional center of mass as calculated from the model agrees with previously published data. The presented COM (Figure 47) trajectory was normalized by subtracting $COM_X(t = HS)$, $COM_Y(t = HS)$, and $COM_Z(t = HS)$ from $COM_X(t)$, $COM_Y(t)$, and $COM_Z(t)$ for all time. In comparison, Winter [136] reported vertical COM displacements

normalized to the mean at different cadences (slow, normal, and fast) and thus, the magnitudes of the graphs do not match the current results, although the qualitative shape of the graphs are similar. For a subject with a height of 6ft (1828.8 mm) Winter's data [136] translates to a range of approximately 60 mm about the mean, which would be very similar to the results from the current model.

The COM velocity in the direction of progression as reported in Winter [136] was normalized to mean stride velocity. However, the overall shape of that graph is similar to the un-normalized, unfiltered velocity resulting from our model. In addition, the range of anterior-posterior (AP) velocity from Winter was approximately 0.35 m/s (about a mean velocity of 1.0) while the current model resulted in a mean AP velocity of about 0.25 m/s, well within the standard deviations from Winter's data [136].

2.4   DISCUSSION

As with typical movement analysis based on experimental data collection, a number of factors contribute to kinematic and kinetic errors, including skin motion artifacts, joint center estimation errors, and anthropometry scaling issues. Soft tissue artifacts can cause significant differences in the calculated joint angles, especially the ab/adduction and int/external rotation kinematic estimations [28, 54, 90, 91, 115]. Joint center mislocation is an additional basis for error in both kinetics and kinematics calculations. For example, there are many different techniques which focus on predicting the location of the hip joint center [10, 76, 120]. The effect of hip joint and knee joint center mislocation has a significant impact on angle and moment calculations [7, 65, 123]. Some segment orientations (e.g., hand) were approximated and this may also have contributed to model errors. Relocating markers present in the static trial but removed for dynamic trials may have introduced error as well, especially when the remaining markers either may have moved relative to each other or when the underlying segment was not truly rigid. The errors that these discrepancies might introduce to the kinematic and kinetic measures (as well as COM determination) were assumed to be small. Another potential source of error for this model is related to segment definition vectors that are orthogonal to a plane. When such a plane is defined using markers that are relatively close together, the segment definition is very sensitive

47

to noise in those marker trajectories. This planar sensitivity was particularly troublesome for the toe segments. Finally, static maker relocations that are based on noisy or otherwise unreliable trajectories have the potential to greatly impact segment definitions.

The estimations in anthropometry parameters, which include segment length, mass, and inertial properties are also a possible source of error [75], especially given the age distribution and activity levels of our subjects as compared to the population used by de Leva [47]. Additionally, de Leva's segmentation was not precisely followed (e.g., torso, pelvis, and head segment lengths – see Table 3). Although some age relevant anthropometry research has been done [106], the work of de Leva [47] appears to present the most complete, gender specific relationships for this type of research. Previous studies suggest that changes in segmental parameters do have a small but statistically significant impact on kinetics [108].

3.0 GAIT PARAMETERS AS PREDICTORS OF SLIP SEVERITY IN YOUNGER AND OLDER ADULTS

Slips were the most frequent event leading to fall and overexertion related injuries in the Swedish labor force [44] and were the most common fall initiating event for employees in the UK [55]. The US National Health Interview Survey questionnaire administered by the National Center for Health Statistics in 1997 revealed a clear majority (64%) of work-related falls were attributable to slipping, tripping, or stumbling and indicated that 43% of occupational same-level fatal falls were most commonly triggered by a slip [44]. According to the Bureau of Labor Statistics, nearly 30% (28.7%) of workers that sustained injuries from slips and/or falls missed 31 days of work or more [26]. Further, 14% of accidental deaths in the workplace were reportedly caused by falls [25]. In addition to the risk of fall related injuries and fatalities, slip recovery efforts have been shown to contribute to high rates of overexertion injuries [45]. De Laet and Pols [46] estimated that the annual direct cost of all fall-related occupational injuries in the U.S. alone was approximately six billion dollars.

The risk of slip and fall accidents increases with age. A ten-fold increase in the incidence of falls was reported in the elderly (65+) compared to younger individuals (16-64) [129] and Lloyd and Stevenson [85] indicated that while slips and trips caused 32% of falls for young people, 67% of falls for the elderly were initiated by slips. Falls on the same level caused roughly 20% of all injuries to older workers as compared to around 10% for the general population with "floor and ground surfaces" listed as the most common source of non-fatal injuries among workers in the 55 year and older age group [110]. In 2004, over one third (39%) of the occupational fatal fall victims were 55 and older [25], more than double that age group's share of the work force (16%) [24].

Just as the risk for slips and falls increases with age, so to does the severity of the outcome of these accidents. Falls are often listed among the leading causes of serious

unintentional injuries, disability, and death among older adults [46, 73, 74, 92, 117]. Approximately 65% of all serious injuries (Injury Severity Score > 15) and 55% of deaths were attributed to falls for patients aged 65 years and over, compared to 11% and 7.5% in the younger population, respectively [125]. Fatality rates from falls showed a significant increase for workers as young as 45 to 54 years old [1]. Additionally, Personick and Windau [110] suggested that older workers are at a greater risk of non-fatal injuries resulting from slips, even those not resulting in falls, due to overexertion during recovery attempts.

There has been some disagreement in the literature regarding the characteristics of a recoverable slip. Perkins [109] commented that longer slip distances and slip velocities exceeding gait speed increased the likelihood for loss of balance. Perkins also characterized slips as full or "macro-slips" if the slipping distance was greater than 10 cm [109]. Leamon and Li [80] used a 3 cm threshold to differentiate full or macro-slips from smaller slips. Strandberg and Lanshammar [127] suggested that slip distances of greater than 10 cm and slip velocities greater than 0.5 m/s typically resulted in falls and reported a continuum of slip severity, mini-, midi-, and maxi- slips, correlated to slip distance and peak slip velocity. Research by Cham and Redfern [34] indicated that falls were typically associated with slip distances greater than 10 cm and peak slip velocities greater than 0.8 m/s. Other research results suggest that these velocity and distance thresholds may be too conservative, i.e., individuals are able to avoid falls for slips with peak slip velocities far exceeding 1.0 m/s [18], but still indicate that longer, faster slips are more likely to result in falls. Lockhart et al. [89] reported slip severity thresholds of 1.44 m/s and 1.07 m/s for younger and older adults respectively walking on a motor oil contaminated surface. Regardless of whether a slip distance or slip velocity threshold is chosen, it seems reasonable to define slip severity based on one of these slip magnitude measures in that longer, faster slips have been associated with an increased risk of falls.

Why, given the same environmental conditions, are some slips unlikely to lead to falls ("non-hazardous slips", short slipping distance and slow slipping velocity), while other slips are much more likely to lead to falls ("hazardous slips", greater slipping distances and faster slipping velocity)? Although there are clearly other contributors (environmental conditions, subject mindset, etc), two general subjective factors (these are clearly not independent factors) likely contribute to slip severity including (1) the state of the body and, perhaps more importantly, of the perturbed foot at slip initiation, and (2) corrective reactions generated in response to slipping.

50

This chapter focuses on the first group of factors. Specifically, walking speed, step length, foot angle at heel strike, heel velocity, and cadence as these have previously been implicated as affecting peak slip velocity [127] and thus influencing fall potential [18, 34, 97, 122]. However, these variables have not previously been studied in a systematic way.

The goal of this research project was to investigate the relationship between slip severity and general gait characteristics including initial conditions at heel strike onto an unexpectedly slippery floor. This relationship was evaluated for younger and older subjects. The underlying hypothesis of this study was that pre-slip parameters would differentiate hazardous from non-hazardous slips classified using a peak slipping velocity threshold of 1 m/s. Because these initial condition variables may be modified via training, a greater understanding of the impact of these variables on slip severity may help to reduce fall incidents precipitated by slips.

3.1   METHODS

This study included 11 older individuals aged 55 to 67 years old and 16 younger individuals aged 20 to 33 years old (Table 6). Written informed consent, approved by the University of Pittsburgh Institutional Review Board, was obtained prior to participation. Exclusionary criteria included a clinically significant history of neurological, orthopedic, cardiovascular and pulmonary abnormalities as well as any other difficulties hindering normal gait. In addition, subjects were excluded if a clinical neurological examination revealed abnormalities that might affect balance.

Table 6: Average subject age, height, and weight with standard deviations

	Female	Male	Age	Height (cm)	Weight (kg)
Young	9	7	23.5 (3.2)	171.2 (8.9)	67.6 (10.5)
Old	7	4	60.9 (4.0)	166.2 (8.1)	78.2 (10.9)

Subjects walked along an 8.5 m long vinyl-tiled walkway. An eight M2-camera Vicon 612 (Oxford Metrics, Vicon Peak – UK) motion measurement system recorded three dimensional motion data at 120 Hz from seventy-nine reflective markers placed on the body and shoes. Ground reaction forces (two Bertec type 4060a force plates embedded into the walkway)

were recorded at 1080 Hz and synchronized with motion data. This chapter describes a subset of the recorded data, including foot kinematics at heel strike and general gait biomechanical variables. Markers used in this analysis include those on the right and left hind foot segment (Figure 19). All participants wore the same brand/model of polyvinyl chloride hard-soled shoes. A harness system connected to an overhead trolley protected subjects from ground contact injuries. The harness caught the subject in the event of an irrecoverable balance loss, but did not impede walking or slipping.
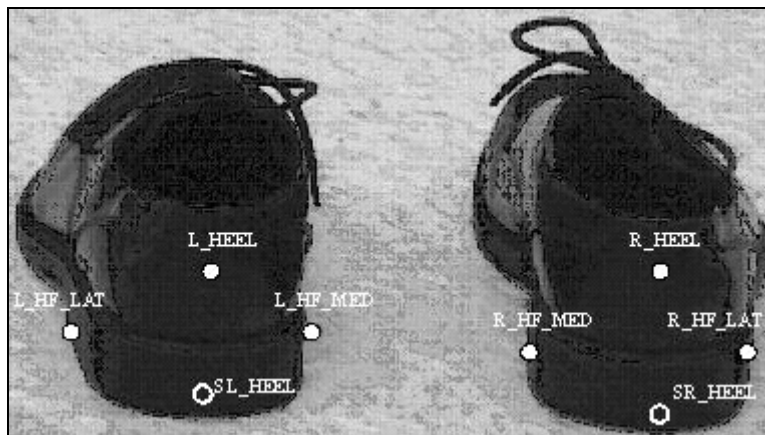
Figure 19: Reflective marker placement

In Figure 19, filled circles (L_HEEL, L_HF_LAT, L_HF_MED, R_HEEL, R_HF_LAT, and R_HF_MED) represent markers that remain on shoes during dynamic trials and hollow circles (SL_HEEL and SR_HEEL) represent markers that are removed after static trials and virtually recreated from other markers during dynamic trials.

Participants were all exposed to the same protocol. Prior to actual data collection, subjects were allowed to practice walking along the gait path while the starting position was adjusted such that the participant appropriately (right foot on first plate, left foot on second plate) hit each force plate with one and only one foot. The lights were then dimmed to prevent the subject from discerning the potential application of the slippery contaminant on the floor and additional practice trials were conducted. Participants were instructed to walk as naturally as possible at a self-selected comfortable pace throughout the experiment.

Prior to each recorded trial, subjects walked to the start of the gait path, faced away from the walkway, and listened to music via headphones for one minute. The music was intended to

disguise any audible hints of contaminant application. At the end of each one-minute waiting period, subjects were asked to turn around, to verify their set starting point, to focus on a target placed at eye-level on the far wall, and to wait for a researcher to signal them to start the trial.

To ensure that participants walked as naturally as possible, they were informed that the first few trials would be non-slippery. Two or three dry trials were then collected ("baseline dry") ensuring that appropriate foot contact was maintained. Then, without the participant's knowledge, a diluted glycerol solution (75% glycerol, 25% water) was applied to the left/leading foot force plate (the surface of this plate was extended such that its dimensions were 0.75 x 0.4 m) and another gait trial was conducted ("unexpected slip"). The coefficient of friction of the shoe-floor interface was 0.53 and 0.03 for the dry and slippery surfaces, respectively, as measured with the English XL VIT Slipmeter ® (ASTM F1679) [5].

Variables of interest were estimated from the force plate and marker data. Heel strike and toe off were determined via analyses of changes in vertical ground reaction forces compared to no load levels. HS was identified as the first data point larger than the mean plus one standard deviation (SDV) as determined from a one second average unloaded measurement. This chosen point was accepted as HS if and only if the normal force remained larger than one SDV and increased to three SDV. HS determination was verified both by visual inspection of the normal force trace and through inspection of the heel marker vertical displacement. Toe off was determined using the same method but with the data reversed in time.

Kinematic variables were calculated from the marker data using a customized routine in Vicon BodyBuilder (Oxford Metrics, Vicon Peak – UK). A heel marker was not used during gait trials because it was easily knocked off by contact with the floor. Instead, a rigid-body analysis technique using static calibration markers was used. The location of a heel marker in the local frame of the hind foot segment was recorded along with all other markers during a standing calibration trial. This information was used to reconstruct the trajectory of the heel marker during walking without attaching a physical marker to the heel. The foot-floor angle (FFA) and its derivative (FFAS) were estimated as the angle between the hind-foot segment and the floor. Other variables of interest, calculated using the heel marker (SL_HEEL, Figure 19), were cadence (CAD – steps/min), vertical and horizontal (square root of the sum of the squares of back-to-front and side-to-side) velocity of the left heel at heel strike (V_VEL and H_VEL – m/s), and step length normalized to leg length, i.e., "step length ratio" (SLR – m/m of left leg

53

length). Slip distance (SD - cm) describes the heel marker's travel distance along the floor from heel strike [58] to a stable zero velocity. For hazardous slips, slip distance was determined by accruing the heel's travel distance from heel strike to the time when the subject either slipped beyond the contaminated force plate or he/she relied on the harness to regain balance as determined by visual inspection of the videos.

Gait speed (GS – m/s) was defined as the average whole body center of mass (COM) velocity along the direction of travel prior to slip initiation. COM was determined using scaled anthropometry based on Chandler [37] and regression equations from Chaffin and Anderson [30] to determine masses and centers of mass for the head, upper and lower arms, trunk, pelvis, thighs, shanks, and feet segments. Segment locations and orientations were determined using at least three, non-collinear reflective markers per segment.

Trial slip severity was categorized as either non-hazardous (NH) or hazardous (H) using the peak velocity of the slipping heel virtual marker. Typical plots of the position and velocity of the left heel, as well as FFA, for both non-hazardous and hazardous slip trials are illustrated in Figure 20. At HS, horizontal heel velocity was often higher than the eventual peak slipping velocity (Figure 20B); for that reason and to accommodate transients occurring at HS, peak slip velocity (PSV) was identified as the local maximum horizontal heel velocity occurring after 50 ms from HS. Hazardous slips were defined as having a PSV greater than 1.0 m/s. This PSV threshold was chosen to agree with slip velocities for larger slips as reported in previous studies [89, 126]. PSV was chosen rather than slip distance (SD) both to allow the inclusion of trials with indeterminate results (recoveries or falls) although, as illustrated in Figure 21, an alternative SD severity threshold of 10 cm would have generated approximately equivalent slip severity classification results.
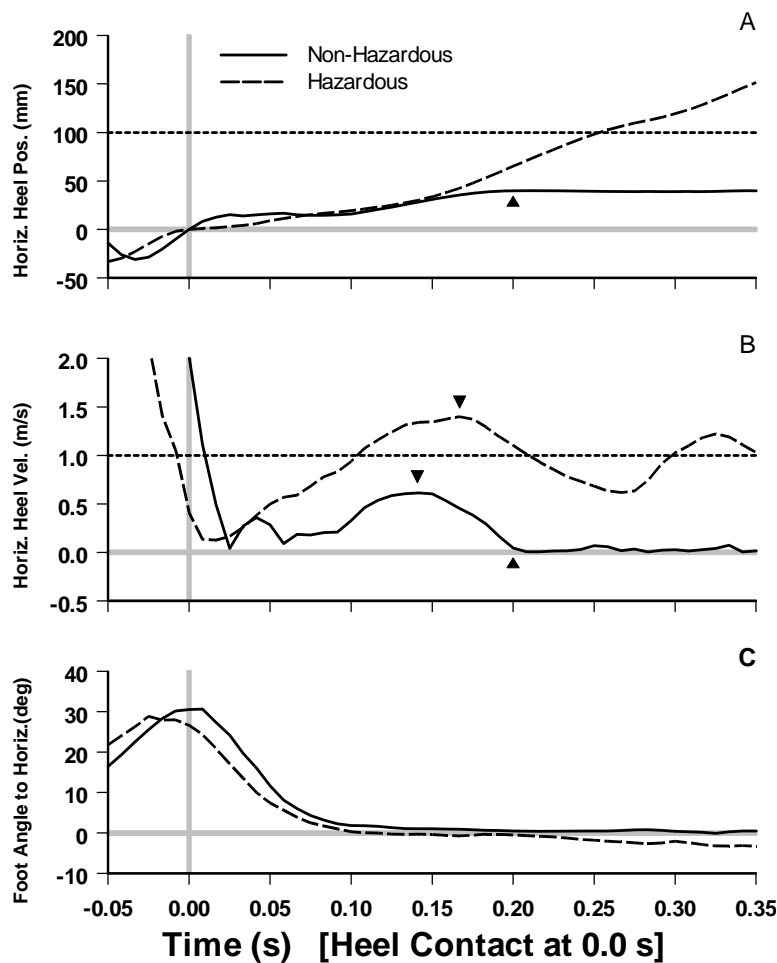
Figure 20: Typical plots for time dependent variables from two slip trials, hazardous and non-hazardous

In Figure 20, heel strike occurs at time = 0. Upward pointing triangles indicate slip distance (SD) locations and downward pointing triangles indicate peak slip velocity (PSV). In Figure 20A, the horizontal position of the left heel relative to heel strike location is given with a dotted horizontal line illustrating a potential SD severity threshold at 100 mm. Positive SD values are in the direction of travel. In Figure 20B, the left heel horizontal velocity is given with a dotted horizontal line illustrating the PSV severity threshold of 1 m/s. In Figure 20C, the foot-floor angle (FFA) is illustrated. All solid and dashed lines in Figure 20 illustrate data from the same non-hazardous/hazardous trials respectively.

3.2   RESULTS

None of the slip events classified as non-hazardous based on the 1 m/s PSV threshold resulted in falls (although some of the non-hazardous slips did elicit post-slip responses), while hazardous slips resulted in recoveries, falls, slips completely off of the force plate, or harness-assisted recoveries. For unexpected slips, *younger and older subjects experienced hazardous slips at about the same rate: 64% (7/11) for older subjects and 69% (11/16) for younger subjects.*

Many of the pre-slip baseline-dry gait characterization parameters were strongly correlated (magnitude of $r > 0.5$) as shown by the correlation coefficients summarizing the strength of the linear relationships between each pair of variables in Table 7. PSV was highly correlated with SD ($r = 0.89$ overall) for both for younger ($r = 0.87$) and older subjects ($r = 0.98$) (Figure 21). All trials categorized as hazardous save one also had a slip distance greater than 10.0 cm. There was only weak correlation (magnitude of $r < 0.3$, $p = 0.36$) between CAD and SLR for these experiments, suggesting that in this study cadence and step length were independently controlled. GS was strongly correlated with SLR and CAD ($r = 0.51$, $p < 0.01$ for each) and FFA at heel strike was strongly correlated with SLR ($r = 0.67$, $p < 0.01$) as well.

Table 7: Correlations among variables of interest – significant correlations ($p < 0.05$) indicated with *

PSV	0.89 *	-0.32	0.49 *	0.17	0.48 *	-0.44 *	-0.24	-0.47
	SD	-0.36	0.58 *	0.32	0.45 *	-0.46 *	-0.08	-0.34
		CAD	-0.18	0.51 *	-0.38 *	0.13	0.50 *	0.34 *
			SLR	0.51 *	0.67 *	-0.70 *	-0.26	-0.54
				GS	0.17	-0.43 *	0.24 *	-0.27
					FFA	-0.73 *	-0.13	-0.55
						FFAS	0.33	0.68 *
							H_VEL	0.28
								V_VEL
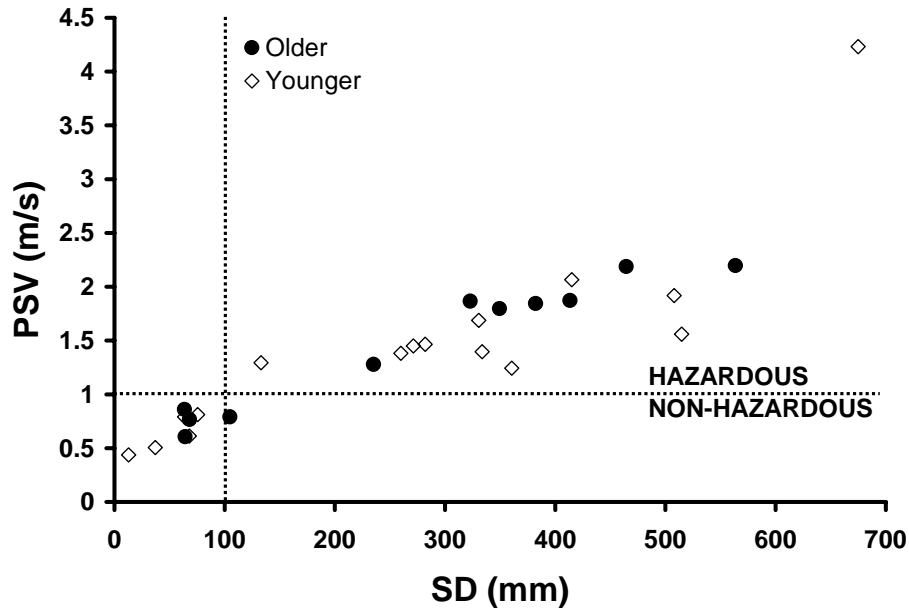
Figure 21: Relationship between peak slip velocity (PSV) and slip distance (SD)

In Figure 21, the vertical dotted line indicates a potential SD slip severity threshold of 100 mm proposed in the literature while the horizontal dotted line illustrates the actual PSV slip severity threshold of 1.0 m/s used for this report. Only one trial would have been classified differently using the two different thresholds.

Two-factor ANOVAs were conducted to determine the associations between the pre-slip gait characterization parameters and the independent variables slip severity (H or NH), age group and their interaction (Table 8). Age did not have a significant effect on CAD, H_VEL, or V_VEL ($p = 0.49$, 0.50, and 0.19 respectively). A trend for older subjects to walk slower (GS) than younger subjects did not reach statistical significance ($p = 0.09$). Significant age effects were seen for SLR, FFA at heel strike, and FFAS at heel strike. Specifically, older subjects walked with shorter step lengths relative to their leg length (SLR) ($p = 0.03$), with smaller foot floor angles (closer to flat foot) at heel strike (FFA) ($p < 0.01$), and with slower FFA rate of change (FFAS) at heel strike ($p = 0.02$).

Table 8: Statistical relationship (p values) among variables of interest, age group, and slip severity as determined via ANOVA – significant correlations ($p < 0.05$) indicated with *

Variable	Age Effect (Y/O)	Slip Severity Effect (H/NH)	Interaction Effect (Y/O x H/NH)
CAD	0.49	0.03 *	0.64
SLR	0.03 *	< 0.01 *	0.46
GS	0.09	0.80	0.93
FFA	< 0.01 *	< 0.01 *	0.48
FFAS	0.021 *	< 0.01 *	0.42
H_VEL	0.50	0.34	0.97
V_VEL	0.19	0.06	0.20

H_VEL and V_VEL were not found to be significantly related to slip severity ($p = 0.34$ and $p = 0.06$) although a trend linking higher vertical velocity to hazardous slips is possible. Significance was found relating slip severity to CAD, SLR, FFA, and FFAS ($p = 0.03$, $p < 0.01$, $p < 0.01$, and $p < 0.01$ respectively). Decreased CAD, longer SLR, higher FFA at heel strike, and faster FFAS at heel strike occurred during hazardous slips. There were no significant interaction effects of slip severity cross age for any of the variables (all p > 0.2). The relationships among these variables, age group, and slip severity are illustrated in Figure 22.
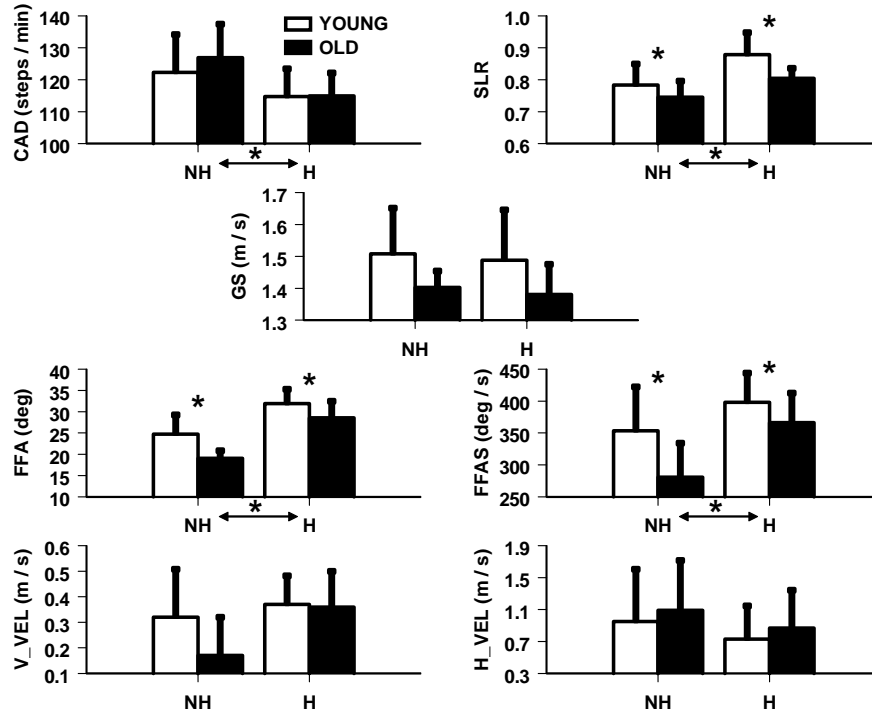
Figure 22: Associations among age-group and variables of interest

In Figure 22, unfilled = younger, filled = old; slip type: Non-Hazardous (NH) and Hazardous (H); and variables of interest. Positive foot-floor angle slope (FFAS) indicate decreasing foot-floor angle (FFA). In Figure 22, positive horizontal velocity (H_VEL) was in the direction of travel and positive vertical velocity (V_VEL) was into the floor surface. Significant results ($p < 0.05$) in Figure 22 are indicated with *.

A stepwise logistic regression analysis was performed in an attempt to relate common initial conditions and gait characteristics to slip severity (H or NH) for younger and older subjects combined. Initial included variables were CAD, SLR, GS and age group (Y/O). FFA was not included due to high correlations with the other variables. The stepwise regression found two variables (CAD ($p = 0.05$) and SLR ($p = 0.02$)) associated with slip severity. The overall model resulted in a $R^2 = 0.45$ with a likelihood $\chi^2 = 15.30$ ($p < 0.01$). Parameters of the logistic regression model for SLR and CAD were 28.2 and -0.16, respectively. This model resulted in the probability plot shown in Figure 23. Increasing SLR (longer steps) and decreasing CAD (slower steps / min) resulted in increasing probability of a hazardous slip. CAD and SLR were not highly correlated with each other ($r = -0.18$, $p = 0.36$) and therefore supplied

relatively independent contributions to the model. GS and age group were not good predictors of slip severity, either alone, or in combination with the other variables.
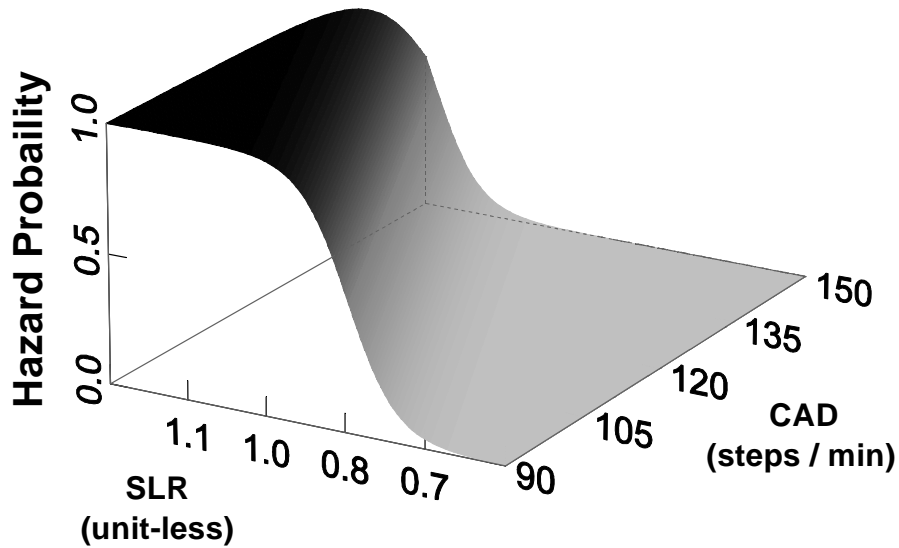
Figure 23: Probability of hazardous slip during first exposure to slippery environment based upon logistic model including step length ratio (SLR) and cadence (CAD)

An alternative logistic regression analysis was conducted using a single initial condition variable, FFA, and age group, since FFA was well correlated with SLR, CAD, and FFAS (Table 7), all of which were statistically related to slip severity (Table 8). This analysis showed a strong logistic relationship for FFA with no age group significance ($R^2 = 0.53$, $\chi^2 = 16.55$; $p < 0.01$). The probability model is given in Figure 24. Increasing FFA resulted in increasing probability of a hazardous slip.
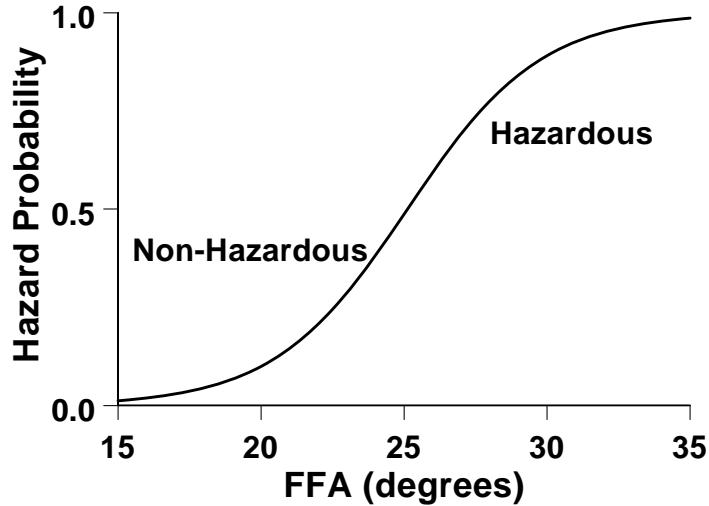
Figure 24: Relationship (logistic regression parameter of 0.43) between hazardous slip event and foot-floor angle (FFA) at heel strike

3.3   DISCUSSION

The findings of this study suggest that initial conditions contribute to the severity of slips. In particular, cadence, normalized step length, and the angle of the foot relative to the floor were found to be important. Decreased cadence, longer step lengths normalized to leg length, higher foot-floor angle at heel strike, and faster foot-floor angular velocity at heel strike were found during hazardous slips. Older subjects were found to have gait that was generally less-hazardous as characterized by smaller step length ratios, smaller foot-floor angles at heel strike, and slower rates of change of the foot-floor angle at heel strike as compared to younger subjects, even though older subjects had equivalent numbers of hazardous slips.

This research was based upon a classification of slips into two categories, hazardous and non-hazardous, rather than differentiating falls from recoveries. This has two major implications on the interpretation of the results. From a practical point of view, it avoids the issue of recovery efforts that are potentially assisted through reliance on the safety harness, slipping completely off of the contaminated force plate, or other indeterminate ground contact. From a theoretical point of view, the results must be interpreted differently from those based on a recovery/fall criterion.

61

Our hazardous criterion, based upon PSV, relies on biomechanical events that occur within 250 ms of heel contact, and thus does not capture the influences of longer latency aspect of the postural control system in any recovery. Therefore, we have focused on the effects of initial conditions on slip severity independent of reactive postural responses during recovery efforts. Using a recovery/fall criterion, the results would be due to a mixture of initial condition factors and reactive postural control factors. This difference is important in the interpretation of the similarities and differences between the young and older subjects, which are discussed later.

Hazardous slips were associated with longer steps (SLR) compared to non-hazardous slips. This agrees with the previously reported relationship between step length and slip risk [6, 18, 33, 83, 89, 98, 102]. The effect of longer step length on slip severity may be due to increases in the ratio of required shear to normal force at heel strike for longer steps [58, 89]. Additionally, longer steps imply greater excursions of the foot with respect to the center of mass, causing the foot to accelerate faster than it would for shorter steps and suggesting an increase in the magnitude of any required action needed to arrest resulting sliding motion of the foot. Finally, taking long steps modifies the tension of lower extremity muscles (e.g., stretching the hamstrings), which may impact the ability to generate faster reflexive torque responses of appropriate magnitude in the face of external perturbations.

Increasing FFA at heel strike was a contributor to slip severity as well, a finding in support of previously published reports [18, 34, 36, 96, 112, 127]. This finding may be due to a number of factors. First, decreased FFA at HS increases the shoe-floor contact area at landing. Also, foot-flat gait reduces the braking impulse at heel strike. Finally, decreased FFA, along with faster cadences and shorter step length ratios impact the dynamics of the center of mass excursions, increasing the center of mass to base of support safety margin, decreasing inertial loading on the foot at heel strike, and thus reducing the frictional requirements needed to prevent a slip [58].

Gait speed did not appear to differentiate between hazardous and non-hazardous slips. However, several researchers have previously reported that peak slip velocities exceeding gait speed increased the likelihood of falls [34, 58, 89, 109, 127, 143]. For the present study, subjects walked at self-selected gait speeds ranging from 1.2 to 1.8 m/s for both hazardous and non-hazardous slips classified based on a PSV threshold of 1.0 m/s. Thus, the range of speeds was not great and it is therefore understandable that a significant relationship between severity and

GS was not found. Perhaps this relationship would be a more valuable differentiator of recoveries and falls.

While the correlation analysis confirmed a number of suspected relationships among gait variables, it also revealed interesting interactions that appear to be in disagreement with previously published literature. For example, in this study CAD and SLR were not well correlated with each other (r = -0.18, p = 0.36), which is in contrast to significant positive correlations reported in the literature [135]. Our lack of correlation is probably due to the limited range of GS induced by the self-paced constraint. Thus, within the self-paced limits it appears that CAD and SLR are independently controlled. Some effects were similar to those reported in the gait literature [18] such as larger foot-floor angles (more vertical orientation of the foot) occurring as longer steps are taken (r= 0.67, p < 0.01) and a slower cadence is adopted (r = -0.38, p = 0.048).

Horizontal heel velocity at heel contact (H_VEL) was not found to have a significant effect on slip severity. In contrast, other studies have shown that greater H_VEL results in greater numbers of slips and falls [18, 86, 88, 136]. However, there tends to be variability in H_VEL at HS, with the heel either slipping forward, backward, or matching ground speed [136]. This variability is probably a function of the instructions to the subject in the experiment and the subjects' mindset (i.e., anticipation of the environmental conditions). Measurements of the coefficient of friction have been shown to be impacted by the velocity of the tests, with greater velocities resulting in lower coefficients of friction (see [38] for review) thus one would anticipate that H_VEL would have an effect on the available coefficient of friction with higher H_VEL more likely to result in hazardous slips. However, our expectation that H_VEL would predict slip severity was not verified in the experiments.

Two logistic regression models were considered to predict slip hazardousness. The choice of predictor variables was based on three factors. First, the explanatory variables were general gait variables that are conventionally thought of affecting slip potential and/or outcome. Second, significant differences in the predictor variables were found between hazardous and non-hazardous slips. Third, independent variables included in the same model were only weakly correlated with each other. The first logistic model included CAD and SLR, both of which are widely used in gait research. These variables were also predictive of slip severity and they were not strongly correlated with each other in this investigation (r = -0.18, p = 0.36); therefore SLR

and CAD were deemed to be good choices for the first logistic regression model (Figure 23). The second model considered only FFA as an explanatory variable predicting slip hazardousness. Because FFA was correlated with both SLR and CAD, and because significant differences in FFA were found between H and NH slips, it seemed a reasonable choice to use FFA as a single predictor of slip severity (Figure 24).

Age group was not found to be primarily associated with the classification of the slip. Thus, gait characteristics dominated the association with slip classification. However, even though younger and older subjects experienced hazardous slips at about the same rate (64% (7/11) for older subjects and 69% (11/16) for younger subjects), older subjects appeared to adopt "safer" gait styles, with shorter SLR, shallower FFA at heel strike, and slower FFAS. Thus, there may be some influence of age that is counteracted by the changes in gait characteristics seen in older adults. Some possibilities include other unmeasured gait characteristics, psychophysical differences related to concern about slipping that could affect the mental set in this experiment, biomechanical differences, or possible reflexive response differences. In addition, our older subjects were as a group slightly heavier than our younger subjects (increased BMI) which could be a covariate for future investigation. Deficiencies in reactive responses to slips have been cited as explanations for slips resulting in falls [88]; however, as PSV occurs within the first 200 ms after HS, it is unlikely that non-reflexive responses would influence slip hazard as defined in this research. Further research is needed to understand the interplay among initial gait characteristics, postural control responses, hazardous slips and aging.

This study's results were limited by the relatively small number of slips analyzed, one per subject; a necessity to avoid anticipation and learning effects [33]. Although study participants were requested to walk naturally and were given ample unperturbed practice trials, it is not possible to determine the effect of the laboratory environment and experimental conditions on subject responses to slips. Although we found no significant kinematic differences at heel strike between the slippery trial and preceding known dry trials, slip anticipation may have influenced all gait trials included in the testing session. Additionally, the older subject group was arguably not sufficiently old to impact general gait variables or may have been healthier than the general population as they were willing to volunteer for a slip study.

One of the potential long-term benefits of this study is its contribution to our understanding of the interplay among fundamental gait parameters, slip potential, and age. The

"human factors" involved in slipping are an important component that deserves increased attention. The results of this study suggest that hazardous slip potential can be reduced by modifying specific gait parameters. This finding may influence training regimens to reduce hazardous slips. Importantly, it appears that adjusting gait may be equally useful across the age groups tested here, although future research is needed to determine if the same associations hold for very old adults. This research will also significantly contribute to definitions of important human factors that may some day be incorporated into new methods of slip resistance testing. There is general agreement within the slip testing community that increasing the 'biofidelity' of slip resistance testing will improve the tests ability to define useful slip measures towards preventing falls. Further understanding of the relation of human gait parameters to slip hazard could be useful in this regard. Finally, the concept of using hazardous versus non-hazardous slips instead of falls and recoveries could benefit future studies investigating interactions of floors and human locomotion. Other human slip studies may want to include this concept in defining the impact of floor condition, age, etc on the potential for slip-related injurious, not only due to falls but also due to the larger responses required to recover from hazardous slips.

4.0 TRAILING LEG STRATEGIES IN RESPONSE TO SLIP PERTURBATIONS DURING GAIT

The incidence of falls is a well-acknowledged public health and occupational concern. Slips are recognized as a major contributor to falls. Slips were the most frequent event leading to fall and overexertion related injuries in the Swedish labor force [44] and were the most common fall initiating event for employees in the UK [55]. The US National Health Interview Survey questionnaire administered by the National Center for Health Statistics in 1997 revealed a clear majority (64%) of work-related falls were attributable to slipping, tripping, or stumbling and indicated that 43% of occupational same-level fatal falls were most commonly triggered by a slip [44]. According to the Bureau of Labor Statistics (2003), nearly 30% (28.7%) of workers that sustained injuries from slips and/or falls missed 31 days of work or more. Further, 14% of accidental deaths in the workplace were reportedly caused by falls [25]. De Laet and Pols [46] estimated that the annual direct cost of all fall-related occupational injuries in the U.S. alone was approximately six billion dollars. According to the Centers for Disease Control and Prevention, falls were the leading cause of injuries requiring hospitalization (22%) and were the second leading cause of fatalities in 2000 [52]. In addition, falls were the most significant mechanism leading to injury related medical costs, leading to lifetime medical costs of around $26.9 billion [52]. Slip recovery efforts have also been shown to contribute to high rates of overexertion injuries [45].

The risk of slip and fall accidents increases with age. A 10-fold increase in the incidence of falls was reported in the elderly (65+) compared to younger individuals (16-64) [129] and Lloyd and Stevenson [85] indicated that while slips and trips caused 32% of falls for young people, 67% of falls for the elderly were initiated by slips. Falls on the same level caused roughly 20% of all injuries to older workers as compared to around 10% for the general population with "floor and ground surfaces" listed as the most common source of non-fatal

injuries among workers in the 55 year and older age group [110]. In 2004, over one third (39%) of the occupational fatal fall victims were 55 and older [25], more than double that age group's share of the work force (16%) [24].

Just as the risk for slips and falls increases with age, so to does the severity of the outcome of these accidents. Falls are often listed among the leading causes of serious unintentional injuries, disability, and death among older adults [46, 73, 74, 92, 117]. Approximately 65% of all serious injuries (Injury Severity Score > 15) and 55% of deaths were attributed to falls for patients aged 65 years and over, compared to 11% and 7.5% in the younger population, respectively [125]. Fatality rates from falls showed a significant increase for workers as young as 45 to 54 years old [1]. Specifically, nearly half of the fatal falls in the US workforce occur in adults aged 45 years and older [132]. The CDC reported that the elderly (75+) experienced 5 times the risk of death due to falls than for any other age group in 2000 [52]. Additionally, Personick and Windau [110] suggested that older workers are at a greater risk of non-fatal injuries resulting from slips, even those not resulting in falls, due to overexertion during recovery attempts.

The simple task of walking on dry floors necessitates the performance of complex processes involved in the initiation of movement and balance maintenance. In the presence of slippery environments, preventing falls becomes more challenging, requiring appropriate biomechanical corrective reactions to recover from slip events. Thus, causes of slips and falls involve the interaction of complex environmental and human factors [57]. Environmental factors include the frictional properties of the foot-floor interface, material properties of walking surfaces/shoes and lighting. Human factors, often affected by aging, include gait biomechanics, sensory information processing, neuromuscular and vestibular mechanisms relevant to locomotion. Other human factors, less often investigated, include the perception of the danger of slipping.

Findings of biomechanical gait studies have been important in slips/falls prevention research [22, 61, 98, 109, 114, 116, 127]. (For a detailed review of the impact of experimental gait studies on slip/fall prevention research, the reader is referred to a review paper by Redfern et al. [113]). In addition to their contribution to the field of tribology, gait studies have improved our understanding of the complex relationship between gait biomechanics and slip-precipitated falls. For example, researchers have identified the frictional requirements

needed to prevent a slip during gait [22, 61, 114, 127]. Gait studies have also shown that kinematic variables such as heel velocity at heel contact and stride length/duration may also influence slipping risks [100, 102, 116].

Another important finding of experimental studies relates to the nature of corrective reactions generated in response to a slip. The body must generate a quick and effective corrective response to re-establish dynamic balance and to maintain upright posture while, for recoverable slips, continuing with the locomotion task. Corrective joint moments have been identified experimentally during gait on contaminated floors [32, 70, 128], however the causal relationship between the timing/magnitude characteristics of these responses and the severity of the slips has not been established, presumably due to the confounding factors that cannot be disentangled through experiments alone.

The results from standing posture studies provide a foundation of understanding for the relationships between perturbation and response for gait. Open-loop, pre-determined automatic postural responses have been proposed to result based on stimuli thresholds [66]. These responses, linked to perturbation magnitudes, have even been termed "strategies" [67, 78, 103]. More dynamic reactions to perturbed standing posture, including compensatory steps are likely more relevant to recovery efforts for perturbed gait. The objective of these stepping responses has been reported to be linked to stability – the dynamic relationship between the body's center of mass and foot placement [95]. Although strategies of response have been identified, these strategies are likely not open-loop, pre-determined motor programs but have been reported to be modulated based on the efficacy of response [3, 95, 105, 133]. The timing of responses relative to sensory input has also been reported, implicating both vestibular and proprioceptive input as likely triggers for response [3]. Finally, these standing posture studies have examined the effects of aging and support the hypothesis that older individuals likely respond to perturbations differently [95].

To better understand the risk of a falls that a given slip presents to a subject, the severity of slips, indicating elevated risk for falls, has been characterized as either hazardous or non-hazardous based on the horizontal velocity of the heel of the slipping foot [100]. Qualitatively, non-hazardous (NHAZ) slips end relatively quickly and are characterized by smaller (less than 1.0 m/s) peak horizontal velocities of the slipping foot (PSV) and shorter sliding distances (SD) (less than 10 cm) by definition. These NHAZ slips thus require relatively minor postural

responses for subjects to continue to walk with approximately normal gait. Hazardous (HAZ) slips, on the other hand, typically last longer and are typified by PSV greater than 1.0 m/s and SD greater than 10 cm. Although recovery from these larger hazardous slips may be possible, more aggressive postural responses appear to be required to avoid falls.

Given that younger and older subjects experienced HAZ slips at similar rates in the laboratory [87, 100] while older individuals fell more in the workplace [52], it was surprising to find that older adults utilized "safer" walking styles than younger adults, i.e., their gait was characterized by shorter step lengths and shallower foot-to-floor angles. Although unmeasured pre-slip gait parameters could explain this apparent contradiction, *it is also likely that differences in slip response could lead to more falls for older adults*. This chapter thus examines differences in the biomechanical responses to hazardous slips for older and younger subjects.

In addition, although recovery from HAZ slips is possible, falls are a likely outcome, perhaps as a direct result of the initial conditions of the slip (some slips may be so severe that recovery is not possible regardless of response) or perhaps due to inadequacy of the response. We propose that, regardless of age, differences in response may determine outcome (falls versus recoveries) for some HAZ slips where recovery is possible. Thus, the studies of biomechanical responses are key to potentially understanding the factors of fall recovery.

Finally, this research was performed to better understand of the dynamics of slip response. Clearly, the slipping leg, the trailing leg, and the upper body (including arms) all contribute, in a coordinated manner, to the complete postural response to HAZ slips [18, 32, 50, 97]. However, lower extremity responses, especially as related to slip dynamics, seem particularly relevant to recovery likelihood [32, 50, 97]. Thus, this study focuses on slipping and trailing leg responses to HAZ slips for younger and older subjects.

4.1 METHODS

This study included 13 older individuals aged 55 to 67 years old and 18 younger individuals aged 20 to 33 years old (Table 9). Written informed consent, approved by the University of Pittsburgh Institutional Review Board, was obtained prior to participation. Exclusionary criteria included a clinically significant history of neurological, orthopedic, cardiovascular and pulmonary

abnormalities as well as any other difficulties hindering normal gait. In addition, subjects were excluded if a clinical neurological examination revealed abnormalities that might affect balance.

Table 9: Study participant characteristics (means with standard deviations illustrated)

	Female	Male	Age	Height (cm)	Weight (kg)
Younger	10	8	23.9 (3.3)	171.1 (8.4)	69.7 (13.2)
Older	8	5	61.1 (3.7)	165.8 (7.7)	78.2 (11.8)

All participants wore the same brand/model of polyvinyl chloride hard-soled shoes with a ¾ inch thick heel. A harness system connected to an overhead trolley protected subjects from ground contact injuries in the event of irrecoverable losses of balance, but did not impede walking or slipping [61, 114]. Subjects were first allowed to practice walking along the gait path while the starting position was adjusted such that the participant appropriately (right foot on first plate, left foot on second plate) hit each force plate with one and only one foot. Room lighting were then dimmed to conceal the eventual application of contaminant onto the floor and additional practice trials were conducted. Participants were instructed to walk as naturally as possible at a self-selected comfortable pace throughout the experiment.

Prior to each recorded trial, subjects walked to the start of the gait path, faced away from the walkway, and listened to music via headphones for one minute to disguise any audible hints of contaminant application. At the end of each one-minute waiting period, subjects were instructed to turn around, to verify their set starting point, to focus on a target placed at eye-level on the far wall, and to wait for a researcher to signal them to start walking.

To ensure that participants walked as naturally as possible, they were informed that the first few trials would be non-slippery. Two or three dry trials were then collected ("baseline dry") ensuring that appropriate foot contact was maintained. Then, without the participant's knowledge, a diluted glycerol solution (75% glycerol, 25% water) was applied to the leading force plate and another gait trial was conducted ("unexpected slip"). The left foot was always the lead/slipping foot. The coefficient of friction of the shoe-floor interface was 0.53 and 0.03 for the dry and slippery surfaces, respectively, as measured with the English XL VIT Slipmeter ® (ASTM F1679) [5]. Only one unexpected slip per subject was recorded.

The experimental protocol was designed to produce unexpected slip perturbations. Previous research performed using the same protocol has shown that subjects do not alter their gait from their preceding dry trials for the unexpected slip trial [32]. Supporting this contention, the contact angle for the leading foot at heel strike was not significantly different from dry to slip ($p = 0.515$). This is a good indication that slip trials were truly unexpected based on previous research by Cham and Redfern [33] and Marigold and Patla [97], who reported that FFA was significantly shallower when subjects anticipate slippery conditions.

An eight M2-camera Vicon 612 motion measurement system (Oxford Metrics, Vicon Peak – UK) recorded 3 dimensional motion data at 120 Hz from seventy-nine reflective markers placed on the body and shoes while subjects stood in a static posture (Figure 25). Nineteen of these markers were then removed for subsequent dynamic trials during which subjects walked along an 8.5 m long vinyl-tiled walkway. Ground reaction forces were recorded at 1080 Hz, synchronized with motion data, from two Bertec type 4060a force plates embedded into the walkway. The surface of the trailing leg (right) force plate was 0.4 x 0.6 m. The surface of the leading leg (left) force plate was extended such that its dimensions were 0.75 x 0.4 m. The leading leg force plate was offset 0.15 m to the left and 0.15 m along the direction of travel from the trailing leg force plate.
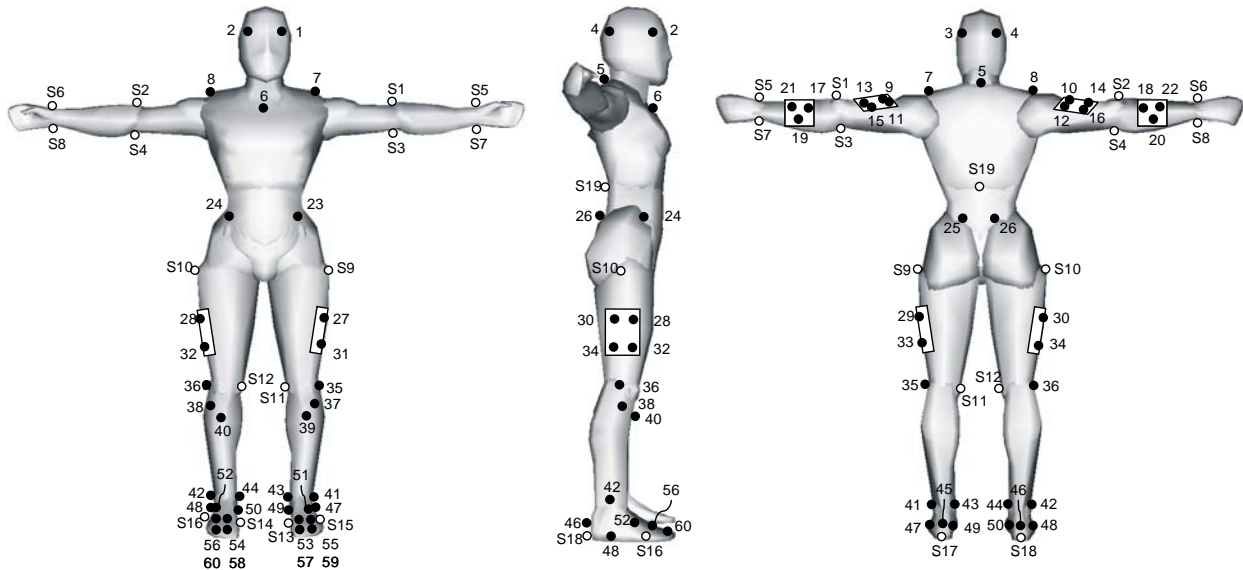
Figure 25: Reflective markers used for dynamic (solid) and static (solid and hollow) trials – static posture illustrated

Static markers removed for dynamic trials were virtually relocated based on their relative locations to markers on the same rigid bodies as determined from static posture (see thesis Section 2.0 for details). Heel strike (HS) and toe off (TO) were determined via analyses of changes in vertical ground reaction forces compared to unloaded force levels. HS was identified at the first normal force measurement greater than two standard deviations above baseline data that subsequently increased beyond 20 Newtons. HS determination was verified both by visual inspection of the normal force trace and through inspection of the heel marker (S17 and S18 in Figure 25) vertical velocity. TO was determined using the same method but with the data reversed in time and was verified by inspection of virtual toe markers' (average of markers 58 and 60 for the right toe and 57 and 59 for the left toe - Figure 25) vertical displacement. When force data was unavailable due to technical difficulties (two subjects) or when a subject's heel or toe was not directly over the force plate for HS and TO (about 10% of trials), these points were determined and verified using heel vertical velocity and toe marker vertical displacement only.

Slip severity, implying an increased risk of falling, was characterized as either hazardous (HAZ) or non-hazardous (NHAZ) based on the horizontal velocity of the heel of the slipping foot using the peak velocity of the slipping heel virtual marker (S17 in Figure 25). To accommodate transients occurring at slipping foot HS, peak slip velocity (PSV) was identified as the local maximum horizontal heel velocity occurring after 50 ms from HS. Hazardous slips were defined as having a PSV greater than 1.0 m/s [100]. Slip distance (SD) describes the heel marker's travel distance along the floor from heel strike [58] to a stable zero velocity. For hazardous slips, slip distance was determined by accruing the slipping heel virtual marker's travel distance from HS to the time when the subject either slipped beyond the contaminated force plate or he/she relied on the harness to regain balance as determined by visual inspection of the video record of the trial. A PSV based severity threshold was chosen rather than a SD threshold because SD determination was affected by slip termination mechanism while PSV was not [100]. However, an alternative SD severity threshold of 10 cm would have generated approximately equivalent slip severity classification results with only one non-hazardous slip trial being re-classified as hazardous.

72

4.2   DATA PROCESSING

Gait speed was determined using the center of mass location at heel strike of the trailing foot on its force plate and the next trailing foot heel strike (one stride). The distance, in the direction of travel, from the center of mass location at these two instances divided by the elapsed time between the two heel strike events yielded gait speed. Participants were instructed to walk at a self-selected purposeful pace. As illustrated in Figure 26, older subjects walked more slowly compared to younger subjects ($p = 0.03$), 1.35 (0.10) and 1.45 (0.13) m/s respectively, but no significant difference in gait speed between hazardous and non-hazardous slips was identified.
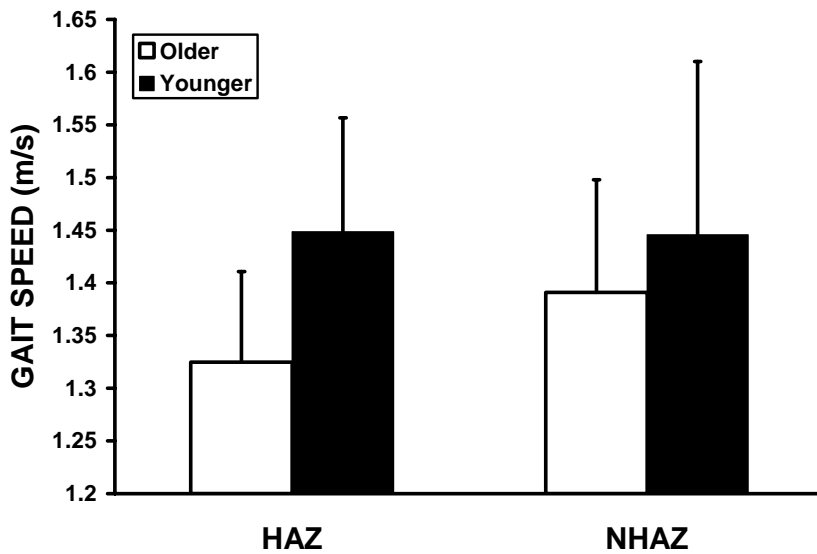
Figure 26: Gait speeds for younger and older subjects by slip severity

The HMBL (University of Pittsburgh) 15 segment, whole body model was utilized for lower extremity kinematic and kinetic variable determination based on marker and ground reaction force data (see Section 2.0 for details). This model includes toe, heel, shank, thigh, upper arm, and forearm segments for the right and left sides of the body, as well as pelvis, torso and head segments. Local coordinate systems (origins and axes) for each segment were defined using markers from that segment and were based definitions from by de Leva [47] whenever possible with reasonable effort extended to align local coordinate systems with ISB recommendations especially for the pelvis, thigh, shank, and feet segments [2, 9, 121, 142, 141].

Gender specific segmental masses (as a percentage of total body mass), center of mass locations, and radii of gyration were adapted from de Leva [47]. Joint moments have been reported in the coordinate system of the more proximal segment and have been normalized to body mass.

For comparative analyses (trial to trial, subject to subject, etc), all time dependent data were normalized to leading leg stance duration from baseline-dry trials. MATLAB's (The MathWorks, Inc.) `interp1` function interpolated from the original data (collected at 120 Hz) from contact (0%) to toe-off (100%) for the leading(slipping) foot using shape-preserving piecewise cubic interpolation.

The outcome of a slip was classified as a fall or recovery based on a fall criterion similar to that of Pai and colleagues [104, 107]. Specifically, a slip trial was classified as a fall if the mid point between hip joint centers dropped below 95% of its minimum height measured during normal gait. This fall definition agreed with visual inspection of recorded trials for all obvious falls and identified trials as falls that were otherwise difficult to visually classify as falls or recoveries.

Lower extremity kinetics were unavailable for two of the thirty-one subjects: for one of these subjects, force plate data was not collected while the other did not contact the force plates in a manner allowing inverse dynamics calculations to be performed. The first of these subjects was younger and responded to a HAZ slip with a FF strategy (see section 4.3.1) resulting in a fall. The second subject was also younger but responded to a NHAZ slip with a MIN strategy (see section 4.3.1) and recovered. Whenever possible these two subjects have been included in statistical analyses and plots that are unrelated to joint torques. In addition to the excluded data from these two subjects, force plate technical difficulties led to the exclusion of two trials from slipping leg torque-related analyses, one for an older subject who responded to a HAZ slip with a FF strategy (see section 4.3.1) and recovered and the other for a younger subject, who responded to a NHAZ slip with a MIN strategy (see section 4.3.1) and thus recovered. Finally, a single younger subject who responded to a HAZ slip with a MID strategy (see section 4.3.1) and fell walked much more aggressively compared to other subjects (larger, faster steps) and had a slip characterized by a peak slip velocity almost twice that of the next fastest slip. This perturbation was deemed to be significantly different from that experienced by other subjects. Thus, this individual was classified as an outlier and was excluded from further analyses.

4.3   RESULTS

Responses to slips were categorized, based on trailing leg dynamics, into four discrete strategies termed minimum (MIN), foot-flat (FF), mid-flight (MID), and toe-down (TD).   This results section first qualitatively describes these response strategies and then reports quantitative analyses of relevant descriptive parameters.   Sagittal plane kinematics and kinetics for the slipping and trailing leg are then presented (Figure 30 and Figure 31). Key parameters of leading and trailing leg hip and knee torques were identified and their relationships to response strategy, age group, and slip outcome are explored.   Finally, the relationships among response strategy, age group, slip outcome, and continuous measures of slip severity are reported.

4.3.1   Observed Response Strategies

Four observed response strategies are qualitatively described in the following sections.   These strategies were identified primarily through observations of the postural dynamics of the trailing leg; specifically, trailing foot orientation at the next ground contact occurring after toe-off.

4.3.1.1 Minimum   The minimum response strategy (MIN) was similar to baseline walking on the non-slippery surface (i.e. dry gait).   Most subjects that had NHAZ slips utilized this strategy (Table 10).   No trials with MIN strategies resulted in falls and, although some did result in other observable responses to the slip (e.g., arm responses), these slips typically ended without the subjects appearing to substantially alter their gait.

75

4.3.1.2 Foot-Flat Foot-flat (FF) responses were typified by the entire shoe sole of the trailing foot contacting the ground either parallel with or slightly behind the slipping foot. The trailing leg then remained in contact with the ground for the duration of the slip for HAZ slips. For NHAZ slips, the trailing foot briefly contacted the floor (a "tap") and then continued with flight, similar to a more typical gait cycle. This strategy was utilized by both older and younger subjects resulting in recoveries for NHAZ slips and in both falls and recoveries for HAZ slips (Table 10).

4.3.1.3 Mid-flight The mid-flight strategy was typified by the sole of the toe segment from the trailing foot contacting the floor parallel to the ground while the heel segment remained slightly elevated: the trailing foot did not become horizontal as the slip progressed. This strategy was utilized, only during HAZ slips, by both older and younger subjects resulting in both falls and recoveries (Table 10). Ground contact for this strategy occurred more quickly and more posteriorly with respect to the slipping foot compared to the FF strategy.

4.3.1.4 Toe-Down Toe-down (TD) responses were typified by the tip of the toe (as opposed to the sole) contacting the floor with the foot inclined substantially, immediately after trailing foot toe-off. This strategy occurred exclusively for HAZ slips and always resulted in falls (Table 10). The immediacy of toe contact for this strategy dictated more posterior and faster responses compared to both FF and MID responses.

Table 10: Severity, age, and response strategy summary

Severity	Strategy	N Young	N Old	N Total
NHAZ	MIN	6	3	9
	FF	0	2	2
	MID	0	0	0
	TD	0	0	0
	Total	6	5	11
HAZ	MIN	0	0	0
	FF	5	3	8
	MID	6	3	9
	TD	1	2	3
	Total	12	8	20
	Total Slips	18	13	31

4.3.2   Response Strategy Characterizations

Hazardous (HAZ) trials were associated with FF, MID, and TD strategies (Table 10). For all HAZ trials, flight phase was interrupted with the trailing foot contacting the ground prematurely, behind or even with the leading foot. The leading foot may or may not have been slipping at the instant of this subsequent trailing foot touch down. Flight time was defined as the elapsed time from trailing leg toe off (TO) to the next trailing foot ground contact (Figure 27). The identified response strategies had different flight times. Mean flight times for MIN responses were not significantly different from baseline dry flight times ($p = 0.45$). ANOVA indicated a significant difference in flight time across strategies when all responses strategies were considered ($p < 0.001$) and when only hazardous trials were considered ($p < 0.001$) (Figure 27). Post-hoc Student's t-tests revealed that MIN flight times were statistically the longest, followed by FF ($p < 0.001$), MID ($p \leq 0.01$), and TD ($p < 0.001$), which was as expected based on qualitative observations (Figure 27A). These results were also verified when only HAZ trial flight times were compared (Figure 27B). In Figure 27, standard deviations are illustrated. Statistically different flight times are indicated with *.
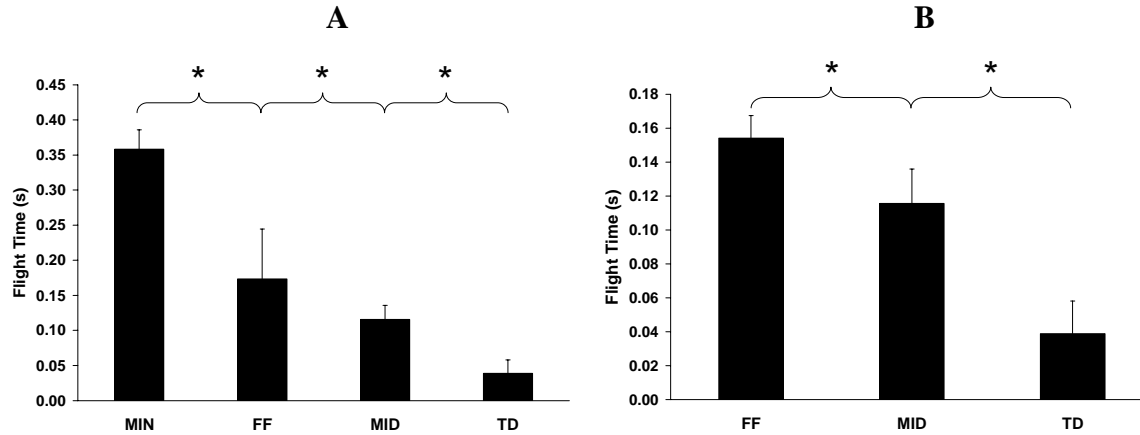
Figure 27: Trailing foot flight times – from toe off to subsequent ground contact – A) for all trials and B) for hazardous trials only.

Qualitative observations of trends for flight distance and foot orientation at subsequent ground contact for the trailing leg were verified through statistical analysis. Flight distances were different across strategies ($p < 0.011$) (Table 11). Post-hoc Student t-tests showed all distances significantly different from each other ($p < 0.01$) with the shortest distance for TD responses, longer distances for MID responses, longer still for FF responses, and longest for MIN responses. Flight distances for MIN responses were less than baseline dry flight distances ($p < 0.01$) indicating that subjects took shorter steps after small slips even though the kinematics looked qualitatively the same as the non-slip dry trials.

Trailing leg foot-to-floor contact angle defined as the sagittal plane angle between the foot and the floor (positive with the heel elevated) at the end of flight, decreased from TD to MID ($p \leq 0.01$), from MID to FF ($p \leq 0.01$), and from FF to MIN ($p < 0.001$) as determined using Student's t-tests of pair wise comparisons. Although observations of FF responses suggested that the trailing foot contacted the floor roughly parallel to the surface, the foot was actually oriented at about 26 degrees from horizontal (heel higher than toe) at the instant of initial trailing foot contact. For FF responses, the trailing foot quickly became parallel with the floor after initial contact. For the MID and TD strategies, the trailing foot remained elevated throughout the trial. The contact angle for MIN slip responses was significantly greater than baseline dry ($p = 0.01$) indicating that, in addition to taking significantly shorter steps after small slips, subjects also contacted the floor with the trailing foot closer to horizontal (Table 11).

78

Characteristics beginning with N in Table 11 report values that have been normalized to baseline dry gait. Across all strategies, contact angles decreased as flight time increased, as shown in Figure 28 (positive rotations indicate an elevated heel).

Table 11: Response strategy characteristics, means, and standard deviations

STRATEGY	BASELINE DRY	MIN	NHAZ FF	FF (NHAZ & HAZ)	HAZ FF	MID	TD
Flight Time (s)	0.38 (0.03)	0.36 (0.03)	0.23 (0.14)	0.17 (0.07)	0.15 (0.01)	0.12 (0.02)	0.04 (0.02)
N Flight Time (s/s)	-	0.98 (0.07)	0.66 (0.37)	0.48 (0.21)	0.41 (0.06)	0.30 (0.07)	0.10 (0.06)
Flight Distance (mm)	1403 (137)	1320 (80)	810 (589)	659 (291)	603 (92)	446 (94)	115 (64)
N Flight Distance (mm/mm)	-	0.96 (0.04)	0.59 (0.37)	0.47 (0.19)	0.43 (0.07)	0.31 (0.08)	0.08 (0.05)
Contact Angle (deg)	-28.2 (5.3)	-10.4 (15.7)	4.1 (9.7)	19.8 (17.4)	25.7 (16.1)	39.9 (13.1)	70.7 (4.2)
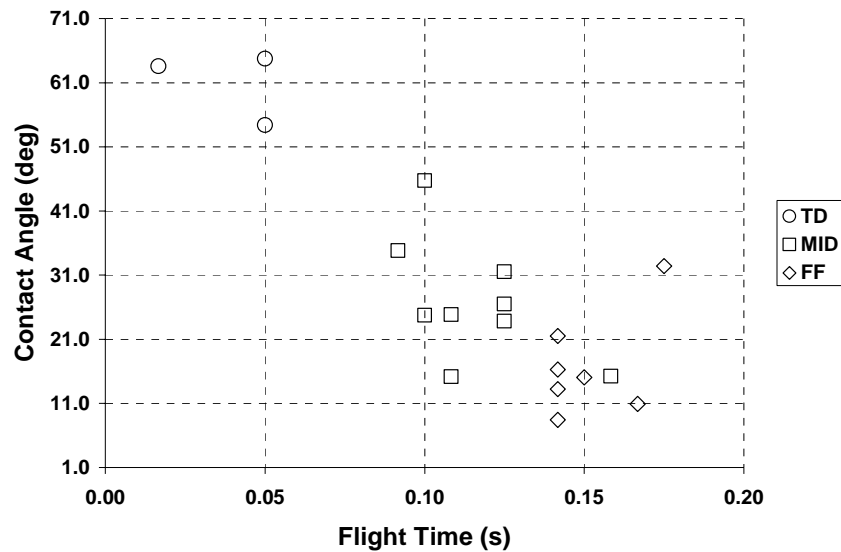
Figure 28: Trailing foot sagittal contact angle with the floor versus flight time for hazardous (PSV > 1.0 m/s) trials

Peak slip velocity (PSV) of the leading leg was related to the response strategy of the trailing leg, with significant differences in PSV across strategies ($p < 0.001$). Post-hoc Student t-tests revealed that PSV for MIN responses were associated with the slowest PSVs while TD responses were associated with the fastest PSVs. When only HAZ trials were considered, the relationship between response strategy and PSV did not reach significance ($p = 0.11$).

The relationship between the response strategy used and slips was explored with another measure of slip severity, termed the Slip Velocity Threshold (SVT). SVT was defined as the

time relative to heel strike at which the slipping velocity reached a threshold of 1 m/s. SVT is thus related to the acceleration of the slipping foot. A faster SVT results from a greater acceleration of the slipping foot after contact with the floor. SVT is a continuous measure of severity for HAZ slips, with shorter SVT implying increased severity of the slip. ANOVA of response strategy versus SVT did not show a significant relationship (p=.33) (Figure 29). The finding that a relationship between strategy and SVT was not identified indicates that slip severity alone does not determine response strategy for HAZ slips A contrast was performed to test the hypothesis that SVT was significantly different between with FF and MID combined compared to TD. This contrast showed a significance level of $p = 0.056$, indicating that the relationship approached significance.
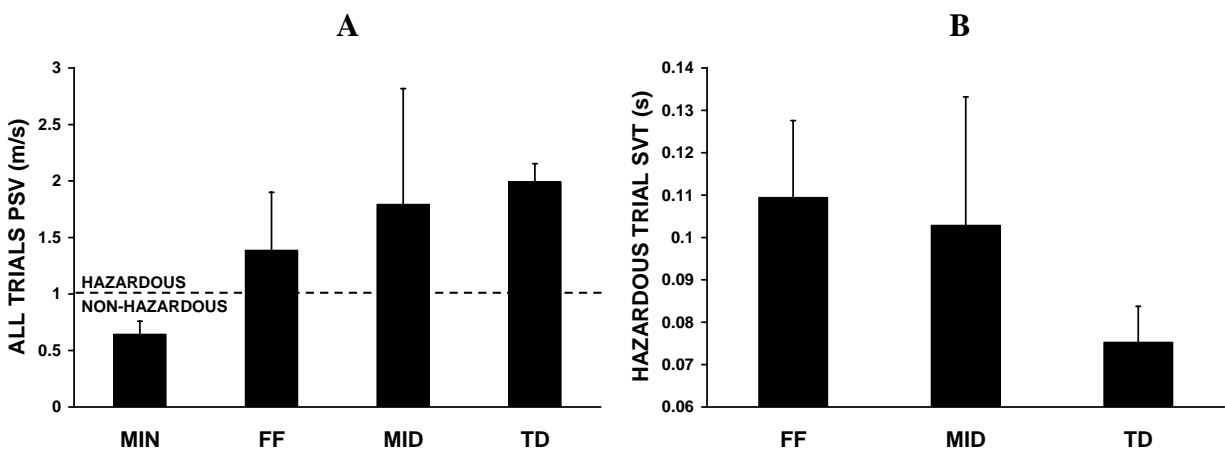
Figure 29: A) Relationship between peak slip velocity and response strategy for all slip trials (FF includes both HAZ and NHAZ slips) and B) Relationship between slip velocity threshold time and response strategy for hazardous slip trials – standard deviations illustrated

4.3.3   Biomechanical Responses to Slips

To further examine postural response strategies for both HAZ and NHAZ slips, lower extremity kinematics and kinetics were examined. Typical examples of hip, knee, and ankle flexion/extension joint angles and torques for the leading/slipping (left) leg are presented in Figure 30 for all four strategies. Similar trailing (right) leg curves are presented in Figure 31. All plots illustrate variables from both an unexpected slip trial and baseline dry trial from the

same-subject. Each strategy's response resulted from a different subject as only one unexpected slip response per subject was recorded. While the MIN example illustrates a response to a NHAZ slip, the FF, MID, and TD examples depict responses to HAZ slips. Among the HAZ slip examples, the FF response resulted in a recovery while the other two strategies resulted in falls. These figures will be referred to in the subsequent descriptions of the biomechanical responses.
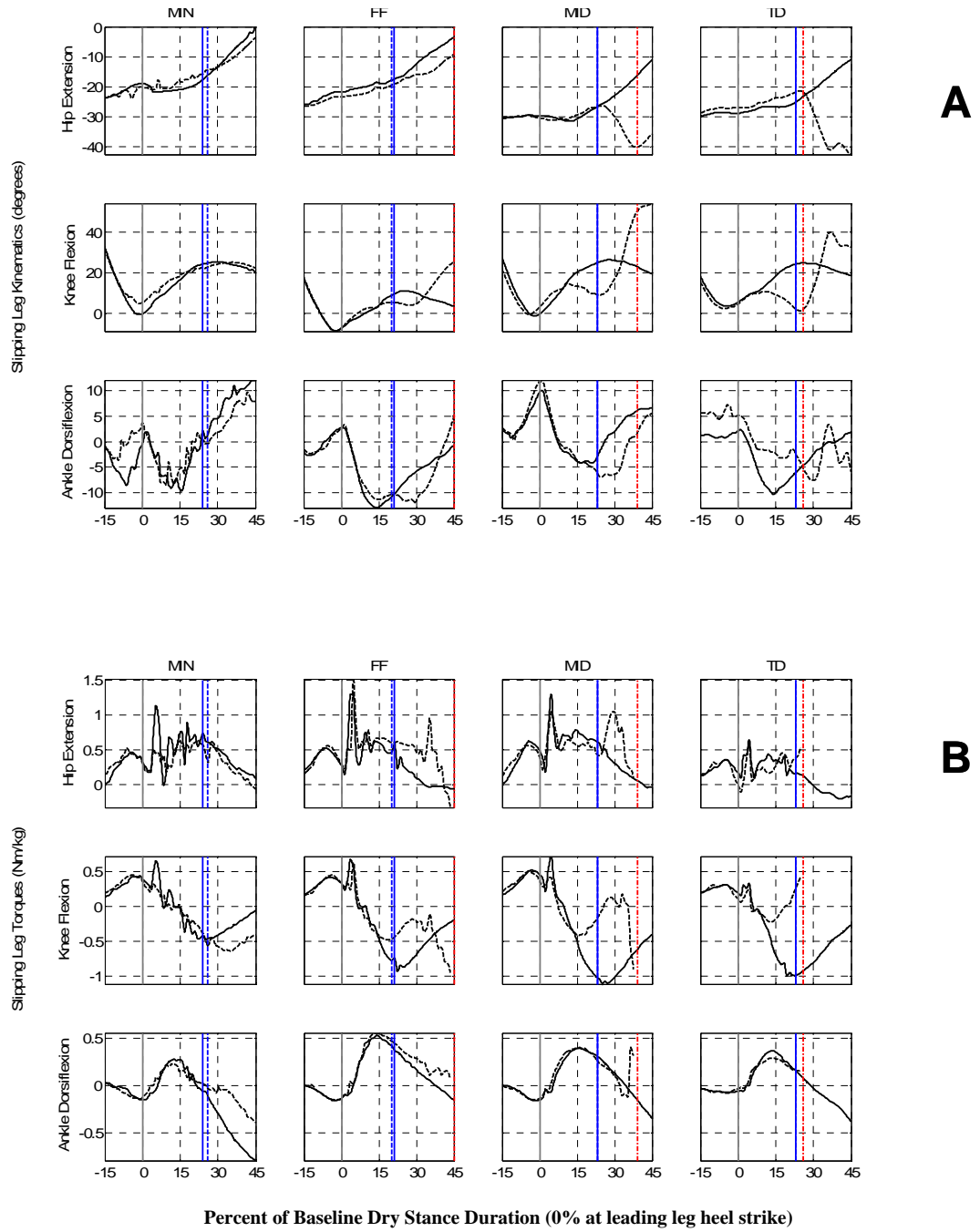
Figure 30: Typical flexion/extension kinematics A) and kinetics B) of the slipping leg for four slip response strategies
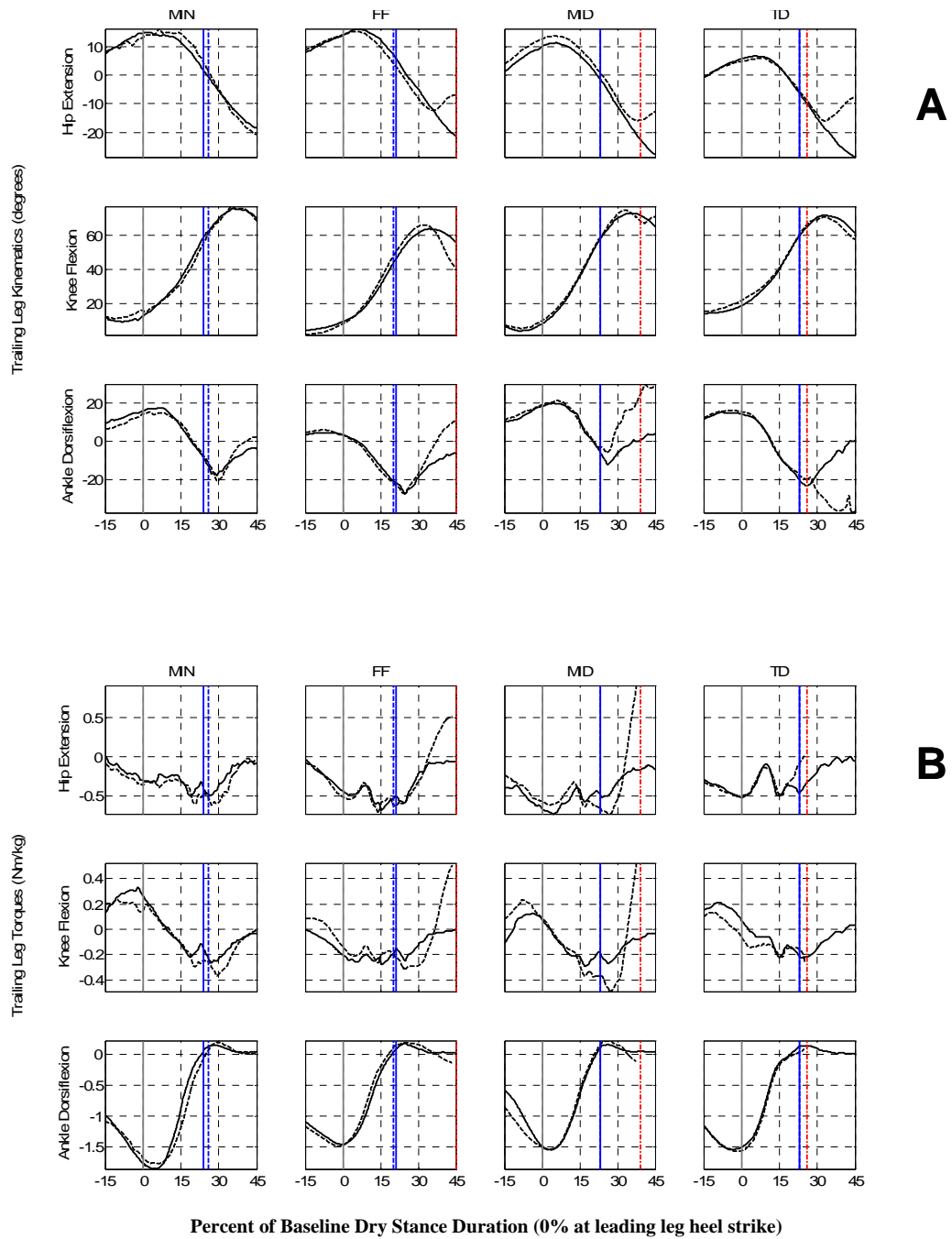
Figure 31: Typical flexion/extension kinematics A) and kinetics B) of the trailing leg for four slip response strategies

In Figure 30 and Figure 31 ordinate labels indicate positive values. All plots have been time normalized to leading foot stance duration from baseline dry trial. Solid traces depict baseline dry trial values and dashed traces illustrate slip trial values from the same subject. The solid gray vertical line at 0% corresponds to leading leg heel strike (HS) for both baseline dry and slip data. The blue vertical lines indicate trailing foot TO for baseline dry (solid) and slip (dashed) trials – solid obscures dashed lines for MID and TD examples. For FF, MID, and TD examples, the red, dash-dot vertical line indicates the trailing foot's subsequent ground contact for the slip trial. Torque traces for slip trials terminate at this red vertical line due to inverse dynamics calculation difficulties. Joint angles are relative to upright standing posture and joint torques have been normalized to subject body mass.

4.3.4 Joint Torque Analyses of Slip Responses

Responses to slips were characterized through parametric analyses of the left/slipping and right/trailing hip and knee torques. For these four torques, a pattern was observed for typical responses to slips consisting of initial transients due to leading foot contact with the floor, followed by a passive torque component and, for some trials, an active torque component. The passive component is defined as the small changes in the torque response for slips compared to dry trials due to slip induced changes in posture. Passive response components for knee torques are identifiable in Figure 30B as the portion of the slip data (dashed), deviating from dry data between 12% and 15% of stance for FF, MID and TD responses and leading up to a peak extensor moment. The active component of response is identified by large changes in torque compared to baseline, indicative of an attempt by the subject to alter postural dynamics [31]. Active components were significantly different from normal dry gait. In Figure 30B, active responses are identifiable as the rapidly changing torques occurring after a peak extensor moment at about 15% of stance, again for FF, MID and TD responses.

Table 12 summarizes the frequency of passive and active components observed by joint and strategy. Note that for NHAZ slips, active components of response were commonly not observed. Further, passive components of response were commonly not observed for leading and trailing leg hip torques. Trials included in Table 12 as "Missing Data" rows indicate missing data due to technical issues.

Table 12: Observed components of response summary

STRATEGY	RESPONSE	LEFT HIP		LEFT KNEE		RIGHT HIP		RIGHT KNEE	
		PASSIVE	ACTIVE	PASSIVE	ACTIVE	PASSIVE	ACTIVE	PASSIVE	ACTIVE
MIN	Observed	4	0	6	5	7	3	7	5
	Not Observed	2	6	0	1	0	4	0	2
	Missing Data	2	2	2	2	1	1	1	1
NHAZ FF	Observed	2	0	3	1	3	3	3	3
	Not Observed	1	3	0	2	0	0	0	0
	Missing Data	0	0	0	0	0	0	0	0
HAZ FF	Observed	6	5	6	6	6	7	6	7
	Not Observed	0	1	0	0	1	0	1	0
	Missing Data	2	2	2	2	1	1	1	1
MID	Observed	4	9	9	9	7	9	9	9
	Not Observed	5	0	0	0	2	0	0	0
	Missing Data	0	0	0	0	0	0	0	0
TD	Observed	2	3	3	3	3	3	3	2
	Not Observed	1	0	0	0	0	0	0	1
	Missing Data	0	0	0	0	0	0	0	0

Three parameters for each joint were identified to characterize the passive and active components of torque response. The first parameter, passive onset, identified the initiation of the passive component of response and was typically associated with a persistent change (from baseline) in the slope of the torque of interest. Passive onset and the second parameter, active onset, were both measured relative to slipping leg heel strike. Active onset identified the initiation of the active component of response and was typically associated with a local maximum or minimum torque. The third parameter, active slope, characterized the rate of change of a given joint torque occurring after active onset. These three parameters are illustrated in Figure 32.

Figure 32 was produced using baseline and slip trial hip and knee torque data from a typical young male subject who experienced a HAZ slip, responded with a MID strategy, and fell. Transient effects due to leading leg heel strike are readily observable for the leading leg hip and knee torques within the first 0.05 seconds. In addition, the onset of the passive component (passive onset, up pointing triangle), the onset of the active component (active onset, down pointing triangle), and the slope of the active response (active slope, red line connecting two circles) are shown for leading and trailing leg hip and knee torques. Figure 32 also illustrates

temporal relationships between leading leg heel strike (time = 0 s) and trailing leg toe-off and subsequent ground contact (flight time) using blue vertical lines. Further, slip progression for a HAZ slip is indicated in Figure 32 by green vertical lines at the time to the slip velocity threshold (SVT), the time at which the peak slip velocity was reached (PSV), and at the end of the slip (although the leading foot did stop sliding in this example, it may have stopped only after reaching the end of the contaminated surface). The vertical red line in Figure 32 indicates the time at which the conditions for a fall were met for this trial, i.e., the subject's hips dropped below 95% of their minimum height during baseline gait.
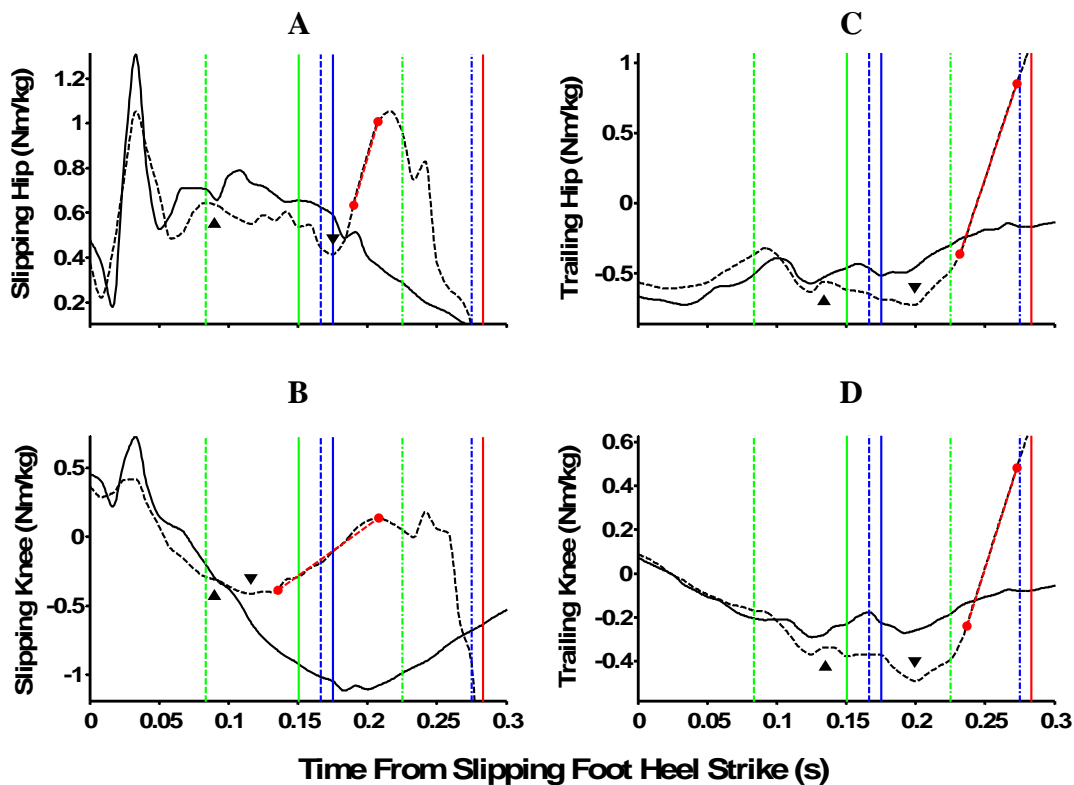
Figure 32: Slipping leg (A and B) and trailing leg (C and D) hip and knee joint torques for a typical HAZ slip with a MID response strategy, leading to a fall

In Figure 32, the displayed 0.3 seconds corresponds to 50 % of baseline dry stance duration for this subject. All torques are normalized to body mass (Nm/kg). Positive hip torques indicate extension moments while positive knee torques indicate flexion moments. Solid black lines are dry trial torques while dashed black lines are slip trial torques. The vertical blue lines

indicate trailing leg toe off for dry (solid) and slip (dashed) trials as well as touch down (dash-dot) of the trailing foot. The vertical green lines indicate when heel slip velocity exceeded the 1.0 m/s threshold (dashed), reached its peak (solid), and when slipping ended (dash-dot). The vertical red line indicates when the hip height criteria for a fall was met. Upward pointing triangles identify passive onset while downward pointing triangles indicate active onset. Active slopes are characterized by dashed red lines terminated with solid red circles.

The following sections describe typical NHAZ and HAZ torque profiles for the joints of interest. Then, for each joint, the relationships between the parameters of response (passive onset, active onset, and active slope) and strategy (MIN, FF, MID, TD), age group (younger and older), and outcome (falls and recoveries) for each joint are presented.

Table 13 indicates the passive and active onsets and active slopes to be discussed and analyzed in the following sections. Onsets in Table 13 are presented both as time (seconds) from slipping leg heel strike and as percentages of stance duration to allow comparisons between subjects with different gait speeds. Missing values in Table 13 indicate that a component of response was not typically observed for a particular joint or strategy (Table 12) and thus was not analyzed. Significant findings for HAZ slips as reported in the following sections are summarized in Table 14.

Table 13: Average and standard deviations for passive onsets (for trials with a passive component of response) and both active onsets and active slopes (for trials with an active component of response) to accompany parametric analyses of response torques

	STRATEGY	MIN	NHAZ FF	HAZ FF	MID	TD
LEFT HIP	Passive Onset (s)	0.10 (0.01)	0.10 (0.03)	-	-	-
	Passive Onset (%)	0.15 (0.02)	0.17 (0.04)	-	-	-
	Active Onset (s)	-	-	0.19 (0.02)	0.17 (0.03)	0.17 (0.01)
	Active Onset (%)	-	-	0.29 (0.04)	0.25 (0.05)	0.24 (0.03)
	Active Slope (Nm/kg/s)	-	-	6.8 (5.3)	8.0 (8.3)	17.5 (6.5)
LEFT KNEE	Passive Onset (s)	0.10 (0.02)	0.07 (0.01)	0.09 (0.02)	0.09 (0.01)	0.07 (0.01)
	Passive Onset (%)	0.15 (0.02)	0.12 (0.02)	0.13 (0.02)	0.13 (0.02)	0.10 (0.01)
	Active Onset (s)	-	-	0.13 (0.01)	0.12 (0.02)	0.10 (0.00)
	Active Onset (%)	-	-	0.19 (0.02)	0.17 (0.03)	0.14 (0.01)
	Active Slope (Nm/kg/s)	-	-	5.2 (0.3)	6.6 (6.4)	7.3 (0.8)
RIGHT HIP	Passive Onset (s)	0.16 (0.02)	0.15 (0.01)	-	-	-
	Passive Onset (%)	0.24 (0.02)	0.25 (0.03)	-	-	-
	Active Onset (s)	-	-	0.19 (0.04)	0.18 (0.03)	0.16 (0.02)
	Active Onset (%)	-	-	0.28 (0.05)	0.27 (0.03)	0.23 (0.02)
	Active Slope (Nm/kg/s)	-	-	21.8 (11.1)	29.8 (10.6)	22.3 (12.2)
RIGHT KNEE	Passive Onset (s)	0.17 (0.02)	0.15 (0.01)	0.14 (0.02)	0.15 (0.03)	0.13 (0.01)
	Passive Onset (%)	0.25 (0.03)	0.26 (0.02)	0.21 (0.03)	0.23 (0.05)	0.18 (0.03)
	Active Onset (s)	-	-	0.22 (0.03)	0.20 (0.03)	0.19 (0.01)
	Active Onset (%)	-	-	0.33 (0.04)	0.30 (0.03)	0.26 (0.02)
	Active Slope (Nm/kg/s)	-	-	15.3 (6.7)	18.0 (5.3)	5.4 (11.0)

4.3.4.1 Slipping Leg Hip Torques Hip torques of the slipping leg for NHAZ slips differed from those during baseline dry trials. For baseline dry trials, left hip torques (see Figure 30B and Figure 32A) included an extension torque peak occurring just after HS that gradually decreased, at a nearly constant rate, crossing zero and becoming flexion torques at between 35% and 50% of stance. For NHAZ slips, transients in leading leg hip torque were reduced in magnitude compared to baseline and occurred to about 10% of stance. These transients then lead to an apparent delay in the onset of the steady reduction in extension torque as observed for unperturbed gait. Although delayed, the rate of change in hip torque after passive onset for NHAZ slips was similar to the rate of change for baseline dry trials (Figure 32A) The active components of hip response to the slip (active onset and active slope) were not identifiable for MIN or FF responses to NHAZ slips (Table 12 and Table 13). However, later in the gait cycle (> 45% of stance), changes in slipping leg hip torques compared to dry gait (slip torques were

similar in shape but compressed in time during swing phase) were observed for both MIN and NHAZ FF responses, presumably related to the resumption of normal gait.

Slipping leg hip torques for HAZ trials typically included an active component of response, initiated from a local extension torque minimum at around 25% of stance (active onset). From active onset forward, hip torque for HAZ trials deviated dramatically from baseline torques, rapidly became more extensive at a steady rate (active slope) until the slip ended, the trailing leg contacted the floor, or the subject slipped off of the force plate or fell into the harness (see Figure 32A) making torque estimates unreliable. These extensive torques acted to resist the postural changes of the slipping leg and bring the foot back towards the body.

ANOVA analyses did not reveal a clear relationship between response strategy and the parameters (passive onset, active onset, or active slope) of response for slipping leg hip torque for HAZ slips. However, a trend ($p = 0.09$) relating strategy and slipping leg hip torque active slope was observed with post-hoc Student's t-tests revealing steeper active slopes for TD responses compared to FF and MID responses ($p = 0.03$ and $p = 0.02$ respectively). Neither age group (young/old) nor outcome (fall/recovery) were found to be significantly related to these same parameters of response.

4.3.4.2 Slipping Leg Knee Torques Knee torques of the leading leg (see Figure 30B and Figure 32B) for NHAZ slips varied from the torques determined for baseline dry trials. Knee torque during the dry trials transitioned from peak flexion, which occurred just prior to heel strike, to peak extension, which occurred at around 25% of stance, at an approximately constant rate. Some transient effects were evident immediately after heel strike (< 10 % of stance). These transients appeared to have smaller magnitudes for slip trials compared to dry. Responses to NHAZ slips had slightly less extension in torque compared to baseline dry (termed this difference the passive component), initiating between 10% and 15% of stance (passive onset). Although NHAZ slips typically ended prior to peak extension torque, slipping leg knee torques approached peak extension at slower rates than for dry gait.

Slipping leg knee torques for HAZ slips were initially similar to NHAZ slips: passive response began at passive onset and followed a similar steady increase from extension torque toward more flexion but at a slower rate than for dry. For HAZ slips however, the increase in extension torque was quickly reversed at active onset with active responses to the slip causing a

89

steady reduction in knee torque at a near constant rate (active slope), leading to flexion moments for more extreme slips (see Figure 32B).

ANOVAs investigating the relationships between slipping leg knee torque passive onset, active onset, and active slope with strategy (FF, MID, and TD) for HAZ trials identified a significant relationship between active slope and strategy ($p = 0.02$) with TD responses having steeper active slopes than MID and FF ($p < 0.01$ for both). Although not significant, a trend ($p = 0.06$) for FF and MID responses to have later passive onsets as a percentage of baseline dry stance compared to TD responses ($p = 0.02$ and $p = 0.01$ respectively from post-hoc Student's t-tests) was observed. Age group (young/old) was not found to be statistically related to any slipping knee torque parameters of response (passive onset, active onset, or active slope). Active slope was found to be significantly related to outcome ($p < 0.01$) with falls characterized by torques changing from extension toward flexion faster compared to recoveries (Figure 33). Positive slopes indicate torques becoming less extensive or more flexive. Active slope for TD responses was significantly greater compared to FF and MID responses ($p = 0.02$ and $p = 0.01$ respectively). Recoveries had significantly lower active slopes compared to falls ($p < 0.01$).
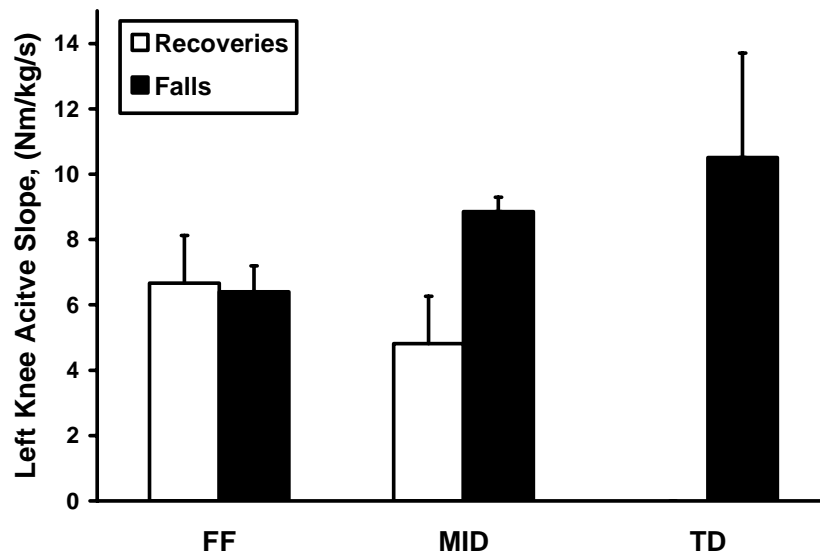
Figure 33: Relationship among outcome, strategy and slipping leg knee active slope (standard deviations illustrated)

4.3.4.3 Trailing Leg Hip Torques Trailing leg hip torques for NHAZ slips also differed from baseline dry, primarily due to passive dynamics. For baseline dry gait, trailing leg hip torques (Figure 31B and Figure 32C) followed a typically periodic trend with peak flexion moments occurring within the first 10% of leading leg stance (just prior to trailing leg toe off) and peak extensor moments occurring near trailing leg heel strike. Trailing leg hip torques followed this same pattern for NHAZ slip responses to about 15% of leading leg stance (passive onset), with slip perturbation tending to delay peak flexion. Once peak flexion was reached for NHAZ slips, torques progressed toward peak extension more quickly than for dry for those trials identified as having an active component of response. Whether an active component of response was observed for a NHAZ slip or not, differences in trailing leg hip torques were observed later in stance which compensated for any slip-induced delays and allowed normal gait to resume quickly.

Trailing leg hip torques for HAZ slip responses followed a pattern that was initially similar to baseline dry gait and NHAZ slips (Figure 31B and Figure 32C). When passive onset was identified, it occurred at around 20% of leading leg stance. After passive onset, these torques briefly became more flexive for HAZ slips than for baseline dry; typically, reaching peak flexion (active onset) at between 21% and 35% of leading leg stance. When passive onset was not identifiable, leading leg hip torques followed a similar trend as observed for baseline dry gait until active onset. After active onset, these torques typically changed quickly at a nearly constant rate (active slope), becoming extensive torques.

A significant relationship ($p < 0.001$) between trailing leg hip torque active onset and strategy was identified for HAZ slips, with TD responses characterized by earlier active onsets than MID or FF ($p < 0.001$ for both). Passive onset was not significantly related to response strategy. Neither age group nor outcome were significantly related to passive onset, active onset, or active slope for the trailing leg hip torque.

4.3.4.4 Trailing Leg Knee Torques Trailing leg knee torques for NHAZ slips followed a pattern similar to baseline dry gait until about 20% of leading leg stance (passive onset). Baseline dry trailing leg knee torques typically progressed from near zero at leading leg heel strike to a local extensor maximum at about 20% of leading leg stance - about the same time as trailing leg toe off. From that extensor maximum, trailing leg knee torques typically progressed

to a maximum flexion preparing for trailing leg heel strike at about 75% to 80% of leading leg stance for dry gait and the nearly sinusoidal pattern then repeated itself (Figure 30B and Figure 32D). Typically, trailing leg knee torque remained near maximum extension in response to NHAZ slips until active onset occurred at between 21% and 35% of stance. Active responses to NHAZ and HAZ slip perturbations were characterized by an increased active slope for trailing leg knee torque compared to same-subject dry gait. The active response produced torques that progressed from maximum extension toward maximum flexion.

ANOVAs with strategy as the main effect revealed a significant relationship with passive onset for the trailing leg knee torque ($p = 0.03$) with post-hoc Student t-test revealing that MID responses had later passive onsets compared to FF or TD ($p = 0.02$ and $p = 0.01$ respectively) for HAZ trials. A trend ($p = 0.08$) relating active onset of the trailing leg knee torque to strategy was observed with post-hoc analyses indicating that TD responses had earlier active onsets than FF responses ($p = 0.02$). There were no significant relationships between trailing leg knee parameters of response and age group or outcome.

4.3.4.5 Joint Torque Parameters and Slip Severity The relationships between severity of slips (both SVT and PSV) and joint torque response parameters (Passive onset, active onset, and active slope for the hip and knee torques) were explored using regression analyses. A summary of identified significant relationships is presented in Table 6. Slipping leg knee torque active onset and SVT were related ($p = 0.02$), with faster SVT corresponding to faster active onsets. A relationship between slipping leg knee torque active onset and PSV did not reach significance ($p = 0.06$). Slipping leg knee torque active slope was found to be related to SVT ($p < 0.01$) with faster SVT leading to steeper active slopes. A significant relationship between slipping leg knee active slope and PSV was identified ($p = 0.04$). No other parameters of response for any of the joints studied were found to be significantly related to SVT or PSV.

JOINT	PARAMETER	STRATEGY	AGE	OUTCOME	SVT (S)	PSV (m/s)
Slipping Hip	Passive Onset (s)	-	-	-	-	-
	Active Onset (s)	-	-	-	-	-
	Active Slope (Nm/kg/s)	**TD > (FF & MID) †**	-	-	-	-
Slipping Knee	Passive Onset (s)	-	-	-	-	-
	Active Onset (s)	-	-	-	**PROP**	**INV PROP †**
	Active Slope (Nm/kg/s)	**TD > (FF & MID)**	-	**F > R**	**INV PROP**	**PROP**
Trailing Hip	Passive Onset (s)	-	-	-	-	-
	Active Onset (s)	**TD < (FF & MID)**	-	-	-	-
	Active Slope (Nm/kg/s)	-	-	-	-	-
Trailing Knee	Passive Onset (s)	**MID > (FF & TD) ‡**	-	-	-	-
	Active Onset (s)	**TD < FF †**	-	-	-	-
	Active Slope (Nm/kg/s)	-	-	-	-	-

† = Trends (0.05 < p < 0.1) not reaching significance
‡ = Trend identified for passive onset normalized to stance duration
PROP indicates that a parameter was proportionally related to the severity measure
INV PROP indicates an inversely proportional relationship

4.3.5 Slip Severity, Strategy, Age Group and Outcome

Outcome (fall or recovery) was associated with SVT for HAZ slips (p<0.001). Horizontal velocity of the slipping foot for falls reached SVT sooner than for recoveries. Similarly, a significant relationship between outcome and PSV ($p < 0.001$) was identified with falls having higher PSV than recoveries. SVT occurs prior to any observed torque response, so therefore indicates the magnitude of the perturbation, while PSV combines the perturbation magnitude with initial response effects. SVT and PSV are related, with increased PSV associated with decreased SVT (Figure 34).
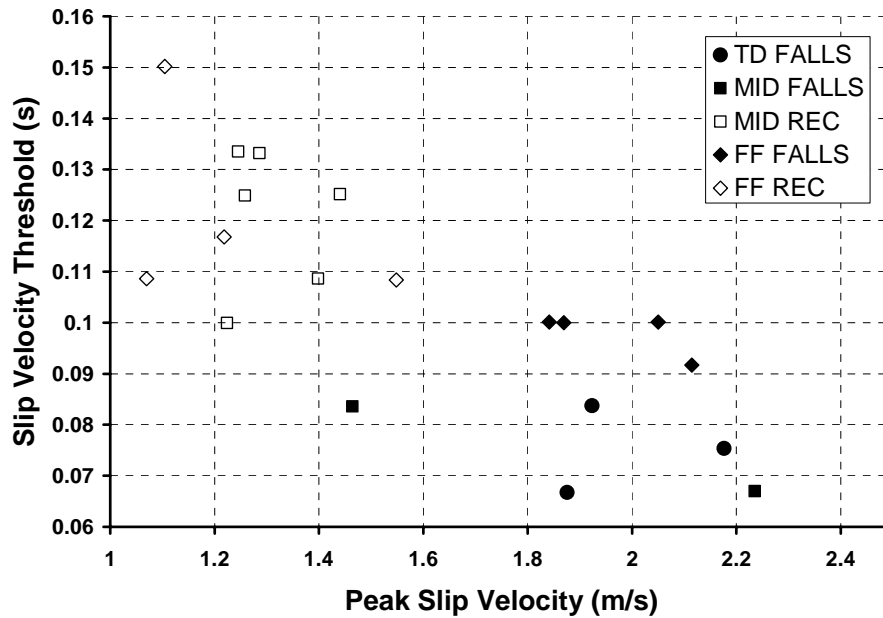
Figure 34: For hazardous slips, the time at which the velocity of the slipping foot exceeded a threshold of 1.0 m/s (SVT) versus peak slip velocity (PSV) – solid symbols illustrate falls, hollow symbols illustrate recoveries

Response strategy and age group were examined, looking for relationships to explain falls. As Table 15 indicates, all TD responses resulted in falls while FF and MID responses to HAZ slips resulted in a mix of fall and recovery outcomes for both younger and older adults. However, a significant relationship between strategy and outcome was not identified ($p = 0.17$). Similarly, age group and outcome were not found to be related ($p = 0.27$). The significant relationships among strategy, age group, outcome, and slip severity for HAZ slips are summarized in Table 15 and Table 16.

Table 15: Relationship among strategy, age group, and outcome for HAZ slips

Outcome	Strategy	Younger	Older	Total
Recoveries	FF	3	1	4
	MID	4	2	6
	TD	0	0	0
	Total	7	3	10
Falls	FF	2	2	4
	MID	2	1	3
	TD	1	2	3
	Total	5	5	10
HAZARDOUS RESPONSES		12	8	20

Table 16: Significant findings summary for strategy, age group, outcome and two measures of slip severity

	AGE	OUTCOME	SVT (S)	PSV (m/s)
STRATEGY	-	-	-	-
AGE		-	-	-
OUTCOME			R > F	F > R

4.3.6   Coordination of Passive and Active Onsets

Coordination of passive and active response to HAZ slips was explored by examining the temporal relationships between joint torque activations. Passive onsets were compared to better understand proprioceptive stimulus presentation while active onsets were compared to better understand response synchrony.   Slipping leg proprioception was hypothesized to initiate primary responses to the slip perturbation while trailing leg proprioception was hypothesized to initiate secondary responses due to postural changes.

Analysis of passive onsets revealed significant difference between joints of the same leg and for joints between legs. Average hip torque passive onset occurred 40 ms earlier for the slipping leg compared to the trailing leg. Similarly, average knee torque passive onset occurred 60 ms earlier for the slipping leg compared to the trailing leg. T-tests determined these

differences to be significant ($p = 0.002$ and $p < 0.001$ respectively). A comparison of passive onsets within the slipping leg revealed that the knee torque onset lead the hip torque onset by 20 ms on average ($p = 0.01$). Conversely, the trailing leg knee torque onset occurred after the trailing leg hip torque by 4 ms on average ($p = 0.05$), which although statistically significant, is temporally insignificant. This analysis indicates that slipping leg torques changed passively sooner than trailing leg torques and that, for the slipping leg, knee torque changed earlier compared to hip torque.

In a similar analysis, differences in active onsets between and within slipping and trailing leg joints were found. Average hip torque active onset occurred 20 ms earlier ($p = 0.005$) while average knee torque active onset occurred 80 ms earlier ($p < 0.001$) for the slipping leg compared to the trailing leg. Active onsets comparisons within the joints of the slipping leg revealed that the knee torque lead the hip torque by 50 ms ($p < 0.001$) while the relationship between trailing leg knee and hip torque active onsets, with an average separation of 9 ms, was not significant ($p = 0.06$). These results parallel the passive onset results, indicating that slipping leg torques changed actively sooner than trailing leg torques and that, for the slipping leg, knee torque changed earlier compared to hip torque.
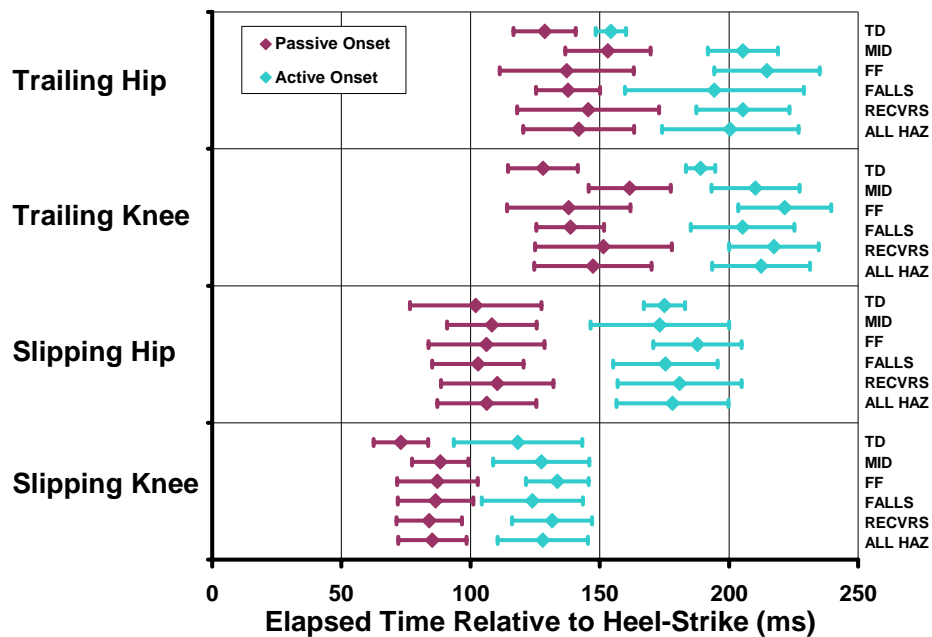
Figure 35: Timing, from heel-strike, of passive and active torque responses for the slipping and trailing leg knees and hips
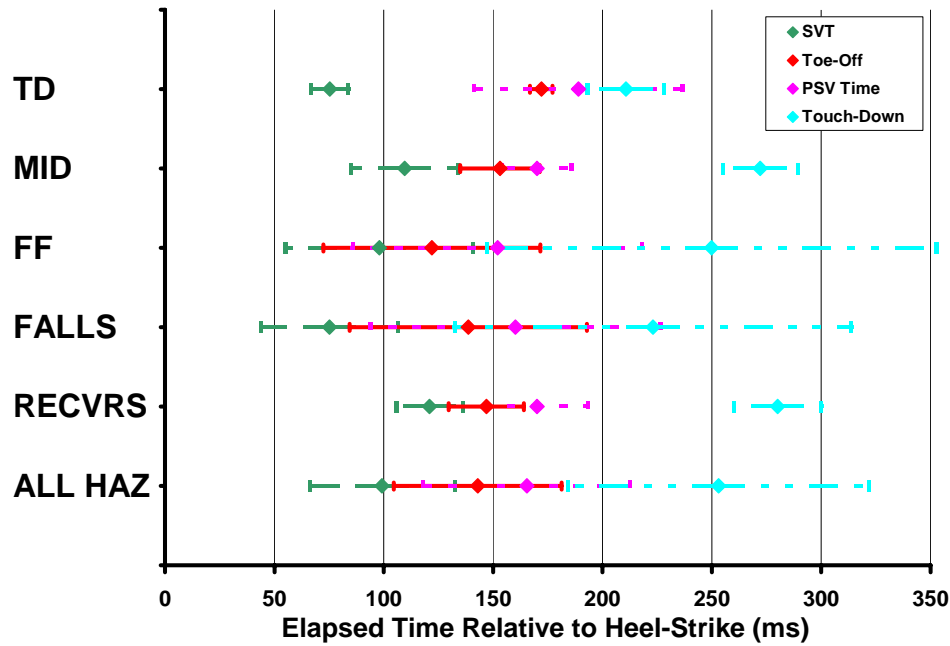
Figure 36: Timing, from heel strike, of gait events for all HAZ slips, recoveries, falls, and HAZ FF, MID, and TD strategies.

In Figure 35, average values with standard deviations are presented for, from bottom to top, HAZ, recoveries, falls, and HAZ FF, MID, and TD responses. SVT, toe-off of the trailing foot, PSV time, and touch down of the trailing foot are illustrated in Figure 36 for reference. Toe off was delayed for TD compared to MID and FF responses to HAZ slips (Figure 35). A significant relationship between toe-off time (Figure 36) and strategy (Figure 35) was not identified ($p = 0.09$), although Student's t-tests did indicated that toe-off occurred earlier for FF compared to MID ($p = 0.047$) and TD (0.026). Although SVT occurred later for recoveries than for falls, (Figure 36) all joints EXCEPT slipping knee appear to have later passive onsets for falls compared to recoveries (Figure 35).

4.4   DISCUSSION

This study examined lower extremity responses to unexpected slips, caused by the application of glycerol, unbeknownst to the subjects, to an area of the floor. Based on trailing leg postural

dynamics, four slip response strategies were identified: MIN, FF, MID, and TD. Trailing foot flight times, flight distances and foot-floor contact angles for touch-down after the slip were related to response strategy. MIN responses were similar to baseline dry gait. The other strategies had decreasing flight times and flight distances and increasing ground contact angles. TD had the fastest flight time, MID had the next fastest and FF had flight times between MID and MIN. Slip severity was greatest for TD and minimal for MIN. Slip severity was not different between FF and MID responses, suggesting that strategy may be a subjective choice rather than resulting purely from slip magnitude, at least for some slips.

Kinetic analyses found differences in torque responses to slip, depending on strategy (Table 14). Slipping leg knee torque responses were greater (i.e. increased active slope) for TD compared to other responses. Trailing leg hip active onset was faster for TD responses than for MID or FF. Trailing leg knee passive onset was later for MID than for FF or TD responses. Additional analyses revealed that slipping leg knee active slope was faster for falls than recoveries. Neither trailing leg response strategy nor any trailing leg hip or knee torque response parameters were found to be related to outcome. Age group (younger/older) was not found to be significantly related to response strategy, slip severity, or outcome.

A discussion of why some slips lead to falls while others lead to recoveries will follow. This section will cover topics such as the importance of slip severity (determined primarily by initial conditions), the importance of an effective response (fast enough, forceful enough), and the importance of coordination, both within each leg and between legs (bringing the slipping foot backwards forcefully enough and fast enough without establishing a new base of support with the trailing foot might end the slip but it would still likely result in a fall. Both legs must work together to accomplish the two objectives) will be discussed.

4.4.1 Response Strategies

A qualitative assessment of strategy was made in the analysis of the responses to slips in an attempt to understand the human responses that lead to falls or recoveries. These identified strategies were categorized based upon trailing leg kinematics, primarily the flight times. However, there were also other characteristics of these strategies that distinguished them from each other. The following discusses these characteristics.

4.4.1.1 MIN Responses MIN responses qualitatively appeared to be very similar to unperturbed or dry gait. All MIN responses were associated with NHAZ slips. However, there were subtle postural changes typified by short delays in lower extremity torques soon after slip initiation followed by minor alterations allowing the resumption of normal ambulation. These small torque changes appear to allow individuals to adjust to the slip perturbation to maintain a normal gait style, direction, and speed. MIN responses may be similar to postural responses occurring for minor, sub-perception slips encountered with every step as previously reported [34, 81].

4.4.1.2 FF Responses to NHAZ Slips FF responses to NHAZ slips resembled a quick foot tap (horizontal to the floor) which, according to Marigold et al. [96], serves to widen the base of support to provide additional security, leading to an increase in stability. This foot tap always happened after the slip had ended and was thus likely a response related to postural changes induced by the slip and not directly in response to the slip. Slip anticipation effects or passive or reflexive response components could have been responsible for limiting the severity of these trials.

4.4.1.3 FF and MID Response Strategies For HAZ slips, the two dominant strategies were FF and MID. Both FF and MID responses resembled the "surfing" response strategy reported by [20, 21, 42, 96, 97,]. FF responses were characterized by longer trailing foot flight times and resulted in shallower trailing foot-floor contact angles compared to MID responses. The trailing foot for MID responses contacted the floor more posteriorly compared to FF responses. Not only did the trailing foot for MID responses initially contact the floor with an elevated heel, but the heel also remained elevated for the duration of the response. These two response strategies led to both recoveries and falls (Table 15).

Our results suggest that slips that include either FF or MID responses use the trailing leg to contribute to the recovery of postural stability. As suggested by Marigold, et al. [97], it appears that lateral stability is of primary importance. For FF trials the trailing foot was placed on the floor parallel to the slipping foot supplying a primarily lateral base of support and creating a platform from which subjects could arrest downward acceleration of the center of mass. This base of support did not provide an increased base of support in the anterior-posterior (AP) direction since the foot landed lateral to the slipping foot. Thus, keeping the center of mass

within the base of support in the AP direction required complex interactions of joint torques in the lower extremities, potentially assisted by upper body dynamics. The MID response strategy had a longer AP base-of-support than the FF but, based on observations of foot orientation and ankle posture, appeared to require additional lower extremity strength to support body weight. Lateral base of support reduction was related to the severity of the slip as anterior excursion of the slipping foot prior to trailing foot toe down was longer for more severe slips.

An argument that FF and MID responses should be considered as a single response strategy could be made, with slight differences in ground clearance during swing phase leading to the increased flight times and shallower ground contact angles for FF compared to MID responses. Ground clearance would be impacted by the subject's sensorimotor capabilities (i.e. reaction time, sensory capabilities, strength, cognition). However, postural stability requirements argue against MID and FF being variants of the same continuous postural response. The choice between FF and MID response strategies may depend upon stability requirements resulting from postural perturbation. Dynamic stability has been shown to be a critical determinate of foot placement for compensatory stepping [94, 95]. As suggested previously, lateral stability requirements may necessitate a more anterior trailing foot placement (i.e. a FF strategy). Conversely, when more AP stability is required, foot placement requirements would dictate increased AP torque responses (i.e., a MID strategy). Note that trailing hip active slopes for the MID responses had steeper active slopes compared to FF responses.

Slip severity and outcome (fall or recovery) were related to MID and FF strategies. Interestingly, slip severity *prior to any active response*, as determined via SVT, was practically identical for FF and MID responses (Table 17). This initial slip severity appears to be a good predictor of outcome, with shorter SVTs (i.e. faster initial accelerations of the slipping foot) resulting in falls regardless of the strategy used.

Slip severity *after the active response had been initiated*, as determined via PSV, appears to depend on response strategy. Faster PSV (i.e. increased slipping velocities) for FF responses leading to falls compared to MID responses leading to falls. However, recoveries accomplished via FF responses appeared to have slightly slower PSVs compared to MID responses (Table 17). This divergence in slip severity following the initial response and its relationship to outcome suggests a possible reason that individuals might utilize one strategy over the other although

some caution regarding this conclusion should be taken, since this finding was not statistically significant, presumably due to small sample size.

Table 17: Slip severity comparisons for FF and MID responses to HAZ slips

STRATEGY	N (Rec/Falls)	Recovery SVT (s)	Fall SVT (s)	Recovery PSV (m/s)	Fall PSV (m/)
FF	4 / 4	0.121 (0.020)	0.075 (0.050)	1.24 (0.22)	1.97 (0.13)
MID	6 / 2	0.121 (0.013)	0.076 (0.012)	1.31 (0.09)	1.85 (0.55)

4.4.1.4 TD Responses The TD responses were characterized by the shortest flight times and distances, resulting in the foot touching down posterior to the slipping foot. This strategy resulted in an unstable lateral base of support. In addition, this strategy required subjects to accept large portions of body weight on the trailing toe with the ankle extremely plantar-flexed exposing subjects potentially to ankle roll-over and collapse. Thus, TD strategies resulted in the least stable postures during the slips. Note that all slips that were associated with TD responses resulted in falls. Thus, either the observed TD responses were inadequate to recover from such severe slips (i.e., slip severity led to falls) or TD responses are inherently unstable with minimal base of support and low potential for generating corrective actions (i.e., TD strategy increased the risk for falls). Because all TD responses resulted in falls, and based on the limited number of observations, it is unclear whether recovery from falls is possible utilizing this type or response.

Interestingly, slip severity for slips associated with TD responses were comparable to other severe slips associated with MID responses (see Figure 34). This observation suggests that, even for "irrecoverable" slips, response strategy may not be determined by slip severity alone but is also likely influenced by the same considerations that lead to FF versus MID responses for less severe slips. This also reinforces the idea that the trailing leg responses are not in response to the slip, but rather to the postural disturbance to the body that the slip creates. Human factors that could possibly influence whether a TD or MID strategy are used for severe slips include strength, reaction time, sensory acuity, and experience.

4.4.2 Is Response Strategy a Choice?

A fundamental question is whether the trailing leg response is chosen by the subject, or is it rather a function of the conditions of the slip (i.e., a result of the passive dynamics). Flexibility in choosing a strategy is supported by the findings for HAZ slips. Note that response strategies for HAZ slips were not associated with slip severity (either determined via SVT or by PSV); thus, the magnitude of the slip perturbation alone cannot predict the trailing leg response. However, strategy choice may be part of a pre-determined automatic postural response, chosen based upon the induced perturbation to the body. The strategy is triggered by some aspect of this perturbation to the body, such as the magnitude and/or direction of the perturbation. Thus, it may not be the slip severity that initiates a particular response, but rather the ensuing postural destabilization of the body which is sensed by other systems (i.e., a proprioceptive or a vestibular trigger). This concept is consistent with work performed in standing postural control during perturbations [3, 4, 13, 14, 29].

Standing postural perturbations have been found to elicit specific responses based upon the characteristics of the perturbations [66]. These specific "strategies" in response to a perturbation are likely continuously modulated based upon available sensory input regarding the perturbation, especially for dynamic activities [105, 133]. For rapid and relatively large perturbations during quiet stance, the so-called "hip strategy" is seen where recovery motions occur predominantly at the hips. For small or slow perturbations, the body responds with motions about the ankle (i.e. "ankle strategy") [67, 78, 103]. The same strategy concept is believed to be involved in response to slips. Specific strategies are invoked based upon the perturbation induced to the body. However, it is not clear from this study whether the initiation of these strategies is "automatic" or can be modified by experience or potentially modulated based on postural stability feedback as suggested in the literature on postural responses to quiet standing perturbations [3, 66]. Response strategies to slips are likely modified based upon prior knowledge of the perturbation and with experience [33, 97]. In addition, the sensorimotor capabilities of individuals, especially as related to age, are expected to impact the stepping response strategies used [95].

4.4.3   Why Do Only Some HAZ Slips Lead to Falls?

Slip severity appears to be the most critical variable related to outcome. Active onset and active slope of the slipping leg knee torque were linked to severity while active slope was also related to outcome. When slip severity (SVT) was included in an ANOVA relating slipping leg knee torque active slope to outcome, only the relationship between SVT and outcome was found to be significant. Thus, the severity of the slip perturbation appears to drive both the change in the analyzed torque parameters and the outcome of the slip.

4.4.3.1 The Importance of Slip Severity Falls were shown to depend on slip severity with the most severe slips, based on slip velocity measures (both SVT and PSV), leading to falls. This finding agrees with previous research which has identified relationships between slip severity and various pre-slip gait characteristics [18, 89, 100]. The most-severe slips may have been "irrecoverable" implying that, regardless of the chosen response strategy and the efficacy of its implementation, falls were inevitable. Including these trials likely overwhelmed the sensitivity of statistical tests examining the effectiveness of recovery strategy and parameters of response torques (such as passive onset, active onset, or active slope) in preventing falls for "recoverable" slips. Indeed, response strategy was not found to be related to slip severity or to outcome for HAZ slips, although this finding should be interpreted understanding the limitations of the relatively small number of TD responses available for analysis.

4.4.3.2 The Importance of Response Effectiveness Differences in the magnitude and timing of response (i.e., active slopes and active onsets) for the leading and trailing leg knee and hip torques may contribute to fall outcomes. Neither repose strategy nor knee and hip torque parameters of response were found to be relevant contributors to recovery for this study. Only slipping leg knee torque active slope was linked to outcome with falls characterized by steeper active slopes compared to recoveries. Because SVT precedes any active response, it appears as if the magnitude of the slip perturbation resulted in the slipping leg knee torque active slope increases. Likewise, a relationship between SVT and slipping leg active onsets was identified. So, either subjects perceived the magnitude of the fall risk and generated larger responses faster,

attempting to avoid falls or more severe slips led to postures that resulted in larger torques sooner.

Torque responses of the trailing leg had earlier onsets for those response strategies requiring faster foot down responses. The onsets for the trailing hip and knee were earlier for the TD compared to the MID and FF strategies. Thus, delays in active onset – whether due to perception delays or reaction time issues - for any of these strategies might increase the risk of a fall. Further conclusions regarding the effect of response on outcome are made difficult by the limited number of trials available for analysis.

4.4.4 Is Response Coordinated Across Joints?

A coordinated effort across joints is likely required to arrest slipping foot motion and to avoid falls. Slipping leg torque responses found for this study were similar to those found by Cham and Redfern [32] with onsets and magnitudes approximately being the same. Interestingly, the slipping leg torque responses for this study were found to be related to response strategy of the trailing foot. Thus, leading leg knee torques are likely utilized to slow slip progression while individuals appear to utilize trailing leg knee and hip torques to position the trailing foot to accept body weight.

An examination of the temporal relationships among slipping leg and trailing leg knee and hip torque onsets (illustrated in Figure 35) indicated that slipping knee passive onsets preceded slipping leg hip torque passive onset and both knee and hip passive onsets for the trailing leg. Slipping knee torque active onset occurred prior to trailing leg toe-off while slipping hip and trailing knee and hip passive onsets occurred at about the same time as toe-off. **Of the joint torques investigated for this thesis, slipping knee torque was the only active response present prior to peak slip velocity thus was likely involved in arresting slipping foot motion,** agreeing with previous findings [32]**. Rather, slipping hip and trailing hip and knee torques appear to be coordinated to control trailing foot placement relative to center of mass acceleration.** The trailing leg knee and hip appear to work in concert to get the trailing foot to a desirable location to either accept weight (and thus change the base of support) OR to get the COM over the slipping base of support (elevating strategy).

As previously discussed, the association seen between slipping leg knee torque response parameters and strategy (Table 14) could also be due to slip severity. Indeed, knee torque active onset times and active slopes for the slipping leg were related to slip severity with faster SVT corresponding to faster active onsets and steeper slopes. This suggests that when more rapid foot slips occur, there is an earlier recognition of the slip and a faster torque response generated. The fast onset times and increased magnitude of response (i.e., active slopes) suggest that the sensory signal initiating response may be slipping leg knee joint proprioception, although vestibular triggers (i.e., vertical COM acceleration) have been implicated in the standing posture literature for anterior-posterior perturbations [3]. Onsets, both passive and active, for the slipping leg hip torque and the trailing leg knee and hip torques were well coupled, albeit delayed, to slipping knee onsets. Interestingly, these parameters of response were not significantly related to slip severity. Thus, it appears as if the trigger for active response at these joints may be the same, namely, slipping leg knee proprioception.

Once triggered, trailing leg hip and knee torques were modulated to achieve an appropriate foot placement. It is unclear whether the goal for this placement was purely to stabilize body posture or if slowing slip progression was also an objective. However, trailing leg hip angle deviated from baseline dry prior to the trailing foot contacting the floor in the opposite direction from what segmental momentum would generate. This demonstrates that lower extremity joint torques accomplished more than basic error tracking for normal gait joint angles and were able to alter lower extremity posture. The dorsiflexion torque at the trailing leg ankle increased toe clearance, allowing subsequent foot contact to occur in a more stable manner, later in the flight phase of gait. This activity occurred in conjunction with the increased trailing leg knee flexion torque and increased hip extension torques (compared to baseline dry), all of which combined to delay ground contact such that the resulting base of support was better able to support the body in a stable configuration. This result supports the hypothesis that dynamic stability (i.e. positioning the trailing foot to provide a base of support to decelerate the body's center of mass) is the critical factor influencing foot placement and agrees with findings from standing posture research [94].

For all joints (including the slipping knee), active onset was earlier for recoveries compared to falls although this relationship was only statistically significant for the slipping leg knee torque. A test of the relationship among slipping knee active onset, SVT, and Outcome

identified a significant relationship between this active onset and SVT ($p = 0.004$) and a trend related this onset to Outcome ($p = 0.06$) with earlier SVTs (i.e., more severe slips) leading to earlier active onsets as expected and Student's t-tests revealing that earlier active onsets of the slipping knee were associated with recoveries ($p = 0.03$). Thus, it appear as though these active onsets were independently related to outcome and suggest that **training techniques to decrease active onset of the slipping leg (perhaps by earlier slip detection) may lead to a higher likelihood for recoveries from HAZ slips.**

4.4.5 Aging and Response Strategies

Response strategy was not related to age group; no significant findings relating parameters of response torques to age group were identified; and, although older subjects were found to walk more slowly compared to younger subjects, no significant difference in slip severity for older compared to younger subjects was found. Older subjects had previously been found to utilize safer pre-slip gait than younger subjects [100] yet did not appear to benefit as expected (i.e., they experienced HAZ slips at the same rates as younger subjects) from decreased stride lengths, more shallow foot-floor contact angle at heel strike, or increased cadence. One of the aims of this research was to explore differences in response between older and younger participants that might explain the divergence in results from expectations as well as potentially explaining the higher rates of slips and falls reported for older individuals in the workplace. The lack of significant benefits resulting from older individuals' safer gait may have been due to 1) their safer gait was not safe enough to realize a detectible benefit for this study 2) there was some other, uncharacterized initial condition that offset the benefit of their other more conservative parameters, or 3) a characteristic of older subjects' response offset the potential benefit of their safer initial conditions. Another possibility was that our older subject group may not have been old enough to capture aging effects. Much of the data supporting higher injury rates for older adults suggest that "older" implies greater than 70 years old while our older subjects were between 55 and 67 years old.

Conducting studies with subjects older than those in this study would be anticipated to have an impact on slip responses. Aging has been shown to diminish sensory and musculoskeletal acuity [71, 131, 138] as well as cognitive function [140] perhaps leading to late

or erroneous perception of slips. In addition aging-related physical strength reduction may lead to overconfident gait for which a person might incorrectly, subconsciously assume that any slip resulting from his/her walking style would be recoverable given internal estimations of their ability to respond. Further, even for individuals adopting an appropriately cautious gait style, exposure to a slip perturbation might lead to response strategy choices that were inappropriate given reduced sensory acuity, diminished reaction times, and lessened strength/power generation abilities that accompany aging. This risk is further compounded due to a lack of exposure to slips that prevents individuals from appropriately modulating their walking style and/or correctly modifying their pre-programmed responses or strategy choices to agree with their abilities. If the efficacy of response (both choice and implementation) is related to outcome, some exposure to destabilization to learn which strategy is best for a person's abilities may be helpful but is a luxury that most individuals do not have.

Including additional subjects, especially individuals older than the currently examined population may yield more age-related effects. Ongoing research into postural control mechanisms has done just that but there is a limit to the benefits of experimentally based slip and fall research that can not be reconciled with the risks of injury, especially for sufficiently older individuals. Therefore, future research aims include the creation of accurate computer models, capable of simulating age-appropriate sensory and muscular deficits for this type of research.

4.4.6   Limitations

There were several limitations to this study. First, the data analysis focused on lower extremity responses as the primary actions in response to the slip. Clearly, there are response components beyond the leading and trailing leg hip and knee torques that could influence outcome. Among these are upper body and arm responses which have been reported [96]. These responses are currently being examined for the same subject population and experimental protocol described herein. Second, within the lower extremity analysis, knee and hip torques were the major focus. This focus was based on previous research in our laboratory that found ankle moments were not important in recovery efforts for larger slips [32]. However, there may be ankle moment contributions to response under certain circumstances, as seen in quiet standing BOS translations [104]. Third, the older subjects in this study were all below 67 years old. This cut-off probably

reduces any possibility of aging effects that would be seen in an older population. Fifth, joint moments could only be calculated while the foot was on the force platform. Once the foot slipped off the platform, the kinetic analysis was not possible, and further joint reactions could not be evaluated.

5.0   DISCUSSION

Slips leading to falls are a serious health problem with costs to society and personal loss of quality of life. Both in the workplace and in the general population, slip-precipitated falls have been definitively shown to be a significant source of mortality and morbidity with increasing risks linked to aging. With such demonstrated prevalence and detrimental outcomes, efforts to reduce these accidents are worthy of attention.

This thesis was focused on the biomechanics of slips during gait, to better understand the relationships among pre-slip gait characteristics, responses to slips, and the severity of resulting outcomes. This work will support efforts to reduce both the quantity and severity of slip and fall accidents. Insights resulting from this thesis may make it possible to identify individuals at risk for slip induced falls a priori and may suggest interventions that could be used to reduce slip risk and/or the severity of slip outcomes.

In addition to the knowledge added toward the long-term goal of slip and fall prevention, a major product of this thesis includes the experimental and analysis toolset developed for the Human Movement and Balance Laboratory (HMBL) at the University of Pittsburgh. Data collection hardware and software tools; algorithms and software based techniques for data analysis; and tools, including a whole-body segmental model, for post-processing of data were developed as general purpose gait laboratory utilities. These utilities have been and will continue to be used for a variety of beneficial human movement research.

5.1   SLIP SEVERITY AND FALLS

Defining the results of a slip is one critical component of studying the biomechanics and potential risk. The most obvious categorization of outcome is whether or not a subject fell.

However, this definition is not sufficient to truly understand the impact of a slip. This study focused initially on the severity of the slip to relate the impact of the slip on the resulting biomechanics [100]. The definition of 'slip severity' has a very specific meaning in the analysis presented in chapter three and a slightly different meaning in chapter four. In chapter three, 'slip severity' refers to a binary slip classification, either hazardous (HAZ) or non-hazardous (NHAZ), based on the peak horizontal velocity (PSV) of the sliding heel. When PSV exceeded 1.0 m/s, a slip was classified as HAZ, suggesting slips with elevated, but not guaranteed, likelihood of fall outcomes. In chapter four, 'slip severity' classification (HAZ, NHAZ) continued to be based on PSV. In addition, chapter four introduced the concept of slip velocity threshold (SVT) as another measure of slip severity. SVT was defined as the time from heel contact to when slip velocity reached 1.0 m/s. Thus, SVT is related to the acceleration of the slipping heel. SVT occurred earlier in the slip compared to PSV (99 (33) ms for SVT versus 165 (47) ms for PSV). The utility of SVT was to identify severe slips prior to the active biomechanical responses. This was an attempt to identify some marker of slip severity that preceded any postural response, thus de-coupling the slip and the response.

Assuming that SVT occurs prior to any active response for HAZ slips suggests two approaches for reducing the risks and costs of slip induced falls that may prove beneficial. The first of these approaches is to identify gait characteristics that lead to HAZ slips. HAZ slip likelihood may then be reduced by changing individuals' pre-slip gait such that the initial conditions of slips are less likely to lead to HAZ slips. The second approach is to identify subjective differences between HAZ slips leading to falls and HAZ slips leading to recoveries. It may then be possible to train individuals to respond to HAZ slips appropriately to reduce the rate for resulting falls. This two-pronged approach fits the structure of this thesis with Section 3.0 corresponding to the first approach and Section 4.0 to the second.

Fall outcomes were defined for outcome analysis in Chapter four. Falls are sometimes difficult to define in an experimental paradigm, due to the harness constraint and safety issues. Some previous studies have used forces in the harness to define falls [18, 139] while others have defined falls based on slip distance or slip velocity thresholds [32, 89, 109, 127]. In this study, a slip trial was classified as a fall if the mid point between hip joint centers dropped below 95% of its minimum height measured during normal gait. This definition was consistent with visual inspection and biomechanical analyses as well as with previous sit-to-stand research fall

definition [104, 107]. Prior to the adoption of this fall outcome classification technique, HAZ slip outcomes included falls, recoveries, and trials with unknown outcomes due to subjects slipping off of the force plate or relying on the harness for support. The concept that HAZ slips present increased risks for falls was re-enforced by the analysis from chapter four which indicated eleven recoveries and zero falls for NHAZ slips and eleven recoveries and nine falls for HAZ slips.

Unfortunately, HAZ slip outcomes (falls or recoveries) were somewhat confounded by the nature of the laboratory environment. The impact of slipping beyond the contaminated force plate remains unknown; however, the mid-hip height does seem to be a reasonable fall criteria even for these slips.

5.2   SIGNIFICANT FINDINGS

As discussed in Section 3.0, pre-slip gait characteristics including cadence, the length of a step relative to leg length (SLR), and the foot-floor angle at heel strike (FFA) and its first derivative (FFAS) were linked to slip severity classification (HAZ or NHAZ). Faster cadence, shorter SLRs, shallower FFA, and reduced FFAS were all associated with NHAZ slips. Older subjects' gait was characterized by shorter SLRs, shallower FFA and reduced FFAS compared to younger subjects. Although these age-related gait differences suggest that older subjects should have had a reduced likelihood for HAZ slips, this was not found. Rather, both older and younger subjects experienced HAZ slips at approximately the same rates (8/13 or 61.5% for older subjects compared to 12/18 or 66.7% for younger subjects –from Chapter 4 data set). Thus, there may be some influence of age that counters the changes in gait characteristics seen in older adults. Some possibilities include other unmeasured pre-slip gait characteristics, psychophysical differences related to concern about slipping that could affect the mental set in this experiment, biomechanical differences, or possible reflexive response differences. In addition, older subjects were, as a group, slightly heavier than the younger subjects (with increased BMI), which could be a covariate for future investigation.

One goal of this work was to identify gait characteristics that are associated with slip severity. Pre-slip characteristics were of particular interest, since these factors could be

controlled and potentially modified in an attempt to reduce injurious falls. Two logistic regression models were considered to predict slip hazardousness based on pre-slip gait characteristics. The first logistic model included cadence and SLR, which were found to be predictive of slip severity and were not strongly correlated with each other. The second logistic model considered only FFA as it was correlated with both SLR and cadence and because significant differences in FFA were found between HAZ and NHAZ slips. **These logistic regression models indicated that pre-slip gait characteristics could be used to predict slip severity *a priori*.** These results suggest that Individuals whose gait was determined to be pre-disposed to HAZ slips could be trained or modified to reduce the potential for injurious slips. Potential factors are shorter steps, increased cadence, and shallower foot-to-floor contact angles.

The biomechanics of slip responses were examined in Section 4.0, looking to test the hypothesis that differences in response might explain divergent outcomes for HAZ slips. Four slip response strategies (MIN = Minimal, FF = Foot Flat, MID = Mid-Flight, and TD = Toe-Down) were identified based on trailing leg postural dynamics with three of these strategies (FF, MID, and TD) utilized for HAZ slips. Additionally, bilateral knee and hip flexion/extension torques for slip responses were compared to baseline dry gait torques. These comparisons suggested that response torques consisted of initial passive components due to postural or reflexive differences followed by an active component with much larger deviations from baseline. The onset of the passive component and the onset and magnitude (slope) of the active component for the slipping and trailing leg knee and hip flexion/extension torques were determined.

Relationships among slip severity (SVT or PSV), outcome (fall or recovery), age group (young or old), strategy (FF, MID, or TD), and the parameters of response torques for HAZ slips were explored. ***The most important finding resulting from this analysis is that HAZ slip outcomes appear to be largely determined by slip severity***. The identified response strategies were not found to be related to age group, outcome, or continuous measures of slip severity (for HAZ slips). However, response strategy did appear to be influenced by slip severity with NHAZ slips leading to MIN of minor FF responses while HAZ slips led to FF, MID and TD responses. Significantly, FF and MID strategies both appeared to be appropriate responses to HAZ slips of comparable severity indicating that slip severity alone did not drive response strategy.

Differences in trailing leg knee and hip onsets were found to be related to response strategy – relationships that did not appear to be confounded to slip severity.

Although slipping leg knee torque parameters of response were found to be related to outcome and to slip severity, slip severity dominated this association: there was no independent relationship between slipping leg knee torque parameters and outcome. While the slipping leg response was dominated by slip severity, trailing leg response was not. This may indicate that the objective of trailing leg response was different from the objective of slipping leg response for this study. An examination of the temporal relationships among slipping leg and trailing leg knee and hip torque onsets (illustrated in Figure 35) indicated that slipping knee passive onsets preceded slipping leg hip torque passive onset and both knee and hip passive onsets for the trailing leg. Slipping knee torque active onset occurred prior to trailing leg toe-off while slipping hip and trailing knee and hip passive onsets occurred at about the same time as toe-off. **Of the joint torques investigated for this thesis, slipping knee torque was the only active response present prior to peak slip velocity thus was likely involved in arresting slipping foot motion.** Interestingly, active onset for slipping leg hip torque occurred after PSV and thus was likely not involved in arresting slipping foot motion. **Rather, slipping hip and trailing hip and knee torques appear to be coordinated to control trailing foot placement relative to center of mass acceleration.**

5.3   FUTURE RESEARCH DIRECTION

The results of this thesis provide direction guiding future research. The limited number of subjects coupled with the necessary limitation of a single unexpected trial per subject made it difficult to interpret findings of this research. Thus, additional experimental research is progressing with plans to monitor unexpected slips from roughly three times as many subjects as were included in this thesis. In addition, future studies should investigate human capabilities and their importance in response. Factors such as reaction times, sensory capabilities, and strength should be correlated with outcomes and biomechanical parameters.

Although this thesis did not identify major age-related differences in response, future studies should investigate this further. Epidemiological data strongly suggests that older adults,

particularly beyond 70 years of age, are at risk of falls during slips. The subjects in this study were not in this age range, and this is believed to be reason for the lack of age-related findings. By studying subjects that are older (> 70) compared to those in the "older" range used for this thesis (55 - 67), further age-related factors may be found. However, there are risks involved that need to be considered. The increased risks for traumatic injury due to ground contact, harness support, and sprains and strains for older individuals counters such potential benefits. Careful evaluation of the methods used and inclusionary criteria will need to be considered. One potential alternative is to use computer simulation techniques to explore the impacts of age indirectly. The experimental findings from this thesis and other ongoing experimental studies can be combined to drive gait simulations with slip outcomes. These simulations can then be used to explore "what-if" situations to more fully understand contributors to slip hazard and fall outcomes.

The biomechanical analyses in this study were limited to exploring the reactions in the lower extremities. There are also important reactions that occur in the torso and upper extremity. The biomechanical model developed for this thesis is also capable of evaluating upper extremity responses to slips and the relationship between of the dynamic location of center of mass and to the base of support. These studies need to be performed, and the results considered in light of the lower extremity responses found here.

APPENDIX A

PLOTS OF TYPICAL KINEMATIC AND KINETIC RESULTS

The plots in this section illustrate results from analyses of a typical young male gait trial. All data presented in this section has been time normalized to a single step using heel strike (HS) and toe off (TO) from the left foot to define 0% and 100% respectively. Segment-to-segment joint coordinate system (JCS) rotations were obtained using segment local coordinate systems as previously described with the first rotation occurring about the parent's flexion axis, the last rotation occurring about the child's long axis, and the middle rotation occurring about an axis orthogonal to the other two axes. Segment local coordinate systems used to obtain reasonable JCS and Euler rotations were not always identical. For Euler angles with respect to the Global coordinate system (X forward, Y to the subjects' left, and Z up), sagittal plane rotations occurred about the Y axis, frontal plane rotations were about the X axis, and transverse rotations were about the Z axis, with the signs of these rotations determined via the right hand rule. Similarly, ground reaction moments were about the same axes. Ground reaction forces and moments and all joint moments resulting from inverse dynamics analyses were normalized to subject mass. Joint moments have been reported about the axes defining the parent segments' local coordinate systems. Due to issues with the manner in which ground reaction forces and moments were automatically connected to the either the massless to segment or the lumped mass heel segment, moments at the MP joint were not considered to be reliable and thus are not presented here.

For all figures in this section, static posture rotations are indicated by dashed horizontal lines (see Table 4). All moments have been normalized to body mass. X axis illustrates 200% (-50% to +150%) of a step, with left foot heel strike at 0% and left foot toe off at 100%.

115
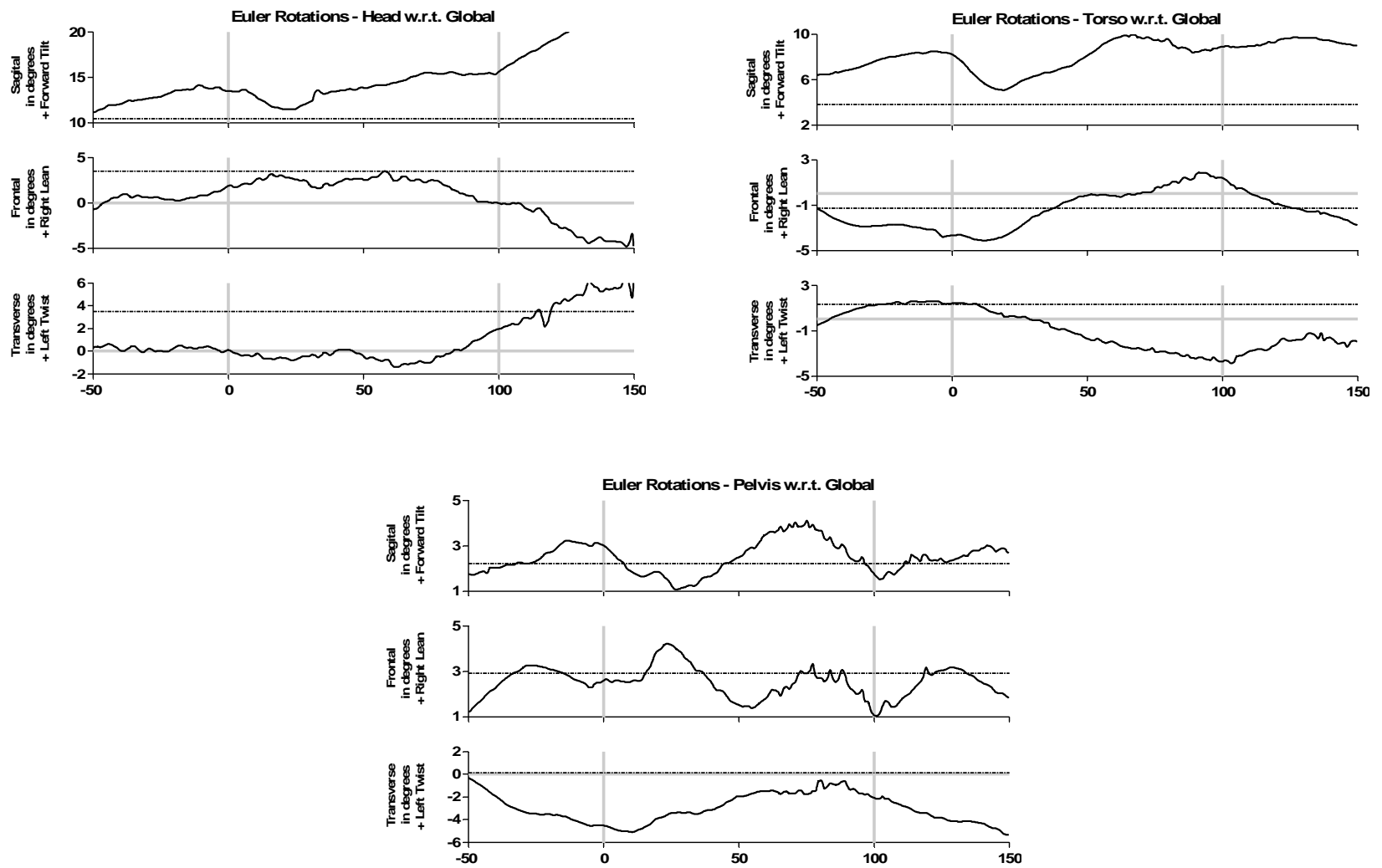
Figure 37: Typical orientations of the head, torso, and pelvis segments with respect to global
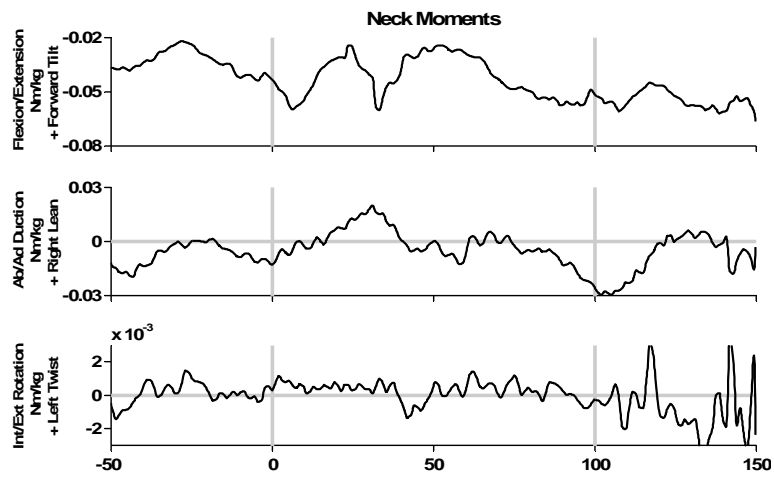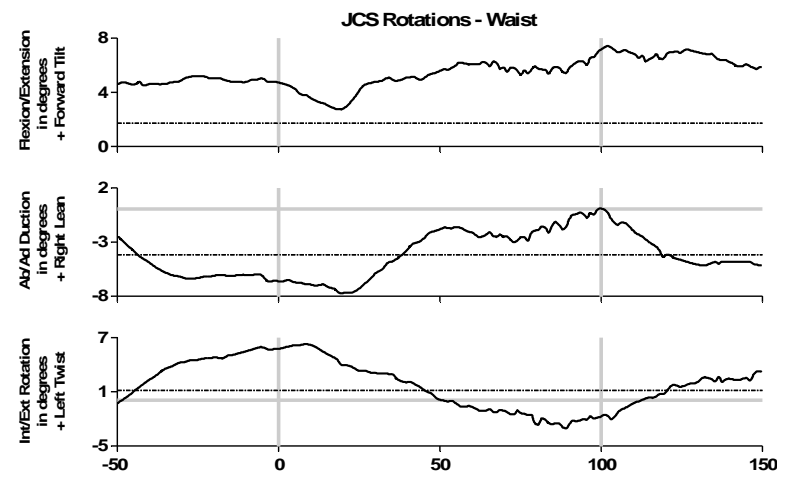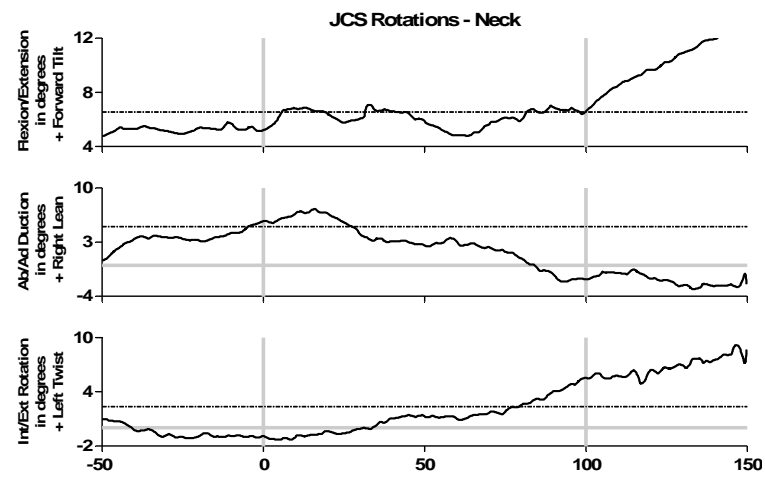
Figure 38: Typical kinematic and kinetic results for the neck and waist. Neck moments reported in torso coordinates and waist moments reported in pelvis coordinates.
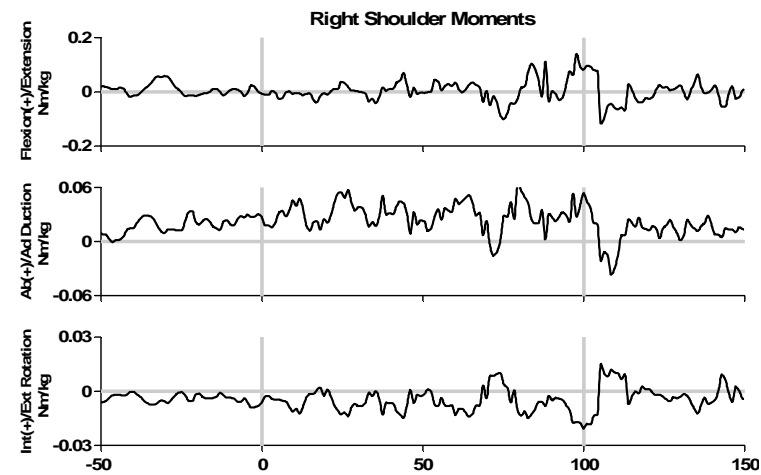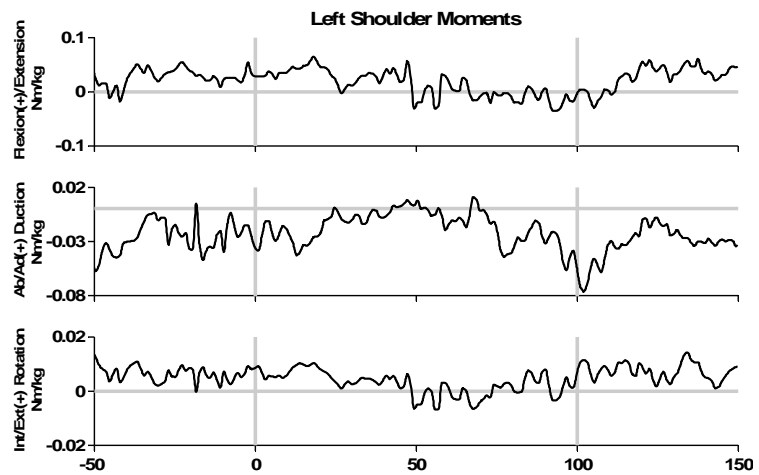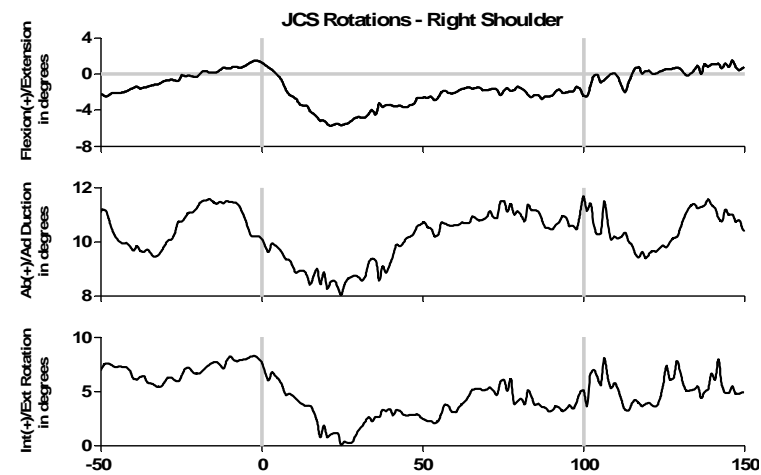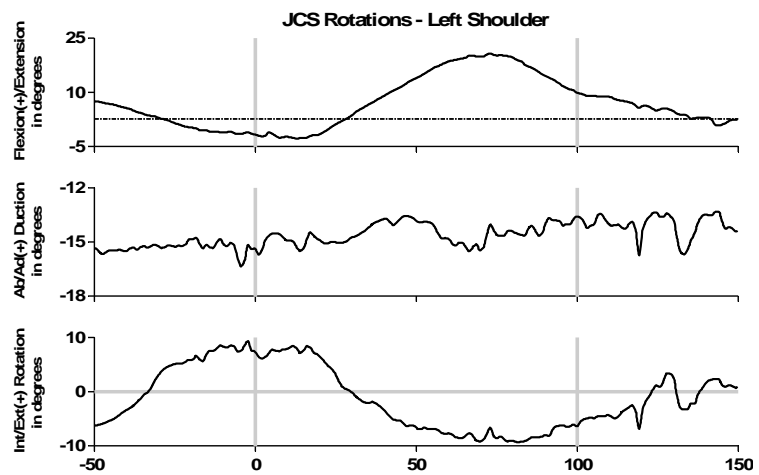
Figure 39: Typical kinematic and kinetic results for the shoulders. Moments reported in torso coordinates.
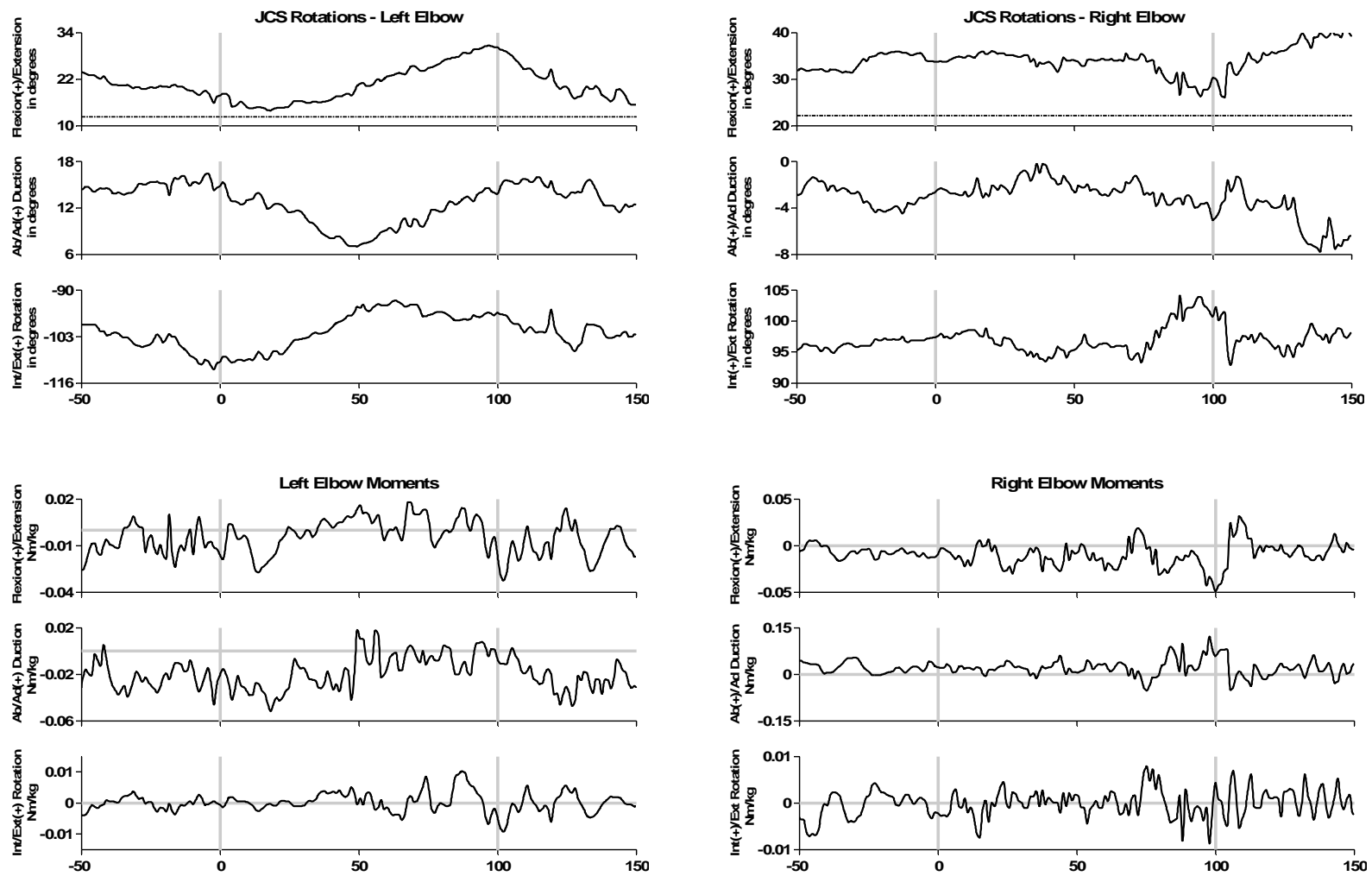
Figure 40: Typical kinematic and kinetic results for the elbows - moments reported in upper arm coordinates
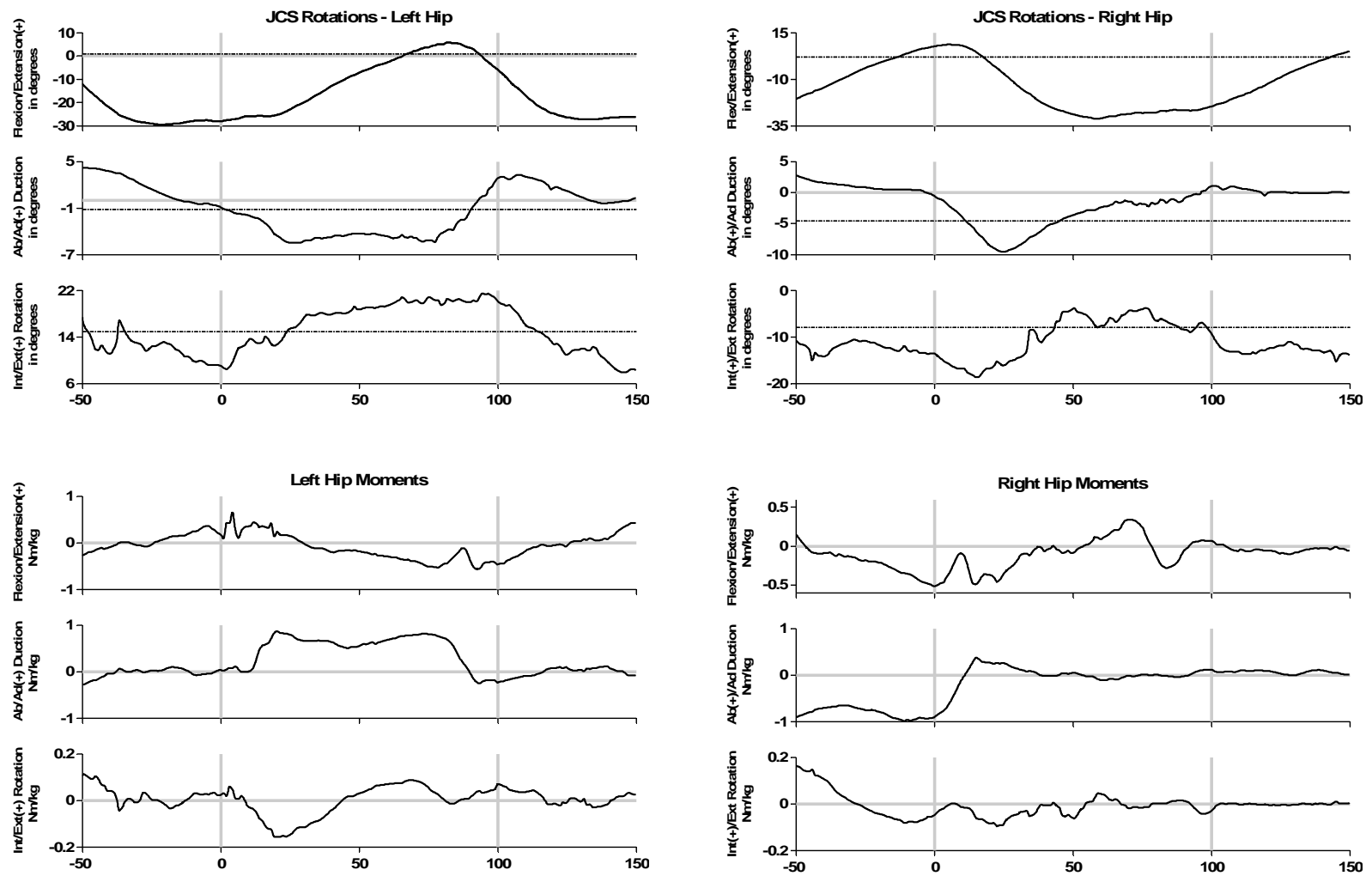
Figure 41: Typical kinematic and kinetic results for the hips - moments reported in pelvis coordinates and normalized to body mass
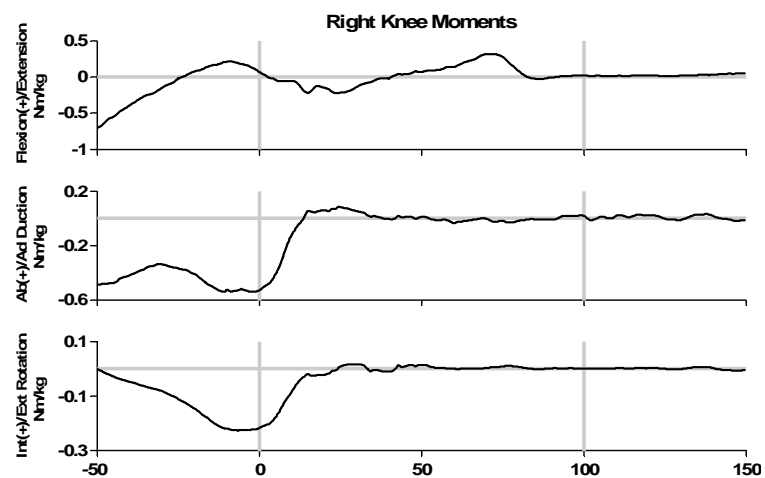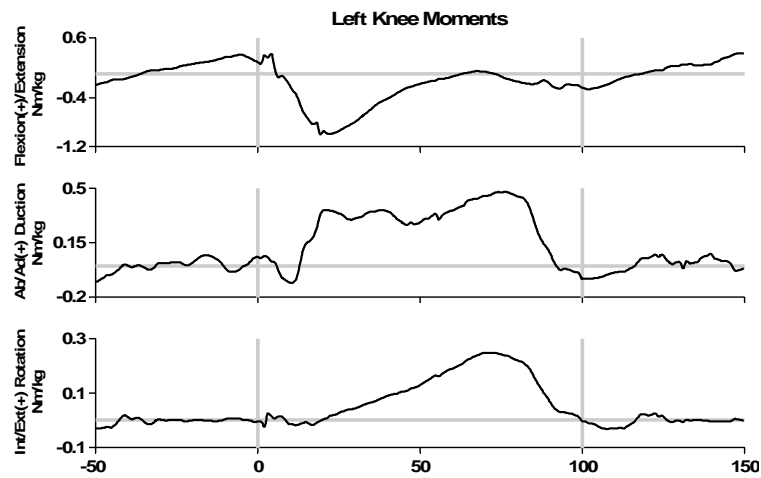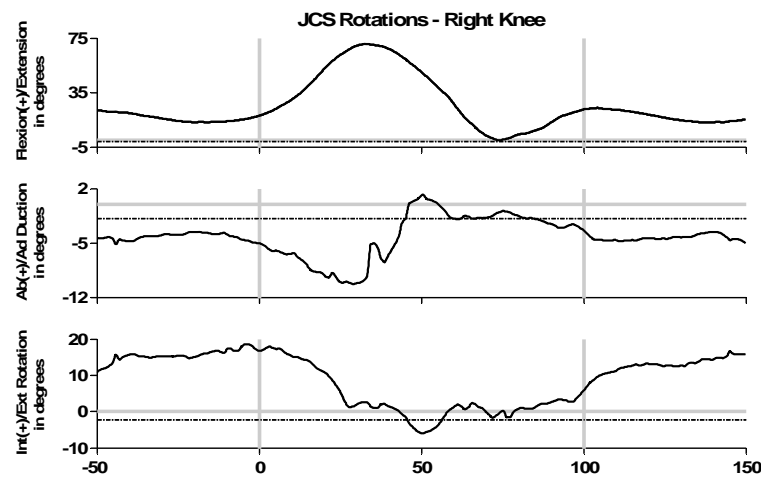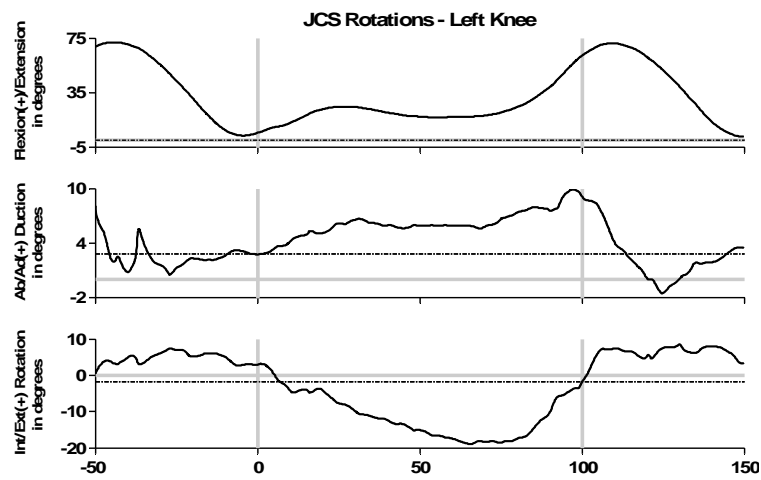
Figure 42: Typical kinematic and kinetic results for the knees - moments reported in thigh coordinates

121
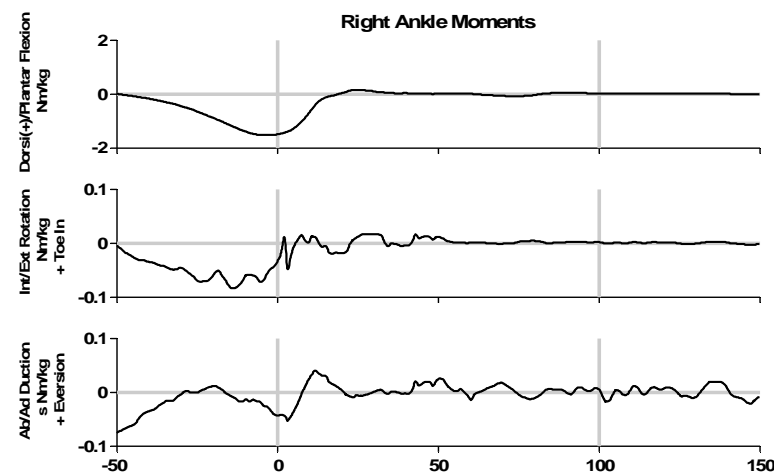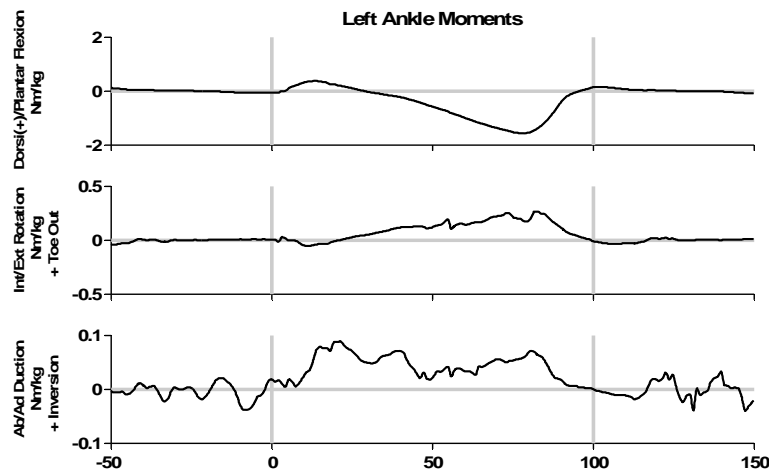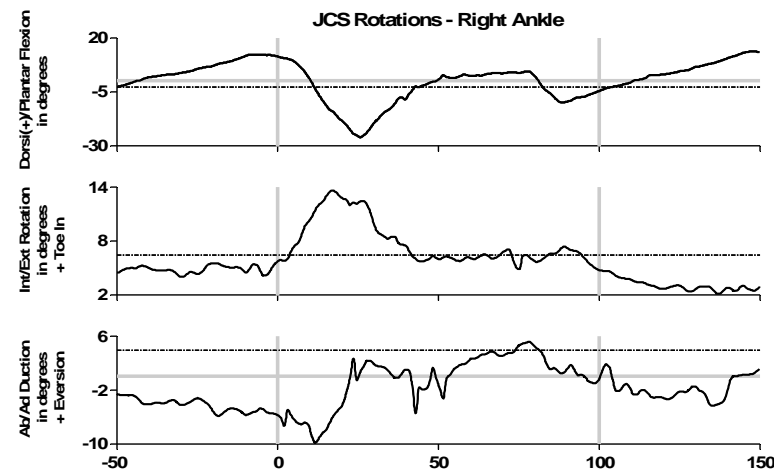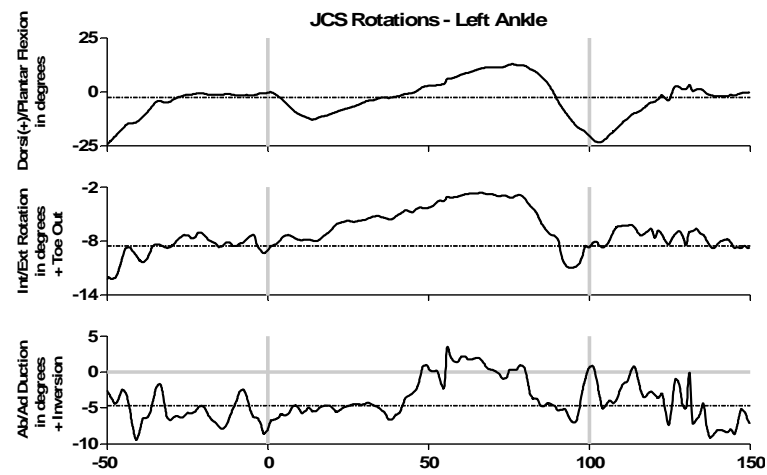
Figure 43: Typical kinematic and kinetic results for the ankles - moments reported in shank coordinates
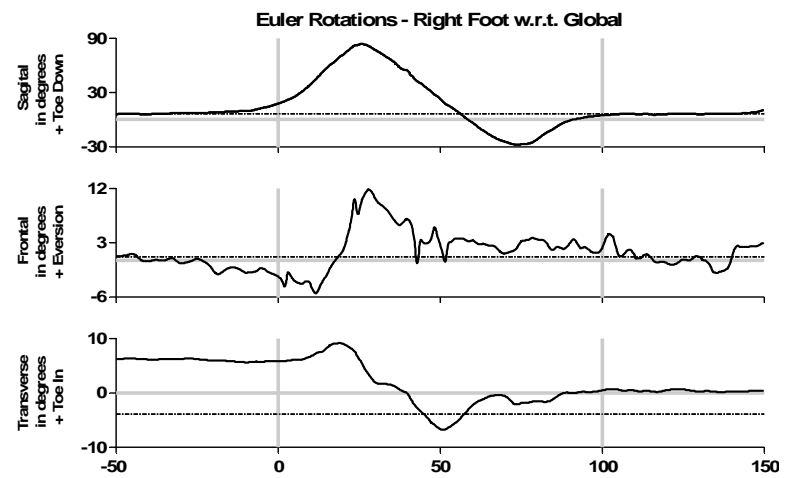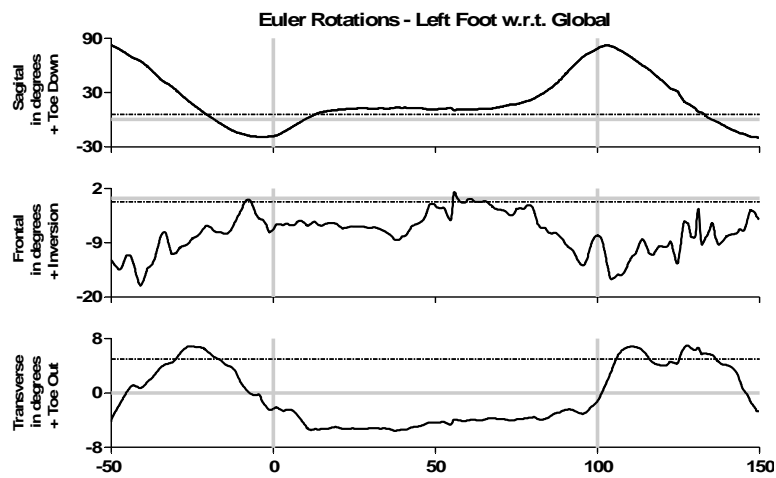
Figure 44: Typical orientations of the feet segments with respect to global
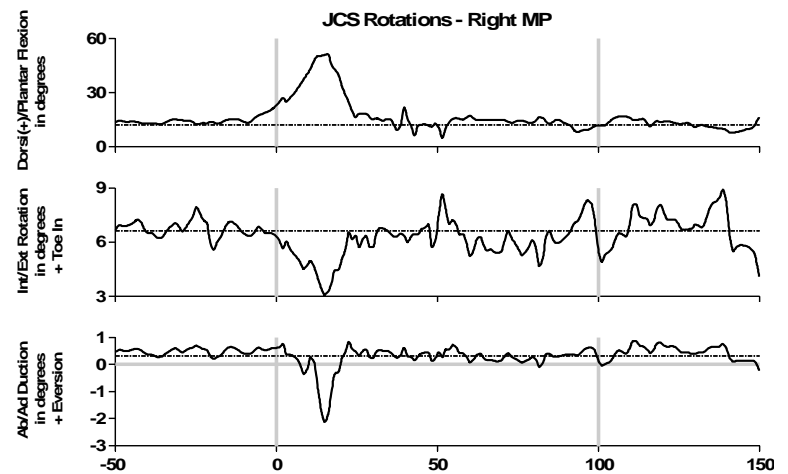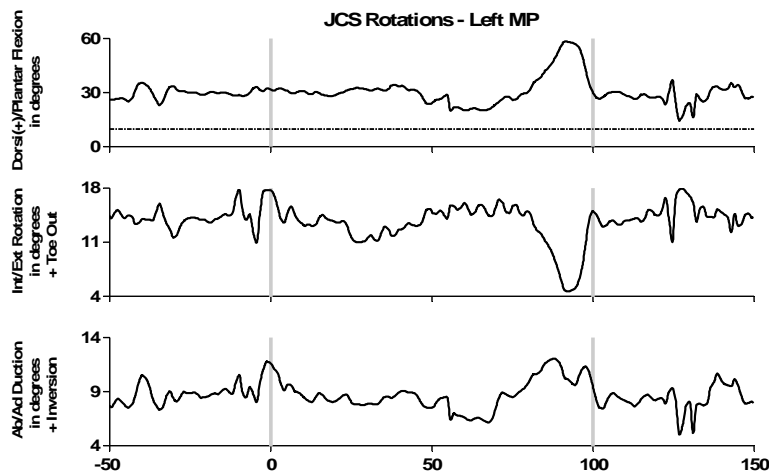
Figure 45: Typical rotations at the MP joints - moments at the MP joints were not considered reliable and are thus not presented here

123
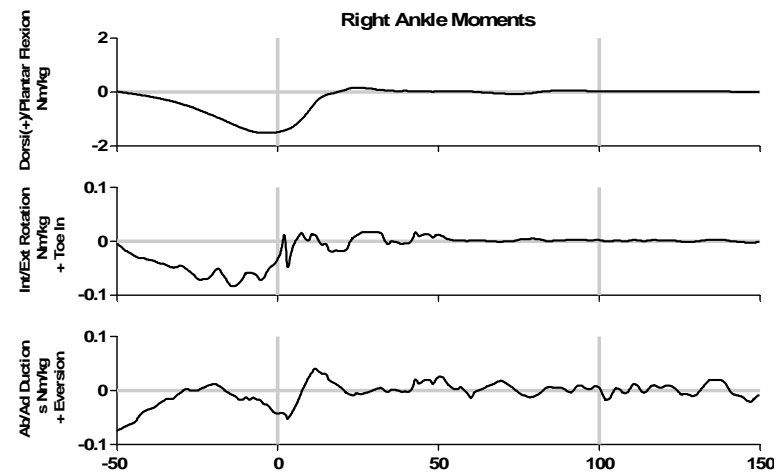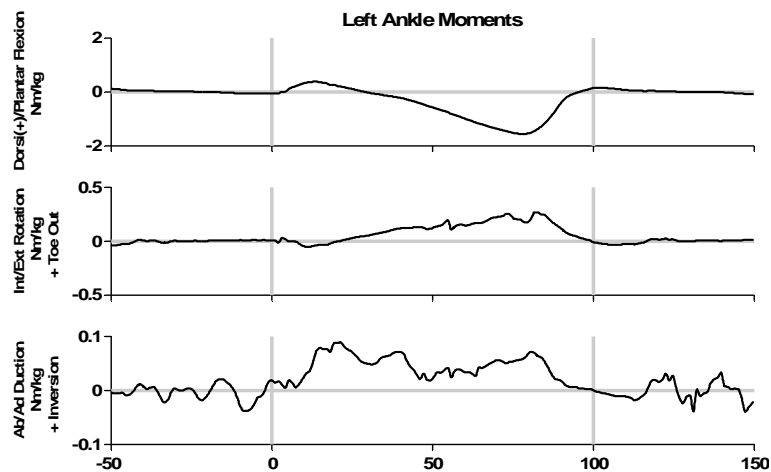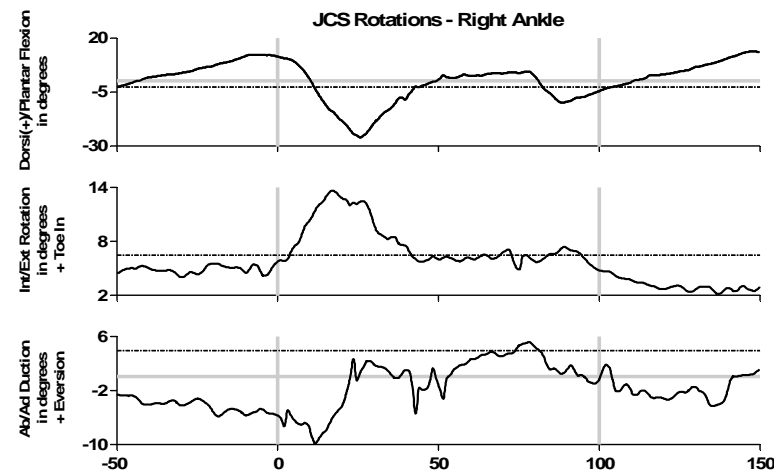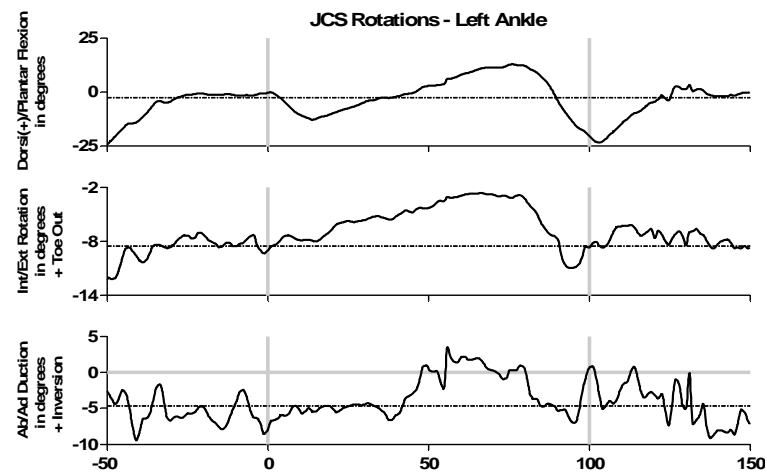
Figure 46: Typical left and right ground reaction forces and moments - both normalized to body mass

124
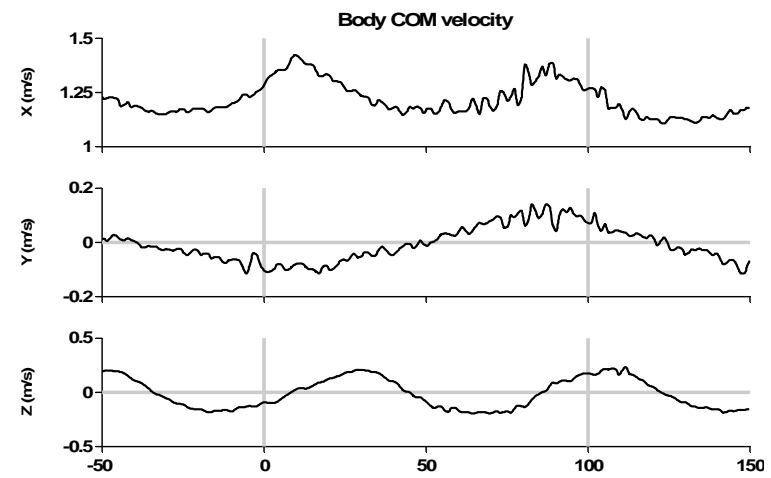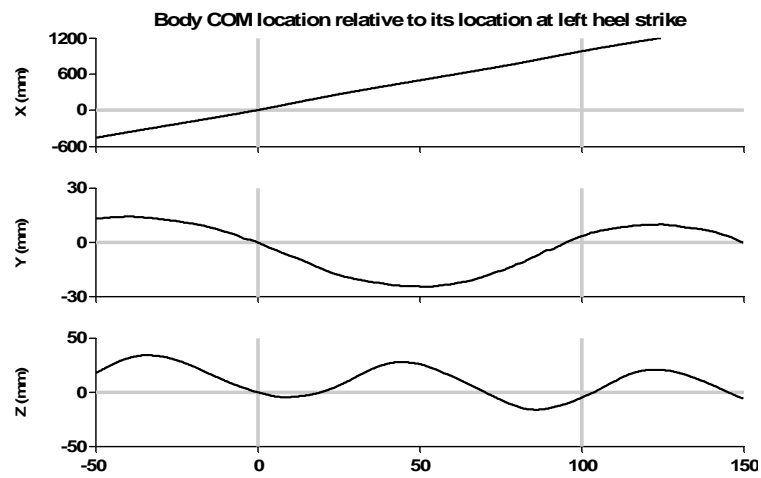
Figure 47: Typical whole body center of mass (COM) trajectory relative to its location at left foot heel strike and COM velocity - Global defined with X forward, Y to the subjects' left, and Z up

APPENDIX B

MARKER LABELS AND DESCRIPTIONS

The following three tables describe the trajectories used in the model. A consistent naming convention has been used for all named items in the marker and model files. The general naming format is:

```
<$ or %><Prefix><V or S><L or R>_<Anatomical Descriptor>_Name_<modifier>
```

`<$ or %>`	The dollar sign indicates that a value is a constant value that has been or will be written to the parameters file (see Appendix E). The percent symbol indicates that a value is in a local coordinates rather than in global.
`<Prefix>`	Identifies the type of object being named. Acceptable prefixes are:

`T`	A marker or trajectory
`P`	A point (X, Y, Z) (like an average value for a trajectory)
`C`	A constant
`Ln`	Length
`Dpth`	Depth
`Wdth`	Width
`G`	Segment created within the model file
`D`	Dummy segment created within the model file (e.g., one used to locate static markers)
`E`	Euler angle rotations
`J`	JCS (Grood and Suntay) rotations
`F`	Forces
`M`	Moments
`X`	Reactions (combination of F, M, and point)
`V`	Velocities

A	Accelerations
I, Ixx, Iyy, Izz	Inertial Property
Ms	Mass
Ux, Uy, Uz	Unit vectors for the axes of the LCS for the named segment

<V or S or none>   Indicates either a (S)tatic marker which would be physically present only in static trials and would be reproduced using its relative location to other markers on the same rigid body for dynamic trials or a (V)irtual trajectory which is created or derived within the model file - i.e., a calculated trajectory.

<L or R>   Indicates whether the item being labeled is from the subject's left or right side

<Anatomical Descriptor>   Indicates other relevant information enabling correct identification of a trajectory. Some typical examples include:

LAT	Lateral
MED	Medial
DOR	Dorsal
SUP	Superior
ANT	Anterior
INF	Inferior
DIS	Distal
PRX	Proximal

<Modifier>   Could be COM for center of mass, Origin, Attach, Offset, etc. These may be strung together as appropriate with underscores separating appended terms.

B.1 DYNAMIC MARKERS

Table 18: This table enumerates the markers present for both static and dynamic trials

Number	Label	Description
1	TL_ANT_Head	Left front head marker
2	TR_ANT_Head	Right front head marker
3	TL_POS_Head	Left back head marker
4	TR_POS_Head	Right back head marker
5	T_C7	Cervical spinal segment 7
6	T_INF_Sternum	Inferior end of sternum
7	TL_Acr	Acromonium (shoulder)
8	TR_Acr	Acromonium (shoulder)
9	TL_SUPANT_Hum	Superior anterior up arm plate
10	TR_SUPANT_Hum	Superior anterior up arm plate
11	TL_SUPPOS_Hum	Superior posterior up arm plate
12	TR_SUPPOS_Hum	Superior posterior up arm plate
13	TL_INFANT_Hum	Inferior anterior up arm plate
14	TR_INFANT_Hum	Inferior anterior up arm plate
15	TL_INFPOS_Hum	Inferior posterior up arm plate
16	TR_INFPOS_Hum	Inferior posterior up arm plate
17	TL_SUPANT_Ulna	Superior anterior forearm plate
18	TR_SUPANT_Ulna	Superior anterior forearm plate
19	TL_MEDPOS_Ulna	Medial posterior forearm plate
20	TR_MEDPOS_Ulna	Medial posterior forearm plate
21	TL_INFANT_Ulna	Inferior anterior forearm plate
22	TR_INFANT_Ulna	Inferior anterior forearm plate
23	TL_ASIS	Left ASIS (TL_ANTSUP_Iliac)
24	TR_ASIS	Right ASIS (TR_ANTSUP_Iliac)
25	TL_PSIS	Left PSIS (TR_POSSUP_Iliac)
26	TR_PSIS	Right PSIS (TR_POSSUP_Iliac)
27	TL_SUPANT_Femur	Superior anterior femur plate
28	TR_SUPANT_Femur	Superior anterior femur plate
29	TL_SUPPOS_Femur	Superior posterior femur plate
30	TR_SUPPOS_Femur	Superior posterior femur plate
31	TL_INFANT_Femur	Inferior anterior femur plate
32	TR_INFANT_Femur	Inferior anterior femur plate
33	TL_INFPOS_Femur	Inferior posterior femur plate
34	TR_INFPOS_Femur	Inferior posterior femur plate
35	TL_LAT_Epic	Lateral epicondyle of femur
36	TR_LAT_Epic	Lateral epicondyle of femur
37	TL_LAT_FibHead	Fibular head of shank
38	TR_LAT_FibHead	Fibular head of shank
39	TL_TibTub	Tibial tuberosity
40	TR_TibTub	Tibial tuberosity
41	TL_LAT_Mal	Lateral malleolus
42	TR_LAT_Mal	Lateral malleolus
43	TL_MED_Mal	Medial malleolus
44	TR_MED_Mal	Medial malleolus
45	TL_SUPPOS_Heel	Left heel (closer to top of shoe)
46	TR_SUPPOS_Heel	Right heel (closer to top of shoe)
47	TL_LAT_Heel	Lateral marker on heel
48	TR_LAT_Heel	Lateral marker on heel
49	TL_MED_Heel	Medial marker on heel
50	TR_MED_Heel	Medial marker on heel
51	TL_LATDOR_HFoot	Lateral dorsal marker on heel
52	TR_LATDOR_HFoot	Lateral dorsal marker on heel
53	TL_MEDPOS_FFoot	Medial, toward heel on toe seg
54	TR_MEDPOS_FFoot	Medial, toward heel on toe seg
55	TL_LATPOS_FFoot	Lateral, toward heel on toe seg
56	TR_LATPOS_FFoot	Lateral, toward heel on toe seg
57	TL_MEDANT_FFoot	Medial toe marker
58	TR_MEDANT_FFoot	Medial toe marker
59	TL_LATANT_FFoot	Lateral toe marker
60	TR_LATANT_FFoot	Lateral toe marker

B.2   STATIC TRIAL MARKERS

Table 19: This table enumerates the markers present only for static trials and relocated using other markers from the same rigid body for dynamic trials

Number	Label	Description
S1	TSL_LAT_Elb	Static lateral elbow
S2	TSR_LAT_Elb	Static lateral elbow
S3	TSL_MED_Elb	Static medial elbow
S4	TSR_MED_Elb	Static medial elbow
S5	TSL_LATDIS_Radius	Static wrist thumb side
S6	TSR_LATDIS_Radius	Static wrist thumb side
S7	TSL_MEDDIS_Radius	Static wrist pinky side
S8	TSR_MEDDIS_Radius	Static wrist pinky side
S9	TSL_Gtro	Static greater trocanter
S10	TSR_Gtro	Static greater trocanter
S11	TSL_MED_EpiC	Static medial epicondyle
S12	TSR_MED_EpiC	Static medial epicondyle
S13	TSL_MEDPRX_Met1	Static medial 1rst metatarsal
S14	TSR_MEDPRX_Met1	Static medial 1rst metatarsal
S15	TSL_LATPRX_Met5	Static lateral 5th metatarsal
S16	TSR_LATPRX_Met5	Static lateral 5th metatarsal
S17	TSL_INFPOS_Heel	Static heel marker
S18	TSR_INFPOS_Heel	Static heel marker
S19	TS_T10	Static thoracic spine seg 10

B.3   VIRTUAL MARKERS

Table 20: This table enumerates the virtual trajectories calculated by the model

Number	Label	Description
V1	TV_Head_Origin	Top of head
V2	TV_Head_COM	Head center of mass
V3	TV_Torso_Origin	Caculated C7 height on long axis of torso
V4	TV_Torso_COM	Torso center of mass
V5	TVL_SJC	Shoulder joint center
V6	TVR_SJC	Shoulder joint center
V7	TVL_UArm_COM	Upper arm center of mass
V8	TVR_UArm_COM	Upper arm center of mass
V9	TVL_EJC	Elbow joint center
V10	TVR_EJC	Elbow joint center
V11	TVL_FArm_COM	Forearm center of mass
V12	TVR_FArm_COM	Forearm center of mass
V13	TVL_WJC	Wrist joint center
V14	TVR_WJC	Wrist joint center
V15	TV_Torso_Attach	Joint center between pelvis and torso
V16	TV_BODY_COM	Whole body center of mass
V17	TV_Pelvis_COM	Pelvis center of mass
V18	TV_MIDH	Midpoint of hip joint centers
V19	TVL_HJC	Hip joint center
V20	TVR_HJC	Hip joint center
V21	TVL_Thigh_COM	Thigh center of mass
V22	TVR_Thigh_COM	Thigh center of mass
V23	TVL_KJC	Knee joint center
V24	TVR_KJC	Knee joint center
V25	TVL_Shank_COM	Shank center of mass
V26	TVR_Shank_COM	Shank center of mass
V27	TVL_AJC	Ankle joint center
V28	TVR_AJC	Ankle joint center
V29	TVL_Combo_COM	Foot center of mass for combined heel and toe
V30	TVR_Combo_COM	Foot center of mass for combined heel and toe
V31	TVL_Foot_Origin	Between toe markers from static trial
V32	TVR_Foot_Origin	Between toe markers from static trial
V33	TVL_MPJC	MP joint center
V34	TVR_MPJC	MP joint center
V35	TVL_Toe	Between toe markers – moves with markers
V36	TVR_Toe	Between toe markers – moves with markers
V37	TVL_HJC2	HJC estimate from Bell
V38	TVR_HJC2	HJC estimate from Bell
V39	TV_PJC	Average of two ASIS and two PSIS markers

APPENDIX C

VICON MARKER FILE

The marker file used with the model (see Appendix D) follows. This marker file was used to facilitate autolabeling as well as to organize markers into useful display sets for use in Vicon's Workstation and BodyBuilder applications (Oxford Metrics, Vicon Peak – UK). Comments have been added to clarify sections and must be removed for this to actually work with Vicon's software.

```
!MKR#2
[Autolabel]

#     Only 32 characters allowed for descriptions

#     Although  the  order  of  the  markers  in  each
      section  is  unimportant  a  marker  must  be
      listed  before  being  used  for  a  segment
      definition or for drawing lines

#     The Autolabel section is used by Workstation
      to identify which markers to show AND which
      markers to look for.

#     The order of markers in this section may be
      changed to make the manual labeling process
      easier.

#       HEAD SEGMENT
TR_ANT_Head         Right front
TL_ANT_Head         Left front
TL_POS_Head         Left back
TR_POS_Head         Right back

#       TORSO SEGMENT
TR_Acr              Right acromonium (shoulder)
TL_Acr              Left acromonium (shoulder)
T_C7                Cervical spinal segment 7
T_INF_Sternum       Inferior end of sternum
TS_T10              Low back thoracic spine seg 10

#       PELVIS SEGMENT
TR_ASIS             Right ASIS (TR_ANTSUP_Iliac)
TL_ASIS             Left ASIS (TL_ANTSUP_Iliac)
TL_PSIS             Left PSIS (TR_POSSUP_Iliac)
TR_PSIS             Right PSIS (TR_POSSUP_Iliac)

#       RIGHT UPPER ARM SEGMENT
TR_SUPANT_Hum       Superior anterior plate
TR_SUPPOS_Hum       Superior posterior plate
TR_INFPOS_Hum       Inferior posterior plate

TR_INFANT_Hum       Inferior anterior plate

TSR_MED_Elb         Static medial elbow
TSR_LAT_Elb         Static lateral elbow

#       RIGHT FORE ARM SEGMENT
TR_SUPANT_Ulna      Superior anterior plate
TR_MEDPOS_Ulna      Medial posterior plate
TR_INFANT_Ulna      Inferior anterior plate

TSR_MEDDIS_Radius Static wrist pinky side
TSR_LATDIS_Radius Static wrist thumb side

#       RIGHT FEMUR SEGMENT
TSR_Gtro            Static greater trocanter
TR_SUPANT_Femur     Superior anterior plate
TR_SUPPOS_Femur     Superior posterior plate
TR_INFPOS_Femur     Inferior posterior plate
TR_INFANT_Femur     Inferior anterior plate

TSR_MED_EpiC        Static medial epicondyle
TR_LAT_EpiC         Lateral epicondyle

#       RIGHT SHANK SEGMENT
TR_LAT_FibHead      Fibular head
TR_TibTub           Tibial tuberosity
TR_MED_Mal          Medial malleolus
TR_LAT_Mal          Lateral malleolus

#       RIGHT HIND FOOT SEGMENT
TSR_INFPOS_Heel     Static HEEL MARKER
TR_SUPPOS_Heel      Right  heel  (closer  to  top  of
                             shoe)
TR_MED_Heel         Medial right shoe heel
TR_LAT_Heel         Lateral right on heel
TR_LATDOR_HFoot     Dorsal lateral right hind-foot

TSR_MEDPRX_Met1     Static medial 1rst metatarsal
TSR_LATPRX_Met5     Static lateral 1rst metatarsal

#       RIGHT FORE FOOT SEGMENT
```

132

```
TR_MEDPOS_FFoot    Medial toward heel fore-foot        TL_SUPPOS_Heel     Left  heel  (closer  to  top  of
TR_LATPOS_FFoot    Lateral toward heel fore-foot                          shoe)
TR_MEDANT_FFoot    Medial TOE MARKER fore-foot         TL_MED_Heel        Medial left shoe heel
TR_LATANT_FFoot    Lateral toward toe fore-foot        TL_LAT_Heel        Lateral left on heel
                                                       TL_LATDOR_HFoot    Dorsal lateral left hind-foot
#      LEFT UPPER ARM SEGMENT
TL_SUPANT_Hum      Superior anterior uparm plate       TSL_MEDPRX_Met1    Static medial 1rst metatarsal
TL_SUPPOS_Hum      Superior posterior uparm plate      TSL_LATPRX_Met5    Static lateral 1rst metatarsal
TL_INFPOS_Hum      Inferior posterior uparm plate
TL_INFANT_Hum      Inferior anterior uparm plate       #      LEFT FORE FOOT SEGMENT
                                                       TL_MEDPOS_FFoot    Medial toward heel fore-foot
TSL_MED_Elb        Static medial left elbow            TL_LATPOS_FFoot    Lateral toward heel fore-foot
TSL_LAT_Elb        Static lateral left elbow           TL_MEDANT_FFoot    Medial TOE MARKER fore-foot
                                                       TL_LATANT_FFoot    Lateral toward toe fore-foot
#      LEFT FORE ARM SEGMENT
TL_SUPANT_Ulna     Superior anterior forarm plate      #      End of autolabel marker definitions
TL_MEDPOS_Ulna     Medial posterior forearm plate
TL_INFANT_Ulna     Inferior anterior forearm plate     #      Segment  definitions  define  green  stick
                                                              figure  AND  determine  which  markers  are
TSL_MEDDIS_Radius Static left wrist pinky side                assumed  to  remain  approximately  equidistant
TSL_LATDIS_Radius Static left wrist thumb side                for autolabeling

#      LEFT FEMUR SEGMENT
TSL_Gtro           Static left greater trocanter       #      PELVIS is set to the ROOT segment and will
TL_SUPANT_Femur    Superior posterior femur plate             be the first segment labeled
TL_SUPPOS_Femur    Superior posterior femur plate
TL_INFPOS_Femur    Inferior posterior femur plate      G_Head  =  TR_ANT_Head,  TL_ANT_Head,  TL_POS_Head,
TL_INFANT_Femur    Inferior anterior femur plate             TR_POS_Head
                                                       ROOT = TR_Acr, T_C7, TL_Acr, T_INF_Sternum
TSL_MED_EpiC       Static medial epicondyle
TL_LAT_EpiC        Lateral epicondyle                  G_Pelvis = TR_ASIS, TR_PSIS, TL_PSIS, TL_ASIS

#      LEFT SHANK SEGMENT                               GR_UArm      =      TR_SUPANT_Hum,      TR_SUPPOS_Hum,
TL_LAT_FibHead     Fibular head                               TR_INFPOS_Hum, TR_INFANT_Hum
TL_TibTub          Tibial tuberosity                   GL_UArm      =      TL_SUPANT_Hum,      TL_SUPPOS_Hum,
TL_MED_Mal         Medial malleolus                          TL_INFPOS_Hum, TL_INFANT_Hum
TL_LAT_Mal         Lateral malleolus
                                                       GR_FArm      =      TR_SUPANT_Ulna,      TR_MEDPOS_Ulna,
#      LEFT HIND FOOT SEGMENT                                 TR_INFANT_Ulna
TSL_INFPOS_Heel    Static HEEL MARKER                  GL_FArm      =      TL_SUPANT_Ulna,      TL_MEDPOS_Ulna,
                                                              TL_INFANT_Ulna
```

```
GR_Thigh   =   TR_SUPANT_Femur,   TR_SUPPOS_Femur,
    TR_INFPOS_Femur,           TR_INFANT_Femur,
    TR_LAT_EpiC
GL_Thigh   =   TL_SUPANT_Femur,   TL_SUPPOS_Femur,
    TL_INFPOS_Femur,           TL_INFANT_Femur,
    TL_LAT_EpiC

GR_Shank = TR_TibTub, TR_LAT_FibHead, TR_LAT_Mal,
    TR_MED_Mal
GL_Shank = TL_TibTub, TL_LAT_FibHead, TL_LAT_Mal,
    TL_MED_Mal

GR_Foot    =    TR_SUPPOS_Heel,    TR_MED_Heel,
    TR_LAT_Heel, TR_LATDOR_HFoot
GL_Foot    =    TL_SUPPOS_Heel,    TL_MED_Heel,
    TL_LAT_Heel, TL_LATDOR_HFoot

GR_Toe   =   TR_MEDPOS_FFoot,   TR_LATPOS_FFoot,
    TR_MEDANT_FFoot, TR_LATANT_FFoot
GL_Toe   =   TL_MEDPOS_FFoot,   TL_LATPOS_FFoot,
    TL_MEDANT_FFoot, TL_LATANT_FFoot

#    Connecting  segments  to  imply  joints  for
     autolabeling

G_Head, ROOT
ROOT, GR_UArm
ROOT, GL_UArm
ROOT, G_Pelvis
G_Pelvis, GR_Thigh
G_Pelvis, GL_Thigh
GR_Thigh, GR_Shank
GL_Thigh, GL_Shank
GR_Shank, GR_Foot
GL_Shank, GL_Foot
GR_Foot, GR_Toe
GL_Foot, GL_Toe


[LCS]
```

```
#    This  section  designed  to  display  the  LCSs
     (origins and axes) for each segment as well
     as  for  displaying  the  Euler  and  JCS
     rotations

#    These  are  the  Euler  angle  rotations  of  the
     child  WRT  the  parent  about  the  parent  axes
     and  the  JCS  rotations  using  the  floating
     axis Cole et al. approach

J_Neck
E_Head_Global

JR_Shld
JL_Shld
JR_Elbow
JL_Elbow

E_Torso_Global
J_Waist
E_Pelvis_Global

JR_Hip
JL_Hip

JR_Knee
JL_Knee

JR_Ankle
JL_Ankle

ER_FFA            Global angle of foot-to-floor
EL_FFA            Global angle of foot-to-floor
JR_MP
JL_MP


#    For drawing local coordinate system axes

TV_Head_Origin    Top of head
UxG_Head
UyG_Head
```

134

```
UzG_Head                                             UzGL_Thigh

TV_Torso_Origin   Calculated  C7  height  on  long   TVR_AJC              Right Ankle Joint Center
                            axis                      UxGR_Shank
UxG_Torso                                             UyGR_Shank
UyG_Torso                                             UzGR_Shank
UzG_Torso
                                                      TVL_AJC              Left Ankle Joint Center
TVR_EJC           Right Elbow Joint Center            UxGL_Shank
UxGR_UArm                                             UyGL_Shank
UyGR_UArm                                             UzGL_Shank
UzGR_UArm
                                                      TR_SUPPOS_Heel    Heel marker
TVL_EJC           Left Elbow Joint Center             UxGR_Foot
UxGL_UArm                                             UyGR_Foot
UyGL_UArm                                             UzGR_Foot
UzGL_UArm
                                                      TL_SUPPOS_Heel    Heel marker
TVR_WJC           Right Wrist Joint Center            UxGL_Foot
UxGR_FArm                                             UyGL_Foot
UyGR_FArm                                             UzGL_Foot
UzGR_FArm
                                                      TVR_Toe              Moving mid-toe marker
TVL_WJC           Left Wrist Joint Center             UxGR_Toe
UxGL_FArm                                             UyGR_Toe
UyGL_FArm                                             UzGR_Toe
UzGL_FArm
                                                      TVL_Toe              Moving mid-toe marker
TV_MIDH           Midpoint of HJCs                    UxGL_Toe
UxG_Pelvis                                            UyGL_Toe
UyG_Pelvis                                            UzGL_Toe
UzG_Pelvis
                                                      #    Connect  origin  and  axes  markers  to  draw
TVR_KJC           Right Knee Joint Center                  lines
UxGR_Thigh
UyGR_Thigh                                            TV_Head_Origin, UxG_Head
UzGR_Thigh                                            TV_Head_Origin, UyG_Head
                                                      TV_Head_Origin, UzG_Head
TVL_KJC           Left Knee Joint Center
UxGL_Thigh                                            TV_Torso_Origin, UxG_Torso
UyGL_Thigh                                            TV_Torso_Origin, UyG_Torso
```

```
TV_Torso_Origin, UzG_Torso                       TL_SUPPOS_Heel, UxGL_Foot
                                                 TL_SUPPOS_Heel, UyGL_Foot
TVR_EJC, UxGR_UArm                               TL_SUPPOS_Heel, UzGL_Foot
TVR_EJC, UyGR_UArm
TVR_EJC, UzGR_UArm                               TVR_Toe, UxGR_Toe
                                                 TVR_Toe, UyGR_Toe
TVL_EJC, UxGL_UArm                               TVR_Toe, UzGR_Toe
TVL_EJC, UyGL_UArm
TVL_EJC, UzGL_UArm                               TVL_Toe, UxGL_Toe
                                                 TVL_Toe, UyGL_Toe
TVR_WJC, UxGR_FArm                               TVL_Toe, UzGL_Toe
TVR_WJC, UyGR_FArm
TVR_WJC, UzGR_FArm

TVL_WJC, UxGL_FArm                               [Forces]
TVL_WJC, UyGL_FArm                               #    These are the measured forceplate quantities
TVL_WJC, UzGL_FArm                                    and center of pressure as well as the forces
                                                      and moments at the joints resulting from
TV_MIDH, UxG_Pelvis                                   inverse dynamics
TV_MIDH, UyG_Pelvis
TV_MIDH, UzG_Pelvis                              FR_FP            Right Foot force plate forces
                                                 FL_FP            Left Foot force plate forces
TVR_KJC, UxGR_Thigh                              MR_FP            Right Foot force plate moments
TVR_KJC, UyGR_Thigh                              ML_FP            Left Foot force plate moments
TVR_KJC, UzGR_Thigh
                                                 FR_FP_VIS        Right Foot force plate forces
TVL_KJC, UxGL_Thigh                              FL_FP_VIS        Left Foot force plate forces
TVL_KJC, UyGL_Thigh                              MR_FP_VIS        Right Foot force plate moments
TVL_KJC, UzGL_Thigh                              ML_FP_VIS        Left Foot force plate moments

TVR_AJC, UxGR_Shank                              TR_CFP           Center of plate
TVR_AJC, UyGR_Shank                              TL_CFP           Center of plate
TVR_AJC, UzGR_Shank                              TR_COP           Center of pressure
                                                 TL_COP           Center of pressure
TVL_AJC, UxGL_Shank
TVL_AJC, UyGL_Shank                              FR_Hip
TVL_AJC, UzGL_Shank                              MR_Hip
                                                 FL_Hip
TR_SUPPOS_Heel, UxGR_Foot                        ML_Hip
TR_SUPPOS_Heel, UyGR_Foot
TR_SUPPOS_Heel, UzGR_Foot                        FR_Knee
```

MR_Knee		TV_Torso_Origin	Caclulated C7 height on long axis
FL_Knee			
ML_Knee		TV_Torso_COM	Torso Center of Mass
		TVR_SJC	Right Shoulder Joint Center
FR_Ankle		TVL_SJC	Left Shoulder Joint Center
MR_Ankle		TV_Torso_Attach	Between Pelvis and Torso
FL_Ankle			
ML_Ankle		TVR_UArm_COM	Right Upper Arm Center of Mass
		TVR_EJC	Right Elbow Joint Center
FR_MP		TVL_UArm_COM	Left Upper Arm Center of Mass
MR_MP		TVL_EJC	Left Elbow Joint Center
FL_MP			
ML_MP		TVR_FArm_COM	Right ForeArm Center of Mass
		TVR_WJC	Right Wrist Joint Center
FR_FP_VIS, TR_COP		TVL_FArm_COM	Left ForeArm Center of Mass
FL_FP_VIS, TL_COP		TVL_WJC	Left Wrist Joint Center
F_Neck		TV_Pelvis_COM	Pelvis Center of Mass
M_Neck		TV_MIDH	Midpoint of HJCs
F_Waist		TVR_HJC	Right Hip Joint Center
M_Waist		TVL_HJC	Left Hip Joint Center
FR_Elb		TVR_Thigh_COM	Right Thigh Center of Mass
MR_Elb		TVR_KJC	Right Knee Joint Center
FL_Elb		TVL_Thigh_COM	Left Thigh Center of Mass
ML_Elb		TVL_KJC	Left Knee Joint Center
FR_Shld		TVR_Shank_COM	Right Shank Center of Mass
MR_Shld		TVR_AJC	Right Ankle Joint Center
FL_Shld		TVL_Shank_COM	Left Shank Center of Mass
ML_Shld		TVL_AJC	Left Ankle Joint Center
		TVR_Combo_COM	Right Foot Center of Mass
[Stick]		TR_SUPPOS_Heel	heel marker
# Use this for drawing a stick figure with COM stuff too		TVR_Foot_Origin	Between toe markers from static trial
TV_Head_Origin Top Of Head		TVL_Combo_COM	Left Foot Center of Mass
TV_Head_COM Head Center of Mass		TL_SUPPOS_Heel	heel marker
		TVL_Foot_Origin	Between toe markers from static trial

137

```
TVR_MPJC          Center of the MP joint
TVR_Toe           Between toe markers
TVL_MPJC          Center of the MP joint
TVL_Toe           Between toe markers


TV_BODY_COM       Whole Body Center of Mass


#     Again any markers reused below must
#     be listed before used

TV_Head_Origin, TV_Head_COM
TV_Head_COM, TV_Torso_Origin
TV_Torso_Origin, TVR_SJC
TV_Torso_Origin, TVL_SJC
TV_Torso_Origin, TV_Torso_COM
TV_Torso_COM, TV_Torso_Attach


TVR_SJC, TVR_UArm_COM
TVR_UArm_COM, TVR_EJC
TVL_SJC, TVL_UArm_COM
TVL_UArm_COM, TVL_EJC


TVR_EJC, TVR_FArm_COM
TVR_FArm_COM, TVR_WJC
TVL_EJC, TVL_FArm_COM
TVL_FArm_COM, TVL_WJC


TV_Torso_Attach, TV_Pelvis_COM
TV_Pelvis_COM, TV_MIDH
TV_MIDH, TVR_HJC
TV_MIDH, TVL_HJC


TVR_HJC, TVR_Thigh_COM
TVR_Thigh_COM, TVR_KJC
TVL_HJC, TVL_Thigh_COM
TVL_Thigh_COM, TVL_KJC


TVR_KJC, TVR_Shank_COM
TVR_Shank_COM, TVR_AJC
TVL_KJC, TVL_Shank_COM
```

```
TVL_Shank_COM, TVL_AJC

TVR_AJC, TVR_Combo_COM, TR_SUPPOS_Heel
TVR_Combo_COM, TVR_MPJC
TVL_AJC, TVL_Combo_COM, TL_SUPPOS_Heel
TVL_Combo_COM, TVL_MPJC


TVR_MPJC, TVR_Toe
TVL_MPJC, TVL_Toe



            [Velocities]


#     These are the calculated velocities
#     of the heel and COM
#     For visualization include the
#     position as well in this set


TSR_INFPOS_Heel
VTSR_INFPOS_Heel
TSL_INFPOS_Heel
VTSL_INFPOS_Heel


TVR_Foot_Origin
VTVR_Foot_Origin
TVL_Foot_Origin
VTVL_Foot_Origin


TVL_Toe
VTVL_Toe


TV_Body_COM
VTV_Body_COM
```

APPENDIX D

BODY BUILDER MODEL

The following model was used to generate the typical data plots for this chapter (see Appendix B and Appendix C for information about variables names). This code requires that the frame rate and subject height, weight, gender, and shoe size be present in a related model parameter file (*.mp). See Appendix E, for a typical mp file.

```
{*    This Bodylanguage script was developed at the Human Movement and Balance Laboratory, Department of
      Bioengineering, University of Pittsburgh, Pittsburgh PA, 15905, USA. This code may not be reused
      without acknowledgment.


           Revision November, 2005


           This model file is requires a companion maker set and model parameters files.
*}


{*    MACROS
*}
MACRO DISPLAYAXES(ASeg)
      Ux#ASeg = ASeg(0) + 150*ASeg(1)
      Uy#ASeg = ASeg(0) + 150*ASeg(2)
      Uz#ASeg = ASeg(0) + 150*ASeg(3)


      OUTPUT(Ux#ASeg, Uy#ASeg, Uz#ASeg)
ENDMACRO



MACRO REPLACE4(p1, p2, p3, p4)
      s234 = [p3, p2 - p3, p3 - p4]
      p1V = Average(p1/s234)*s234
      s341 = [p4, p3 - p4, p4 - p1]
      p2V = Average(p2/s341)*s341
      s412 = [p1, p4 - p1, p1 - p2]
      p3V = Average(p3/s412)*s412
      s123 = [p2, p1 - p2, p2 - p3]
      p4V = Average(p4/s123)*s123


      p1 = p1 ? p1V
      p2 = p2 ? p2V
      p3 = p3 ? p3V
      p4 = p4 ? p4V


      OUTPUT(p1, p2, p3, p4)
ENDMACRO



MACRO LINVELACC(Point)
      FrameTimeLength = 1/$SamplingRate
```

```
        V#Point = ((Point[-2] - (8*Point[-1]) + (8*Point[1]) - Point[2])/(12*FrameTimeLength))/1000
        A#Point = ((V#Point[-2] - (8*V#Point[-1]) + (8*V#Point[1]) - V#Point[2])/(12*FrameTimeLength))

        OUTPUT(V#Point, A#Point)
ENDMACRO


{*      OPTIONAL POINTS

        If we forgot a marker for a static or dynamic trial, add it here.
        Previously difficult markers include the upperback, T_C7, and fore foot markers.
*}
OPTIONALPOINTS(TS_T10)
OPTIONALPOINTS(TSR_MED_Elb, TSR_LAT_Elb, TSR_LATDIS_Radius, TSR_MEDDIS_Radius)
OPTIONALPOINTS(TSL_MED_Elb, TSL_LAT_Elb, TSL_LATDIS_Radius, TSL_MEDDIS_Radius)
OPTIONALPOINTS(TSR_Gtro, TSR_MED_EpiC)
OPTIONALPOINTS(TSL_Gtro, TSL_MED_EpiC)
OPTIONALPOINTS(TSR_INFPOS_Heel, TSR_MEDPRX_Met1, TSR_LATPRX_Met5)
OPTIONALPOINTS(TSL_INFPOS_Heel, TSL_MEDPRX_Met1, TSL_LATPRX_Met5)


{*      REPLACE MISSING MARKERS
*}
REPLACE4(TR_ANT_Head, TL_ANT_Head, TL_POS_Head, TR_POS_Head)
REPLACE4(TR_Acr, TL_Acr, T_INF_Sternum, T_C7)
REPLACE4(TR_SUPANT_Hum, TR_SUPPOS_Hum, TR_INFPOS_Hum, TR_INFANT_Hum)
REPLACE4(TL_SUPANT_Hum, TL_SUPPOS_Hum, TL_INFPOS_Hum, TL_INFANT_Hum)
REPLACE4(TR_ASIS, TL_ASIS, TL_PSIS, TR_PSIS)
REPLACE4(TR_SUPANT_Femur, TR_SUPPOS_Femur, TR_INFPOS_Femur, TR_INFANT_Femur)
REPLACE4(TL_SUPANT_Femur, TL_SUPPOS_Femur, TL_INFPOS_Femur, TL_INFANT_Femur)
REPLACE4(TR_SUPANT_Femur, TR_SUPPOS_Femur, TR_INFPOS_Femur, TR_LAT_EpiC)
REPLACE4(TL_SUPANT_Femur, TL_SUPPOS_Femur, TL_INFPOS_Femur, TL_LAT_EpiC)
REPLACE4(TR_TibTub, TR_LAT_FibHead, TR_LAT_Mal, TR_MED_Mal)
REPLACE4(TL_TibTub, TL_LAT_FibHead, TL_LAT_Mal, TL_MED_Mal)
REPLACE4(TR_SUPPOS_Heel, TR_MED_Heel, TR_LAT_Heel, TR_LATDOR_HFoot)
REPLACE4(TL_SUPPOS_Heel, TL_MED_Heel, TL_LAT_Heel, TL_LATDOR_HFoot)
REPLACE4(TR_MEDPOS_FFoot, TR_LATPOS_FFoot, TR_LATANT_FFoot, TR_MEDANT_FFoot)
REPLACE4(TL_MEDPOS_FFoot, TL_LATPOS_FFoot, TL_LATANT_FFoot, TL_MEDANT_FFoot)


{*      STATIC MARKER RELOCATION
```

```
*}
D_Torso = [T_C7, TR_Acr - TL_Acr, T_C7 - T_INF_Sternum]
DR_UArm = [TR_INFANT_Hum, TR_INFANT_Hum - TR_SUPPOS_Hum, TR_INFPOS_Hum - TR_INFANT_Hum]
DL_UArm = [TL_INFANT_Hum, TL_INFANT_Hum - TL_SUPPOS_Hum, TL_INFPOS_Hum - TL_INFANT_Hum]
DR_FArm = [TR_SUPANT_Ulna, TR_MEDPOS_Ulna - TR_SUPANT_Ulna, TR_INFANT_Ulna - TR_SUPANT_Ulna]
DL_FArm = [TL_SUPANT_Ulna, TL_MEDPOS_Ulna - TL_SUPANT_Ulna, TL_INFANT_Ulna - TL_SUPANT_Ulna]
DR_Thigh = [TR_LAT_EpiC, TR_SUPPOS_Femur - TR_LAT_EpiC, TR_INFANT_Femur - TR_INFPOS_Femur]
DL_Thigh = [TL_LAT_EpiC, TL_SUPPOS_Femur - TL_LAT_EpiC, TL_INFANT_Femur - TL_INFPOS_Femur]
DR_HFoot = [TR_SUPPOS_Heel, TR_LATDOR_HFoot - TR_SUPPOS_Heel, TR_MED_Heel - TR_LAT_Heel]
DL_HFoot = [TL_SUPPOS_Heel, TL_LATDOR_HFoot - TL_SUPPOS_Heel, TL_MED_Heel - TL_LAT_Heel]
DR_FFoot = [TR_MEDANT_FFoot, TR_MEDPOS_FFoot - TR_MEDANT_FFoot, TR_MEDANT_FFoot - TR_LATANT_FFoot]
DL_FFoot = [TL_MEDANT_FFoot, TL_MEDPOS_FFoot - TL_MEDANT_FFoot, TL_MEDANT_FFoot - TL_LATANT_FFoot]

{*    Average location of removable markers from static trial to mp file
*}
IF ($Static == 1)
     $%PS_T10 = TS_T10/D_TORSO
     $%PSR_MED_Elb = TSR_MED_Elb/DR_UArm
     $%PSR_LAT_Elb = TSR_LAT_Elb/DR_UArm
     $%PSL_MED_Elb = TSL_MED_Elb/DL_UArm
     $%PSL_LAT_Elb = TSL_LAT_Elb/DL_UArm
     $%PSR_LATDIS_Radius = TSR_LATDIS_Radius/DR_FArm
     $%PSR_MEDDIS_Radius = TSR_MEDDIS_Radius/DR_FArm
     $%PSL_LATDIS_Radius = TSL_LATDIS_Radius/DL_FArm
     $%PSL_MEDDIS_Radius = TSL_MEDDIS_Radius/DL_FArm
     $%PSR_GTro = TSR_GTro/DR_Thigh
     $%PSL_GTro = TSL_GTro/DL_Thigh
     $%PSR_MED_EpiC = TSR_MED_EpiC/DR_Thigh
     $%PSL_MED_EpiC = TSL_MED_EpiC/DL_Thigh
     $%PSR_INFPOS_Heel = TSR_INFPOS_Heel/DR_HFoot
     $%PSL_INFPOS_Heel = TSL_INFPOS_Heel/DL_HFoot
     $%PSR_MEDPRX_Met1 = TSR_MEDPRX_Met1/DR_FFoot
     $%PSR_LATPRX_Met5 = TSR_LATPRX_Met5/DR_FFoot
     $%PSL_MEDPRX_Met1 = TSL_MEDPRX_Met1/DL_FFoot
     $%PSL_LATPRX_Met5 = TSL_LATPRX_Met5/DL_FFoot

     PARAM($%PS_T10, $%PSR_MED_Elb, $%PSR_LAT_Elb, $%PSL_MED_Elb, $%PSL_LAT_Elb, $%PSR_LATDIS_Radius)
     PARAM($%PSR_MEDDIS_Radius, $%PSL_LATDIS_Radius, $%PSL_MEDDIS_Radius, $%PSR_Gtro, $%PSL_Gtro)
     PARAM($%PSR_MED_EpiC, $%PSL_MED_EpiC, $%PSR_INFPOS_Heel, $%PSL_INFPOS_Heel, $%PSR_MEDPRX_Met1)
     PARAM($%PSR_LATPRX_Met5, $%PSL_MEDPRX_Met1, $%PSL_LATPRX_Met5)
ENDIF
```

```
TS_T10 = $%PS_T10*D_TORSO
TSR_MED_Elb = $%PSR_MED_Elb*DR_UArm
TSR_LAT_Elb = $%PSR_LAT_Elb*DR_UArm
TSL_MED_Elb = $%PSL_MED_Elb*DL_UArm
TSL_LAT_Elb = $%PSL_LAT_Elb*DL_UArm
TSR_LATDIS_Radius = $%PSR_LATDIS_Radius*DR_FArm
TSR_MEDDIS_Radius = $%PSR_MEDDIS_Radius*DR_FArm
TSL_LATDIS_Radius = $%PSL_LATDIS_Radius*DL_FArm
TSL_MEDDIS_Radius = $%PSL_MEDDIS_Radius*DL_FArm
TSR_GTro = $%PSR_GTro*DR_Thigh
TSL_GTro = $%PSL_GTro*DL_Thigh
TSR_MED_EpiC = $%PSR_MED_EpiC*DR_Thigh
TSL_MED_EpiC = $%PSL_MED_EpiC*DL_Thigh
TSR_INFPOS_Heel = $%PSR_INFPOS_Heel*DR_HFoot
TSL_INFPOS_Heel = $%PSL_INFPOS_Heel*DL_HFoot
TSR_MEDPRX_Met1 = $%PSR_MEDPRX_Met1*DR_FFoot
TSR_LATPRX_Met5 = $%PSR_LATPRX_Met5*DR_FFoot
TSL_MEDPRX_Met1 = $%PSL_MEDPRX_Met1*DL_FFoot
TSL_LATPRX_Met5 = $%PSL_LATPRX_Met5*DL_FFoot


OUTPUT(TS_T10)
OUTPUT(TSR_MED_Elb, TSR_LAT_Elb, TSL_MED_Elb, TSL_LAT_Elb)
OUTPUT(TSR_LATDIS_Radius, TSR_MEDDIS_Radius, TSL_LATDIS_Radius, TSL_MEDDIS_Radius)
OUTPUT(TSR_Gtro, TSL_Gtro, TSR_MED_EpiC, TSL_MED_EpiC)
OUTPUT(TSR_INFPOS_Heel, TSL_INFPOS_Heel)
OUTPUT(TSR_MEDPRX_Met1, TSR_LATPRX_Met5, TSL_MEDPRX_Met1, TSL_LATPRX_Met5)



{*      SEGMENT/LCS DEFS
*}
NN = $Ms_Body



{*      Replace original GLOBAL with more meaningful coordinate system
*}
G_GLOBAL = [{0, 0, 0}, {0, 0, 1}-{0, 0, 0}, {0, 0, 0}-{0, 1, 0}, zyx]



{*      PELVIS
*}
```

143

```
TV_PJC1 = (TL_ASIS + TR_ASIS)/2
dir1 = NORM(TR_ASIS, TL_ASIS, (TR_PSIS + TL_PSIS)/2)

G_Pelvis = [TV_PJC1, TL_ASIS - TR_ASIS, {0, 0, 0} - dir1, yxz]

IF ($Static == 1)
      $Wdth_Pelvis = DIST(TR_ASIS, TL_ASIS)
      $Dpth_Pelvis = DIST((TR_PSIS + TL_PSIS)/2, (TR_ASIS + TL_ASIS)/2)
      $LnR_ASISAnkle = DIST(TR_ASIS, TR_MED_Mal)
      $LnL_ASISAnkle = DIST(TL_ASIS, TL_MED_Mal)

      PARAM($Wdth_Pelvis, $Dpth_Pelvis, $LnR_ASISAnkle, $LnL_ASISAnkle)
ENDIF

{*    Leardini 1999
*}
TVR_HJC = { -0.096*$LnR_ASISAnkle, 0.09*$Wdth_Pelvis - 111, -0.31*$Dpth_Pelvis}*G_Pelvis
TVL_HJC = { -0.096*$LnL_ASISAnkle, -0.09*$Wdth_Pelvis + 111, -0.31*$Dpth_Pelvis}*G_Pelvis

{*    Bell 1990
*}
TVR_HJC2 = {-0.30*$Wdth_Pelvis, -0.36*$Wdth_Pelvis, -0.19*$Wdth_Pelvis}*G_Pelvis
TVL_HJC2 = {-0.30*$Wdth_Pelvis, 0.36*$Wdth_Pelvis, -0.19*$Wdth_Pelvis}*G_Pelvis

{*    Relocates the pelvis origin to be consistent with anthropometry ref
*}
TV_PJC = (TL_ASIS + TR_ASIS + TR_PSIS + TL_PSIS)/4
TV_MIDH = (TVR_HJC + TVL_HJC)/2

G_Pelvis = [TV_MIDH, TL_ASIS - TR_ASIS, {0, 0, 0} - dir1, yxz]
DISPLAYAXES(G_Pelvis)

{*    Gender 1 is male  *}
IF ($Gender == 1)
      Mult1 = 1 - 61.15/100
      Mult2 = 11.17/100
      Rx = 61.5/100
      Ry = 55.1/100
      Rz = 58.7/100
ELSE
      Mult1 = 1 - 49.20/100
```

144

```
        Mult2 = 12.47/100
        Rx = 43.3/100
        Ry = 40.2/100
        Rz = 44.4/100
ENDIF


IF ($Static == 1)
        $Ln_Pelvis = TS_T10(3) - TV_MIDH(3)
        Ln = $Ln_Pelvis

        $%P_Pelvis_COM = {0, 0, $Ln_Pelvis * Mult1}

        $Ms_Pelvis = Mult2*NN
        Ms = $Ms_Pelvis

        Ix = Ms*(Ln*Rx)*(Ln*Rx)
        Iy = Ms*(Ln*Ry)*(Ln*Ry)
        Iz = Ms*(Ln*Rz)*(Ln*Rz)

        $I_Pelvis = {Ix, Iy, Iz}

        PARAM($%P_Pelvis_COM)
        PARAM($Ln_Pelvis, $Ms_Pelvis, $I_Pelvis)
ENDIF

TV_Pelvis_COM = $%P_Pelvis_COM * G_Pelvis

OUTPUT(TVR_HJC, TVL_HJC, TVR_HJC2, TVL_HJC2, TV_PJC, TV_MIDH, TV_Pelvis_COM)


{*      TORSO
*}
IF ($Gender == 1)
        Mult1 = 50.66/100 {*    distance percentage to UPT COM from origin      *}
        Mult2 = 45.02/100 {*    distance percentage to MPT COM from midway point      *}
        Mult3 = 15.96/100 {*    Mass from UPT *}
        Mult4 = 16.33/100 {*    Mass from MPT *}
        Mult5 = 50.7262/100     {*    Distance from origin to combined COM      *}
        L_ratio = 52.9065/100   {*    How much of overall length comes from UPT *}
        d1 = 0.239238     {*    Distance from UPT COM to new COM as fraction of total length      *}
        d2 = -0.23382     {*    Distance from MPT COM to new COM as fraction of total length      *}
```

145

```
      R1x = 50.5/100      {*    1 refers to UPT, 2 to MPT      *}
      R1y = 32.0/100
      R1z = 46.5/100
      R2x = 48.2/100
      R2y = 38.3/100
      R2z = 46.8/100
ELSE
      Mult1 = 50.50/100
      Mult2 = 45.12/100
      Mult3 = 15.45/100
      Mult4 = 14.65/100
      Mult5 = 49.6549/100
      L_ratio = 52.6194/100
      d1 = 0.230821
      d2 = -0.24343
      R1x = 46.6/100
      R1y = 31.4/100
      R1z = 44.9/100
      R2x = 43.3/100
      R2y = 35.4/100
      R2z = 41.5/100
ENDIF

IF ($Static == 1)
      $%PV_Torso_Attach = {0, 0, $Ln_Pelvis}

      PV_Torso_Origin1 = (T_C7 + T_Inf_Sternum)/2
      PV_Torso_Origin1 = {PV_Torso_Origin1(1), PV_Torso_Origin1(2), T_C7(3)}
      $%PV_Torso_Origin = PV_Torso_Origin1/D_Torso

      PARAM($%PV_Torso_Attach, $%PV_Torso_Origin)
ENDIF

TV_Torso_Origin = $%PV_Torso_Origin * D_Torso
TV_Torso_Attach = $%PV_Torso_Attach * G_Pelvis

dir3 = NORM(TL_Acr, TR_Acr, TV_Torso_Attach)

G_Torso = [TV_Torso_Origin, TV_Torso_Origin - TV_Torso_Attach, {0, 0, 0} - dir3, zyx]
G_Torso2 = [TV_Torso_Origin, TV_Torso_Origin - TV_Torso_Attach, dir3 - {0, 0, 0}, zyx]
DISPLAYAXES(G_Torso)
```

```
IF ($Static == 1)
      $Ln_Torso = DIST(TV_Torso_Origin, TV_Torso_Attach)
      Ln = $Ln_Torso

      $%P_Torso_COM = {0, 0, -$Ln_Torso*Mult5}

      Ln1 = Ln*L_ratio
      Ln2 = Ln*(1 - L_ratio)
      $Ms_Torso = (Mult3 + Mult4)*NN
      $Ms_1 = Mult3*NN
      $Ms_2 = Mult4*NN

      K1x_S = R1x*Ln1*R1x*Ln1
      K1y_S = R1y*Ln1*R1y*Ln1
      K1z_S = R1z*Ln1*R1z*Ln1

      K2x_S = R2x*Ln2*R2x*Ln2
      K2y_S = R2y*Ln2*R2y*Ln2
      K2z_S = R2z*Ln2*R2z*Ln2

      d1_S = d1*Ln*d1*Ln
      d2_S = d2*Ln*d2*Ln

      Ix = (K1x_S + d1_S)*$Ms_1 + (K2x_S + d2_S)*$Ms_2
      Iy = (K1y_S + d1_S)*$Ms_1 + (K2y_S + d2_S)*$Ms_2
      Iz = K1z_S*$Ms_1 + K2z_S*$Ms_2

      $I_Torso = {Ix, Iy, Iz}

      PARAM($%P_Torso_COM)
      PARAM($Ln_Torso, $Ms_Torso, $I_Torso)
ENDIF

TV_Torso_COM = $%P_Torso_COM * G_Torso

G_Torso = [G_Torso, G_Pelvis, TV_Torso_Attach, $Ms_Torso, $%P_Torso_COM, $I_Torso]

OUTPUT(TV_Torso_Origin, TV_Torso_Attach, TV_Torso_COM)
```

147

```
{*     HEAD
*}
TV_Head_Origin1 = (TR_ANT_Head + TL_ANT_Head + TL_POS_Head + TR_POS_Head)/4
dir4 = NORM(T_C7, TR_POS_Head, TL_POS_Head)

G_Head = [TV_Head_Origin1, TL_ANT_Head - TR_ANT_Head, {0, 0, 0} - dir4, yzx]

IF ($Gender == 1)
     Mult1 = 50.2/100
     Mult2 = 6.94/100
     Rx = 30.3/100
     Ry = 31.5/100
     Rz = 26.1/100
ELSE
     Mult1 = 48.41/100
     Mult2 = 6.68/100
     Rx = 27.1/100
     Ry = 29.5/100
     Rz = 26.1/100
ENDIF

IF ($Static == 1)
     $Ln_Head = $Height + 30 - T_C7(3)

     C_Head_TOP_Offset = $Height + 30 - TV_Head_Origin1(3)
     C_Head_COM_Offset = Mult1 * $Ln_Head - C_Head_TOP_Offset

     $%P_Head_COM = -{0, 0, C_Head_COM_Offset}
     $%P_Head_TOP =  {0, 0, C_Head_TOP_Offset}

     $Ms_Head = Mult2*NN
     Ms = $Ms_Head

     Ln = $Ln_Head

     Ix = Ms*(Ln*Rx)*(Ln*Rx)
     Iy = Ms*(Ln*Ry)*(Ln*Ry)
     Iz = Ms*(Ln*Rz)*(Ln*Rz)

     $I_Head = {Ix, Iy, Iz}
```

```
        PARAM($%P_Head_COM, $%P_Head_TOP)
        PARAM($Ln_Head, $Ms_Head, $I_Head)
ENDIF


TV_Head_COM = $%P_Head_COM*G_Head
TV_Head_Origin = $%P_Head_TOP*G_Head


G_Head = [TV_Head_Origin, TL_ANT_Head - TR_ANT_Head, {0, 0, 0} - dir4, yzx]
DISPLAYAXES(G_Head)


G_Head = [G_Head, G_Torso, TV_Torso_Origin, $Ms_Head, $%P_Head_COM, $I_Head]


OUTPUT(TV_Head_Origin)
OUTPUT(TV_Head_COM)



{*      UPPER ARMS
*}
TVR_EJC = (TSR_LAT_Elb + TSR_MED_Elb)/2
TVL_EJC = (TSL_LAT_Elb + TSL_MED_Elb)/2


IF ($Gender == 1)
        Delta = -34.5 - 9.5         {*      9.5 = MARKER HEIGHT to center *}
        Mult1 = 1 - 57.72/100
        Mult2 = 2.71/100
        Rx = 28.5/100
        Ry = 26.9/100
        Rz = 15.8/100
ELSE
        Delta = -33.7 - 9.5
        Mult1 = 1 - 57.54/100
        Mult2 = 2.55/100
        Rx = 27.8/100
        Ry = 26.0/100
        Rz = 14.8/100
ENDIF


TVR_SJC = (TR_Acr/G_Torso + {0, 0, Delta})*G_Torso
TVL_SJC = (TL_Acr/G_Torso + {0, 0, Delta})*G_Torso


IF ($Static == 1)
```

149

```
        $LnR_UArm = DIST(TVR_SJC, TVR_EJC)
        $LnL_UArm = DIST(TVL_SJC, TVL_EJC)


        $%PVR_UArm_COM = {0, 0, Mult1*$LnR_UArm}
        $%PVL_UArm_COM = {0, 0, Mult1*$LnL_UArm}


        $Ms_UArm = Mult2*NN


        Ms = $Ms_UArm


        Ln = $LnR_UArm


        Ix = Ms*(Ln*Rx)*(Ln*Rx)
        Iy = Ms*(Ln*Ry)*(Ln*Ry)
        Iz = Ms*(Ln*Rz)*(Ln*Rz)


        $IR_UArm = {Ix, Iy, Iz}


        Ln = $LnL_UArm


        Ix = Ms*(Ln*Rx)*(Ln*Rx)
        Iy = Ms*(Ln*Ry)*(Ln*Ry)
        Iz = Ms*(Ln*Rz)*(Ln*Rz)


        $IL_UArm = {Ix, Iy, Iz}


        PARAM($%PVR_UArm_COM, $%PVL_UArm_COM)
        PARAM($LnR_UArm, $LnL_UArm, $Ms_UArm, $IR_UArm, $IL_UArm)
ENDIF

GR_UArm = [TVR_EJC, TVR_SJC - TVR_EJC, TSR_LAT_Elb - TSR_MED_Elb, zxy]
GL_UArm = [TVL_EJC, TVL_SJC - TVL_EJC, TSL_MED_Elb - TSL_LAT_Elb, zxy]
DISPLAYAXES(GR_UArm)
DISPLAYAXES(GL_UArm)

TVR_UArm_COM = $%PVR_Uarm_COM * GR_UArm
TVL_UArm_COM = $%PVL_Uarm_COM * GL_UArm

GR_UArm = [GR_UArm, G_Torso, TVR_SJC, $Ms_Uarm, $%PVR_Uarm_COM, $IR_UArm]
GL_UArm = [GL_UArm, G_Torso, TVL_SJC, $Ms_Uarm, $%PVL_Uarm_COM, $IL_UArm]
```

```
OUTPUT(TVR_SJC, TVL_SJC)
OUTPUT(TVR_EJC, TVL_EJC)
OUTPUT(TVR_UArm_COM, TVL_UArm_COM)


{*      FOREARMS (incl HANDS)
*}
TVR_WJC = (TSR_MEDDIS_Radius + TSR_LATDIS_Radius)/2
TVL_WJC = (TSL_MEDDIS_Radius + TSL_LATDIS_Radius)/2

GR_FArm = [TVR_WJC, TVR_EJC - TVR_WJC, TSR_LATDIS_Radius - TSR_MEDDIS_Radius, zxy]
GL_FArm = [TVL_WJC, TVL_EJC - TVL_WJC, TSL_MEDDIS_Radius - TSL_LATDIS_Radius, zxy]
DISPLAYAXES(GR_FArm)
DISPLAYAXES(GL_FArm)

{*      Segment 1 = forearm, Segment 2 = hand == > origin placed at WJC   *}
IF ($Gender == 1)
      Mult1 = 54.26/100 {*     percent length of forearm to forearm COM  *}
      Mult2 = 79/100    {*     percent length of hand to hand COM  *}
      Mult3 = 1.62/100  {*     percent total body mass for forearm *}
      Mult4 = 0.61/100  {*     percent total body mass for hand    *}
      L_ratio = 0.320565      {*    How long is the hand w.r.t. forearm length      *}

      R1x = 27.6/100
      R1y = 26.5/100
      R1z = 12.1/100


      R2x = 62.8/100
      R2y = 51.3/100
      R2z = 40.1/100
ELSE
      Mult1 = 54.41/100
      Mult2 = 74.74/100
      Mult3 = 1.38/100
      Mult4 = 0.56/100
      L_ratio = 0.295119183

      R1x = 26.1/100
      R1y = 25.7/100
      R1z = 9.4/100
```

151

```
        R2x = 53.1/100
        R2y = 45.4/100
        R2z = 33.5/100
ENDIF

IF ($Static == 1)
        $LnR_FArm = DIST(TVR_EJC, TVR_WJC)
        $LnL_FArm = DIST(TVL_EJC, TVL_WJC)

        {* Previously for dynamic as well as static?
        *}

        scale_factor = (Mult1*Mult3 - L_ratio*Mult2*Mult4)    {*    distance from origin to combo COM    *}
        d1 = (mult1 - scale_factor)   {*    distance from forearm COM to combo COM relative to forearm length
            *}
        d2 = (scale_factor + L_ratio*mult2) {*    distance from hand COM to combo COM relative to forearm
            length       *}

        Ms_1 = Mult3*NN
        Ms_2 = Mult4*NN

        $%PVR_FArm_COM = {0, 0, scale_factor*$LnR_FArm}
        $%PVL_FArm_COM = {0, 0, scale_factor*$LnL_FArm}

        $Ms_FArm = (Mult3 + Mult4)*NN

        {*    First Right and then Left    *}

        Ln = $LnR_FArm
        Ln2 = Ln*L_ratio

        d1_S = d1*Ln*d1*Ln
        d2_S = d2*Ln*d2*Ln

        K1x_S = R1x*Ln*R1x*Ln
        K1y_S = R1y*Ln*R1y*Ln
        K1z_S = R1z*Ln*R1z*Ln

        K2x_S = R2x*Ln2*R2x*Ln2
        K2y_S = R2y*Ln2*R2y*Ln2
        K2z_S = R2z*Ln2*R2z*Ln2
```

```
        Ix = (K1x_S + d1_S)*Ms_1 + (K2x_S + d2_S)*$Ms_2
        Iy = (K1y_S + d1_S)*Ms_1 + (K2y_S + d2_S)*$Ms_2
        Iz = K1z_S*Ms_1 + K2z_S*Ms_2

        $IR_FArm = {Ix, Iy, Iz}

        {* NOW LEFT *}

        Ln = $LnL_FArm
        Ln2 = Ln*L_ratio

        d1_S = d1*Ln*d1*Ln
        d2_S = d2*Ln*d2*Ln

        K1x_S = R1x*Ln*R1x*Ln
        K1y_S = R1y*Ln*R1y*Ln
        K1z_S = R1z*Ln*R1z*Ln

        K2x_S = R2x*Ln2*R2x*Ln2
        K2y_S = R2y*Ln2*R2y*Ln2
        K2z_S = R2z*Ln2*R2z*Ln2

        Ix = (K1x_S + d1_S)*Ms_1 + (K2x_S + d2_S)*$Ms_2
        Iy = (K1y_S + d1_S)*Ms_1 + (K2y_S + d2_S)*$Ms_2
        Iz = K1z_S*Ms_1 + K2z_S*Ms_2

        $IL_FArm = {Ix, Iy, Iz}

        PARAM($%PVR_FArm_COM, $%PVL_FArm_COM)
        PARAM($LnR_FArm, $LnL_FArm, $Ms_FArm, $IR_FArm, $IL_FArm)
        PARAM(scale_factor)
ENDIF

TVR_FArm_COM = $%PVR_FArm_COM*GR_FArm
TVL_FArm_COM = $%PVL_FArm_COM*GL_FArm

GR_FArm = [GR_FArm, GR_UArm, TVR_EJC, $Ms_FArm, $%PVR_FArm_COM, $IR_FArm]
GL_FArm = [GL_FArm, GL_UArm, TVL_EJC, $Ms_FArm, $%PVL_FArm_COM, $IL_FArm]

OUTPUT(TVR_WJC, TVL_WJC)
```

```
OUTPUT(TVR_FArm_COM, TVL_FArm_COM)


{*     THIGHS
*}
TVR_KJC = (TSR_MED_EpiC + TR_LAT_EpiC)/2
TVL_KJC = (TSL_MED_EpiC + TL_LAT_EpiC)/2
dir5 = NORM(TVR_HJC, TR_LAT_EpiC, TSR_MED_EpiC)
dir6 = NORM(TVL_HJC, TSL_MED_EpiC, TL_LAT_EpiC)

GR_Thigh = [TVR_KJC, dir5 - {0, 0, 0}, TVR_HJC - TVR_KJC, xyz]
GL_Thigh = [TVL_KJC, dir6 - {0, 0, 0}, TVL_HJC - TVL_KJC, xyz]
DISPLAYAXES(GR_Thigh)
DISPLAYAXES(GL_Thigh)

IF ($Gender == 1)
     Mult1 = 1 - 40.95/100
     Mult2 = 14.16/100
     Rx = 32.9/100
     Ry = 36.4/100
     Rz = 14.9/100
ELSE
     Mult1 = 1 - 36.12/100
     Mult2 = 14.78/100
     Rx = 36.9/100
     Ry = 36.4/100
     Rz = 16.2/100
ENDIF

IF ($Static == 1)
     $LnR_Thigh = DIST(TVR_HJC, TVR_KJC)
     $LnL_Thigh = DIST(TVL_HJC, TVL_KJC)

     $%PVR_Thigh_COM = {0, 0, Mult1*$LnR_Thigh}
     $%PVL_Thigh_COM = {0, 0, Mult1*$LnL_Thigh}

     $Ms_Thigh = Mult2*NN
     Ms = $Ms_Thigh

     Ln = $LnR_Thigh
```

```
        Ix = Ms*(Ln*Rx)*(Ln*Rx)
        Iy = Ms*(Ln*Ry)*(Ln*Ry)
        Iz = Ms*(Ln*Rz)*(Ln*Rz)

        $IR_Thigh = {Ix, Iy, Iz}

        $Ln = $LnL_Thigh

        Ix = Ms*(Ln*Rx)*(Ln*Rx)
        Iy = Ms*(Ln*Ry)*(Ln*Ry)
        Iz = Ms*(Ln*Rz)*(Ln*Rz)

        $IL_Thigh = {Ix, Iy, Iz}

        PARAM($%PVR_Thigh_COM, $%PVL_Thigh_COM)
        PARAM($LnR_Thigh, $LnL_Thigh, $Ms_Thigh, $IR_Thigh, $IL_Thigh)
ENDIF

TVR_Thigh_COM = $%PVR_Thigh_COM*GR_Thigh
TVL_Thigh_COM = $%PVL_Thigh_COM*GL_Thigh

GR_Thigh = [GR_Thigh, G_Pelvis, TVR_HJC, $Ms_Thigh, $%PVR_Thigh_COM, $IR_Thigh]
GL_Thigh = [GL_Thigh, G_Pelvis, TVL_HJC, $Ms_Thigh, $%PVL_Thigh_COM, $IL_Thigh]

OUTPUT(TVR_KJC, TVL_KJC)
OUTPUT(TVR_Thigh_COM, TVL_Thigh_COM)


{*      SHANKS
*}
TVR_AJC = (TR_MED_Mal + TR_LAT_Mal)/2
TVL_AJC = (TL_MED_Mal + TL_LAT_Mal)/2
dir7 = NORM(TVR_KJC, TR_LAT_Mal, TR_MED_Mal)
dir8 = NORM(TVL_KJC, TL_MED_Mal, TL_LAT_Mal)

GR_Shank = [TVR_AJC, dir7 - {0, 0, 0}, TVR_KJC - TVR_AJC, xyz]
GL_Shank = [TVL_AJC, dir8 - {0, 0, 0}, TVL_KJC - TVL_AJC, xyz]

GR_Shank2 = [TVR_AJC, dir7 - {0, 0, 0}, TVR_AJC - TVR_KJC, zyx]
GL_Shank2 = [TVL_AJC, dir8 - {0, 0, 0}, TVL_AJC - TVL_KJC, zyx]
DISPLAYAXES(GR_Shank)
```

```
DISPLAYAXES(GL_Shank)

IF ($Gender == 1)
      Mult1 = 1 - 43.95/100
      Mult2 = 4.33/100
      Rx = 25.1/100
      Ry = 24.6/100
      Rz = 10.2/100
ELSE
      Mult1 = 1 - 43.52/100
      Mult2 = 4.81/100
      Rx = 26.7/100
      Ry = 26.3/100
      Rz = 9.2/100
ENDIF

IF ($Static == 1)
      $LnR_Shank = DIST(TVR_KJC, TVR_AJC)
      $LnL_Shank = DIST(TVL_KJC, TVL_AJC)

      $%PVR_Shank_COM = {0, 0, Mult1*$LnR_Shank}
      $%PVL_Shank_COM = {0, 0, Mult1*$LnL_Shank}

      $Ms_Shank = Mult2*NN
      Ms = $Ms_Shank

      Ln = $LnR_Shank

      Ix = Ms*(Ln*Rx)*(Ln*Rx)
      Iy = Ms*(Ln*Ry)*(Ln*Ry)
      Iz = Ms*(Ln*Rz)*(Ln*Rz)

      $IR_Shank = {Ix, Iy, Iz}

      Ln = $LnL_Shank

      Ix = Ms*(Ln*Rx)*(Ln*Rx)
      Iy = Ms*(Ln*Ry)*(Ln*Ry)
      Iz = Ms*(Ln*Rz)*(Ln*Rz)

      $IL_Shank = {Ix, Iy, Iz}
```

156

```
        PARAM($%PVR_Shank_COM, $%PVL_Shank_COM)
        PARAM($LnR_Shank, $LnL_Shank, $Ms_Shank, $IR_Shank, $IL_Shank)
ENDIF


TVR_Shank_COM = $%PVR_Shank_COM*GR_Shank
TVL_Shank_COM = $%PVL_Shank_COM*GL_Shank

GR_Shank = [GR_Shank, GR_Thigh, TVR_KJC, $Ms_Shank, $%PVR_Shank_COM, $IR_Shank]
GL_Shank = [GL_Shank, GL_Thigh, TVL_KJC, $Ms_Shank, $%PVL_Shank_COM, $IL_Shank]

OUTPUT(TVR_AJC, TVL_AJC)
OUTPUT(TVR_Shank_COM, TVL_Shank_COM)


{*     FEET
*}
IF ($Static == 1)
        TVR_Foot_Origin = (TR_MEDANT_FFoot + TR_LATANT_FFoot)/2
        TVL_Foot_Origin = (TL_MEDANT_FFoot + TL_LATANT_FFoot)/2

        $%PVR_Foot_Origin = TVR_Foot_Origin / DR_HFoot
        $%PVL_Foot_Origin = TVL_Foot_Origin / DL_HFoot

        PARAM($%PVR_Foot_Origin, $%PVL_Foot_Origin)
ENDIF

TVR_Foot_Origin = $%PVR_Foot_Origin*DR_HFoot
TVL_Foot_Origin = $%PVL_Foot_Origin*DL_HFoot

dir9 = NORM(TR_SUPPOS_Heel, TSR_LATPRX_Met5, TSR_MEDPRX_Met1)
dir10 = NORM(TL_SUPPOS_Heel, TSL_MEDPRX_Met1, TSL_LATPRX_Met5)

GR_Foot = [TR_SUPPOS_Heel, dir9 - {0, 0, 0}, TVR_Foot_Origin - TR_SUPPOS_Heel, xyz]
GL_Foot = [TL_SUPPOS_Heel, dir10 - {0, 0, 0}, TVL_Foot_Origin - TL_SUPPOS_Heel,  xyz]

GR_Foot2 = [TR_SUPPOS_Heel, dir9 - {0, 0, 0}, TR_SUPPOS_Heel - TVR_Foot_Origin, zyx]
GL_Foot2 = [TL_SUPPOS_Heel, dir10 - {0, 0, 0}, TL_SUPPOS_Heel - TVL_Foot_Origin, zyx]

DISPLAYAXES(GR_Foot)
DISPLAYAXES(GL_Foot)
```

157

```
IF ($Gender == 1)
      Mult1 = 44.15/100
      Mult2 = 1.37/100
      Rx = 25.7/100
      Ry = 24.5/100
      Rz = 12.4/100
ELSE
      Mult1 = 40.14/100
      Mult2 = 1.29/100
      Rx = 29.9/100
      Ry = 27.9/100
      Rz = 13.9/100
ENDIF

IF($Static == 1)
      $LnR_Foot = DIST(TR_SUPPOS_Heel, TVR_Foot_Origin)
      $LnL_Foot = DIST(TL_SUPPOS_Heel, TVL_Foot_Origin)

      $%PVR_Foot_COM = {0, 0, Mult1*$LnR_Foot}
      $%PVL_Foot_COM = {0, 0, Mult1*$LnL_Foot}

      temp1 = DIST(TR_SUPPOS_Heel, TSR_INFPOS_Heel)
      temp2 = DIST(TL_SUPPOS_Heel, TSL_INFPOS_Heel)

      $%PVR_Shoe_COM = {-temp1, 0, $LnR_Foot/2}
      $%PVL_Shoe_COM = {-temp2, 0, $LnL_Foot/2}

      $Ms_Foot = Mult2*NN

      IF ($LnR_Foot + $LnL_Foot)/2 < 252.66
            $ShoeSize = 5.5
      ELSIF $LnR_Foot < 260.14
            $ShoeSize = 6
      ELSIF $LnR_Foot < 264.63
            $ShoeSize = 6.5
      ELSIF $LnR_Foot < 269.11
            $ShoeSize = 7
      ELSIF $LnR_Foot < 273.59
            $ShoeSize = 7.5
      ELSIF $LnR_Foot < 278.08
```

158

```
        $ShoeSize = 8
ELSIF $LnR_Foot < 282.56
        $ShoeSize = 8.5
ELSIF $LnR_Foot < 287.04
        $ShoeSize = 9
ELSIF $LnR_Foot < 291.53
        $ShoeSize = 9.5
ELSIF $LnR_Foot < 296.01
        $ShoeSize = 10
ELSIF $LnR_Foot < 300.49
        $ShoeSize = 10.5
ELSIF $LnR_Foot < 304.98
        $ShoeSize = 11
ELSIF $LnR_Foot < 309.46
        $ShoeSize = 11.5
ELSIF $LnR_Foot < 313.94
        $ShoeSize = 12
ELSIF $LnR_Foot < 318.43
        $ShoeSize = 12.5
ELSIF $LnR_Foot < 322.91
        $ShoeSize = 13
ELSE
        $ShoeSize = 13.5
ENDIF


$ShoeSize2 = $ShoeSize


$Ms_Shoe = ($ShoeSize*0.0425 + 0.5375)/2


$Ms_Combo = $Ms_Foot + $Ms_Shoe


$%PVR_Combo_COM = ($Ms_Foot * $%PVR_Foot_COM + $Ms_Shoe * $%PVR_Shoe_COM) / $Ms_Combo
$%PVL_Combo_COM = ($Ms_Foot * $%PVL_Foot_COM + $Ms_Shoe * $%PVL_Shoe_COM) / $Ms_Combo


d5 = $%PVR_Combo_COM - $%PVR_Foot_COM
d6 = $%PVR_Combo_COM - $%PVR_Shoe_COM
d7 = DIST($%PVR_Combo_COM, $%PVR_Foot_COM)
d8 = DIST($%PVR_Combo_COM, $%PVR_Shoe_COM)


Ms1 = $Ms_Foot
Ms2 = $Ms_Shoe
```

```
Ln = $LnR_Foot/2

K2x_S = 1/2*(($Ln*$Ln) + (45*45))
K2y_S = 1/6*((3*$Ln*$Ln) + (4*20*20))
K2z_S = 1/6*((3*45*45) + (4*20*20))


Ln = $LnR_Foot


K1x_S = Ln*Rx*Ln*Rx
K1y_S = Ln*Ry*Ln*Ry
K1z_S = Ln*Rz*Ln*Rz


Ix = (K1x_S + d5(3)*d5(3))*Ms1 + (K2x_S + d6(3)*d6(3))*Ms2
Iy = (K1y_S + d5(1)*d5(1))*Ms1 + (K2y_S + d6(1)*d6(1))*Ms2
Iz = (K1z_S + d7*d7)*Ms1 + (K2z_S + d8*d8)*Ms2


$IR_Combo = {Ix, Iy, Iz}


d5 = $%PVL_Combo_COM - $%PVL_Foot_COM
d6 = $%PVL_Combo_COM - $%PVL_Shoe_COM
d7 = DIST($%PVL_Combo_COM, $%PVL_Foot_COM)
d8 = DIST($%PVL_Combo_COM, $%PVL_Shoe_COM)


Ln = $LnL_Foot/2


K2x_S = 1/2*(($Ln*$Ln) + (45*45))
K2y_S = 1/6*((3*$Ln*$Ln) + (4*20*20))
K2z_S = 1/6*((3*45*45) + (4*20*20))


Ln = $LnL_Foot


K1x_S = Ln*Rx*Ln*Rx
K1y_S = Ln*Ry*Ln*Ry
1z_S = Ln*Rz*Ln*Rz


Ix = (K1x_S + d5(3)*d5(3))*Ms1 + (K2x_S + d6(3)*d6(3))*Ms2
Iy = (K1y_S + d5(1)*d5(1))*Ms1 + (K2y_S + d6(1)*d6(1))*Ms2
Iz = (K1z_S + d7*d7)*Ms1 + (K2z_S + d8*d8)*Ms2


$IL_Combo = {Ix, Iy, Iz}
```

```
        PARAM($%PVR_Foot_COM, $%PVL_Foot_COM, $%PVR_Shoe_COM, $%PVL_Shoe_COM, $%PVR_Combo_COM,
             $%PVL_Combo_COM)
        PARAM($LnR_Foot, $LnL_Foot, $ShoeSize2, $Ms_Foot, $Ms_Shoe, $Ms_Combo, $IR_Combo, $IL_Combo)
ENDIF

TVR_Foot_COM = $%PVR_Foot_COM*GR_Foot
TVL_Foot_COM = $%PVL_Foot_COM*GL_Foot

TVR_Shoe_COM = $%PVR_Shoe_COM*GR_Foot
TVL_Shoe_COM = $%PVL_Shoe_COM*GL_Foot

TVR_Combo_COM = $%PVR_Combo_COM*GR_Foot
TVL_Combo_COM = $%PVL_Combo_COM*GL_Foot

GR_Foot = [GR_Foot, GR_Shank, TVR_AJC, $Ms_Combo, $%PVR_Combo_COM, $IR_Combo]
GL_Foot = [GL_Foot, GL_Shank, TVL_AJC, $Ms_Combo, $%PVL_Combo_COM, $IL_Combo]

OUTPUT(TVR_Foot_Origin, TVL_Foot_Origin, TVR_Foot_COM, TVL_Foot_COM, TVR_Shoe_COM, TVL_Shoe_COM)
OUTPUT(TVR_Combo_COM, TVL_Combo_COM)


{*     TOES
*}
TVR_MPJC = (TSR_LATPRX_Met5 + TSR_MEDPRX_Met1) / 2
TVL_MPJC = (TSL_LATPRX_Met5 + TSL_MEDPRX_Met1) / 2
TVR_Toe = (TR_MEDANT_FFoot + TR_LATANT_Ffoot) / 2
TVL_Toe = (TL_MEDANT_FFoot + TL_LATANT_Ffoot) / 2
dir11 = NORM(TVR_Toe, TSR_MEDPRX_Met1, TSR_LATPRX_Met5)
dir12 = NORM(TVL_Toe, TSL_LATPRX_Met5, TSL_MEDPRX_Met1)

GR_Toe = [TVR_Toe, dir11 - {0, 0, 0}, TVR_Toe - TVR_MPJC, xyz]
GL_Toe = [TVL_Toe, dir12 - {0, 0, 0}, TVL_Toe - TVL_MPJC, xyz]
DISPLAYAXES(GR_Toe)
DISPLAYAXES(GL_Toe)

GR_Toe = [GR_Toe, GR_Foot, TVR_MPJC, 0, {0, 0, 0}, {0, 0, 0}]
GL_Toe = [GL_Toe, GL_Foot, TVL_MPJC, 0, {0, 0, 0}, {0, 0, 0}]

OUTPUT(TVR_MPJC, TVL_MPJC, TVR_Toe, TVL_Toe)
```

```
{*     KINETICS
*}
ForceThreshold = 2       {*     Force must be bigger than 2 Newtons *}
DistanceThreshold = 80   {*     Attachment or origin must be closer than 80 mm  *}
VelocityThreshold = 4000      {*     Closest end must be moving slower than 4000 mm/s *}


{*     WARNING - In order for these to make sense, every trial must have its
       forceplate setup configured from 2 to 10 AND NOT from 10 to 9
*}


{*     Moments are in Nmm, converted to Nm at the time of output
*}
NN = $Ms_Body + $Ms_Shoe*2
IF EXIST(ForcePlate1)
       FR_FP = ForcePlate1(1)
       MR_FP = ForcePlate1(2)
       TR_CFP = ForcePlate1(3)

       IF (ABS(FR_FP(3)) > 5)
              TVR_COP = TR_CFP + {-MR_FP(2)/FR_FP(3), MR_FP(1)/FR_FP(3), -TR_CFP(3)}
              FPR_Connect = 1
       ELSE
              TVR_COP = TR_CFP
              FPR_Connect = 0
       ENDIF

       XR_FP = |FR_FP, MR_FP, TR_CFP|
       FR_FP_VIS = FR_FP + TR_CFP
       MR_FP_VIS = MR_FP/1000
       FR_FP = ForcePlate1(1)/(9.81*NN)
       MR_FP = ForcePlate1(2)/(9.81*NN*1000)

       OUTPUT(FR_FP, MR_FP, FR_FP_VIS, MR_FP_VIS, TR_CFP, TVR_COP)
ENDIF

IF EXIST(ForcePlate2)
       FL_FP = ForcePlate2(1)
       ML_FP = ForcePlate2(2)
       TL_CFP = ForcePlate2(3)
```

```
        IF (ABS(FL_FP(3)) > 5)
                TVL_COP = TL_CFP + {-ML_FP(2)/FL_FP(3), ML_FP(1)/FL_FP(3), -TL_CFP(3)}
                FPL_Connect = 1
        ELSE
                TVL_COP = TL_CFP
                FPL_Connect = 0
        ENDIF

        XL_FP = |FL_FP, ML_FP, TL_CFP|
        FL_FP_VIS = FL_FP + TL_CFP
        ML_FP_VIS = ML_FP/1000
        FL_FP = FL_FP/(9.81*NN)
        ML_FP = ML_FP/(9.81*NN*1000)

        OUTPUT(FL_FP, ML_FP, FL_FP_VIS, ML_FP_VIS, TL_CFP, TVL_COP)
ENDIF

{*      ANKLES
*}
%XR_Ankle = REACTION(GR_Foot)
XR_Ankle = %XR_Ankle*GR_Shank
FR_Ankle = XR_Ankle(1)/NN
MR_Ankle = %XR_Ankle(2)/(NN*1000)

%XL_Ankle = REACTION(GL_Foot)
XL_Ankle = %XL_Ankle*GL_Shank
FL_Ankle = XL_Ankle(1)/NN
ML_Ankle = %XL_Ankle(2)/(NN*1000)

OUTPUT(FR_Ankle, MR_Ankle)
OUTPUT(FL_Ankle, ML_Ankle)

{*      KNEES
*}
%XR_Knee = REACTION(GR_Shank)
XR_Knee = %XR_Knee*GR_Thigh
FR_Knee = XR_Knee(1)/NN
MR_Knee = %XR_Knee(2)/(NN*1000)

%XL_Knee = REACTION(GL_Shank)
XL_Knee = %XL_Knee*GL_Thigh
```

163

```
FL_Knee = XL_Knee(1)/NN
ML_Knee = %XL_Knee(2)/(NN*1000)

OUTPUT(FR_Knee, MR_Knee)
OUTPUT(FL_Knee, ML_Knee)

{*      HIPS
*}
%XR_Hip = REACTION(GR_Thigh)
XR_Hip = %XR_Hip*G_Pelvis
FR_Hip = XR_Hip(1)/NN
MR_Hip = %XR_Hip(2)/(NN*1000)

%XL_Hip = REACTION(GL_Thigh)
XL_Hip = %XL_Hip*G_Pelvis
FL_Hip = XL_Hip(1)/NN
ML_Hip = %XL_Hip(2)/(NN*1000)

OUTPUT(FR_Hip, MR_Hip)
OUTPUT(FL_Hip, ML_Hip)

{*      Neck
*}
%X_Neck = REACTION(G_Head)
X_Neck = %XR_Hip*G_Torso
F_Neck = X_Neck(1)/NN
M_Neck = %X_Neck(2)/(NN*1000)

OUTPUT(F_Neck, M_Neck)

{*      Elbows
*}
%XR_Elb = REACTION(GR_FArm)
XR_Elb = %XR_Elb*GR_UArm
FR_Elb = XR_Elb(1)/NN
MR_Elb = %XR_Elb(2)/(NN*1000)

%XL_Elb = REACTION(GL_FArm)
XL_Elb = %XL_Elb*GL_UArm
FL_Elb = XL_Elb(1)/NN
ML_Elb = %XL_Elb(2)/(NN*1000)
```

164

```
OUTPUT(FR_Elb, MR_Elb)
OUTPUT(FL_Elb, ML_Elb)

{*      Shoulders
*}
%XR_Shld = REACTION(GR_UArm)
XR_Shld = %XR_Shld*G_Torso
FR_Shld = XR_Shld(1)/NN
MR_Shld = %XR_Shld(2)/(NN*1000)

%XL_Shld = REACTION(GL_UArm)
XL_Shld = %XL_Shld*G_Torso
FL_Shld = XL_Shld(1)/NN
ML_Shld = %XL_Shld(2)/(NN*1000)

OUTPUT(FR_Shld, MR_Shld)
OUTPUT(FL_Shld, ML_Shld)


{*      Waist
*}
%X_Waist = REACTION(G_Torso)
X_Waist = %X_Waist*G_Pelvis
F_Waist = X_Waist(1)/NN
M_Waist = %X_Waist(2)/(NN*1000)

OUTPUT(F_Waist, M_Waist)


{*      COM CALCS
*}
$Ms_SUM = $Ms_Head + $Ms_Torso + 2*($Ms_UArm + $Ms_FArm) + $Ms_Pelvis + 2*($Ms_Thigh + $Ms_Shank +
      $Ms_Combo)

TV_Low_Body_COMx = ($Ms_Combo*TVL_Combo_COM(1) + $Ms_Combo*TVR_Combo_COM(1) + $Ms_Shank*TVR_Shank_COM(1) +
      $Ms_Shank*TVL_Shank_COM(1) + $Ms_Thigh*TVR_Thigh_COM(1) + $Ms_Thigh*TVL_Thigh_COM(1))
TV_Mid_Body_COMx = ($Ms_Pelvis*TV_Pelvis_COM(1) + $Ms_Head*TV_Head_COM(1) + $Ms_Torso*TV_Torso_COM(1))
TV_Up_Body_COMx = ($Ms_UArm*TVL_UArm_COM(1) + $Ms_UArm*TVR_UArm_COM(1) + $Ms_FArm*TVL_FArm_COM(1) +
      $Ms_FArm*TVR_FArm_COM(1))
TV_Body_COMx = (TV_Low_Body_COMx + TV_Mid_Body_COMx + TV_Up_Body_COMx)/$Ms_SUM
```

165

```
TV_Low_Body_COMy = ($Ms_Combo*TVL_Combo_COM(2) + $Ms_Combo*TVR_Combo_COM(2) + $Ms_Shank*TVR_Shank_COM(2) +
      $Ms_Shank*TVL_Shank_COM(2) + $Ms_Thigh*TVR_Thigh_COM(2) + $Ms_Thigh*TVL_Thigh_COM(2))
TV_Mid_Body_COMy = ($Ms_Pelvis*TV_Pelvis_COM(2) + $Ms_Head*TV_Head_COM(2) + $Ms_Torso*TV_Torso_COM(2))
TV_Up_Body_COMy = ($Ms_UArm*TVL_UArm_COM(2) + $Ms_UArm*TVR_UArm_COM(2) + $Ms_FArm*TVL_FArm_COM(2) +
      $Ms_FArm*TVR_FArm_COM(2))
TV_Body_COMy = (TV_Low_Body_COMy + TV_Mid_Body_COMy + TV_Up_Body_COMy)/$Ms_SUM

TV_Low_Body_COMz = ($Ms_Combo*TVL_Combo_COM(3) + $Ms_Combo*TVR_Combo_COM(3) + $Ms_Shank*TVR_Shank_COM(3) +
      $Ms_Shank*TVL_Shank_COM(3) + $Ms_Thigh*TVR_Thigh_COM(3) + $Ms_Thigh*TVL_Thigh_COM(3))
TV_Mid_Body_COMz = ($Ms_Pelvis*TV_Pelvis_COM(3) + $Ms_Head*TV_Head_COM(3) + $Ms_Torso*TV_Torso_COM(3))
TV_Up_Body_COMz = ($Ms_UArm*TVL_UArm_COM(3) + $Ms_UArm*TVR_UArm_COM(3) + $Ms_FArm*TVL_FArm_COM(3) +
      $Ms_FArm*TVR_FArm_COM(3))
TV_Body_COMz = (TV_Low_Body_COMz + TV_Mid_Body_COMz + TV_Up_Body_COMz)/$Ms_SUM

TV_Body_COM = {TV_Body_COMx, TV_Body_COMy, TV_Body_COMz}
OUTPUT(TV_Body_COM)


{*     ANGLES
*}

{*     NECK
*}
J_Neck = -<G_Torso, G_Head, yxz>

{*     GLOBAL HEAD
*}
E_HG = <G_Head, G_GLOBAL, zxy>
E_Head_Global = <E_HG(3), E_HG(2), E_HG(1)>

{*     SHOULDERS
*}
JR_Shld = -<G_Torso2, GR_UArm, yxz>
JL_Shld = -<G_Torso2, GL_UArm, yxz>

{*     ELBOWS
*}
JR_Elbow = -<GR_UArm, GR_FArm, yxz>
JL_Elbow = -<GL_UArm, GL_FArm, yxz>
```

```
{*      GLOBAL TORSO
 *}
E_TG = <G_Torso, G_GLOBAL, zxy>
E_Torso_Global = <E_TG(3), E_TG(2), E_TG(1)>


{*      WAIST
 *}
J_Waist = -<G_Pelvis, G_Torso, yxz>


{*      GLOBAL PELVIS
 *}
E_PG = <G_Pelvis, G_GLOBAL, zxy>
E_Pelvis_Global = <E_PG(3), E_PG(2), E_PG(1)>


{*      HIP
 *}
JR_Hip = -<G_Pelvis, GR_Thigh, yxz>
JL_Hip = -<G_Pelvis, GL_Thigh, yxz>


{*      KNEES
 *}
JR_Knee = -<GR_Thigh, GR_Shank, yxz>
JL_Knee = -<GL_Thigh, GL_Shank, yxz>


{*      ANKLES
 *}
JR_Ankle = -<GR_Shank2, GR_Foot, yxz>
JL_Ankle = -<GL_Shank2, GL_Foot, yxz>


{*      GLOBAL FEET
 *}
ER_FF = <GR_Foot2, G_GLOBAL, zxy>
EL_FF = <GL_Foot2, G_GLOBAL, zxy>
ER_FFA = <ER_FF(3), ER_FF(2), ER_FF(1)>
EL_FFA = <EL_FF(3), EL_FF(2), EL_FF(1)>


{*      MP
 *}
JR_MP = -<GR_Foot, GR_Toe, yxz>
JL_MP = -<GL_Foot, GL_Toe, yxz>
```

```
IF ($Static == 1)
      $J_Neck = J_Neck

      $E_Head_Global = E_Head_Global

      $JR_Shld = JR_Shld
      $JL_Shld = JL_Shld

      $JR_Elbow = JR_Elbow
      $JL_Elbow = JL_Elbow

      $E_Torso_Global = E_Torso_Global

      $J_Waist = J_Waist

      $E_Pelvis_Global = E_Pelvis_Global

      $JR_Hip = JR_Hip
      $JL_Hip = JL_Hip

      $JR_Knee = JR_Knee
      $JL_Knee = JL_Knee

      $JR_Ankle = JR_Ankle
      $JL_Ankle = JL_Ankle

      $ER_FFA = ER_FFA
      $EL_FFA = EL_FFA

      $JR_MP = JR_MP
      $JL_MP = JL_MP

      PARAM($J_Neck, $E_Head_Global, $JR_Shld, $JL_Shld, $JR_Elbow, $JL_Elbow, $E_Torso_Global, $J_Waist)
      PARAM($E_Pelvis_Global, $JR_Hip, $JL_Hip, $JR_Knee, $JL_Knee, $JR_Ankle, $JL_Ankle, $ER_FFA, $EL_FFA,
           $JR_MP, $JL_MP)
ENDIF

OUTPUT(J_Neck, E_Head_Global, JR_Shld, JL_Shld, JR_Elbow, JL_Elbow, E_Torso_Global, J_Waist)
OUTPUT(E_Pelvis_Global, JR_Hip, JL_Hip, JR_Knee, JL_Knee, JR_Ankle, JL_Ankle, ER_FFA, EL_FFA, JR_MP, JL_MP)
```

```
{*      VELOCITIES
*}
LINVELACC(TSR_INFPOS_Heel)
LINVELACC(TSL_INFPOS_Heel)
LINVELACC(TVR_Foot_Origin)
LINVELACC(TVL_Foot_Origin)
LINVELACC(TVR_Toe)
LINVELACC(TVL_Toe)
LINVELACC(TV_BODY_COM)
```

COMPANION SUBJECT PARAMETERS FILE

The first part of this file contains information required to run the model. These parameters are supplied by the analyst. $SamplingRate is in frames per second, $Ms_Body is in Kg, $Height is in mm, $Gender is 1 for male and 0 for female, and $ShoeSize is the U.S. standard shoe size (which can be compared to the calculated shoe size resulting from the model, $ShoeSize2). The second part of this file contains parameters that were calculated by the model during analysis of the static trial and then used for analysis of the dynamic trials. See Appendix B for a detailed description of the parameter naming convention.

```
$SamplingRate = 120
$Ms_Body = 83.64
$Height = 1780
$Gender = 1
$ShoeSize = 10

$%PS_T10 = {39.9931,-351.729,-92.0506}
$%PSR_MED_Elb = {76.2584,-76.9156,79.3571}
$%PSR_LAT_Elb = {60.4154,8.5828,85.9229}
$%PSL_MED_Elb = {81.5319,78.7023,90.9195}
$%PSL_LAT_Elb = {77.1038,-2.61184,84.6558}
$%PSR_LATDIS_Radius = {32.7378,39.2755,129.049}
$%PSR_MEDDIS_Radius = {95.3065,3.61471,105.915}
$%PSL_LATDIS_Radius = {-61.096,32.0566,-52.3742}
$%PSL_MEDDIS_Radius = {0.16372,13.3671,-95.8039}
$%PSR_GTro = {465.971,-41.968,40.6052}
$%PSL_GTro = {445.456,35.6895,25.9832}
$%PSR_MED_EpiC = {-19.8104,-111.853,17.6134}
$%PSL_MED_EpiC = {-26.7841,98.2955,32.5821}
$%PSR_INFPOS_Heel = {-1.97006,43.2253,-10.3862}
$%PSL_INFPOS_Heel = {-5.65573,-40.2816,2.55125}
$%PSR_MEDPRX_Met1 = {45.8243,-41.9722,50.3377}
$%PSR_LATPRX_Met5 = {88.4602,-49.0248,-55.7599}
$%PSL_MEDPRX_Met1 = {62.118,58.7171,41.8251}
$%PSL_LATPRX_Met5 = {88.4735,41.607,-69.4896}
$Wdth_Pelvis = 268.12
$Dpth_Pelvis = 197.526
$LnR_ASISAnkle = 945.532
$LnL_ASISAnkle = 957.415
$%P_Pelvis_COM = {0,0,72.3173}
$Ln_Pelvis = 186.145
$Ms_Pelvis = 9.34259
$I_Pelvis = {122440,98282.3,111545}
$%PV_Torso_Attach = {0,0,186.145}
$%PV_Torso_Origin = {3.95111,32.0932,-69.1436}
$%P_Torso_COM = {0,0,-182.513}
$Ln_Torso = 359.8
$Ms_Torso = 27.0074
$I_Torso = {410040,302632,190480}
$%P_Head_COM = {0,0,-35.2434}
$%P_Head_TOP = {0,0,90.6835}
```

171

```
$Ln_Head = 250.85
$Ms_Head = 5.80462
$I_Head = {33534.5,36243.3,24882.1}
$%PVR_UArm_COM = {0,0,114.66}
$%PVL_UArm_COM = {0,0,121.573}
$LnR_UArm = 271.191
$LnL_UArm = 287.543
$Ms_UArm = 2.26664
$IR_UArm = {13540.2,12062.6,4161.49}
$IL_UArm = {15222.2,13561,4678.46}
$%PVR_FArm_COM = {0,0,1.93608}
$%PVL_FArm_COM = {0,0,1.93735}
$LnR_FArm = 267.219
$LnL_FArm = 267.393
$Ms_FArm = 1.86517
$IR_FArm = {140806,127079,2018.56}
$IL_FArm = {140989,127245,2021.19}
$%PVR_Thigh_COM = {0,0,283.304}
$%PVL_Thigh_COM = {0,0,284.699}
$LnR_Thigh = 479.77
$LnL_Thigh = 482.133
$Ms_Thigh = 11.8434
$IR_Thigh = {295077,361199,60522.5}
$IL_Thigh = {295077,361199,60522.5}
$%PVR_Shank_COM = {0,0,228.021}
$%PVL_Shank_COM = {0,0,230.496}
$LnR_Shank = 406.818
$LnL_Shank = 411.232
$Ms_Shank = 3.62161
$IR_Shank = {37761.5,36272.1,6235.95}
$IL_Shank = {38585.5,37063.5,6372.01}
$%PVR_Foot_Origin = {281.72,29.0105,78.0383}
$%PVL_Foot_Origin = {286.366,-22.7236,75.8126}
$%PVR_Foot_COM = {0,0,129.697}
$%PVL_Foot_COM = {0,0,131.171}
$%PVR_Shoe_COM = {-44.4999,0,146.883}
$%PVL_Shoe_COM = {-40.7612,0,148.551}
$%PVR_Combo_COM = {-13.1617,0,134.78}
$%PVL_Combo_COM = {-12.0559,0,136.311}
$LnR_Foot = 293.765
$LnL_Foot = 297.102
```

```
$ShoeSize2 = 10
$Ms_Foot = 1.14587
$Ms_Shoe = 0.48125
$Ms_Combo = 1.62712
$IR_Combo = {63051,62667.4,2907.29}
$IL_Combo = {63202.6,62695.1,2801.53}
$J_Neck = <6.48107,4.99641,2.34315>
$E_Head_Global = <10.4169,3.5481,3.4968>
$JR_Shld = <-82.7307,40.7278,68.477>
$JL_Shld = <82.2918,-36.9677,77.9887>
$JR_Elbow = <22.0736,16.0181,77.8616>
$JL_Elbow = <12.2325,-18.3756,-69.5907>
$E_Torso_Global = <3.83365,-1.30908,1.30784>
$J_Waist = <1.6949,-4.16528,1.10695>
$E_Pelvis_Global = <2.15131,2.86085,0.116555>
$JR_Hip = <1.93746,-4.59549,-7.95305>
$JL_Hip = <0.8277,-1.15287,14.8732>
$JR_Knee = <-1.01539,-1.93363,-2.44391>
$JL_Knee = <-0.185949,2.81,-1.78713>
$JR_Ankle = <-2.87156,6.39183,3.87236>
$JL_Ankle = <-2.65324,-8.60637,-4.73452>
$ER_FFA = <5.89058,0.580316,-3.94178>
$EL_FFA = <5.72036,-0.837944,4.85112>
$JR_MP = <11.6782,6.5678,0.343466>
$JL_MP = <9.47441,-2.11217,-0.575879
```

APPENDIX F

POST-PROCESSING MATLAB CODE

The following MATLAB code sections work in conjunction with the model to perform much of the processing described in this technical note, including heel strike and toe off determination and time normalization. The data from Vicon is stored in C3D files and is brought into MATLAB via code that has been adapted from free software from Motion Lab Systems and available through www.c3d.org.

'main.m'

The code used to read Vicon's c3d files, to read the mp file, and to determine and verify heel strike and toe off. The resulting data is then stored in mat files for future processing.

```
%   The basic function of this code will:
%   1)  Check to see if heel strike and toe off have been found for a given trial
%          A)  Have been identified (either in a file or manual entry)
%                 - bring up plots for verification
%             i)  Normal force
%             ii) Heel marker or toe marker
%          B)  Have NOT been identified
%             i)  For a dry trial, use the automated algorithm to guess HS and TO and then verify guesses
%                   manually as in A) above
%             ii) For a slip trial, use the automated algorithm for R HS, L HS, and R TO and then use a
%                   previous trial's L TO to estimate current L TO
%   2)  Using the HS and TO values, create time normalized data for all trajectories in the c3d file (SAVE
%          HS AND TO TO A FILE)
%   3)  Write all of the time normalized data to one mat file, the raw data to a second mat file, and the
%          analog data to a third mat file
%          A)  TNN_NORM.mat
%          B)  TNN_RAW.mat
%          C)  TNN_ANALOG.mat

clear

path1 = 'C:\MATLAB7\work';
path2 = 'C:\Data\';

cd(path2)
[inname, path2] = uigetfile('*.c3d', 'Choose a c3d file for processing');
v = findstr(inname,'.c3d');  %   Find the end of the name part

trialnumstr = cell2mat(regexp(inname(1:v-1),'\d+','match'));
number = str2num(trialnumstr);

name = sprintf('Trial_%02d', number);
```

175

```
%   this next bit gets the data from the c3d file

cd(path1)
[nframes, MarkerNames, AnalogNames, analogmulti] = loadc3d([path2 '\' inname]);
load('dummy.mat');
cd(path2)

%   If analog data does not exist due to technical difficulties, then put zeros in for the necessary
%      variables

dead_data_array = zeros(nframes,3);
if (isequal(AnalogNames,{'BadAnalogs'}))
    %   This indicates that analogs were not collected
    AnalogRelated = {'FL_Ankle' 'FL_Elb' 'FL_FP' 'FL_FP_VIS' 'FL_Hip' 'FL_Knee' 'FL_Shld'...
        'FR_Ankle' 'FR_Elb' 'FR_FP' 'FR_FP_VIS' 'FR_Hip' 'FR_Knee' 'FR_Shld' 'F_Neck'...
        'F_Waist' 'ML_Ankle' 'ML_Elb' 'ML_FP' 'ML_FP_VIS' 'ML_Hip' 'ML_Knee' 'ML_Shld'...
        'MR_Ankle' 'MR_Elb' 'MR_FP' 'MR_FP_VIS' 'MR_Hip' 'MR_Knee' 'MR_Shld' 'M_Neck'...
        'M_Waist' 'TL_CFP' 'TL_COP' 'TR_CFP' 'TR_COP'}';
    for i = 1:36
        eval([cell2mat(AnalogRelated(i)) '= dead_data_array;']);;
    end
end

%   analogmulti is the number of analog samples per video frame, i.e., 9
%   when analog rate was 1080 and video rate was 120

disp('c3d File Loaded ...')

%   This next bit of code opens an appropriate mp file to get things like sampling rate, etc.  This DOESN'T
%      WORK PARTICULARLY WELL ANYMORE SINCE THE BATCH PROCESSING PIPELINE IN VICON MESSES WITH THE MP FILE
%      SO THAT IT IS NO LONGER STRUCTURED NICELY

[inname2, path3] = uigetfile('*.mp', 'Choose an mp file for processing');
cd(path1)
read_mp_file([path3 '\' inname2]);
load('dummy_mp.mat');
cd(path2)

disp('mp File Loaded ...')
```

```
frames = (1:nframes)';
time = (0:(1/C_SamplingRate):(nframes/C_SamplingRate - 1/C_SamplingRate))';

%   Now, since the raw trajectory and analog data are here, may as well save them to mat files. To do this,
      will need to get all of the data together correctly.  MarkerNames has all of the trajectory labels in
      it.

%   All unlabeled trajectories and all overlapping trajectories have been carefully removed.  If this isn't
      done, some trials will have too many things and some of them will be garbage.

%   It would be nice if the list of trajectories was always in the same order!
%   Since it isn't as it comes out of Vicon, plotting would be difficult as the column indices would change
      for the same data from trial to trial.  Assuming that, for a given study, the trajectories will
      remain the same from trial to trial, alphabetizing should work

[MarkerNames, order] = sort(MarkerNames);

%   This next bit of code takes the MarkerNames variable and divides it up
%   into X, Y, and Z column names.

MarkerList = '';
for i = 1:length(MarkerNames)
    LColumns(3*i-2:3*i) = [cellstr([char(MarkerNames(i)) '(:,1)']) cellstr([char(MarkerNames(i)) '(:,2)'])
            cellstr([char(MarkerNames(i))'(:,3)'])];

    MarkerList = [MarkerList ' ' char(MarkerNames(i)) ' '];   % this will grow with each new variable name
end

if (isequal(AnalogNames,{'BadAnalogs'}))
    %   no analogs exist so skip saving this file
else
    %   This is the same sort of thing but for analog channel names
    AnalogList = '';
    for i = 1:length(AnalogNames)
        AnalogList = [AnalogList ' ' char(AnalogNames(i)) ' '];   % this will grow with each new variable
name
    end

    %   Save the analog data
    analograte = analogmulti*C_SamplingRate;
    eval(['save ''' name '''_ANALOG.mat analograte AnalogNames' AnalogList]);
```

177

```matlab
    disp('raw analog data saved ...')
end

%   This next bit of code uses the data from the c3d file to determine HS and TO when these estimates do
      not already exist. It is also possible to load these from a mat file (see below for the structure) or
      type them in manually.

%   By default, there are 2 types of data that can be used to determine HS and TO.  The first is analog
      ground reaction force data and the second is heel and toe marker data.  THE FIRST WIL NOT WORK IF
      ANALOG DATA DOES NOT EXIST FOR A TRIAL.  Clearly, there will be problems if the force-plate data
      exists but is unreliable.

%   =====
EventArray = zeros(1,16);


R_Heel = abs(VTSR_INFPOS_Heel(:,3));
L_Heel = abs(VTSL_INFPOS_Heel(:,3));


R_Toe_Z = TVR_Toe(:,3);
L_Toe_Z = TVL_Toe(:,3);


Exist = menu('Do HS and TO estimates already exist for this trial?', 'YES', 'NO');

if (Exist == 1) %   Estimates already exist
    action = menu('Enter manually or load from a file?', 'Enter', 'Load');

    if(action == 1) %   Get estimates from user input

        estimates = menu('Do higher precision (i.e., 1080 Hz) estimates exist?', 'Yes', 'No');
        if(estimates == 1)  %   higher precision available
            disp('If actual analog frequency was higher or lower than 1080,')
            disp('then, use the actual data sample at the higher or lower freq')

            %   NOTE EventArray will contain both higher and lower samples as well as some other data that
                 is related to these estimates
            EventArray(13) = input('Enter sample number for right HS:');
            EventArray(14) = input('Enter sample number for right TO:');
            EventArray(15) = input('Enter sample number for left HS:');
            EventArray(16) = input('Enter sample number for left TO:');
```

178

```
        %   Since the user typed in higher frequency data, automatically calculate the lower frequency
            estimates.
        for i = 1:4
            EventArray(i) = round(EventArray(i + 12) / analogmulti);
        end
        EventArray(17) = analogmulti;

    else    %   only lower precision available
        disp('Frame number refers to the video capture frame number,')
        disp('i.e., data frame N from data typically collected at 120 Hz')

        EventArray(1) = input('Enter frame number for right HS:');
        EventArray(2) = input('Enter frame number for right TO:');
        EventArray(3) = input('Enter frame number for left HS:');
        EventArray(4) = input('Enter frame number for left TO:');

        %   Since the lower frequency estimates have been given, calculate the higher frequency
            estimates
        for i = 1:4
            EventArray(i + 12) = analogmulti * EventArray(i);
        end
        EventArray(17) = analogmulti;

    end %   end of manual HS and TO entry if section

    %   regardless of type of manual estimates, set MEANs and SDs section of EventArray to 0 since they
        were manually entered.  Normally, these would indicate the mean and standard deviations for the
        normal force data for no load sections either before HS or after TO that would have been used
        to estimate HS and TO automatically.

    for i=5:12
        EventArray(i) = 0;
    end

    disp('HS and TO estimates entered ...')

%   Load estimates from a file - assuming that this data is in the correct format
else
    [HSTOfile, path2] = uigetfile('*_HS_TO.mat', 'Choose a c3d file.');
    load(strcat(path2, HSTOfile));
```

179

```matlab
        disp('HS and TO estimates loaded ...')

        %    Some of the older trials did not keep track of the analog multiplier.  If this data is
             reloaded, need to append the analog multiplier to EventArray

        if(length(EventArray)==16)
            EventArray(17) = analogmulti;
        end
    end %    end of enter or load

else    %    Estimates do not already exist so need to automatically figure out HS and TO estimates

    %    First, keep the analogmultiplier in EventArray
    EventArray(17) = analogmulti;

    %    This next section of code uses data to automatically determine HS and TO

    useanalogs = menu('Are analog estimates reliable for this trial?', 'Use Analogs!', 'No');
    if (useanalogs == 1)
        %    Use analog normal forces
        [EventArray] = Get_HS_and_TO(FZ1, FZ2, analogmulti);
    else
        %    Use Heel and Toe marker data only
        [EventArray] = Get_HS_and_TO_2(R_Heel, L_Heel, R_Toe_Z, L_Toe_Z, analogmulti);
    end

    delete(gcf)

    %    For slip trials, TO for the left foot is not determinable via typical methods so...
    if (EventArray(4) == -1)    %    meaning that L_TO needs to be estimated from another file
        %    figure out TO from a different trial - ask the user to choose the other trial OR type in a
             number

        [HSTOfile, path2] = uigetfile('*_HS_TO.mat', 'Choose a c3d file for L_TO determination.');
        name2 = strcat(path2, HSTOfile);

        %    This will replace L_TO with one referenced to another trial's L_TO rel. to L_HS - done using the
             low frequency estimates
        [EventArray] = get_slip_TO(name2, EventArray);

    end %    end of the slip if
```

180

```matlab
    disp('HS and TO estimates determined ...')


end %   End of the whole get HS and TO routine

%   Now, give the user the option to visually inspect and possibly change the automatically OR manually
        entered/loaded HS and TO entries

%   Again, this won't work if the analog data is screwed up so...
useanalogs = menu('Are analog estimates reliable for this trial?', 'Use Analogs!', 'No');

if (useanalogs == 1)
    [EventArray] = Verify_HS_and_TO(FZ1, FZ2, R_Heel, R_Toe_Z, L_Heel, L_Toe_Z, EventArray);
else
    [EventArray] = Verify_HS_and_TO_2(R_Heel, R_Toe_Z, L_Heel, L_Toe_Z, EventArray);
end

disp('HS and TO estimates verified ...')

delete(gcf)

%   These low frequency estimates may have been rounded/changed inside Verify_HS_and_TO
R_HS = EventArray(1);
R_TO = EventArray(2);
L_HS = EventArray(3);
L_TO = EventArray(4);

%   Set up the data and labels to be saved to the HS and TO data file
labels = {'HS_R (120)' 'TO_R (120)' 'HS_L (120)' 'TO_L (120)' 'MEAN for HS_R' 'SD for HS_R'...
        'MEAN for TO_R' 'SD for TO_R' 'MEAN for HS_L' 'SD for HS_L' 'MEAN for TO_L' 'SD for TO_L'...
        'HS_R (High)' 'TO_R (High)' 'HS_L (High)' 'TO_L (High)' 'AnalogMulti'};

eval(['save ''' name '''_HS_TO.mat EventArray labels']);   %   This will save all 17 numbers

disp('HS and TO estimates saved ...')

%   ====
%     Now that HS and TO have been determined, verified, and saved, time to normalize the data
percentnormL = percenttime_normalize(L_HS, L_TO, frames)';
```

181

```matlab
%   Put raw data together - this is just to keep track of the column labels.
LColumns = [cellstr('percentnormL') cellstr('frames') cellstr('time') LColumns];

%   Put data together with extra columns
eval(['data1 = [percentnormL frames time];']);

eval(['data2 = [' MarkerList '];']);
data = [data1 data2];

%   Prior to normalization, should remove the effect of "flipping" of axes
%   i.e., if angle measurements exceed 180, subtract 360 to make sure that trends continue

%   NEED TO DO THIS ONLY FOR ANGLES
    for i = 1:length(LColumns)
        LABELS = char(LColumns(i));
        if (LABELS(1)=='E' | LABELS(1)=='J')

            %   Get rid of 180 degree problem - first get average value
            mean_value = mean(data(R_HS:L_TO,i));

            data_temp = data(:,i);

            %   Look for values outside of allowable range
            big_indicies = find(data_temp>180);
            small_indicies = find(data_temp<-180);
            if (mean_value < 0)
                for j = 1:length(big_indicies)
                    data_temp(big_indicies(j)) = data_temp(big_indicies(j))-360;
                end
            else
                for j = 1:length(small_indicies)
                    data_temp(small_indicies(j)) = data_temp(small_indicies(j))+360;
                end
            end

            %   Now, shift angles that are outside of +/- 180 on average into range

            mean_value = mean(data(R_HS:L_TO,i));

            if (mean_value > 180)
                data_temp(:) = data_temp(:)-360;
```

```
                elseif (mean_value < -180)
                    data_temp(:) = data_temp(:)+360;
                end
                data(:,i)=data_temp;
            end
        end
    end

eval(['save ''' name '''_RAW.mat LColumns data' MarkerList]);

disp('Raw marker data saved ...')

%   time normalize
results(:,1) = (-50:1/10:149.9)';

%   new_y = interp1(old_x, old_y, new_x, 'pchip')
%   only want data at the values from -50% to + 150%
%   So, we want the old x values to be of the same scale as the new - i.e., use the interpolated time scale

results(:,2:size(data,2)) = interp1(data(:,1), data(:,2:size(data,2)), results(:,1), 'pchip');

eval(['save ''' name '''_LNORM.mat LColumns results;']);

disp('Normalized (to LHS and LTO) marker data saved ...')

%   do it again for variables to be normalized to right foot stance time

percentnormR = percenttime_normalize(R_HS, R_TO, frames)';

eval(['data3 = [percentnormR frames time FR_FP(:,1) FR_FP(:,2) FR_FP(:,3)];']);
results2(:,1) = (-50:1/10:149.9)';
results2(:,2:size(data3,2)) = interp1(data3(:,1), data3(:,2:size(data3,2)), results2(:,1),'pchip');

RColumns = {'percentnormR' 'frames' 'time' 'FR_FP(:,1)' 'FR_FP(:,2)' 'FR_FP(:,3)'};
eval(['save ''' name '''_RNORM.mat RColumns results2']);

disp('Normalized (to RHS and RTO) marker data saved ...')
```

'READ_MP_FILE.M'

This handy little function, reads and interprets the parameters stored in the mp file for use in MATLAB.

```
function read_mp_file(filename)

    fid = fopen(filename);

    line = 1;
    while 1
        data = fgetl(fid);
        if ~ischar(data), break, end
        data = strrep(data, '$', 'C_');
        data = strrep(data, '<', '[');
        data = strrep(data, '>', ']');
        data = strrep(data, '%', 'Loc_');
        data = strrep(data, '{', '[');
        data = strrep(data, '}', ']');

        eval([data ';']);
    end
    fclose(fid);

%   NOTE:  To get numbers out of the non-rotation type vectors, use cell2mat for each element
    clear filename
    clear fid

    save dummy_mp.mat
return
```

'loadc3d.m'

This code modified code from Motion Lab Systems (www.c3d.org) and is based on their c3dserver application.

```matlab
function [nFrames, MarkerNames, AnalogNames] = loadc3d(filename)
%       This function uses a filename (complete with path if necessary) to create an activex object
        using the c3dsever application (must be installed on the machine being used to analyze the
        data).

%       The marker data and analog data are retrieved from the file and stored to variables using the
        marker names and analog channel names as variable names.  These variables are then stored to a
        temporary mat file named dummy.mat at the default MATLAB path.  That file will need to be
        loaded by the calling m file to get all of the results.  Other relevant results are available
        using the return variables nFrames, MarkerNames, AnalogNames which may be changed if they are
        not used.

        test = c3dserver;
        openc3d(test, 1, filename)

        h = waitbar(0,['Trial is loading...']);

        nMarkers = test.GetNumber3DPoints;
        nChannels = test.GetAnalogChannels;
        nScale = test.GetHeaderScaleFactor;
        if nScale < 0
                scaled = char(1);
        else
                scaled = char(0);
        end

        nStartFrame = test.GetVideoFrameHeader(0);
        nEndFrame = test.GetVideoFrameHeader(1);
        nFrames = nEndFrame - nStartFrame + 1;
        nFrameRate = test.GetVideoFrameRate;
        nAnalogToVideoRatio = test.GetAnalogVideoRatio;

        nGroups = test.GetNumberGroups();
```

185

```matlab
for i = 1:nGroups
      GroupNames(i) = cellstr(test.GetGroupName(i-1));
end

GroupNames = GroupNames';
%      Example group names in a typical c3d file:
%      'TRIAL'
%      'SUBJECTS'
%      'POINT'
%      'ANALOG'
%      'FORCE_PLATFORM'
%      'SEG'
%      'EVENT_CONTEXT'
%      'EVENT'
%      'MANUFACTURER'

AnaglogGroupIndex = test.GetGroupIndex('ANALOG');
PointGroupIndex = test.GetGroupIndex('POINT');

nParameters = test.GetNumberParameters();

for i = 1:nParameters
      ParameterNames(i) =  cellstr(test.GetParameterName(i-1));
end

ParameterNames = ParameterNames';
%      EXAMPLE PARAMTERS FROM A TYPICAL C3D file…
% TRIAL
%      'ACTUAL_START_FIELD'
%      'ACTUAL_END_FIELD'
%      'CAMERA_RATE'
%      'VIDEO_RATE_DIVIDER'

% SUBJECTS
%      'IS_STATIC'
%      'USES_PREFIXES'
%      'USED'
%      'NAMES'
%      'LABEL_PREFIXES'
%      'MARKER_SETS'
%      'DISPLAY_SETS'
```

186

```
%       'MODELS'
%       'MODEL_PARAMS'

% POINT
%       'USED'
%       'FRAMES'
%       'DATA_START'
%       'SCALE'
%       'RATE'
%       'MOVIE_DELAY'
%       'X_SCREEN'
%       'Y_SCREEN'
%       'UNITS'
%       'ANGLE_UNITS'
%       'SCALAR_UNITS'
%       'TYPE_GROUPS'
%       'LABELS'
%       'DESCRIPTIONS'
%       'SCALARS'
%       'ANGLES'
%       'FORCES'
%       'MOMENTS'
%       'FORCE_UNITS'
%       'MOMENT_UNITS'

% ANALOG
%       'FORMAT'
%       'BITS'
%       'GEN_SCALE'
%       'RATE'
%       'USED'
%       'GAIN'
%       'SCALE'
%       'OFFSET'
%       'UNITS'
%       'LABELS'
%       'DESCRIPTIONS'
%       'BOARDS'
%       'BOARD_LABELS'
%       'BOARD_CHANNELS'
%       'PCHAN'
```

```
% FORCE PLATFORM
%       'USED'
%       'ZERO'
%       'TYPE'
%       'CORNERS'
%       'ORIGIN'
%       'CHANNEL'
%       'CAL_MATRIX'

% SEG
%       'MARKER_DIAMETER'
%       'DATA_LIMITS'
%       'ACC_FACTOR'
%       'MAX_NOISE_FACTOR'
%       'INTERSECTION_LIMIT'
%       'RESIDUAL_ERROR_FACTOR'
%       'PREDICTION_ERROR'

% EVENT CONTEXT
%       'USED'
%       'ICON_IDS'
%       'LABELS'
%       'DESCRIPTIONS'
%       'COLOURS'

% EVENT
%       'USED'
%       'CONTEXTS'
%       'ICON_IDS'
%       'LABELS'
%       'DESCRIPTIONS'
%       'SUBJECTS'
%       'TIMES'
%       'GENERIC_FLAGS'

% MANUFACTURER
%       'COMPANY'
%       'SOFTWARE'
%       'VERSION_LABEL'
```

```matlab
        MarkerNamesIndex = test.GetParameterIndex('POINT', 'LABELS');
        MarkerNamesLength = test.GetParameterLength(MarkerNamesIndex);

        for i = 1:nMarkers %    How many markers are there
            MarkerNames(i,:) = cellstr(test.GetParameterValue(MarkerNamesIndex,i-1));
        %    all of these strings will have trailing spaces that will need to be truncated later
        %    The following gets rid of minus signs, stars, and # signs that might be hanging around
            and will cause problems later if they remained in variable names.

            MarkerNames(i,:)= strrep(MarkerNames(i,:),'-','_');
            MarkerNames(i,:)= strrep(MarkerNames(i,:),'*','Z');
            MarkerNames(i,:)= strrep(MarkerNames(i,:),'#','Z');
        end

        MarkerNames2 = char(MarkerNames);

        AnalogNamesIndex = test.GetParameterIndex('ANALOG', 'LABELS');
        AnalogNamesLength = test.GetParameterLength(AnalogNamesIndex);
        AnalogScaleIndex = test.GetParameterIndex('ANALOG','SCALE');
        AnalogOffsetIndex = test.GetParameterIndex('ANALOG','OFFSET');

        for i = 1:AnalogNamesLength % The number of analog channels
            AnalogNames(i,:) = cellstr(test.GetParameterValue(AnalogNamesIndex,i-1));
        %    all of these strings will have trailing spaces that will need to be truncated later
            AnalogOffsets(i) = test.GetParameterValue(AnalogOffsetIndex,i-1);
            AnalogScales(i) = test.GetParameterValue(AnalogScaleIndex,i-1);
        end

        if exist('AnalogNames') %    Some trials (static) have no analog data present
        else
            AnalogNames = ' ';  %   Since there was no analog data, return a blank
        end

        AnalogNames2 = char(AnalogNames);

outdata = '';      %     This will be used to form the list of variables to write to the mat file
        j=1;
        for i = 1:nMarkers
        temp = deblank(MarkerNames2(i,:)); %    gets rid of trailing spaces in each variable name
        temp2 = strrep(temp,'_','\_'); %   Format the name of the variable currently being loaded so
            it gets displayed correctly (no subscripts)
```

```matlab
        waitbar(i/nMarkers, h, ['Marker ' int2str(i) ' = ' temp2])

        if temp(1) == 'Z'
%       When a single bad character (like a # sign) shows up as the name for a variable, make it
        two characters wide for later
            temp = strrep(temp,'Z','ZZ');
        end

    eval([temp '= zeros(nFrames, 3);']);        %     make  sure  that  our  variables  exist  ahead  of
        time and are of the right size
    eval([temp '(:,1) = cell2mat(test.GetPointDataEx(i-1, 0, nStartFrame, nEndFrame, scaled));']);
        %     x coordinate
    eval([temp '(:,2) = cell2mat(test.GetPointDataEx(i-1, 1, nStartFrame, nEndFrame, scaled));']);
        %     y coordinate
    eval([temp '(:,3) = cell2mat(test.GetPointDataEx(i-1, 2, nStartFrame, nEndFrame, scaled));']);
        %     z coordinate

        if temp(1:2) == 'Ax' | temp(1:2) == 'Ay' | temp(1:2) == 'Az'
%       We  don't  want  to  import  certain  markers  -  in  this  case,  any  markers  used  to
            illustrate the axes for local coordinate systems.
        else
        outdata = [outdata ' ' temp ' '];   % this will grow with each new variable name
            MarkerList(j) = {temp};
            j=j+1;
        end
    end


    j=1;
    for k = 1:nChannels %   The number of analog channels
    temp3 = deblank(AnalogNames2(k,:)); %     gets rid of trailing spaces in each variable name
    temp4 = strrep(temp3,'_','\_');  % Format the name of the variable currently being loaded so
        it gets displayed correctly (no subscripts)
        waitbar((k)/nChannels, h, ['AnalogChannel ' int2str(k) ' = ' temp4])

    eval([temp3    '=   cell2mat(test.GetAnalogDataEx(k-1,   nStartFrame,   nEndFrame,   char(1),
        AnalogOffsets(k), AnalogScales(k), char(1)));']);

eval([temp3 '= -(' temp3 '- double(AnalogOffsets(k)))*AnalogScales(k);']);
        %     scale the data to engineering units
        if temp3(1:2) == 'Ux' | temp3(1:2) == 'Uy' | temp3(1:2) == 'Uz'
        else
```

```matlab
            outdata = [outdata ' ' temp3 ' '];  % this will grow with each new variable name
                    AnalogList(j) = {temp3};
                    j = j+1;
            end
        end

        close(h) % waitbar

eval(['save dummy.mat ' outdata])   %    save the list of variables to a dummy mat file
        MarkerNames = MarkerList;

if (iscell(AnalogNames))
            AnalogNames = AnalogList;
else
            AnalogNames = {'BadAnalogs'}
end
return
```

'Get_HS_and_TO.m'

This function automates determination of heel strike and toe off using normal force data.

```
function [EventArray] = Get_HS_and_TO(FZ_R, FZ_L, multi)
%   This function will generate estimates of HS and TO for data trials by applying the automatic HS and
        TO determination algorithm

    %   First thing to do is to plot the correct data
    for i = 1:4
        %   For L_TO, check if this is a slip trial
        switch i
                case 1
                    Fz = FZ_R;
                    words = 'Right Fz - HS';
                case 2
                    Fz =  FZ_R;
                    Fz = flipud(Fz);
                    words = 'Right Fz - TO';
                case 3
                    Fz = FZ_L;
                    words = 'Left Fz - HS';
                case 4
                    Slip = menu(strcat('Is this a slip trial?'),'YES', 'NO');
                    if (Slip == 1)
                        EventArray(4) = -1;
                        break   %   Get out of here
                    end %   end if
                    Fz = FZ_L;
                    Fz = flipud(Fz);
                    words = 'Left Fz - TO';
        end %   end of switch

        figure(1); clf

        Nsamples = length(Fz);
        %   Set up x axis vector
```

192

```
        t=1:Nsamples;

        %   plot normal force for the correct foot
        plot(t,Fz,'b+');
        hold on

%   Next thing is to get the user to choose the range of data for calculating the mean and standard
    deviation
        title([words, '. Choose beginning of baseline data.'])
        grid on;

        %   Get the point clicked on by the user
        [start_point, dummy]=ginput(1);

        start_point = fix(start_point);

        title([words, '. Choose end of baseline data.'])
        grid on;

        %   Get the point clicked on by the user
        [end_point, dummy]=ginput(1);

        end_point = fix(end_point);

        clf(1)

        %   Calculate standard deviation and mean in range
        BaselineSD = std(Fz(start_point:end_point));
        BaselineMEAN = mean(Fz(start_point:end_point));

%   Not enough noise to really detect the major change needed using multiple SDs - instead, a
    relatively minor change is outside of the envelope.  Rather, use 20 N as initial search

        choice = end_point + 1; %   start looking one sample past the end of baseline data
        while(Fz(choice) < 20)
            choice = choice + 1;
        end

%   Now, work backwards to find the first point BEFORE the breakout point that was less than or
    equal to 2 standard deviations from the mean - this assumes that force should not drop below
    the baseline level for HS OR TO.
```

```
        while(Fz(choice) > (BaselineMEAN + 2 * BaselineSD))
            choice = choice - 1;
        end

        switch i
            case 1
                EventArray(1) = round(choice / multi);
                EventArray(13) = choice;
                EventArray(5) = BaselineMEAN;
                EventArray(6) = BaselineSD;
            case 2
                EventArray(2) = round((Nsamples + 1 - choice) / multi);    % reversed data
                EventArray(14) = (Nsamples + 1 - choice);
                EventArray(7) = BaselineMEAN;
                EventArray(8) = BaselineSD;
            case 3
                EventArray(3) = round(choice / multi);
                EventArray(15) = choice;
                EventArray(9) = BaselineMEAN;
                EventArray(10) = BaselineSD;
            case 4
                EventArray(4) = round((Nsamples + 1 - choice) / multi);    % reversed data
                EventArray(16) = (Nsamples + 1 - choice);
                EventArray(11) = BaselineMEAN;
                EventArray(12) = BaselineSD;
        end %   end of switch

    end %   end of for loop

    EventArray(17) = multi;
return
```

'Get_HS_and_TO2.m'

This function automates determination of heel strike and toe off using marker trajectory data only.

```matlab
function [EventArray] = Get_HS_and_TO_2(R_Heel, L_Heel, R_Toe_Z, L_Toe_Z, multi)
    %   This function will generate estimates of HS and TO for data trials by applying an automatic HS and
    %       TO determination algorithm

    EventArray = [0 0 0 0 0 0 0 0 0 0 0 0 0 0 0 0 0 0 0 0];
    %   First thing to do is to plot the correct data
    for i = 1:4
        switch i
            case 1
                Fz = R_Heel;
                words = 'R Heel Z - HS: Choose baseline data';
                step = -1;
            case 2
                delete(gcf)
                Fz =  R_Toe_Z;
                words = 'R Toe Z - TO: Choose region data';
                step = +1;
            case 3
                delete(gcf)
                Fz = L_Heel;
                words = 'L Heel Z - HS: Choose baseline data';
                step = -1;
            case 4
                delete(gcf)
                %   For L_TO, check if this is a slip trial
                Slip = menu(strcat('Is this a slip trial?'),'YES', 'NO');
                if (Slip == 1)
                    EventArray(4) = -1;
                    break   %   Get out of here
                end %   end if

                Fz = L_Toe_Z;
                words = 'L Toe Z - TO: Choose region data';
```

```
            step = +1;
    end %    end of switch

figure(1); clf

Nsamples = length(Fz);
%    Set up x axis vector
t=1:Nsamples;

%    plot marker movement for the correct foot
plot(t,Fz)
if i == 1 | i == 3
    axis auto
else
    axis([0 Nsamples 0 100])
    axis manual
end
hold on

limits = axis;
if (i == 2 | i == 4)
    line([EventArray(i-1) EventArray(i-1)], [limits(3) limits(4)], 'LineStyle', '--', ...
        'Color', 'k');
end

%    Next thing is to get the user to choose the range of data for calculating the mean and standard
    deviation

title([words, '. Choose beginning.'])
grid on;

%    Get the point clicked on by the user
[start_point, dummy]=ginput(1);

start_point = fix(start_point);

title([words, '. Choose end.'])
grid on;

%    Get the point clicked on by the user
[end_point, dummy]=ginput(1);
```

196

```matlab
end_point = fix(end_point);

clf(1)

%   Calculate standard deviation and mean in range
BaselineSD = std(Fz(start_point:end_point));
BaselineMEAN = mean(Fz(start_point:end_point));

%   get minimum in region
[dataminy,dataminx] = min(Fz(start_point:end_point));

if (i == 1 | i == 3)
    Fz = abs(Fz - BaselineMEAN);
end

hold off

xmin2 = start_point-round(.5*(end_point - start_point));
xmax2 = end_point + round(.5*(end_point - start_point));

if xmin2<=1
    xmin2 = start_point;
end

if xmax2 >= Nsamples
    xmax2 = Nsamples
end

plot(t(xmin2:xmax2),Fz(xmin2:xmax2))
axis auto
hold on

limits = axis;
if (i == 2 | i == 4)
    line([EventArray(i-1) EventArray(i-1)], [limits(3) limits(4)], 'LineStyle',...
            '--', 'Color', 'k');
end

%   Find first point bigger than 4 standard deviations away from the mean occurring after endpoint
```

197

```
        if (i == 1 | i == 3)
            choice = start_point + step; %   start looking one before the
            %   beginning of baseline data or one past the end of the data
            %   depending on step
            while(Fz(choice) < (4 * BaselineSD))
                choice = choice + step; %   Either move forward one or backward
                %   one depending on step
            end
        else
            choice = dataminx+start_point-1;
        end

        plot(choice, Fz(choice),'ko')

        pause

        %   multiply by multi to get into samples numbers
        EventArray(i) = choice;
        EventArray(i+12) = EventArray(1)*multi;
        EventArray(i*2+3) = BaselineMEAN;
        EventArray(i*2+4) = BaselineSD;

    end %   end of for loop

    EventArray(17) = multi;
return
```

'get_slip_TO.m'

This function is used to estimate left foot toe off for slip trials. It adds another trial's left foot stance duration to the slip trial's left foot heel strike to estimate toe off.

```
function [EventArray] = get_slip_TO(name, EventArray)
    %   this function will open a file and return the L_TO from that file

    TempArray = EventArray;

    load(name)
    %   This will return EventArray
    L_HS = EventArray(3);
    L_TO = EventArray(4);

    EventArray = TempArray; %   Get back to current EventArray

    EventArray(4) = (L_TO - L_HS) + EventArray(3);

    %   Need to add EventArray for higher precision estimate of TO
    EventArray(16) = EventArray(17) * EventArray(4);
return
```

'Verify_HS_and_TO.m'

This function uses high frequency ground reaction force and/or lower frequency marker trajectory data to verify that acceptable heel strike and toe off estimates have been chosen.

```
function [EventArray] = Verify_HS_and_TO(FZ_R, FZ_L, R_Heel, R_Toe_Z, L_Heel, L_Toe_Z, EventArray)
    %   This function will use forces and/or marker trajectories to verify  HS and TO

    multi = EventArray(17);

    for i = 1:4
        BaselineMEAN = EventArray(i*2 + 3);
        BaselineSD = EventArray(i*2 + 4);

        switch i
            case 1
                words = 'Right Fz - HS';
            case 2
                words = 'Right Fz - TO';
            case 3
                words = 'Left Fz - HS';
            case 4
                words = 'Left Fz - TO';
        end %   end of switch

        Modify = menu([words, '. Verify with forces?'],'YES','NO');
        if (Modify == 1)
            point = EventArray(i + 12);   %   Use the higher precision estimates

            figure(1); clf

            switch i
                case 1
                    Fz = FZ_R;
                case 2
                    Fz =  FZ_R;
                case 3
```

200

```
        Fz = FZ_L;
    case 4
        Fz = FZ_L;
end %   end of switch

Nsamples = length(Fz);
%   Set up x axis vector
t=1:Nsamples;

%   plot normal force for the correct foot
plot(t, Fz, 'b+');
hold on

%   plot the pre-existing point
plot(t(point), Fz(point), 'ro');

%   plot a mean + 2 * SD line
SDvalue = BaselineMEAN + 2 * BaselineSD;
plot([t(1) t(Nsamples)], [SDvalue SDvalue], 'g-')

title([words, '. Zoom in to check point.'])
grid on
zoom on
hold off

Modify = menu([words, '. Is the chosen point correct?'], 'YES, Keep It', 'NO, Pick a New One');

while Modify ~=1
    plot(t, Fz, 'b+');
    title([words, '. Zoom in, push key, and use the cursor to pick point.'])
    grid on
    hold on
    zoom on

    %   Wait for the user to push a key
    pause

    %   Get the point clicked on by the user
    [point, dummy] = ginput(1);

    zoom out
```

```
        point = fix(point);

        clf

        %    replot Normal Force
        plot(t, Fz, 'b+');
        title([words, '. Zoom in if needed to verify.']);
        hold on

        plot(t(point), Fz(point), 'ro');

        %    plot a mean + 2 * SD line
        SDvalue = BaselineMEAN + 2 * BaselineSD;
        plot([t(1) t(Nsamples)], [SDvalue SDvalue], 'g-')

        grid on
        hold off;
        zoom on

        Modify = menu([words, '. Is this new point OK ?'],'YES, Keep It','NO, Pick a New One');
    end %    end of while

    EventArray(i+12) = point;
    EventArray(i) = round(point / multi);
end %    end verify with forces if

Modify = menu([words, '. Verify with marker trajectories?'], 'YES', 'NO');

if (Modify == 1)
    point = EventArray(i);

    Nframes = length(R_Heel);
    t=1:Nframes;

    switch i
        case 1
            data = R_Heel;
            words = 'Right Heel Vertical Velocity';

        case 2
            data =  R_Toe_Z;
```

202

```matlab
            words = 'Right Toe Vertical Position';
        case 3
            data = L_Heel;
            words = 'Left Heel Vertical Velocity';
        case 4
            data =  L_Toe_Z;
            words = 'Left Toe Vertical Position';
end %   end of switch

%   plot trajectory for the current point
if(i==1 | i ==3)
    data = abs(data - BaselineMEAN);
    plot(t, data)

    axis auto
else
    plot(t, data)
    axis([0 Nframes 0 100])
    axis manual
end

hold on

%   plot the pre-existing point
plot(t(point), data(point),'ro');

limits = axis;
%   plot HS for TO buggers
if (i==2 | i ==4)
    line([EventArray(i-1) EventArray(i-1)], [limits(3) limits(4)], 'LineStyle', ...
'--', 'Color', 'k');
end

title([words, '. Zoom in to check point.'])
zoom on
grid on
hold off

Modify = menu([words, '. Is the chosen point correct?'],'YES, Keep It','NO, Pick a New One');

while Modify ~=1
```

```matlab
if(i==1 | i ==3)
    plot(t, data)
    axis auto
else
    plot(t, data)
    axis([0 Nframes 0 100])
    axis manual
end
title([words, '. Zoom in, push any key, use the cursor to pick point.'])
grid on;
hold on;
limits = axis;
if (i==2 | i ==4)
    line([EventArray(i-1) EventArray(i-1)], [limits(3) limits(4)], ...
  'LineStyle', '--', 'Color', 'k');
end
zoom on;

%   Wait for the user to push a key
pause

%   Get the point clicked on by the user
[point, dummy] = ginput(1);

zoom out

point = fix(point);

clf

%   replot data
if(i==1 | i ==3)
    plot(t, data)
    axis auto
else
    plot(t, data)
    axis([0 Nframes 0 100])
    axis manual
end

limits = axis;
```

```
        hold on
        if (i==2 | i ==4)
            line([EventArray(i-1) EventArray(i-1)], [limits(3) limits(4)], ...
          'LineStyle', '--', 'Color', 'k');
        end

        title([words, '. Zoom in if needed to verify press any key to continue.']);
        hold on

        plot(t(point), data(point),'ro');
        grid on
        hold off;
        zoom on

        %   Wait for the user to push a key
        pause

        Modify = menu([words, '. Is this new point OK ?'],'YES, Keep It','NO, Pick a New One');
    end %   end of while

                    %    If point changes due to marker trajectory verification, need to update
          higher precision point as well.
    if (point ~= EventArray(i))
        EventArray(i) = point;
        EventArray(i + 12) = point * multi;
    end

  end %   end of verify with trajectories if

  %   If no verification, EventArray remains unchanged

end %   end of 4 element for loop

return
```

'Verify_HS_and_TO2.m'

This function uses only lower frequency marker trajectory data to verify that acceptable heel strike and toe off estimates have been chosen.

```
function [EventArray] = Verify_HS_and_TO_2(R_Heel, R_Toe, L_Heel, L_Toe, EventArray)
    %   This function will use forces and/or marker trajectories to verify HS and TO

    multi = EventArray(17);

    for i = 1:4
        BaselineMEAN = EventArray(i*2 + 3);
        BaselineSD = EventArray(i*2 + 4);

        switch i
            case 1
                words = 'Right Fz - HS';
            case 2
                words = 'Right Fz - TO';
            case 3
                words = 'Left Fz - HS';
            case 4
                words = 'Left Fz - TO';
        end %   end of switch

        Modify = menu([words, '. Verify with marker trajectories?'], 'YES', 'NO');

        if (Modify == 1)
            point = EventArray(i);

            Nframes = length(R_Heel);
            t=1:Nframes;

            switch i
                case 1
                    data = R_Heel;
                    words = 'Right Heel Vertical Velocity';
```

206

```matlab
            %   set up the time scale
        case 2
            data =  R_Toe;
            words = 'Right Toe Vertical Position';
        case 3
            data = L_Heel;
            words = 'Left Heel Vertical Velocity';
        case 4
            data =  L_Toe;
            words = 'Left Toe Vertical Position';
end %   end of switch

%   plot trajectory for the current point
if(i==1 | i ==3)
    data = abs(data - BaselineMEAN);
    plot(t, data)

    axis auto
else
    plot(t, data)
    axis([0 Nframes 0 100])
    axis manual
end

hold on

%   plot the pre-existing point
plot(t(point), data(point),'ro');

limits = axis;
%   plot HS for TO buggers
if (i==2 | i ==4)
    line([EventArray(i-1) EventArray(i-1)], [limits(3) limits(4)], ...
        'LineStyle', '--', 'Color', 'k');
end

title([words, '. Zoom in to check point.'])
zoom on
grid on
hold off
```

```matlab
Modify = menu([words, '. Is the chosen point correct?'],'YES, Keep It','NO, Pick a New One');

while Modify ~=1
    if(i==1 | i ==3)
        plot(t, data)
        axis auto
    else
        plot(t, data)
        axis([0 Nframes 0 100])
        axis manual
    end
    title([words, '. Zoom in, push any key, use the cursor to pick point.'])
    grid on;
    hold on;
    limits = axis;
    if (i==2 | i ==4)
        line([EventArray(i-1) EventArray(i-1)], [limits(3) limits(4)], ...
            'LineStyle', '--', 'Color', 'k');
    end
    zoom on;

    %   Wait for the user to push a key
    pause

    %   Get the point clicked on by the user
    [point, dummy] = ginput(1);

    zoom out

    point = fix(point);

    clf

    %   replot data
    if(i==1 | i ==3)
        plot(t, data)
        axis auto
    else
        plot(t, data)
        axis([0 Nframes 0 100])
```

208

```matlab
        axis manual
    end

    limits = axis;
    hold on
    if (i==2 | i ==4)
        line([EventArray(i-1) EventArray(i-1)], [limits(3) limits(4)], ...
            'LineStyle', '--', 'Color', 'k');
    end

    title([words, '. Zoom in if needed to verify press any key to continue.']);
    hold on

    plot(t(point), data(point),'ro');
    grid on
    hold off;
    zoom on

    %   Wait for the user to push a key
    pause

    Modify = menu([words, '. Is this new point OK ?'],'YES, Keep It','NO, Pick a New One');
end %   end of while

%   If point changes due to marker trajectory verification, need to update higher precision
%       point as well.
if (point ~= EventArray(i))
    EventArray(i) = point;
    EventArray(i + 12) = point * multi;
end

end %  end of verify with trajectories if

%  If no verification, EventArray remains unchanged

end %  end of 4 element for loop

return
```

BIBLIOGRAPHY

1. Agnew, J. and Suruda, A.J. (1993) Age and fatal work-related falls. *Human Factors* **35**, 731-6.

2. Allard, P., Cristofolini, L., D'Lima, D., Kirtley, C., Leardini, A., Rosenbaum, D., Schmid, O., Siegler, S., Stokes, I., Whittle, M., Witte, H. and Wu, G., (2003) Response to Dr. Baker's letter to the editor. *J Biomech* **36** (2), 303–304.

3. Allum, J.H., Carpenter, M.G. and Honegger, F. (2003) Directional aspects of balance corrections in man. *IEEE Eng Med Biol Mag* **22**, 37-47.

4. Allum, J.H., Honegger, F. and Schicks, H. (1993) Vestibular and proprioceptive modulation of postural synergies in normal subjects. *J Vestib Res* **3**, 59-85.

5. American Society for Testing and Materials (1996) Standard Test Method for Using a Variable Incidence Tribometer (VIT). ASTM F1679-96. *Annual Book of ASTM Standards* **15**.07.

6. Andres, R.O., O'Connor, D. and Eng, T. (1992) A practical synthesis of biomechanical results to prevent slips and falls in the workplace. In: Anonymous *Advances in Industrial Ergonomics and Safety IV*, pp. 1001-1006. London: Taylor & Francis.

7. Andriacchi, T.P., Strickland, A.B. (1983) Gait analysis as a tool to assess joint kinetics. In Berne, N., Engin, A.E., Correira da Silva, K.M. (Eds), *Proceedings of NATO. Advanced Study Institute Biomechanics of Normal and Pathological Articulating Joints.* Estoril, Portugal, pp. 83-102.

8. Apkarian, J., Naumann, S. and Cairns, B. (1989) A three-dimensional kinematic and dynamic model of the lower limb. *J Biomech* **22**, 143-55.

9. Baker, R. (2003) Letter to the editor regarding ISB recommendation on definition of joint coordinate systems for the reporting of human joint motion—part I: ankle, hip and spine. *J Biomech* **36** (2), 300–302.

10. Bell, A.L., Pedersen, D.R. and Brand, R.A. (1990) A comparison of the accuracy of several hip center location prediction methods. *J Biomech* **23**, 617-21.

11.   Besier, T.F., Sturnieks, D.L., Alderson, J.A. and Lloyd, D.G. (2003) Repeatability of gait data using a functional hip joint centre and a mean helical knee axis. *J Biomech* **36**, 1159-68.

12.   Binda, S.M., Culham, E.G. and Brouwer, B. (2003) Balance, muscle strength, and fear of falling in older adults. *Exp Aging Res* **29**, 205-19.

13.   Bloem, B.R., Allum, J.H., Carpenter, M.G. and Honegger, F. (2000) Is lower leg proprioception essential for triggering human automatic postural responses? *Exp Brain Res* **130**, 375-91.

14.   Bloem, B.R., Allum, J.H., Carpenter, M.G., Verschuuren, J.J. and Honegger, F. (2002) Triggering of balance corrections and compensatory strategies in a patient with total leg proprioceptive loss. *Exp Brain Res* **142**, 91-107.

15.   Bloomberg, J.J., Peters, B.T., Smith, S.L., Huebner, W.P. and Reschke, M.F. (1997) Locomotor head-trunk coordination strategies following space flight. *J Vestib Res* **7**, 161-77.

16.   Bloomberg, J.J., Reschke, M.F., Huebner, W.P. and Peters, B.T. (1992) The effects of target distance on eye and head movement during locomotion. *Ann N Y Acad Sci* **656**, 699-707.

17.   Bojsen-Moller, F. and Lamoreux, L. (1979) Significance of free-dorsiflexion of the toes in walking. *Acta Orthop Scand* **50**, 471-9.

18.   Brady, R.A., Pavol, M.J., Owings, T.M. and Grabiner, M.D. (2000) Foot displacement but not velocity predicts the outcome of a slip induced in young subjects while walking. *J Biomech* **33**, 803-8.

19.   Brown, L.A., Doan, J.B., McKenzie, N.C. and Cooper, S.A. (2006) Anxiety-mediated gait adaptations reduce errors of obstacle negotiation among younger and older adults: Implications for fall risk, *Gait & Posture,* In Press, Corrected Proof, Available online 18 January 2006, www.elsevier.com.

20.   Buchanan, J.J. and Horak, F.B. (1999) Emergence of postural patterns as a function of vision and translation frequency. *J Neurophysiol* **81**, 2325-39.

21.   Buchanan, J.J. and Horak, F.B. (2001) Transitions in a postural task: do the recruitment and suppression of degrees of freedom stabilize posture? *Exp Brain Res* **139**, 482-94.

22.   Buczek, F.L. and Banks, S.A. (1996) High-resolution force plate analysis of utilized slip resistance in human walking. *Journal of testing and evaluation* **24**, 353-358.

23.   Buczek, F.L. and Cavanagh, P.R. (1990) Stance phase knee and ankle kinematics and kinetics during level and downhill running. *Med Sci Sports Exerc* **22**, 669-77.

24. Bureau of Labor Statistics (2004) *Annual averages - household data from the Current Population Survey*. United States Department of Labor. Available from http://www.bls.gov/cps/cpsaat8.pdf.

25. Bureau of Labor Statistics (2004) *National census of fatal occupational injuries in 2004*. United States Department of Labor 05-1598. Available from http://www.bls.gov/news.release/pdf/cfoi.pdf.

26. Bureau of Labor Statistics (2003) *Lost-worktime injuries and illnesses: characteristics and resulting days away from work*. United States Department of Labor 05-521, Available from http://www.bls.gov/news.release/pdf/osh2.pdf.

27. Cappozzo, A., Catani, F., Croce, U.D. and Leardini, A. (1995) Position and orientation in space of bones during movement: anatomical frame definition and determination. *Clin Biomech (Bristol, Avon)* **10**, 171-178.

28. Cappozzo, A., Catani, F., Leardini, A., Benedetti, M.G. and Croce, U.D. (1996) Position and orientation in space of bones during movement: experimental artifacts. *Clin Biomech (Bristol, Avon)* **11**, 90-100.

29. Carpenter, M.G., Allum, J.H. and Honegger, F. (2001) Vestibular influences on human postural control in combinations of pitch and roll planes reveal differences in spatiotemporal processing. *Exp Brain Res* **140**, 95-111.

30. Chaffin, D.B. and Anderson, D.B. (1991) *Occupational Biomechanics*, 2nd ed. Hoboken: John Wiley and Sons.

31. Cham, R., Moyer B.E. and Redfern, M.S. (2002) Whole body biomechanics of responses to slips. In *Proceedings of the American Society of Biomechanics (ASB) in conjunction with the IVth World Congress of Biomechanics,* Calgary, Alberta, Canada, 4-9 August, # 231, ID# 1044.

32. Cham, R. and Redfern, M.S. (2001) Lower extremity corrective reactions to slip events. *J Biomech* **34**, 1439-45.

33. Cham, R. and Redfern, M.S. (2002) Changes in gait when anticipating slippery floors. *Gait & Posture* **15**, 159-71.

34. Cham, R. and Redfern, M.S. (2002) Heel contact dynamics during slip events on level and inclined surfaces. *Safety Science* **40**, 559-576.

35. Chamberlin, M.E., Fulwider, B.D., Sanders, S.L. and Medeiros, J.M. (2005) Does fear of falling influence spatial and temporal gait parameters in elderly persons beyond changes associated with normal aging? *J Gerontol A Biol Sci Med Sci* **60**, 1163-7.

36.   Chambers, A.J., Margerum, S., Redfern, M.S. and Cham, R. (2003) Kinematics of the foot during slips. *Occupational Ergonomics* **3**, 225-233.

37.   Chandler, R.F., Clauser, C.E., McConville, J.T., Reynolds, H.M. and Young, J.W. (1975) *Investigation of inertial properties of the human body*. DOT HS-801 430, Washington, DC: U.S. Department of Transportation.

38.   Chang, W.R., Gronqvist, R., Leclercq, S., Myung, R., Makkonen, L., Strandberg, L., Brungraber, R.J., Mattke, U. and Thorpe, S.C. (2001) The role of friction in the measurement of slipperiness, Part 1: friction mechanisms and definition of test conditions. *Ergonomics* **44**, 1217-32.

39.   Chao, E.Y., Laughman, R.K., Schneider, E. and Stauffer, R.N. (1983) Normative data of knee joint motion and ground reaction forces in adult level walking. *J Biomech* **16**, 219-33.

40.   Chapra, S.C., and Canale, R.P. (1988) *Numerical Methods for Engineers*. 2nd ed. New York: McGraw-Hill, Inc.

41.   Cole, G.K., Nigg, B.M., Ronsky, J.L. and Yeadon, M.R. (1993) Application of the joint coordinate system to three-dimensional joint attitude and movement representation: a standardization proposal. *J Biomech Eng* **115** (4A):344-9.

42.   Corna, S., Tarantola, J., Nardone, A., Giordano, A. and Schieppati, M. (1999) Standing on a continuously moving platform: is body inertia counteracted or exploited? *Exp Brain Res* **124**, 331-41.

43.   Courtney, T.K., Chang, W-R., Grönqvist, R. and Redfern, M.S. (2001) *Ergonomics* **44,** Issue 13.

44.   Courtney, T.K., Sorock, G.S., Manning, D.P., Collins, J.W. and Holbein-Jenny, M.A. (2001) Occupational slip, trip, and fall-related injuries--can the contribution of slipperiness be isolated? *Ergonomics* **44**, 1118-37.

45.   Courtney, T.K. and Webster, B.S. (2001) Antecedent factors and disabling occupational morbidity--insights from the new BLS data. *AIHAJ* **62**, 622-32.

46.   De Laet, C.E. and Pols, H.A. (2000) Fractures in the elderly: epidemiology and demography. *Baillieres Best Pract Res Clin Endocrinol Metab* **14**, 171-9.

47.   de Leva, P. (1996) Adjustments to Zatsiorsky-Seluyanov's segment inertia parameters. *J Biomech* **29**, 1223-30.

48.   Doriot, N. and Cheze, L. (2004) A three-dimensional kinematic and dynamic study of the lower limb during the stance phase of gait using an homogeneous matrix approach. *IEEE Trans Biomed Eng* **51**, 21-7.

49. Eng, J.J. and Winter, D.A. (1995) Kinetic analysis of the lower limbs during walking: what information can be gained from a three-dimensional model? *J Biomech* **28**, 753-8.

50. Ferber, R., Osternig, L.R., Woollacott, M.H., Wasielewski, N.J. and Lee, J.H. (2002) Reactive balance adjustments to unexpected perturbations during human walking. *Gait & Posture* **16**, 238-48.

51. Fingerhut, L.A., Cox, C.S. and Warner, M. (1998) International comparative analysis of injury mortality. Findings from the ICE on injury statistics. International Collaborative Effort on Injury Statistics. *Adv Data* 1-20.

52. Finkelstein, E.A., Corso, P.S., Miller, T.R., and Associates (2006) The Incidence and Economic Burden of Injuries in the United States. New York: Oxford University Press.

53. Frigo, C., Rabuffetti, M., Kerrigan, D.C., Deming, L.C., and Pedotti, A. (1998) Functionally oriented and clinically feasible quantitative gait analysis method. *Med Biol Eng Comput* **36**, 179-185.

54. Fuller, J., Lui, L.J., Murphy, M. C., Mann, R. W. (1997) A comparison of lower-extremity skeletal kinematics measured using skin- and pin mounted markers. *Human Movement Science* **16**, 219-242.

55. Gao, C. and Abeysekera, J. (2004) A systems perspective of slip and fall accidents on icy and snowy surfaces. *Ergonomics* **47**, 573-98.

56. Greenspan, S.L., Maitland, L.A., Myers, E.R., Krasnow, M.B. and Kido, T.H. (1994) Femoral bone loss progresses with age: a longitudinal study in women over age 65, *J Bone Miner Res* **9**, 1959-1965.

57. Grönqvist, R. (1999) Slips and falls. In: Kumar, S., (Ed.) *Biomechanics in Ergonomics*, pp. 351-375. Taylor and Francis.

58. Gronqvist, R., Abeysekera, J., Gard, G., Hsiang, S.M., Leamon, T.B., Newman, D.J., Gielo-Perczak, K., Lockhart, T.E. and Pai, C.Y. (2001) Human-centred approaches in slipperiness measurement. *Ergonomics* **44**, 1167-99.

59. Grood, E.S. and Suntay, W.J. (1983) A joint coordinate system for the clinical description of three-dimensional motions: application to the knee. *J Biomech Eng* **105**, 136-44.

60. Growney, E., Meglan, D., Johnson, M., Cahalan, T. and An K. (1997) Repeated measures of adult normal walking using a video tracking system. *Gait & Posture* **6**, 147-162.

61. Hanson, J.P., Redfern, M.S. and Mazumdar, M. (1999) Predicting slips and falls considering required and available friction. *Ergonomics* **42**, 1619-33.

62. Hausdorff, J.M., Rios, D.A., Edelber, H.K. (2001) Gait variability and fall risk in community-living older adults: a 1-year prospective study. *Archives of Physical Medicine and Rehabilitation* **82**, 1050–1056.

63. Health and Safety Executive (1999) Health and Safety Statistics 1998/9, Sudbury, UK, HSE Books.

64. Hirasaki, E., Moore, S.T., Raphan, T. and Cohen, B. (1999) Effects of walking velocity on vertical head and body movements during locomotion. *Exp Brain Res* **127**, 117-30.

65. Holden, J.P and Stanhope, S.J. (1998) The effect of variation in knee center location estimates on net knee joint moments. *Gait & Posture* **7**, 1-6.

66. Horak, F.B., Diener, H.C. and Nashner, L.M. (1989) Influence of central set on human postural responses. *J Neurophysiol* **62**, 841-53.

67. Horak, F.B. and Nashner, L.M. (1986) Central programming of postural movements: adaptation to altered support-surface configurations. *J Neurophysiol* **55**, 1369-81.

68. Horak, F.B., Nutt, J.G., and Nashner, L.M. (1992) Postural inflexibility in Parkinsonian subjects. *J Neurol Sci* **111**, 46-58.

69. Hornbrook, M.C., Stevens, V.J., Wingfield, D.J., Hollis, J.F., Greenlick, M.R., Ory, M.G. (1994) Preventing falls among community-dwelling older persons: results from a randomized trial. *The Gerontologist* **34**, 16–23.

70. Hsaio, E.T. and Robinovitch, S.N. (1998) Common protective movements govern unexpected falls from standing height. *J Biomech* **31**, 1-9.

71. Judge, J.O., King, M.B., Whipple, R., Clive, J. and Wolfson, L.I. (1995) Dynamic balance in older persons: effects of reduced visual and proprioceptive input. *J Gerontol A Biol Sci Med Sci* **50**, M263-70.

72. Kadaba, M.P., Ramakrishnan, H.K. and Wootten, M.E. (1990) Measurement of lower extremity kinematics during level walking. *J Orthop Res* **8**, 383-92.

73. King, M.B. and Tinetti, M.E. (1995) Falls in community-dwelling older persons. *J Am Geriatr Soc* **43**, 1146-54.

74. King, M.B. and Tinetti, M.E. (1996) A multifactorial approach to reducing injurious falls. *Clin Geriatr Med* **12**, 745-59.

75. Kingma, I., Toussaint, H.M., De Looze, M. P., and Van Dieen, J.H. (1996) Segment inertial parameter evaluation in two anthropometric models by application of a dynamic linked segment model. *J Biomech* **29**, 693-704.

76.   Kirkwood, R.N., Culham, E.G. and Costigan, P. (1999) Radiographic and non-invasive determination of the hip joint center location: effect on hip joint moments. *Clin Biomech (Bristol, Avon)* **14**, 227-35.

77.   Kurlan, R. (2005) "Fear of falling" gait: a potentially reversible psychogenic gait disorder. *Cogn Behav Neurol* **18**, 171-2.

78.   Kuo, A.D. and Zajac, F.E. (1993) A biomechanical analysis of muscle strength as a limiting factor in standing posture. *J Biomech* **26 Suppl 1**, 137-50.

79.   Lafortune, M.A., Cavanagh, P.R., Sommer, H.J. 3rd and Kalenak, A. (1992) Three-dimensional kinematics of the human knee during walking. *J Biomech* **25**, 347-57.

80.   Leamon, T.B. and Li, K.W. (1990) Microslip length and the perception of slipping. In *Twenty Third International Congress on Occupational Health,* Montreal, Canada, 22-28 September, 17-18.

81.   Leamon, T.B. and Son, D. (1989) The natural history of a microslip, in A. Mital (ed), Advances in Industrial Ergonomics and Safety I, (London: Taylor & Francis), 633 – 638.

82.   Leardini, A., Cappozzo, A., Catani, F., Toksvig-Larsen, S., Petitto, A., Sforza, V., Cassanelli, G. and Giannini, S. (1999) Validation of a functional method for the estimation of hip joint centre location. *J Biomech* **32**, 99-103.

83.   Lin, M.L., Hoskin, A.F., Fearn, K.T., Porretta, K.T., Sinelnikov, S., (2006) INJURY FACTS® 2005-2006 edition, National Safety Council Paperback Publisher: Natl Safety Council, Itasca, IL.

84.   Llewellyn, M.G.A. and Nevola, V. R. (1992) Strategies for walking on low-friction surfaces. In W. A. Lotens and G. Havenith (eds) *Proceeding of the Fifth International Conference on Environmental Ergonomics,* Maastricht, The Netherlands, 22-28 September, 156-157.

85.   Lloyd, D.G. and Stevenson, M.G. (1992) Investigation of floor surface profile characteristics that will reduce the incidence of slips and falls. *Mechanical engineering transactions institution of engineers - Australia* **ME17**, 99-105.

86.   Lockhart, T.E. (1997) The ability of elderly people to traverse slippery walking surfaces. In *Proceedings of the Human Factors and Ergonomics Society 41rst Annual Meeting* **1**, Albuquerque, NM, September, 125-129.

87.   Lockhart, T.E. and Kim, S. (2006) Relationship between hamstring activation rate and heel contact velocity: Factors influencing age-related slip-induced falls. *Gait & Posture* **24 (1), 23-34.**.

88.   Lockhart, T.E., Smith, J.L., Woldstad, J.C. and Li, P. (2000) Effects of musculoskeletal and sensory degradation due to aging on the biomechanics of slips and falls.   In *Proceedings of the International Ergonomics Association 14th Triennial Congress and the Human Factors and Ergonomics Society 44th Annual Meeting*, San Diego, CA, August 2000, Vol. 5, 83-86.

89.   Lockhart, T.E., Woldstad, J.C. and Smith, J.L. (2003) Effects of age-related gait changes on the biomechanics of slips and falls. *Ergonomics* **46**, 1136-60.

90.   Lu, T.W. and O'Connor, J.J. (1999) Bone position estimation from skin marker co-ordinates using global optimization with joint constraints. *J Biomech* **32** 129-134.

91.   Lucchetti, L., Cappozzo, A., Cappello, A., and Della Croce, A. (1998) Skin movement artifact assessment and compensation in the estimation of knee-joint kinematics. *J Biomech* **31**, 977-984.

92.   Luukinen, H., Herala, M., Koski, K., Kivela, S.L. and Honkanen, R. (1999) Rapid increase of fall-related severe head injuries with age among older people: a population-based study. *J Am Geriatr Soc* **47**, 1451-2.

93.   Maki, B.E. (1997) Gait changes in older adults: predictors of falls or indicators of fear. *J Am Geriatr Soc* **45.**

94.   Maki, B.E. and McIlroy, W.E. (1999)   The control of foot placement during compensatory stepping reactions: does speed of response take precedence over stability? *IEEE Trans Rehabil Eng* **7**, 80-90.

95.   Maki, B.E., McIlroy, W.E. and Fernie, G.R. (2003)   Change-in-support reactions for balance recovery. *IEEE Eng Med Biol Mag* **22**, 20-6.

96.   Marigold, D.S., Bethune, A.J. and Patla, A.E. (2003) Role of the unperturbed limb and arms in the reactive recovery response to an unexpected slip during locomotion. *J Neurophysiol* **89**, 1727-37.

97.   Marigold, D.S. and Patla, A.E. (2002) Strategies for dynamic stability during locomotion on a slippery surface: effects of prior experience and knowledge. *J Neurophysiol* **88**, 339-53.

98.   McVay, E.J. and Redfern, M.S. (1994) Rampway Safety: Foot forces as a function of rampway angle. *American Industrial Hygiene Association Journal* **55** 626-634.

99.   Melton, L.J., Chrischilles, E.A., Cooper, C., Lane, A.W., Riggs, B.L. (1992) Perspective. How many women have osteoporosis? *J Bone Miner Res* **7**, 1005-10.

100.   Moyer, B.E., Chambers, A.J., Redfern, M.S., and Cham, R. (2006) Gait parameters as predictors of slip severity in younger and older adults. *Ergonomics* **49**, 329-343.

101.   Murray, M.P., Sepic, S.B. and Barnard, E.J. (1967) Patterns of sagittal rotation of the upper limbs in walking. *Phys Ther* **47**, 272-84.

102.   Myung, R. and Smith, J.L. (1997) The effect of load carrying and floor contaminants on slip and fall parameters. *Ergonomics* **40**, 235-46.

103.   Nashner, L.M., and McCollum, G. (1985) The organization of human postural movements: a formal basis and experimental synthesis, *Behav Brain Sci* **8**, 135–172.

104.   Pai, Y.C., Wening, J.D., Runtz, E.F., Iqbal, K. and Pavol, M.J. (2003) Role of feedforward control of movement stability in reducing slip-related balance loss and falls among older adults. *J Neurophysiol* **90**, 755-62.

105.   Park, S., Horak, F.B. and Kuo, A.D. (2004) Postural feedback responses scale with biomechanical constraints in human standing. *Exp Brain Res* **154**, 417-27.

106.   Pavol, M.J., Owings, T.M. and Grabiner, M.D. (2002) Body segment inertial parameter estimation for the general population of older adults. *J Biomech* **35**, 707-12.

107.   Pavol, M.J., Runtz, E.F., Edwards, B.J. and Pai, Y.C. (2002) Age influences the outcome of a slipping perturbation during initial but not repeated exposures. *Journals of Gerontology Series A-Biological Sciences & Medical Sciences* **57** (8):M496-503.

108.   Pearsall, D.J. and Costigan, P.A. (1999) The effect of segment parameter error on gait analysis results. *Gait & Posture* **9**, 173-83.

109.   Perkins, P.J. (1978) Measurement of slip between the shoe and ground during walking. In American society for testing and materials (Ed.) *ASTM-Special-Technical-Publication,* ASTM STP 649, Philadelphia, PA, 71-87.

110.   Personick, M.E. and Windau, J.A. (1995) Characteristics of older workers' injuries. 891, U.S. Department of Labor - Bureau of Labor Statistics.

111.   Pozzo, T., Berthoz, A. and Lefort, L. (1990) Head stabilization during various locomotor tasks in humans. I. Normal subjects. *Exp Brain Res* **82**, 97-106.

112.   Redfern, M.S. and Bidanda, B. (1992) Effects of shoe angle, velocity, and vertical force on shoe/floor slip resistance. In: Kumar, S., (Ed.) *Advances in industrial ergonomics and safety IV*, pp. 997-1000. Taylor and Francis.

113.   Redfern, M.S., Cham, R., Gielo-Perczak, K., Gronqvist, R., Hirvonen, M., Lanshammar, H., Marpet, M., Pai, C.Y. and Powers, C. (2001) Biomechanics of slips. *Ergonomics* **44**, 1138-66.

114.   Redfern, M.S. and DiPasquale, J. (1997) Biomechanics of descending ramps. *Gait and Posture* **6**, 119-125.

115. Reinschmidt, C., van den Bogert, A.J., Nigg, B.M., Lundberg, A. and Murphy, N. (1997) Effect of skin movement on the analysis of skeletal knee joint motion during running. *J Biomech* **30**, 729-32.

116. Rhoades, T.P., and Miller, J.M., (1988) Measurement and comparison of "required" versus "available" slip resistance. In *Proceedings of the Annual Conference of the Human Factors Association of Canada.* 137-140.

117. Rivara, F.P., Grossman, D.C. and Cummings, P. (1997) Injury prevention. Second of two parts. *N Engl J Med* **337**, 613-8.

118. Roux, E., Bouilland, S., Godillon-Maquinghen, A.P. and Bouttens, D. (2002) Evaluation of the global optimization method within the upper limb kinematics analysis. *J Biomech* **35**, 1279-83.

119. Saini, M., Kerrigan, D.C., Thirunarayan, M.A. and Duff-Raffaele, M. (1998) The vertical displacement of the center of mass during walking: a comparison of four measurement methods. *J Biomech Eng* **120**, 133-9.

120. Seidel, G.K., Marchinda, D.M., Dijkers, M. and Soutas-Little, R.W. (1995) Hip joint center location from palpable bony landmarks--a cadaver study. *J Biomech* **28**, 995-8.

121. Sheehan, F.T., Mitiguy, P. (1999) In regards to the "ISB recommendations for standardization in the reporting of kinematic data". *J Biomech* **32**(10), 1135-6.

122. Smeesters, C., Hayes, W.C. and McMahon, T.A. (2001) Disturbance type and gait speed affect fall direction and impact location. *J Biomech* **34**, 309-17.

123. Stagni, R., Leardini, A., Cappozzo, A., Grazia Benedetti, M. and Cappello, A. (2000) Effects of hip joint centre mislocation on gait analysis results. *J Biomech* **33**, 1479-87.

124. Stepnick, L. and Whitelaw N. (2006) A new vision of aging: helping older adults make healthier choices, Center for the Advancement of Health, Issue Briefing No. 2, March, Washington, DC.

125. Sterling, D.A., O'Connor, J.A. and Bonadies, J. (2001) Geriatric falls: injury severity is high and disproportionate to mechanism. *J Trauma* **50**, 116-9.

126. Strandberg, L. (1983) On accident analysis and slip-resistance measurement. *Ergonomics* **26**, 11-32.

127. Strandberg, L. and Lanshammar, H. (1981) The dynamics of slipping accidents. *Journal of occupational accidents* **3**, 153-162.

128. Tang, P.F. and Woollacott, M.H. (1998) Inefficient postural responses to unexpected slips during walking in older adults. *J Gerontol A Biol Sci Med Sci* **53**, M471-80.

129.   Thomas, E.J. and Brennan, T.A. (2000)   Incidence and types of preventable adverse events in elderly patients: population based review of medical records. *BMJ* **320**, 741-4.

130.   Thorstensson, A., Nilsson, J., Carlson, H. and Zomlefer, M.R. (1984) Trunk movements in human locomotion. *Acta Physiol Scand* **121**, 9-22.

131.   Tinetti, M.E., Speechley, M. and Ginter, S.F. (1988) Risk factors for falls among elderly persons living in the community. *N Engl J Med* **319**, 1701-7.

132.   Tinetti, M.E. and Williams, C.S. (1997)   Falls, injuries due to falls, and the risk of admission to a nursing home. *N Engl J Med* **337**, 1279-84.

133.   Tripp, B.P., McIlroy, W.E. and Maki, B.E. (2004)   Online mutability of step direction during rapid stepping reactions evoked by postural perturbation. *IEEE Trans Neural Syst Rehabil Eng* **12**, 140-52.

134.   Vicon Motion Systems Ltd (2000) Details of Kinetic Functions in BodyBuilder.

135.   Winter, D.A. (1983) Biomechanical motor patterns in normal walking. *J Mot Behav* **15**, 302-30.

136.   Winter, D.A. (1991) *The Biomechanics and Motor Control of Human Gait: Normal, Elderly, and Pathological*. 2nd ed. Ontario: University of Waterloo Press.

137.   Winter, D.A. (2005) *Biomechanics and Motor Control of Human Movement*. 3rd ed. Hoboken: John Wiley & Sons, Inc.

138.   Wolfson, L., Judge, J., Whipple, R. and King, M. (1995) Strength is a major factor in balance, gait, and the occurrence of falls. *J Gerontol A Biol Sci Med Sci* **50 Spec No**, 64-7.

139.   Wood, B.H., Bilclough, J.A., Bowron, A., and Walker, R.W. (2002) Incidence and prediction of falls in Parkinson's disease: a prospective multidisciplinary study. *J Neurol Neurosurg Psychiatry* **72**, 721-5.

140.   Woolacott, M.H. and Shumway-Cook, A. (2002)   Attention and the control of posture and gait: a review of an emerging area of research, *Gait & Posture* **16**, 1-14.

141.   Wu, G., Cavanagh, P.R. (1995) ISB recommendations for standardization in the reporting of kinematic data. *J Biomech* **28**(10), 1257-61.

142.   Wu, G., Siegler, S., Allard, P., Kirtley, C., Leardini, A., Rosenbaum, D., Whittle, M., D'Lima, D.D., Cristofolini, L., Witte, H., Schmid, O. and Stokes, I. (2002)   ISB recommendation on definitions of joint coordinate system of various joints for the reporting of human joint motion--part I: ankle, hip, and spine. International Society of Biomechanics. *J Biomech* **35**, 543-8.

143. You, J., Chou, Y., Lin, C. and Su, F. (2001) Effect of slip on movement of body center of mass relative to base of support. *Clin Biomech (Bristol, Avon)* **16**, 167-73.

144. Zatsiorsky, V.M. (1998) *Kinematics of Human Motion*. Human Kinetics.